

UNIVERSITY OF SOUTHAMPTON

FACULTY OF ENGINEERING AND PHYSICAL SCIENCES

School of Electronics and Computer Science

Corrosive Sulphur Condition Monitoring of Oil-Filled Power Transformers

by

Mohd Shahril Bin Ahmad Khiair

Thesis for the degree of Doctor of Philosophy

December 2019

UNIVERSITY OF SOUTHAMPTON

ABSTRACT

FACULTY OF ENGINEERING AND PHYSICAL SCIENCES

School of Electronics and Computer Science

Thesis for the degree of Doctor of Philosophy

Corrosive Sulphur Condition Monitoring of Oil-Filled Power Transformers

Mohd Shahril Bin Ahmad Khiair

The after-effects of corrosive sulphur-related faults on power transformers are disastrous. The existence of sulphur corrosion in transformer insulating oils leads to a formation and deposition of copper sulphide, creating a low resistance path across and through the paper insulation, resulting in internal discharges, flashovers, and ultimately catastrophic transformer failures. The current techniques applied to detect and monitor the progression of sulphur corrosion in transformer insulating oils (i.e. X-ray fluorescence and scanning electron microscopy–energy dispersive X-ray spectroscopy) require relatively expensive equipment and skilled personnel to run the tests, which increases operation costs. In addition, this approach must be carried out in laboratory, which requires a longer time to obtain the results. The existing standard tests, such as the BS EN 62535, ASTM D1275-B, and ASTM copper strip corrosion standard are imprecise because they are based on visual comparison of metal strips against a standard reference colour chart. As a solution, the work presented in this thesis is focused on developing a low-cost, portable, foolproof, and reliable method that provides instantaneous response in detecting the progression of corrosive sulphur compounds present in transformer insulating oils. In particular, the techniques investigated in this study were ultraviolet–visible spectroscopy, direct current conductivity measurements, and interdigitated capacitive sensors. The results reveal that these techniques were not feasible for the detection and condition monitoring of corrosive sulphur. However, obtained results and analysis led to the development of a novel technique based on thin film sacrificial copper strip sensors. It is possible to continuously quantify the elemental sulphur

concentrations in transformer insulating oils instantly on-site and has potential to be implemented as an online condition monitoring tool. The design and development of the sensors were carried out based on the 2^2 factorial design. A regression model was developed, being able to predict the transformed resistance of the sensors as a function of their area and thickness. In use, the sensor change in resistance is a function of the level of corrosive sulphur compounds (i.e. in ppm) in the mineral oil.

TABLE OF CONTENTS

TABLE OF CONTENTS	IV
DECLARATION OF AUTHORSHIP.....	IX
ACKNOWLEDGEMENTS.....	XI
ABBREVIATIONS.....	XII
1 INTRODUCTION	1
<i>1.1 POWER TRANSFORMERS</i>	<i>1</i>
<i>1.2 PROBLEM STATEMENT AND RESEARCH MOTIVATION</i>	<i>2</i>
<i>1.3 RESEARCH OBJECTIVES.....</i>	<i>5</i>
<i>1.4 SIGNIFICANT CONTRIBUTIONS OF THE RESEARCH</i>	<i>6</i>
<i>1.5 ORGANISATION OF THE THESIS</i>	<i>10</i>
2 MONITORING OF OIL-FILLED POWER TRANSFORMER DUE TO SULPHUR CORROSION	12
<i>2.1 INTRODUCTION</i>	<i>12</i>
<i>2.2 MONITORING THE INSULATING OIL: TYPES AND REASONS</i>	<i>12</i>
<i>2.3 MINERAL OILS</i>	<i>14</i>
<i>2.4 SULPHUR CORROSION: TERMINOLOGIES AND GENERAL BACKGROUND..</i>	<i>17</i>
<i>2.5 SULPHUR COMPOUNDS</i>	<i>20</i>
<i>2.6 SULPHUR CORROSION MECHANISM.....</i>	<i>21</i>
<i>2.7 DETECTION AND CONDITION MONITORING OF CORROSIVE SULPHUR.....</i>	<i>27</i>
<i>2.8 COUNTERMEASURES AGAINST CORROSIVE SULPHUR.....</i>	<i>32</i>
<i>2.9 SUMMARY</i>	<i>33</i>
3 IDENTIFICATION OF CORROSIVE OILS USING THE EXISTING STANDARD TECHNIQUE AND UV–VIS SPECTROSCOPY	35
<i>3.1 INTRODUCTION</i>	<i>35</i>
<i>3.2 PREPARATION OF CORROSIVE OIL AND BARE COPPER SAMPLES.....</i>	<i>35</i>
<i>3.3 BS EN 62535 STANDARD TEST METHOD AND SEM–EDX SPECTROSCOPY....</i>	<i>38</i>

3.3.1	<i>FUNDAMENTAL PRINCIPLES OF SEM–EDX SPECTROSCOPY</i>	38
3.3.2	<i>RESULTS AND DISCUSSION</i>	39
3.4	<i>UV–VIS SPECTROSCOPY</i>	43
3.4.1	<i>FUNDAMENTAL PRINCIPLES OF ABSORPTION SPECTROSCOPY</i>	45
3.4.2	<i>FUNDAMENTAL PRINCIPLES OF UV-VIS SPECTROSCOPY AND PREVIOUS APPLICATIONS</i>	46
3.5	<i>EXPERIMENTAL SET-UP</i>	47
3.6	<i>RESULTS AND DISCUSSION</i>	48
3.7	<i>SUMMARY</i>	50
4	SULPHUR CORROSION SENSORS UTILISING DC CONDUCTIVITY MEASUREMENTS AND INTERDIGITATED CAPACITIVE SENSORS	51
4.1	<i>INTRODUCTION</i>	51
4.2	<i>KARL FISCHER (KF) COULOMETRIC TITRATION</i>	51
4.2.1	<i>FUNDAMENTAL PRINCIPLES</i>	51
4.2.2	<i>EQUIPMENT USED AND PROCEDURE</i>	52
4.3	<i>DC CONDUCTIVITY MEASUREMENTS</i>	53
4.3.1	<i>FUNDAMENTAL PRINCIPLE AND PREVIOUS APPLICATIONS</i>	53
4.3.2	<i>EXPERIMENTAL SET-UP</i>	57
4.3.3	<i>RESULTS AND DISCUSSIONS</i>	60
4.4	<i>INTERDIGITATED SENSORS (IDCs)</i>	62
4.4.1	<i>FUNDAMENTAL PRINCIPLES AND PREVIOUS APPLICATIONS</i>	63
4.4.2	<i>DESIGN, CONSTRUCTION AND FABRICATION</i>	66
4.4.3	<i>EXPERIMENTAL SET-UP AND PROCEDURE</i>	67
4.4.4	<i>RESULTS AND DISCUSSION</i>	70
4.5	<i>SUMMARY</i>	72
5	THIN FILM SACRIFICIAL COPPER STRIPS FOR SULPHUR CORROSION SENSING	73
5.1	<i>INTRODUCTION</i>	73

5.2	<i>FABRICATION OF SENSORS</i>	74
5.3	<i>PRINCIPLE OF THE LOW-RESISTANCE MEASUREMENTS</i>	77
5.4	<i>DEVELOPMENT OF THE SENSORS BASED ON THE 2² FACTORIAL DESIGN</i>	79
5.4.1	<i>SCREENING EXPERIMENT</i>	80
5.4.2	<i>RESULTS OF THE SCREENING EXPERIMENT</i>	81
5.4.3	<i>REGRESSION MODEL</i>	83
5.4.4	<i>VALIDATION OF THE REGRESSION MODEL</i>	85
5.5	<i>CHARACTERISTICS OF THE SENSORS IN THE PRESENCE OF CORROSIVE BY-PRODUCTS DUE TO THE BREAKDOWN OF DBDS</i>	86
5.5.1	<i>EXPERIMENTAL SET-UP</i>	87
5.5.2	<i>SURFACE MORPHOLOGIES OF THE SENSORS</i>	87
5.5.3	<i>CHANGES IN THE RESISTANCE OF THE SENSORS FOR INSULATING OILS WITH DIFFERENT DBDS CONCENTRATIONS</i>	90
5.5.4	<i>EFFECT OF AGEING TEMPERATURE ON THE CHARACTERISTICS OF THE SENSORS</i>	91
5.6	<i>CHARACTERISTICS OF THE SENSORS IN THE PRESENCE OF ELEMENTAL SULPHUR</i>	94
5.6.1	<i>EXPERIMENTAL SET-UP</i>	94
5.6.2	<i>SURFACE MORPHOLOGIES OF THE SENSORS</i>	94
5.6.3	<i>CHANGES IN THE RESISTANCE OF THE SENSORS FOR INSULATING OILS WITH DIFFERENT ELEMENTAL SULPHUR CONCENTRATIONS</i>	95
5.6.4	<i>VALIDATION OF THE SENSORS BY ULTRA HIGH PERFORMANCE SUPERCRITICAL FLUID CHROMATOGRAPHY–MASS SPECTROMETRY</i>	96
5.7	<i>A NOVEL ONLINE METHOD FOR QUANTIFICATION OF CORROSIVE SULPHUR IN INSULATING OILS</i>	101
5.7.1	<i>EXPERIMENTAL SET-UP</i>	102
5.7.2	<i>RESULTS AND DISCUSSION</i>	103
5.7.3	<i>LIMITATIONS OF THE SENSORS</i>	111

5.7.4	PROPOSED ONLINE METHOD FOR QUANTIFICATION OF ELEMENTAL SULPHUR IN INSULATING OILS	113
5.8	SUMMARY	116
6	CONCLUSIONS	118
6.1	CONCLUSIONS	118
6.2	FUTURE WORK	119
	APPENDIX A: PUBLISHED PAPERS	121
A.1	CONFERENCE I: M.S.A. Khiar, R.C.D. Brown and P.L. Lewin, “Detection of Sulfur Corrosion in Transformer Insulation Oils Using An Interdigitated Capacitive Sensor Based On Printed Circuit Board Technology,” in <i>IEEE Conference on Electrical Insulation and Dielectric Phenomena (CEIDP)</i> , 2017, pp. 278-281.	121
A.2	CONFERENCE II: M.S.A. Khiar, R.C.D. Brown and P.L. Lewin, “Tracking The Progression of Sulfur Corrosion in Transformer Oil Using Thin Film Sacrificial Copper Strip,” in <i>IEEE 2nd International Conference on Dielectrics (ICD)</i> , 2018, pp. 1-4.	125
A.3	CONFERENCE III: M.S.A. Khiar, R.C.D. Brown and P.L. Lewin, “Effect of Temperature Changes on Thin Film Sacrificial Copper Strips due to Sulfur Corrosion,” in <i>IEEE Conference on Electrical Insulation and Dielectric Phenomena (CEIDP)</i> , 2018, pp. 490-493.	129
A.4	ACADEMIC JOURNAL: M.S.A. Khiar, R.C.D. Brown and P.L. Lewin, “Sacrificial copper strip sensors for sulfur corrosion detection in transformer oils,” <i>Measurement</i> , vol. 148, pp. 1–6, 2019.	133
	APPENDIX B: NATIONAL GRID REPORTS	139
B.1	THE EFFECT OF CORROSIVE OIL ON UV-VIS SPECTROSCOPY	139
B.2	THE EFFECT OF CORROSIVE OIL ON DC CONDUCTIVITY MEASUREMENTS	148
	APPENDIX C: UHPSFC–MS DATA SETS	159
C.1	0 PPM	159
C.2	10 PPM	160
C.3	20 PPM	161
C.4	40 PPM	162
	APPENDIX D: SURFACE MORPHOLOGIES OF THE SENSORS	163

<i>D.1 HIGH-DEFINITION QUALITY IMAGES OF SENSORS AGED AFTER 1 H</i>	<i>163</i>
<i>(10 PPM OF S8 AT 110 °C).....</i>	<i>163</i>
<i>D.2 HIGH-DEFINITION QUALITY IMAGES OF SENSORS AGED AFTER 2.25 H</i>	<i>164</i>
<i>(10 PPM OF S8 AT 110 °C).....</i>	<i>164</i>
LIST OF REFERENCES	165

DECLARATION OF AUTHORSHIP

I, Mohd Shahril Bin Ahmad Khiar

declare that this thesis entitled

“Corrosive Sulphur Condition Monitoring of Oil-Filled Power Transformers”

and the work presented in it are my own and has been generated by me as the result of my own original research.

I confirm that:

1. This work was done wholly or mainly while in candidature for a research degree at this University;
2. Where any part of this thesis has previously been submitted for a degree or any other qualification at this University or any other institution, this has been clearly stated;
3. Where I have consulted the published work of others, this is always clearly attributed;
4. Where I have quoted from the work of others, the source is always given. With the exception of such quotations, this thesis is entirely my own work;
5. I have acknowledged all main sources of help;
6. Where the thesis is based on work done by myself jointly with others, I have made clear exactly what was done by others and what I have contributed myself;
7. Parts of this work have been published as peer reviewed journal paper (•) or conference contributions (-):
 - M. S. Ahmad Khiar, R.C.D. Brown, and P.L. Lewin, “Sacrificial Copper Strip Sensors for Sulfur Corrosion Detection in Transformer Oils,” *Measurement, in Press*.

- M. S. A. Khiar, R. C. D. Brown, and P. L. Lewin, “Detection of Sulfur Corrosion in Transformer Insulation Oils Using an Interdigitated Capacitive Sensor Based on Printed Circuit Board Technology,” in *IEEE Conference on Electrical Insulation and Dielectric Phenomena (CEIDP)*, 2017, pp. 278–281.
- M. S. A. Khiar, R. C. D. Brown, and P. L. Lewin, “Tracking the Progression of Sulfur Corrosion in Transformer Oil using Thin Film Sacrificial Copper Strip,” in *IEEE 2nd International Conference on Dielectrics (ICD)*, 2018, pp. 1–4.
- M. S. A. Khiar, R. C. D. Brown, and P. L. Lewin, “Effect of Temperature Changes on Thin Film Sacrificial Copper Strips due to Sulfur Corrosion,” in *IEEE Conference on Electrical Insulation and Dielectric Phenomena (CEIDP)*, 2018, pp. 490–493.

Signed:

Date:

ACKNOWLEDGEMENTS

Alhamdulillah. All praise be to Allah SWT for His blessings and mercy such that I can complete this thesis. I want to acknowledge the Government of Malaysia, Universiti Teknikal Malaysia Melaka (UTeM), and National Grid plc (UK) for providing me the financial support to pursue my PhD study.

I wish to express my deepest gratitude to supervisors Professor Paul L Lewin and Professor Richard C D Brown, for their continuous guidance, suggestions, and encouragement that have greatly helped me in my research work throughout my postgraduate study. I am grateful to all of the Tony Davies High Voltage Laboratory members, especially to Dr James A. Pilgrims, Neil Palmer, Liz Tillotson, Brian Rodgers, Mark Long White, and Charlie P. Reed. I wish to express my appreciation to Dr Richard Pearce from Ocean and Earth Science, National Oceanography Centre (NOCS), University of Southampton, for the SEM–EDX analysis, and a special thank to Mr. Richard Howell for manufacturing the PCB. In addition, I would like express my sincere gratitude to Professor Harold Chong, Dr Kian Kiang, and Neil Sessions from Electronics and Computer Science, University of Southampton for their support in manufacturing the thin film copper strip sensors.

I am grateful to Allah the Almighty for blessing me with great and supportive parents, Haji Ahmad Khair Bin Haji Zainol and Hajjah Samsiah Binti Kassim. I am also grateful to my lovely wife, Zulaikha Binti Md Radzai, for her great love, care, and continuing support. I also cherished the moments with my cutie pies, Sarah Insyirah, Sophea Insyirah, and Izzah Insyirah for making my PhD journey wonderful and enjoyable. I greatly appreciate the endless prayers and motivations from all of my siblings, in-laws, nephews, and nieces, for your moral support. Thank you for sharing your PhD journey with me, my dearest father-in-law, Datuk Professor Dr Haji Md Radzai Bin Said. Your 30 years of experience as an academician has inspired me to follow your footsteps and disseminate knowledge to other scholars. I am also indebted to my mother-in-law, Datin Hajjah Latifah Binti Mindar and all in-laws for your prayers and support. I specially thank my best friends; Ir Dr Haji Sharin Bin Ab Ghani, Ir Imran Sutan Chairul, Ir Muhammad Syahrani Bin Johal, and all of the High Voltage Engineering Research Laboratory CeRIA FKE UTeM members.

ABBREVIATIONS

AC	Alternating current
Ag	Silver
ANOVA	Analysis of variance
ASTM	American Society for Testing and Materials
BiBZ	Bibenzyl
BS EN	British standard
ΔC	Changes in oil capacitance values
ΔCW	Changes in amount of copper
$^{\circ}\text{C}$	Degree Celsius
CCD	Covered conductor deposition
CH_4	Methane
CIGRE	International Council on Large Electric Systems (in French: <i>Conseil International des Grands Réseaux Électriques</i>)
Cu	Copper
C_2H_2	Acetylene
C_2H_4	Ethylene
C_2H_6	Ethane
DBDS	Dibenzyl disulphide
DBS	Dibenzyl sulphide
DC	Direct current
Df	Degrees of freedom
DGA	Dissolved gas analysis
DIN	German Institute for Standardization (in German: <i>Deutsches Institut für Normung</i>)
DoE	Design of experiments
EDX	Energy dispersive X-ray spectroscopy
eV	electronvolt
ε_0	Permittivity of free space (8.854 pF/m)
ε_r	Permittivity of material

F	Farad
FDS	Frequency domain spectroscopy
FR-4	International grade designation for fibreglass reinforced epoxy laminates that are flame-retardant
g/L	Gram per Litre
g/mol	Gram per mole
h	Hour(s)
IDCs	Interdigitated capacitive sensors
IEC	International Electrotechnical Commission
in	Inch
J s	Joule-second
K	Kelvin
KF	Karl Fischer
KOH	Potassium hydroxide
kV	Kilovolt(s)
m	Metre(s)
mA	Miliampere
mbar	Milibar
mg kg ⁻¹	Milligrams per kilogram
mg L ⁻¹	Milligrams per litre
mHz	Millihertz
mL	Millilitre(s)
mm	Millimetre(s)
mm ²	Square millimetres
m s ⁻¹	Metre per second
<i>MS</i>	Means squares
MVA	Megavoltamperes
nm	Nanometre(s)
OFAT	One-factor-at-a-time
pA	PicoAmpere
PCB	Printed circuit board

PDC	Polarisation and depolarisation current
pF	PicoFarad
pF/m	PicoFarad per metre
ppb	Parts per billion
ppm	Parts per million
PTFE	Polytetrafluoroethylene
Q	Charge
ΔR	Change in resistance
R^2	Coefficient of determination
$RMSE$	Root mean square error
rpm	Revolutions per minute
ΔS_8	Change in elemental sulphur concentration
UHPSFC–MS	Ultra high performance supercritical fluid chromatography–mass spectrometry
s	Second(s)
S	Sulphur
SEM	Scanning electron microscopy
SS	Sum of squares
$\tan \delta$	Loss tangent (dissipation factor)
TC	Technical Committee
TMD	Total mercaptans and disulphides
TOPICSII	Transformer Oil Passivation and Impact of Corrosive Sulphur II
TPP	Triphenylphosphine
TPPS	Triphenylphosphine sulphide
UV–vis	Ultraviolet–visible
ΔV	Potential difference
WG	Working group
wt %	Weight percent
XPS	X-ray photoelectron spectroscopy
2^2	Two-level
μA	Microampere

μL	Microlitre(s)
μm	Micrometre(s)
Ω	Ohm

1 INTRODUCTION

1.1 POWER TRANSFORMERS

Power transformers are the backbone of power system networks. Power transformers enable changes in voltage or current in power system networks while simultaneously maintaining the output power at a constant value [1]. Power transformers enable electrical utilities to transfer power to the end users based on supply and demand through a transmission and distribution network system.

The insulation system is the heart of a power transformer and it is used to insulate a number of critical elements such as tap changers, circuit breakers, bushings, and transformers [2]. Figure 1-1 shows the components of an oil-filled power transformer, which consists of two major insulations: cellulose-based solid insulation, and insulating oil. The insulation system can be divided into two categories: major insulation and minor insulation. The major insulation refers to the insulator (i.e. oil and cellulose-based solid insulation such as pressboard) between the windings and core yoke as well as between the leads and ground. In contrast, the minor insulation refers to the insulator (i.e. oil and cellulose-based solid insulation such as Kraft paper) at the inter-disc and inter-turn windings.

There are two types of power transformers: liquid-filled transformers and dry-type transformers. These transformers are distinguished based on their insulation type. Oil is used as the insulating medium in liquid-filled transformers whereas air or gas is used as the insulating medium in dry-type transformers [3]. In general, there are two types of transformers in which insulating oil is used as the insulating medium: free-breathing transformers and hermetically-sealed transformers.

Liquid-filled transformers are more efficient compared with dry-type transformers because oil is a very effective medium to reduce temperature at hot spots in the coils [2]. Therefore, these transformers are commonplace and for many decades have been used for both distribution and transmission applications [4]. However, the main disadvantage of liquid-filled transformers is the high risk of explosion because oil is highly flammable [5]. Owing

to the substantial volume of oil required for power transformers, this increases the possibility of insulation failure or electrical breakdown, which may lead to ignition or even explosions at excessively high oil temperatures. Power transformer explosions can cause personal injury or even death, environmental hazards (oil spillage), and sudden discontinuity of power supply, which can lead to significant losses to utility companies and commercial businesses [6]. Therefore, it is crucial to monitor the operating conditions of power transformers using online condition monitoring techniques in order to prolong the lifespan of power transformers and minimise breakdowns and catastrophic failures.

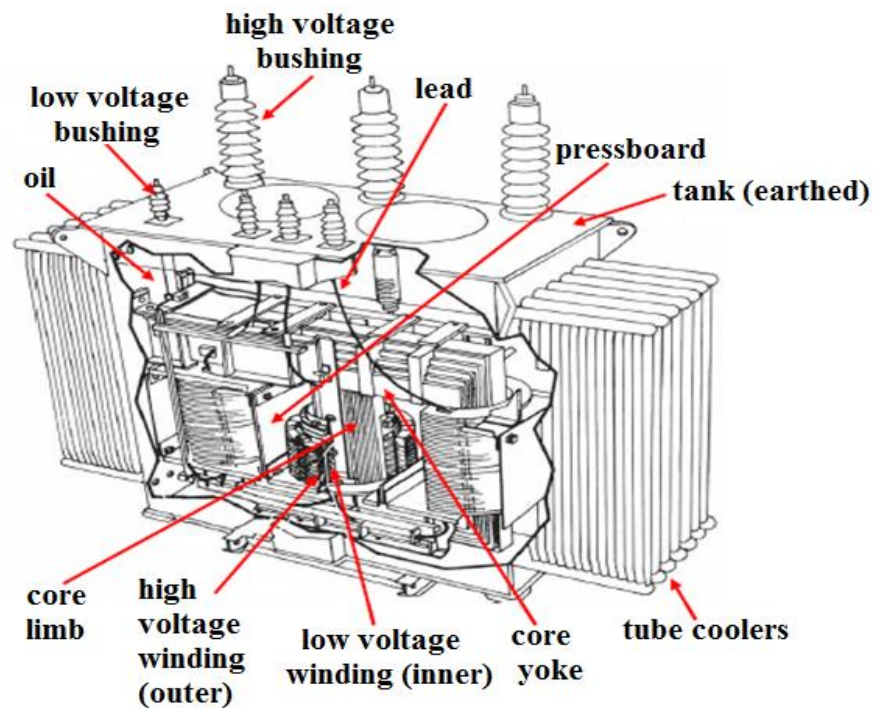


Figure 1-1. Components of an oil-filled power transformer. Modified from [7].

1.2 PROBLEM STATEMENT AND RESEARCH MOTIVATION

Insulator condition serves as an indicator to determine the life expectancy of transformers [1]. The quality of the insulation (oil and paper) determines the health index of the power transformer [8]. Therefore, it is crucial to monitor the degradation of the insulating oil and paper insulation in order to prolong the lifetime of power transformers.

According to the International Council on Large Electric Systems (CIGRE) Technical Report (Working Group A2.40) published in 2015, the two main types of power transformer failures are inter-turn failures and dielectric failures, which constitute 64 % of power transformer failures, as shown in Table 1-1 [9].

Table 1-1. Types of transformer failures [9].

Type	Inter-turn failures	Dielectric failures	Tap-changer faults	Gassing	Mechanical failures
Percentage (%)	39	25	21	11	4

Based on statistics [9], 86 % of the causes of transformer failures are sulphur corrosion-associated faults. Since sulphur corrosion is considered to be a minor technical issue in electrical utilities, there is a lack of in-depth studies regarding this issue, and only a few failure cases have been reported [10]. According to Arvidsson et al. [11], sulphur corrosion has probably been known for many years, beginning from the end of the 1980s in Brazil and South Africa. However, this issue was somewhat resolved in the early 1990s through the enhancement of oil purification techniques and the implementation of oil corrosive tests as part of quality control management systems [12],[13]. However, sulphur corrosion issues resurfaced at the beginning of the 21st century [14] and the number of cases associated with sulphur corrosion has increased significantly since then [10]. The lack of studies related to sulphur corrosion has led major organisations such as CIGRE and Sea Marconi to implement countermeasures to tackle this problem [15],[16].

The after effects of corrosive sulphur on power transformers are disastrous. It is known that the presence of corrosive sulphur in the insulating oils does not only adversely affect copper conductors and other metal surfaces, but also the paper insulation. The existence of copper sulphide, which appears as solid contaminants inside failed power transformers [17], produces a low resistance path across and through the cellulose insulation, which can lead to internal discharges, flashover, and turn-to-turn transformer breakdowns [10], [18]. Several journal articles published by Mitsubishi Electric Corporation supported this argument [19]–[22]. This type of fault is ranked as the highest cause of transformer failures, as shown in

Table 1-1. The number of transformer failures due to sulphur corrosion continues to increase and many transformer units worldwide have failed since the beginning of this decade [23]. Hence, there is a critical need to develop reliable condition monitoring tools in order to monitor the presence of corrosive sulphur species in transformer oils and prevent catastrophic transformer failures.

Initially, the detection of corrosive sulphur species is carried out by the manufacturers of insulating oils to ensure that the oils comply with the relevant international standards. Thereafter, corrosive sulphur species are detected by the operators of transformer systems, who regularly undertake oil quality monitoring processes. To date, there are four common standard corrosion tests, which will be described in Section 2.7. These tests involve comparing the colour of a copper strip with the ASTM copper strip corrosion standard [24] in order to deduce the corrosivity levels of the insulating oils under assessment. Unfortunately, these methods are imprecise because they rely on visual-based observations. In addition, these offline tests involve taking a small volume of oil sample, which may not be representative of the corrosivity level of the total oil volume in the transformer.

As yet, various techniques (see Section 2.7) have been developed to detect the presence of corrosive sulphur compounds that leads to the formation of copper sulphide in insulating oils. In general, all of these techniques involve the use of costly equipment and require skilled personnel to conduct the tests. In addition, these techniques are time-consuming because the oil samples need to be sent to an external laboratory for analysis. To date, there are no studies concerning the application of ultraviolet-visible (UV–vis) spectroscopy, direct current (DC) conductivity measurements, interdigitated capacitive sensors (IDCs), and thin film sacrificial copper strips sensors to detect and monitor the progression of sulphur corrosion in insulating oils, which forms the motivation of this research. Therefore, new experimental techniques have been developed and assessed at the Tony Davies High Voltage Laboratory, University of Southampton, in order to address these issues.

1.3 RESEARCH OBJECTIVES

This research is focused on the development of a feasible method that is able to identify if the transformer is at risk of catastrophic failure due to the presence of corrosive compounds in the insulating oil. The method is developed to measure the corrosive sulphur content of the insulating oil in order to produce an online acquisition system that will allow changes of elemental sulphur concentration to be measured in real-time in in-service plant. The overall aim is to develop a prognostic tool that can be widely used in electrical transmission networks to minimise the risk of unexpected outages. To achieve this aim, this research is divided into three sub-objectives as follows:

Sub-objective 1:

- (a) To study the feasibility of the BS EN 62535 standard test method in analysing copper surface subjected to sulphur corrosion, where the surfaces are aged in mineral oil with different dibenzyl disulphide (DBDS) concentrations.
- (b) To monitor the progression of sulphur corrosion on the copper surface by scanning electron microscopy–energy dispersive X-ray spectroscopy (SEM–EDX).

Sub-objective 2:

- (a) To investigate the feasibility of UV–vis spectroscopy, DC conductivity measurements, and IDCs in tracking the progression of sulphur corrosion due the corrosive by-products as a result of the breakdown of DBDS.

Sub-objective 3

- (a) To develop a regression model based on the two-level (2^2) factorial design in order to estimate the transformation resistance values of the thin film sacrificial copper strips sensors as a function of the area and thickness.
- (b) To investigate the characteristics of the thin film sacrificial copper strips sensors in the presence of corrosive by-products as result of the breakdown of DBDS and elemental sulphur.

- (c) To quantify the elemental sulphur concentration based on the changes in the electrical resistance of the thin film sacrificial copper strip sensors at different temperature range over a period of time.

1.4 SIGNIFICANT CONTRIBUTIONS OF THE RESEARCH

Condition-based monitoring is more important compared with preventive (schedule) monitoring because aged in-service power transformers require frequent inspections to reduce the risk of catastrophic failure. Condition-based monitoring is also more preferable because power utility companies can prioritise on maintaining their in-service transformers rather than replacing the aged transformers with new ones, which is rather costly. Thus, there is a need to develop a practical, reliable and cost-effective condition-based monitoring techniques to detect the progression of sulphur corrosion in insulating oils. The contributions of this research are detailed in Figures 1-2 and 1-3 and are summarised as follows:

- 1) Based on the experimental results, it is found that UV–vis spectroscopy is not a suitable tool to track the progression of sulphur corrosion in insulating oils because it is difficult to distinguish the UV–vis spectra of the aged oil samples, particularly at low DBDS concentrations. Furthermore, the presence of water contributes to changes in the oil capacitance (for measurements using IDCs) and oil conductivity (for DC conductivity measurements), which complicates the interpretation of results.
- 2) A novel technique based on thin film sacrificial copper strips has been developed in this research. The thin film copper strips generate resistance values relative to the level of oil corrosiveness. Compared with the current practice (which involves visually comparing the discolouration of the copper surface with a standard reference colour (i.e. ASTM D130-12 [24]), this technique minimises the possibility of misinterpreting the results because it is based on quantitative analysis. In addition, the technique involves the use of economical sensors and does not require skilled personnel to conduct the tests. The major benefit of the proposed technique over existing techniques is that it could be used to continuously monitor changes of the elemental sulphur content on site in real-time, which will facilitate timely remedial actions.

- 3) The 2^2 factorial design is proposed in this research, which is suitable to investigate the significant effect of two independent variables (area and thickness) on the transformation resistance values of the thin film sacrificial copper strip sensors. This approach significantly reduces the number of test runs and ultimately saves manufacturing time and costs compared with the one-factor-at-a-time (OFAT) approach. The development of a regression model in order to estimate the transformation resistance values of the thin film sacrificial copper strip sensors as a function of the area and thickness has significantly aided the sensor design process.

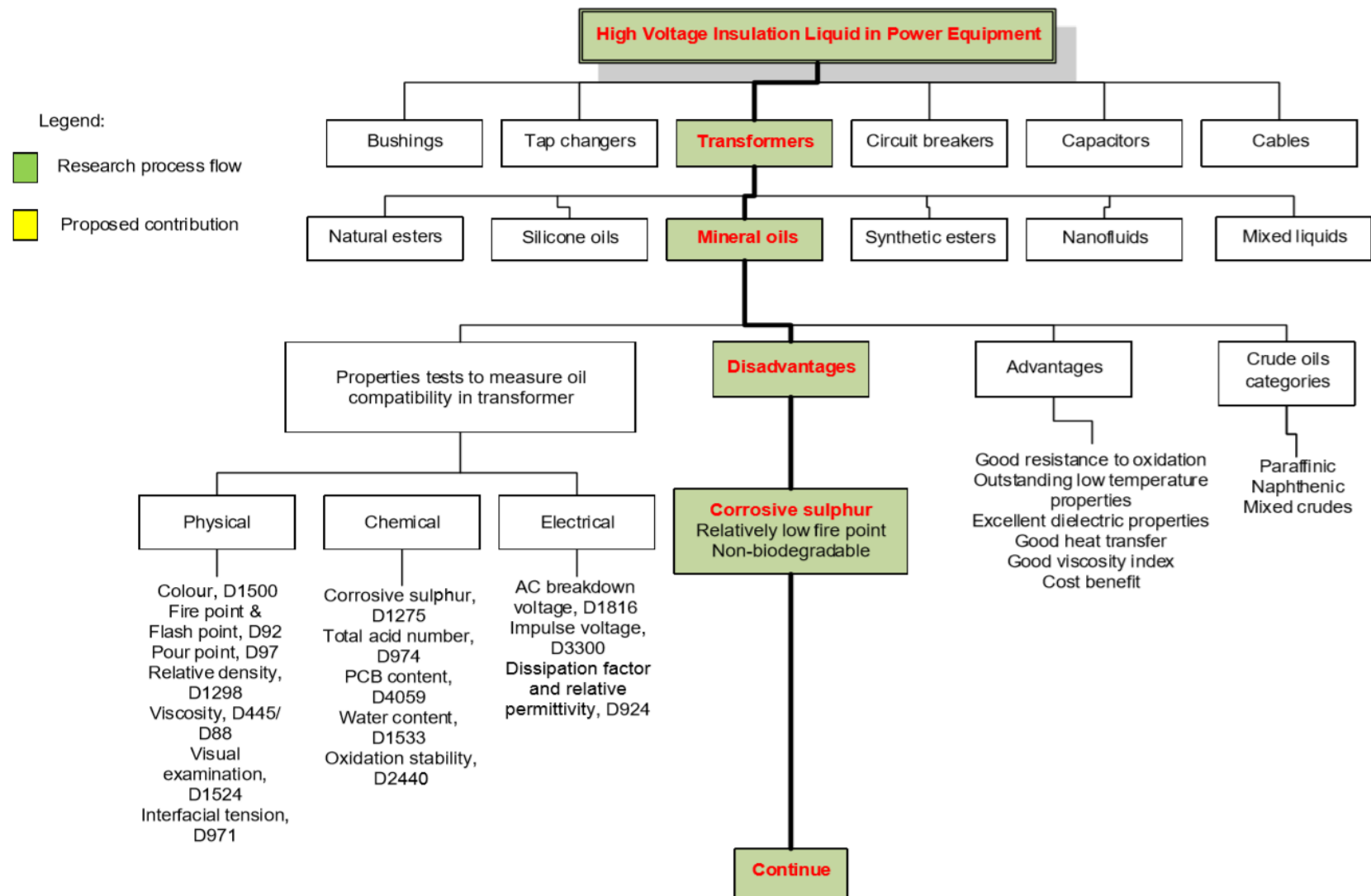


Figure 1-2. The roadmap of research contributions.

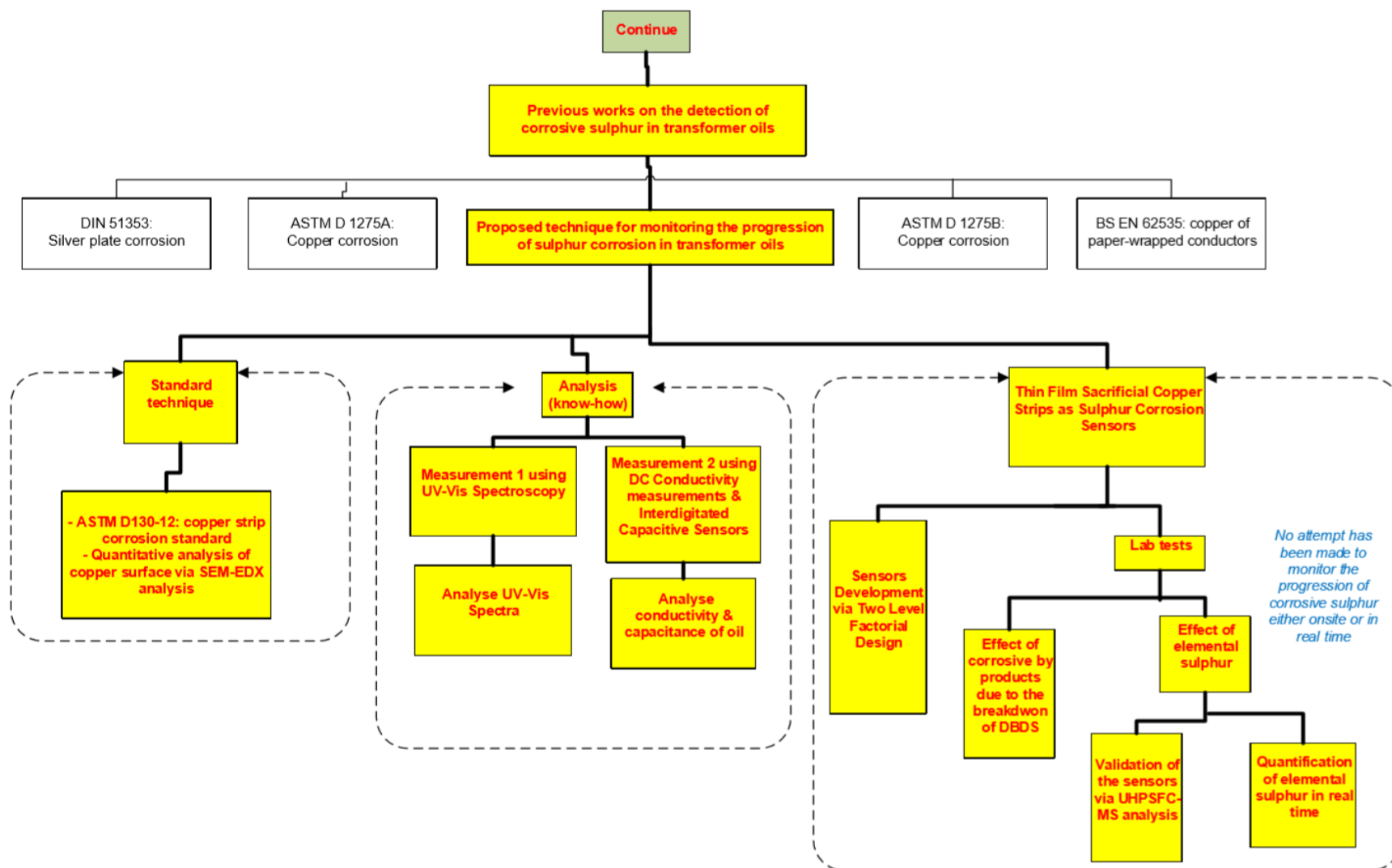


Figure 1-3. The roadmap of research contributions (continued).

1.5 ORGANISATION OF THE THESIS

There are six chapters presented in this thesis, including this chapter. A brief background on power transformers and their insulation systems is first presented, followed by the problem statement and research motivation. The objectives and significant contributions of this research are also presented in this chapter.

Chapter 2 is focused on in-depth review of sulphur corrosion, which includes a description of sulphur compounds and theoretical background on the formation of copper sulphide. Emphasis is given on the detection and condition monitoring of corrosive sulphur because this is the main focus of this research. Studies pertaining to the mitigation techniques of corrosive sulphur in insulating oils are also reviewed in this chapter.

Chapter 3 is focused on the identification of corrosive oil using the standard test method and UV-vis spectroscopy. The sample preparation, experimental set-up, and experimental procedure are presented and discussed in detail. The qualitative results obtained based on the BS EN 62535 standard test method as well as quantitative results obtained from SEM-EDX spectroscopy are also described.

Chapter 4 is focused on the DC conductivity measurements used to assess the corrosivity levels of the insulating oil samples. This is followed by the development of the IDCs as a feasible alternative for sulphur corrosion detection. The fundamental principles, previous applications, experimental set-up, experimental procedure, and results are presented and discussed. Since the presence of water affects the measurements, the equipment, experimental set-up, and experimental procedure for water content measurements are also presented in brief.

Chapter 5 presents the key findings of this research. The feasibility and reliability of thin film sacrificial copper strip sensors in detecting and monitoring the corrosive by-products of DBDS is discussed in detail. In addition, the quantification of elemental sulphur concentration based on the changes in the electrical resistance of the thin film sacrificial copper strip sensors at different temperature range over a period of time is further explained. Ultra high performance supercritical fluid chromatography-mass spectrometry (UHPSFC-

MS) is used to evaluate the relationship between the changes in electrical resistance of the thin film sacrificial copper strip sensors and changes in elemental sulphur concentrations, which is further explained in this chapter. The possibility of using the 2^2 factorial design to develop the regression model is also discussed. The regression model can be used to estimate the transformation resistance values of the thin film sacrificial copper strip sensors as a function of the area and thickness.

Chapter 6 outlines the conclusions drawn based on the research works presented from Chapter 3 to Chapter 5. The recommendations for future work are also presented. The appendices contain published papers, obtained measurement data and images of sensor surfaces as well as reports submitted to National Grid plc (UK) as part of the TOPICSII project.

2 MONITORING OF OIL-FILLED POWER TRANSFORMER DUE TO SULPHUR CORROSION

2.1 INTRODUCTION

This chapter is structured into subsections to describe relevant literature on sulphur corrosion phenomena occurred in oil-filled power transformers. Initially, an overview regarding the types and reasons for monitoring the insulating oils is reported. Before introducing into the main subject (corrosive sulphur), the description of mineral oil is firstly explained. This is followed by a review on the terminologies and general background of sulphur corrosion. The types of sulphur compounds exist in the transformer insulating oils are also reviewed, followed by the sulphur corrosion mechanism, which includes a theoretical background on the formation of copper sulphide. The main issues associated with this research, particularly those about the detection and condition monitoring of corrosive sulphur are discussed in detail. This subsection covers a broad technique to appreciate the concept and practicality of implementing the novel detection technique presented in the following chapters. The final section of this chapter presents the countermeasures applied by the industry in order to mitigate the corrosive sulphur issues.

2.2 MONITORING THE INSULATING OIL: TYPES AND REASONS

Power transformer assessment involves in monitoring insulating oil because insulating oils are the major dielectric system, easily accessible and carry valuable information on the health of power transformer because it comprises degradation products from oil and paper insulation. There are two types of power transformer monitoring, namely schedule-based (preventive) monitoring and condition-based (predictive) monitoring. Schedule-based maintenance is carried out on a running hour basis. However, as power transformer failures may occur before the scheduled maintenance takes place, condition-based monitoring

(particularly on the insulating oil) is a favourable technique. Power transformer condition-based monitoring helps in coordinating the maintenance schedule and improves transformer reliability that will ultimately prolong the operational life. Due to this reason, utilities and industry have switched their way of maintaining their power transformer from schedule-based to condition-based monitoring [25].

Nowadays, there is a significant research associated with transformer online condition monitoring. Additionally, the development of sensors applied for online condition monitoring has gained much attention. Compared to offline condition monitoring, online condition monitoring provides instantaneous information regarding the current condition of the transformer. This technique minimises unnecessary shutdowns which save money, time, and manpower. Currently, dissolved gas analysis (DGA) plays an important role as an online condition monitoring tool for the detection of transformer faults [26] such as local overheating, partial discharge and arcing based on the concentration of gases such as methane (CH_4), acetylene (C_2H_2), ethylene (C_2H_4), ethane (C_2H_6), carbon monoxide, carbon dioxide, oxygen, hydrogen, and nitrogen [27] that are formed due to the chemical decomposition of both oil and paper insulation.

Practically, a power transformer is expected to be operated up to 60 years with the aid of appropriate routine maintenance [25]. However, power transformer failure can occur before end of nominal life and it has been reported by the International Association of Engineering Insurers that between 1997 and 2001, the US incurred a total loss of over 286 million US dollars due to early power transformer failures. The largest power transformer losses rated at 25 MVA occurred in 2000 with a business interruption of over 80 million US dollars [28]. It shall be noted that insulation failure constitutes to the main cause of power transformer failures, as shown in Table 2-1. Four main factors corresponded for those insulation failures namely heat, moisture, oxidation, and acidity. Due to insulation failure, the lifespan of a power transformer was reduced by approximately 40 years compared to its expected nominal life. Approximately half of the total cost was due to insulation failure, even though the number of cases was only a quarter of the total cases. Hence, the need for assessing the condition of a power transformer fleet is ultimately essential to avoid any faults occurrence that leads to an unplanned outage, a risky and costly event.

Table 2-1. Type of power transformer failures [28].

Type of failure	Contribution factors	Number of cases	Cost (US Dollar)
Insulation failure	Heat, moisture, oxidation, acidity	24	149,967,277
Design/material/workmanship	Foreign object left in the tank, poor brazing (metal joining)	22	64,696,051
Oil contamination	Sludge	4	11,836,367
Overloading	Load exceed the capacity written on nameplate	5	8,568,768
Fire/explosion		3	8,045,771
Line surge	Line faults/flashovers	4	4,959,691
Improper maintenance/operation	Accumulation of dirt in oil / corrosion	5	3,518,783
Flood	Man-made/natural caused flood	2	2,240,198
Loose connection	Improper bolt connection	6	2,186,725
Lightning	Lightning surge	3	657,935
Moisture	Pipe leak/roof leak/leaking bushing or fitting	1	175,000
Unknown		15	29,776,245
Total		94	286,628,811

2.3 MINERAL OILS

Different types of insulating oils including mineral oil, silicone based oil, natural ester, and synthetic ester have their benefits and drawbacks, however, carry similarities, and serve as a coolant and electrical insulator to ensure reliable operation of high voltage equipment under normal operating conditions [1]. Since the focus of this research was to monitor the progression of sulphur corrosion in oil-filled power transformers, the discussion on insulating liquid in this thesis concentrates on mineral oils only.

Mineral oil-based dielectric liquids derived from refined crude petroleum were firstly used as insulating media in oil-filled power transformers [29]. Crude oil mainly consists of three hydrocarbons fractions (Figure 2-1). However, it contains a wide range of impurity species; in particular molecules that contain sulphur (hydrogen sulphide, elemental sulphur,

mercaptans, alkyl sulphides, and thiophenes), oxygen (naphthenic acids), and nitrogen (frequently encountered in asphaltenes), as well as metal species and aromatic compounds [1].

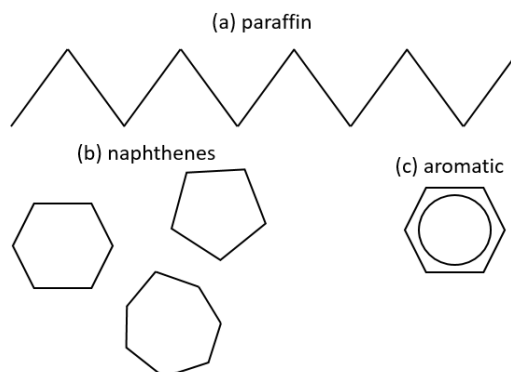


Figure 2-1. Mineral oil mainly consists of three hydrocarbon compounds: (a) paraffin, (b) naphthenes, and (c) aromatic.

Crude oil is required to undergo a refinery process for changing it into refined oil with desired physicochemical properties, thus fulfil the requirements of a specific application as well as to remove impurities [1]. Refined mineral oils are the results of substantively complicated blends based on a mixture of over 3000 different hydrocarbons, predominantly paraffinic and naphthenic compounds with minor concentrations of aromatic compounds [2]. Due to this reason, the characteristic of the oil is determined principally by either naphthenic or paraffinic compounds. The presence of optimum concentrations of aromatic compounds (between 5 % and 10 %) in the oil contributes to a good oxidation resistance as well as preserving thermal properties to be relatively close to either purely paraffinic or naphthenic oil [30].

Paraffinic based mineral oil was firstly used; however, the industry moved to using naphthenic oils from 1925 [2]. Compared to paraffinic crude oils, naphthenic crude oils composed of relatively low paraffinic wax content [1] and therefore in a low-temperature environment, naphthenic crude oils are relatively difficult to crystallise because of their high pour point (pour point is the flowing capability of a liquid at low temperature [31]). Due to this reason, naphthenic- based mineral oils are preferable to be widely used especially in any extreme cool climate places, allowing power transformers to work under normal conditions without risk of liquid insulation failure.

It is essential to have an insulating oil that provides excellent heat dissipation when there is a rise in operating temperature of the transformer created by several factors such as a high load demand and extremely hot weather conditions. When the transformer is operating at high-temperatures, local overheating of the transformer winding can occur, which may lead to catastrophic transformer failure. In this case, naphthenic based mineral oil carries an advantage of having lower kinematic viscosity [32]. A low kinematic viscosity produces a higher circulation flow speed of the insulating oils improving the heat dissipation of the insulating oil.

The degradation of oil-paper dielectrics is subjected to electrical, mechanical, thermal and electrical stresses, yielding transformer failures. In prolonging the lifespan of a power transformer, naphthenic based mineral oils are preferable due to their relatively good solubility which aids in dissolving any oil sludge produced from those stresses [32]. It is worth noting that the after-effect of oil sludge is disastrous because it increases the operating temperature of power transformer caused by blockages of transformer cooling pipes/fins as well as increasing abrasion of cellulose surfaces by circulating components of the sludge.

Despite its good properties, naphthenic crude oils have several drawbacks. Naphthenic crude oils is limited by its availability because it is considered as a rare resource since less than 5 % of the world's crude oils are naphthenic [33]. Naphthenic based mineral oils have less oxidation stability compared to paraffinic based mineral oils which may reduce the lifespan of power transformers. The poor resistance to oxygen causes the accumulation of acids in the oil and leads to the formation of sludge, reducing the oil dielectric strength [34]. Besides, the presence of oxygen in insulating oils produces carboxylic acids that eventually degrade the paper insulation.

An excellent insulating oil should have the following characteristics, namely; high breakdown voltage (minimum: 70 kV), high level of flash point (minimum: 135 °C), low viscosity (maximum: 12 mm²/s at 40 °C), and low pour point (maximum: – 40 °C). Other characteristics that should be taken into consideration are good impulse strength (minimum: 145 kV at 25 °C), and non-toxicity towards the surrounding environment. It is indeed impossible to have the insulating oils that meet all the properties mentioned; therefore, a balanced compromise between the oil properties is essential.

Up to present, mineral oils are still being used in power transformers due to their cost benefits, good ageing characteristics, good dielectric strength, low viscosities, good oxidation stability, as well as due to the availability of petroleum resources [2]. In the absence of any other issues, mineral oils enable the operation of transformers to be relatively constant between 60 °C and 80 °C [35]. However, the performance of mineral oils is far from optimum in terms of the flash and fire points when the operating temperature is 130 °C or above [36]. Compared to vegetable oils, mineral oil is non-biodegradable, toxic and non-environmentally friendly, making it hazardous towards aquatic life in onshore and offshore environments [37].

Several tests for in-service mineral oils have been produced (Table 2-2) to ensure the ability of the transformer to continue functioning appropriately as well as to minimise any chances of failures. It can be seen that corrosive sulphur needs a special investigation which reveals a critical need of monitoring the sulphur corrosion in power transformer. Therefore, the following subsections will focus mainly on this matter.

Table 2-2. Mineral oil tests for in-service transformer [31].

Group	Parameter	
I: Routine tests	Colour & appearance	Acidity
	Breakdown voltage	Dielectric dissipation factor
	Water content	Inhibitor content
II: Complementary tests	Sediment sludge	Particles
	Interfacial tension	
III: Special investigation tests	Oxidation stability	Viscosity
	Flash point	Polychlorinated biphenyls
	Compatibility	Corrosive sulphur
	Pour point	DBDS content
	Density	Passivator content

2.4 SULPHUR CORROSION: TERMINOLOGIES AND GENERAL BACKGROUND

Corrosion is defined as “the deterioration of a material, usually a metal, that results from a reaction with its environment” [38]. According to the ASTM D2864 – Standard Terminology Relating to Electrical Insulating Liquids and Gases, corrosive sulphur is defined as

“elemental sulphur and thermally unstable sulphur compounds in electrical insulation oil that can cause corrosion of certain transformer metals such as copper and silver” [39]. Perceiving that corrosion is a deterioration process of metal, the corrosiveness level is significantly associated with the initial condition of both corrosive species and the metal. It shall be noted that the presence of other variables such as inhibitors and catalysts responsible for the corrosion process are generally assumed.

The sulphur corrosion issues begin in the middle of 20th century whereby the method of detecting corrosive sulphur species in transformer oils known as ASTM Committee D 27 (currently known as ASTM D 1275) was first documented in 1948 [40]. However, this issue gained great attention from the utilities since the beginning of the 21st century [14] because there has been a significant increase in the number of cases of oil-filled transformer failures related to sulphur corrosion [41]. A report published by CIGRE [10] highlights that even though transformers are designed following the established industrial standards without major manufacturing defects, transformer failures are still a major issue. Failure still occurs although the transformers are operated within the range of loads and temperatures specified by industrial standards. It is suspected that the type of oil used in some transformers may create new corrosive compounds [10]. This is evident from the unfavourable outcomes observed when the transformers were tested according to the BS EN 62535 standard corrosion test [42]. After some thought, it was concluded that the sulphur corrosion issue was due to the insulating oil itself or the addition of newly formulated additives into the insulating oils after installation which may create a corrosive environment [10].

Historically, the amount of sulphur in mineral oils has reduced over the last two decades due to advances in the petrochemical industry [43]. Figure 2-2 shows the decrease in the total sulphur content of mineral oils from 1964 to 2008 [18]. It can be seen that the total sulphur content drops significantly from the beginning of the 1990s. However, Figure 2-3 shows a contradictory pattern compared with Figure 2-2. Approximately 50 % of the transformers installed during the 1990s tested positive for corrosive sulphur. The increasing trend in corrosive oil is may be due to changes in the transformer design (an increase of 10 K in their average winding temperature) in the 1980s [44]. Hence, the decreasing trend shown in Figure 2-2 indicates that the refinery process only reduces the sulphur content of mineral oils

and this does not reduce the occurrence of corrosive sulphur in oils. As a result, in the past two decades, extensive research have been carried out trying to identify potentially corrosive compounds, understand the sulphur corrosion mechanism and the formation of copper sulphide, and develop effective methods to sense and track the corrosive sulphur species in insulating oils which will be further reviewed in Section 2.5–2.7.

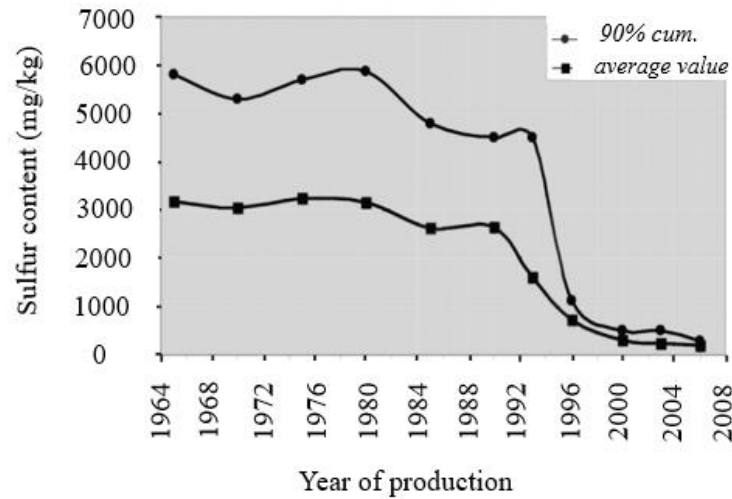


Figure 2-2. Decreasing trend of the total sulphur content of mineral oils used in transformer or shunt reactors from 1964 to 2008 [18].

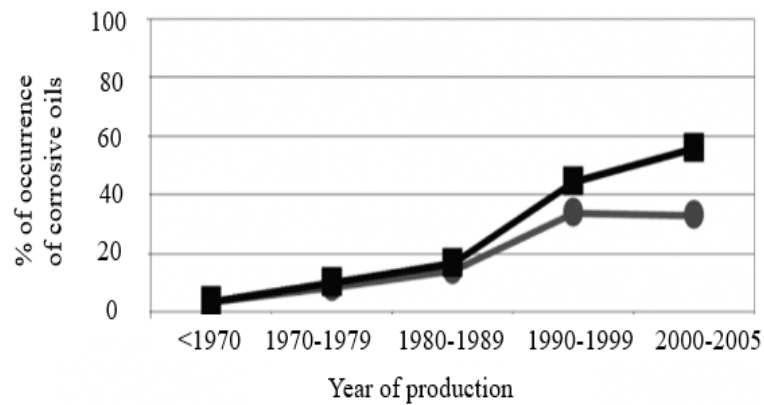


Figure 2-3. Occurrence of corrosive oils for naphthenic oils from 1970 to 2005 according to ASTM D1275A. Note that the circle data markers indicate normal operation whereas the square data markers indicate a 48-h extension [18].

2.5 SULPHUR COMPOUNDS

Insulating oils typically contain 0.001–0.5 % of sulphur [17]. Sulphur can be found in the mineral oil in elemental form or in organosulphur molecules, namely thiophenes, disulphides, polysulphides, dialkyl sulphides (thioethers), and mercaptans (thiols). Each compound has its own unique reaction rate with copper, which ultimately forms copper sulphide species, as solid corrosion products or complexes, depending upon the concentration of the compounds, copper surface condition, temperature, and ageing time [17]. The corrosive levels of sulphur are ranked from elemental sulphur > mercaptans > sulphides > disulphides > thiophenes [45]. Hence, elemental sulphur is considered as the most reactive compound with copper, followed by reactive mercaptans. Meanwhile, thiophenes are non-reactive sulphur compounds, whereas disulphides are relatively stable. Nevertheless, disulphides can degrade into benzyl mercaptans, resulting in more corrosive species [46] as illustrated in Figure 2-4. It can be seen that heat causes the linkage of disulphides to be cleaved, which in turn forms the reactive benzyl mercaptan. A further increase in heat results in the formation of ethyl benzene and copper sulphide. Lewand et al. [46] reported that the degradation of aromatic disulphide which is known as DBDS (molecular formula of $C_{14}H_{14}S_2$) happened when the insulating oils were thermally aged at a low temperature of 80 °C within only 2 months. It shall be noted that under high oxygen concentrations, thermal decomposition of DBDS or mercaptans could lead to the formation of the most corrosive sulphur compound namely elemental sulphur [47].

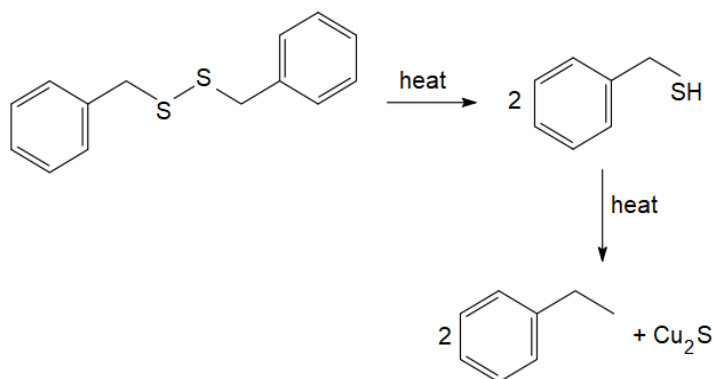


Figure 2-4. Degradation of a stable DBDS into reactive benzyl mercaptan and further into ethyl benzene and copper sulphide [30].

Researchers and utilities agree that some corrosive sulphur compounds originate from crude oils, whereas others may have been introduced during the manufacturing process [48]. Unsophisticated oil manufacturing technology and refining processes [49], as well as the replenishment of additives such as antioxidants used to prolong the oxidation stability [18] of mineral oils are the two aspects closely related to the manufacturing process. Sulphides and disulphides are the two types of sulphur compounds commonly used as secondary oil antioxidants [48] to protect against the oxygen ingested during transformer operation [44]. DBDS is one of the common disulphides that is used in power transformers as an antioxidant in transformer insulating oils. At a temperature of less than 150 °C, DBDS exhibits a good oil oxidation inhibitory characteristic by preventing any cleaving of S–S bond linkage thus, reducing hydroperoxides levels [49]. Increasing the level of peroxides results in the increased amount of aldehyde, which in turn degrades the paper insulation. However, eliminating this type of sulphur that is already present in the oil may reduce oil oxidation stability and leads to an increase in oil viscosity and accelerates the sludge growth.

In oil-filled power transformers, few materials including gaskets and glues contain sulphur [41]. While only a few sulphur compounds are corrosive, the presence of these materials makes several contributions to the sulphur corrosion phenomenon particularly when the transformer is operating at higher temperatures which may transform the stable sulphur species into the reactive sulphur [40]. It is known that three materials are considered to be the primary causes of sulphur corrosion reaction, namely oil, paper, and copper [50].

2.6 SULPHUR CORROSION MECHANISM

The mechanism of sulphur corrosion in insulating oils is not only due to a single corrosive sulphur compound — rather, there are tens to hundreds of sulphur compounds in mineral oils [46] which may be among the contributing factors. Sulphur corrosion is initiated by the chemical reaction between conductors (i.e. copper or silver) and corrosive or potentially corrosive insulating oils, even though the power transformers are operating at their nominal condition, which in turn forms copper sulphide [51]. It is understood that the dissolution of

copper in the insulating oil and the formation of a copper complex, which is oil soluble, contributes to the copper sulphide formation [48], [52].

Some extensive models have been proposed to explain the formation of copper sulphide in insulating oils and paper insulation. A model developed in [52] proposes a formation of copper sulphide via two-step process whereby the first step involves the coordination of oil-soluble copper complexes which consist of copper and particulate disulphides (i.e. DBDS). The dissolution of oil-soluble complexes is then diffused via the insulating oil, which in turn absorbed on the paper insulation. The next step involves the decomposition of the oil-soluble complexes into copper sulphide deposits and another formation of complexes by-products, namely dibenzyl sulphide (DBS) and bibenzyl (BiBZ). This model was developed based on an experimental investigation which shows that at a high temperature of 150 °C, the copper strip weight increased because the decomposition of copper sulphide on copper strips was more pronounced than the formation complexes by-products in insulating oils. This whole chemical process is visualised diagrammatically in Figure 2-5.

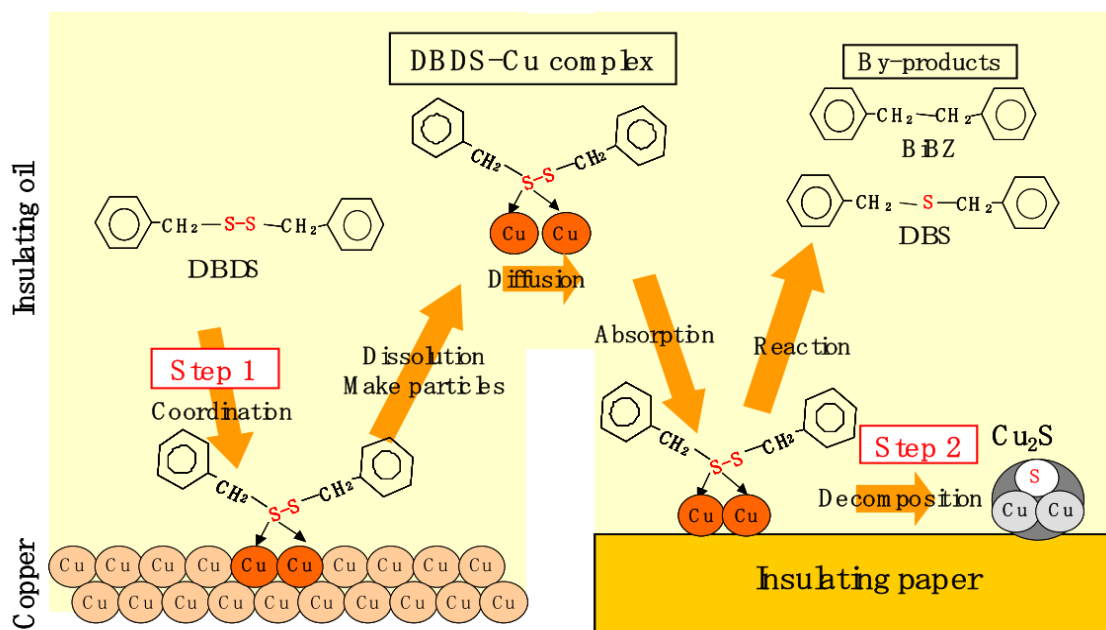


Figure 2-5. Formation of copper sulphide deposits [51].

Recently, in 2014, Facciotti et al. [43] proposed two concurrent mechanisms of paper insulation contaminated by copper sulphide, based on the experimental investigations employing environmental SEM (penetration range: 0.5–5 μm) and X-ray photoelectron spectroscopy (XPS) (penetration range: 10–20 nm). As illustrated in Figure 2-6, the first mechanism involves a high rate reaction, which likely results in a higher amount of copper sulphide. DBDS reacts with copper to form a layer of copper sulphide, where the stoichiometric ratio is $\sim 2:1$. The copper sulphide layer eventually displaces from copper surface once the interaction with the bulk surface breaks. This reaction accelerates in the presence of oxygen. The paper insulation retains most of the copper sulphide particles, which causes a deposition on its surface. However, the second mechanism is slower compared with the first mechanism, and it is primarily responsible for the bulk contamination of the paper insulation. DBDS reacts with copper, creating complexes which diffuse from the copper surface. It is expected that the concentration profile will decrease exponentially with an increase in distance from the copper surface. These complexes eventually break down to form copper sulphide and other by-products. The probability that the copper sulphide deposits formed also decreases exponentially when the distance from the copper surface is increases.

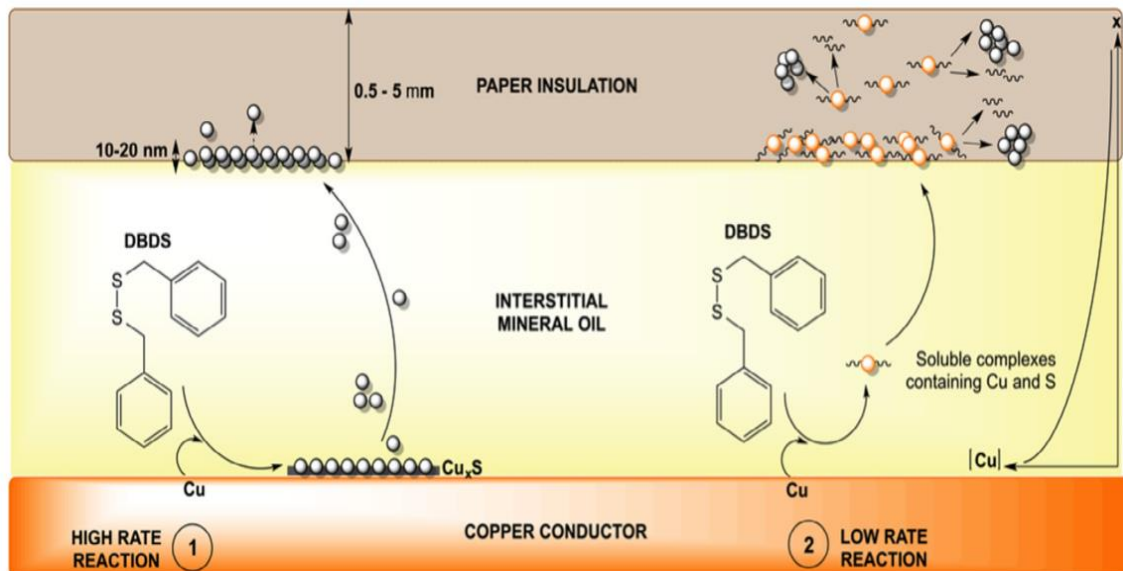


Figure 2-6. Schematic diagram of two concurrent mechanisms for:
 (1) surface contamination and (2) bulk contamination of the paper insulation proposed by Facciotti et al. [43].

CIGRE, through their Working Group A2.40, proposed a mechanism on the formation, migration, and deposition of copper sulphide on paper insulation in 2015 [9]. They gave a detailed account of the chemical reaction associated with the formation of copper sulphide in insulating oils, as shown in Figure 2-7. The formation of copper sulphide begins with the dissolution of copper in the insulating oil, followed by the adsorption of copper species on the paper insulation. Lastly, the reaction between copper and sulphur takes place, resulting in the deposition of copper sulphide on the paper insulation.

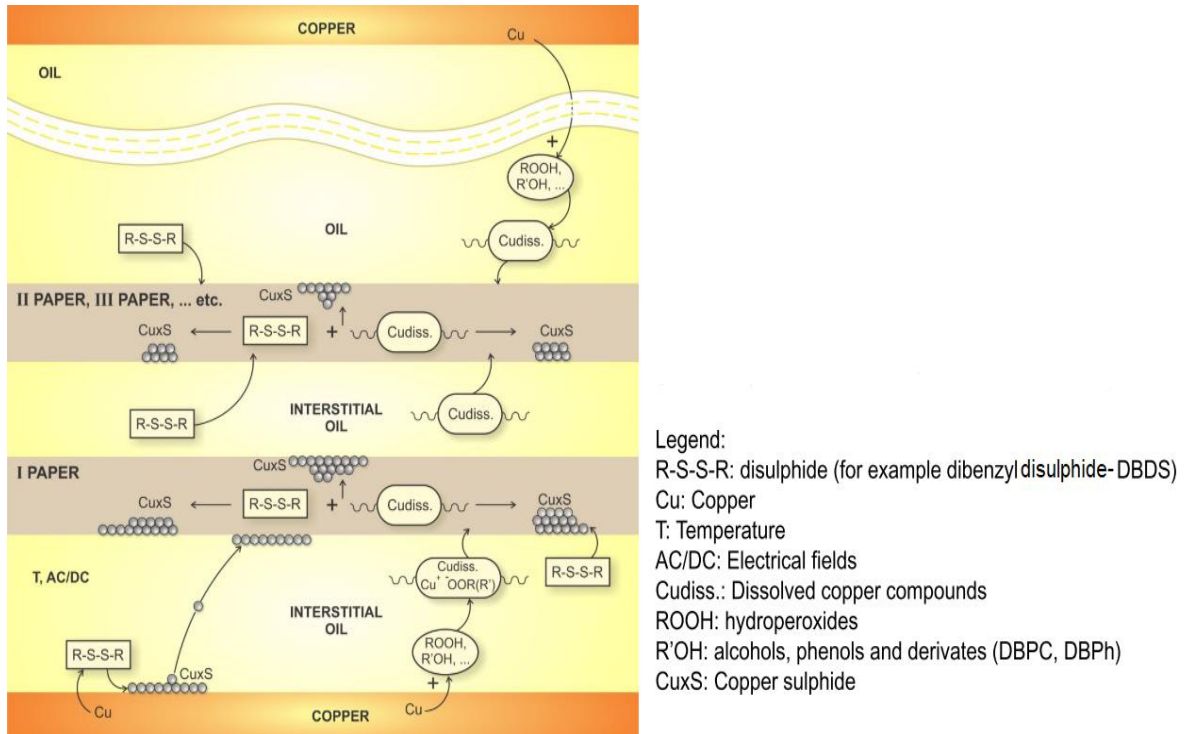


Figure 2-7. Mechanism of copper sulphide formation on insulation paper proposed by the CIGRE [9].

The latest experimental evidence obtained from X-ray diffraction analysis in 2016 [53] shows that the formation of copper sulphide was due to the thermal degradation of copper thiolate complexes. It can be seen from Figure 2-8 that the formation of copper thiolate complexes was due to the degradation products of DBDS, including DBS and benzyl mercaptan. It has been suggested that the formation of copper thiolate complexes is initiated by the heterogeneous reaction between copper oxide and benzyl mercaptan.

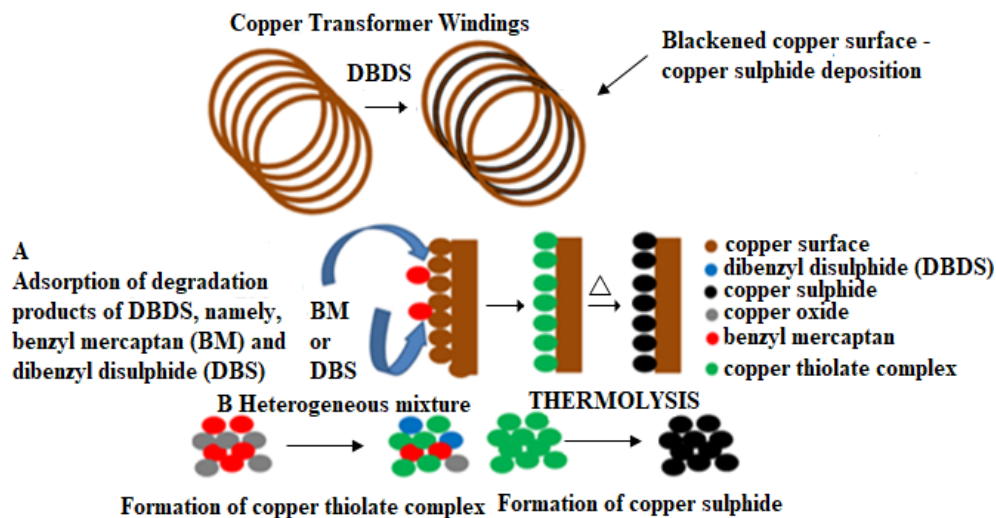


Figure 2-8. Alternative pathway for the formation of copper thiolate complexes resulting in the deposition of copper sulphide on the copper conductor [53].

The presence of DBDS in the insulating oils was identified as the main cause of corrosive sulphur-related faults [16], [17] and this type of compound is indeed adequate in encouraging the deposition of copper sulphide [46]. An experimental investigation demonstrated that the presence of extremely low DBDS concentration of 1 mg kg^{-1} was sufficient to render a noticeable deposition of copper sulphide on the paper insulation [54]. Instead of DBDS, other type of disulphides, mercaptans, and elemental sulphur, may also contribute to the formation of copper sulphide [10], [17], [48], [52], [55]. Under high oxygen concentrations, thermal decomposition of DBDS or mercaptans could lead to the formation of the most corrosive sulphur compound — elemental sulphur [47].

A report provided by Doble Engineering USA [46] demonstrated that there was an unambiguous relationship between the DBDS concentrations and oils corrosivity level. According to this report, the transformer insulating oils that were suffered from the corrosive sulphur-related failures were examined to have high DBDS concentrations. In addition, there was a reduction trend in the DBDS concentrations over time found in the highly loaded power transformers. The reduction in DBDS concentrations provides a clear evidence that DBDS was degraded and formed corrosive by-products, as depicted in Figure 2-4. Following this, the DBDS presence in insulating oils from three in-service shunt reactors was examined (Figure 2-9) [18]. After 18 months of operation, there was a decrease in DBDS

concentrations for Reactors A, B, and C. However, no significant changes occurred in the Spare Reactor (no load current). This study supports the empirical theory given in Figure 2-9 whereby the presence of heat due to a high operating temperature of Reactors A, B, and C causes the degradation of DBDS into other corrosive by-products, which in turn reduces the concentration of DBDS.

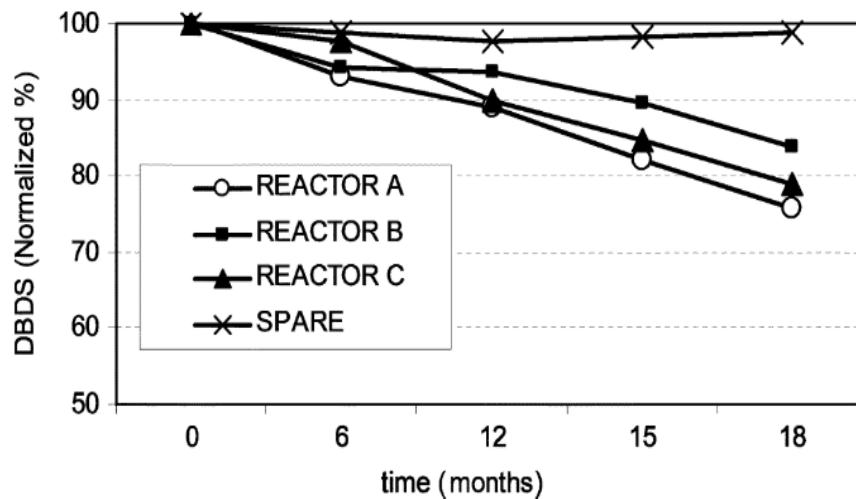


Figure 2-9. The decreasing trend in DBDS concentrations for three in-service shunt reactors. It shall be noted that the spare shunt reactor consists of no load [18].

Although the breakdown of DBDS is believed to play a major role in the sulphur corrosion process, insulating oils are still found to be corrosive in the absence of DBDS [51], hence indicating that other sulphur species can induce a corrosive environment. In addition, a study indicated that insulating oils exhibit a corrosive behaviour, regardless it contains DBDS or not [18].

The formation and deposition of copper sulphide in the insulation system are devastating. Copper sulphide could move (either in the form of dissolved or suspended) into the bulk of insulating oils [56] which worsens the dielectric properties of the insulating oils. The effect of copper dissolved in insulating oils is even worse than that of insulating oils that contain suspended copper particles [57]. The conductive copper sulphide may deposit on either copper conductor [56] or paper insulation [58], and may diffuse into the porous cellulose fibre that causes the paper insulation to be conductive [16]. It is interesting to note that the

presence of visible copper sulphide contaminant on oil-impregnated Kraft paper caused an increase in $\tan \delta$ value from 0.003 to greater than 1 [17], which indicates that copper sulphide contaminants contributes to an increase in dielectric losses of paper insulation which may leads to the power transformer failure. The deposition of copper sulphide on copper surfaces diminishes the amount of copper in the transformer parts (i.e. winding and tap changer), increasing the rate of copper losses which degrades transformer electrical properties [41].

2.7 DETECTION AND CONDITION MONITORING OF CORROSIVE SULPHUR

The detection of corrosive sulphur species is initially carried out by manufacturers of insulating oils in order to ensure that the oils comply with the relevant industrial standards. Following this, detection of corrosive sulphur species is carried out by the transformer system operators who conduct most of the oil quality monitoring processes [49].

At present, there are four different standard corrosion tests, as shown in Table 2-3. All of these standard tests are based on visual comparison between the discolouration of the copper surface (non-corrosive/suspected corrosive/corrosive) and the ASTM copper strip corrosion standard, as shown in Figure 2-10. These techniques are fairly subjective as it depends on the qualitative analysis, resulting in numerous drawbacks: (a) difficulty in getting the same colour of new copper strip when compared to the ASTM copper strip corrosion standard, (b) people see colour in their own way and therefore different operators might give diverse ratings of the same strip, (c) the comparison between discolouration of the copper surface and the ASTM copper strip corrosion standard is highly subjected to the lighting rate, (d) the lithograph has a nonlinear response progression (for example, with reference to Figure 2-10, 2d entirely differs from 2c and 3a is only slightly more tarnished than 1b), (e) the strips must be rated immediately after being removed from the fluid, which is occasionally problematic if the test is conducted on-site, (f) some of the colour descriptors used on the lithograph, such as claret, that are rarely used and may be confusing, and (g) the results of the test are very dependent on strip preparation.

Table 2-3. Standard test methods used to determine corrosivity of oils

(*Used in this research work, as described in Chapter 3)

Method	Material	Description (Oil/Metal/Paper)	Temperature (°C)	Time (h)	Oxygen	Remarks
DIN 51353	Ag	100 mL/1600 mm ² /-	100	18	Absent	Silver plate corrosion
ASTM D1275A	Cu	250 mL/300 mm ² /-	140	19	Absent	Copper corrosion
ASTM D1275B	Cu	250 mL/300 mm ² /-	150	48	Absent	Copper corrosion
*BS EN 62535	Cu	15 mL/540 mm ² /540 mm ²	150	72	Limited	Corrosion of paper-wrapped conductors



Figure 2-10. ASTM copper strip corrosion standard [24].

The DIN 51353, ASTM D1275A and ASTM D1275B standard corrosion tests involve immersing a metal (usually copper or silver) in the insulating oil following specific test conditions, as shown in Table 2-3. These standard tests are not reliable since it is impossible to determine the deposition of copper sulphide on the paper insulation. Hence, a new standard test (BS EN 62535) [42] was developed by the CIGRE to address this issue. This test involves immersing a copper strip (length: 30 mm) in 15 mL of insulating oil. Following this, the copper strip is placed inside a vial, which is then aged at a constant temperature of

150 °C for 72 h. There are two types of test in this case, which are bare copper strip and paper-wrapped copper strip. The paper-wrapped copper test, also known as covered conductor deposition (CCD) [18], is designed to determine the ability of the insulating oil to form copper sulphide deposits on the paper insulation. For this reason, the CCD test is closely interlinked with a large number of studies because it is vital to monitor the deposition of copper sulphide on the paper insulation since these deposits lead to turn-to-turn winding short circuits. However, there are a couple of disadvantages to this test. Firstly, the presence of oxygen in the vial can cause oxidation. Secondly, there may be undesirable chemical reactions due to the pressurised oil in the sealed vial at high temperatures [33].

The ASTM D1275A, ASTM D1275B, and BS EN 62535 standard test methods are designed to detect corrosive sulphur or potentially corrosive sulphur in insulating oils and there is no information on identifying corrosive sulphur species in a specific manner. Following this, academics and utilities have developed and employed several techniques in quantifying DBDS (the main cause of sulphur corrosion in insulating oils).

Tumiatti et al. [59] proposed the use of a gas chromatography interfaced with suitable detectors such as electron capture detector, atomic emission detector, sulphur chemiluminescence detector, flame photometric detector, mass spectrometer and tandem mass spectrometer, which can quantify DBDS concentration as low as 5 mg kg⁻¹. According to Toyama et al. [52], the presence of DBS, BiBZ, and DBDS in insulating oils can be detected using solid phase extraction at concentration as low as 0.1 ppm, followed by gas chromatography–mass spectrometry. Both of these two research groups have proposed a reliable technique to detect DBDS at lower concentrations.

According to Scatiggio et al. [18], amongst the 14 unused (uninhibited or inhibited) insulating oils which were inspected to have DBDS, the DBDS concentrations were within the range of 100–350 ppm. This range was found to be higher (100–1000 ppm) by Lewand and Reed [46]. Regardless of the proposed range, the exact amount of DBDS that could correspond towards the corrosive environment is still vague. For this reason, some researchers investigated the threshold of DBDS concentration which could exhibit a corrosive environment.

Maina et al. [60] indicated that the threshold of DBDS that leads to corrosive oil is 20 mg kg^{-1} . Martins et al. [61] concluded that the minimum concentration of DBDS that will make the oil potentially corrosive according to the BS EN 62535 standard is $\sim 10 \text{ mg kg}^{-1}$. The type of oil used in their study was non-corrosive oil (i.e. Shell Diala D). Meanwhile, Oweimreen et al. [62] investigated the relationship between the depletion rate of DBDS and corrosion process. They conducted the experiments following the BS EN 62535 standard test method (72 h at 150°C) and the results show that the DBDS concentration decreased from 150 mg L^{-1} to 53.1 mg L^{-1} using gas chromatography. The results of the copper strip test were positive (indicating the occurrence of corrosion) when the DBDS concentration was only 150 mg L^{-1} . However, solely detecting DBDS does not solve issues linked with sulphur corrosion due to the presence of other sulphur compounds that induces sulphur corrosion [18]. Therefore, it is crucial to develop a non-standardised test which can be used to quantify corrosive sulphur species since this will help one to identify whether DBDS or other corrosive sulphur compounds are the cause of corrosion whenever there are positive results from the CCD test [11].

The International Electrotechnical Commission Technical Committee 10 (IEC TC-10) established a new working group — IEC TC-10 WG-37. This group is given the responsibility to formulate new test methods to quantify sulphur compounds in used and unused mineral insulating oils in an explicit manner. This group has proposed several test methods, which are divided into three parts [63]:

- i) Part 1—Test method for the quantitative determination of DBDS
- ii) Part 2—Test methods for the quantitative determination of total corrosive sulphur
- iii) Part 3—Test methods for the quantitative determination of total mercaptans and disulphides (TMD) and other targeted corrosive sulphur species

Several techniques have been proposed to monitor the progression of copper sulphide within the paper insulation. In addition, several attempts have been made to detect the deposition of copper sulphide by measuring the dielectric response of the oil-paper insulation using frequency domain spectroscopy (FDS) [64]–[66] as well as polarisation and depolarisation current (PDC) technique [67]. Based on the results obtained from these techniques, it is found that the deposition of copper sulphide on the paper insulation affected the dissipation

factor ($\tan \delta$) as well as permittivity of the paper insulation. Hence, the higher the number of corrosive compounds present in the insulation oil, the higher the $\tan \delta$ and permittivity, particularly at lower frequencies starting from 1 mHz [66]. The main disadvantage of these techniques is the presence of other impurities (particularly moisture) that may lead to misinterpretation of the results.

Interestingly, XPS is used to obtain the information regarding the elemental composition of the solid surface (i.e. paper insulation) [43], [68]. However, this technique does not provide any information on the elemental composition of bulk paper insulation [33]. To overcome this issue, many researchers [18], [54], [58], [60], [69]–[74] have employed SEM–EDX (as recommended in the BS EN 62535 standard test method) to semi-quantitatively determine the amount of copper and sulphur deposited on the paper insulation, based on the percentage of atomic concentration. Besides, X-ray micro-analyser coupled with an EDX was also used in one study [54]. However, the implementation of FDS, PDC, XPS, and SEM–EDX in investigating the degree of damage incurred by sulphur corrosion based on the condition of paper insulation is not appropriate for the in-service power transformers because it is destructive. In addition, these techniques can only be carried out during the shutdown period of the transformer at ambient temperature. Also operators need to remove paper insulation or copper specimens (which is suspected of undergoing sulphur corrosion from the windings of the power transformers) which will interrupt the transformer operation. However, these techniques are useful in investigating copper sulphide deposition issues for scrapped or failed transformers, which is very positive. Common condition monitoring tools such as sweep frequency response analysis, return voltage measurement, insulation resistance, partial discharge, turns-ratio, power factor measurement, and DGA have proven to be inappropriate to detect any damage due to corrosive sulphur-related faults [41].

Scientists and researchers are searching for indirect techniques to detect the presence of copper sulphides in insulating oils as a result of sulphur corrosion processes without disassembling of power transformers. A recent test procedure employing X-ray fluorescence has been developed [69], [75], which permits quantitative analysis of sulphur and copper in insulating oils as low as 4.05 ppm and 1.95 ppm, respectively. However, there are a few problems associated with this technique. Firstly, it is necessary for the user to have multiple

points of data so that the data can be normalised with respect to the first data point. This is important since there may be differences in the data when the samples are collected from different batches of the same oil. In addition, the user needs to plot the calibration curves for both copper and sulphur once the oil samples are analysed.

Each of the techniques explained in this section has its own drawbacks and more importantly, all of the techniques are offline condition monitoring tools. Thus, there is a need to develop a simple, reliable, and inexpensive detection system which will greatly facilitate operators in continuously evaluating the quality of insulating oils due to sulphur corrosion on site in real-time, to allow timely remedial actions.

2.8 COUNTERMEASURES AGAINST CORROSIVE SULPHUR

Solving the issues associated with the formation of copper sulphide initiated by sulphur corrosion in insulating oils is crucial. Until now, the search for an approach for eliminating the deposition of copper sulphide on paper insulation has not been successful. Hence, countermeasure strategies have been proposed. Retro-filling (also known as oil change) has been used in the 1980s on polychlorinated biphenyls contaminated oil where 90–95 % of the residues have been removed via this process [76]. The experimental evidence provided [77] indicates that the detrimental effect of sulphur corrosion on the copper strip was reduced by approximately 76 % when the corrosive oil was replaced with a new natural ester. Conversely, replacing the corrosive insulating oils during periodic maintenance is not a feasible solution due to the environmental impact and high cost of insulating oil [43].

Oil reclamation uses adsorbent clays to minimise the soluble or insoluble polar contaminants from the insulating oil [78], thus prolonging the lifespan of a power transformer. Positively, this technique is economical and has minor environmental impact. However, oil reclamation causes the generation of elemental sulphur due to the reactivation of the adsorbent clay (at a high temperature of more than 300 °C) and catalytic (alumosilicate as catalyst) cracking reactions from hydrocarbon and sulphur based compounds [9]. Experimental evidence reveals that the trace of 1 ppm of elemental sulphur attacked the copper surface after been

aged for 19 h at 140 °C [12]. In addition, elemental sulphur will also react with silver at low temperatures [9].

Passivation techniques and additives such as toluotrazole-dialkyl-ammine (commercially known as Irgamet[®]39) have been employed to protect copper conductor surfaces against corrosive sulphur attacks [60], though this technique will not eliminate any corrosive sulphur species. Besides, the addition of passivators into the insulating oils results in a reduction of dissolved copper in oil and copper deposition onto paper insulation. Interestingly, the presence of Irgamet[®]39 in the uninhibited and inhibited insulating oils improved the oils oxidation stability [61]. Nonetheless, the addition of Irgamet[®]39 led to the generation of passivator-induced stray gassing [79] caused by the evolution of hydrogen, carbon monoxide, and carbon dioxide gases. The generation of hydrogen in the insulating oils may cause difficulties in interpreting the DGA results because the released hydrogen is not only due to the effect of Irgamet[®]39 but also depends on other mechanisms such as partial discharge [80]. Either oil reclamation or Irgamet[®]39, both of these mitigation techniques creates another issue — silver corrosion [9], which predominantly forms a silver sulphide deposition on the surfaces of selector contact of on load tap changer [81]. The common adsorbent used for oil reclamation known as Fuller's earth (clay) has been identified as one of the contributors towards the silver corrosion [82]. Research on the detection and removal techniques associated with elemental sulphur is still on going.

2.9 SUMMARY

Condition-based monitoring of power transformers is much preferable by the industry compared to time-based monitoring, which benefits in reduced costs and outages. Monitoring insulating oils (commonly used: mineral oil) of power transformers due to several faults such as corrosive sulphur-related faults gives valuable information on the general health of the power transformer, thus preventing the possibility of catastrophic failures. The sulphur corrosion mechanism in insulating oils remains unclear although it is believed that this phenomenon is initiated by the presence of corrosive by-products of DBDS (i.e. mercaptans and elemental sulphur). There are several models that explain the chemical

reactions, formation, and deposition of copper sulphide in power transformers. Irrespective the mechanism of sulphur corrosion, monitoring the progression of sulphur corrosion in power transformers is critical before any effective countermeasure can be used. The capability and limitation of standard and non-standard corrosion test methods based on the quality of the insulating oils and paper insulations together with current mitigation techniques associated with sulphur corrosion are not ideal. The extensive review provided in this chapter sets out the scope and motivation of this research, leading to the main aim of searching for a reliable quantifiable online condition monitoring tool to track the continuous presence of corrosive sulphur species in transformer insulating oils in real-time.

3 IDENTIFICATION OF CORROSIVE OILS USING THE EXISTING STANDARD TECHNIQUE AND UV–VIS SPECTROSCOPY

3.1 INTRODUCTION

This chapter summarises the investigation into sulphur corrosion in transformer oils using the existing standard technique (i.e. BS EN 62535 standard test method and SEM–EDX analysis). The preparation of the corrosive oil and bare copper samples used in this study is described in detail in Section 3.2. The existing standard technique involves two types of analysis: (1) qualitative analysis (BS EN 62535 standard test method) and (2) quantitative analysis (SEM–EDX). These analyses are described in detail in Section 3.3. The SEM–EDX analysis was carried out entirely by Dr Richard Pearce from the National Oceanography Centre Southampton (NOCS), University of Southampton, using Carl Zeiss Leo 1450VP SEM with Oxford Instruments EDX spectrometer. The fundamental principles and feasibility of UV–vis spectroscopy in sensing the presence of sulphur corrosion in transformer oils are presented in Section 3.4. The experimental set-up, data collection, and data analysis were conducted entirely by the author utilising the facilities available in the Tony Davies High Voltage Laboratory, University of Southampton.

3.2 PREPARATION OF CORROSIVE OIL AND BARE COPPER SAMPLES

Nytro Gemini X mineral oil (courtesy of Nynas AB, Sweden) was used to prepare the corrosive oil samples. The properties (stability) of this non-corrosive oil are presented in Table 3-1. This oil was chosen because it passed the corrosion tests specified in the following standards: (a) DIN 51353, (b) IEC 62535, and (c) ASTM D 1275 B. In addition, the Nytro Gemini X mineral oil is free of DBDS and metal passivator additives with a maximum total sulphur content of 0.05 % [83].

Table 3-1. Properties of the Nytro Gemini X mineral oil used in this study.

Property	Test Method	Typical Data
Total sulphur content (%)	ISO 14596	0.01
Corrosive sulphur	DIN 51353	Non-corrosive
Potentially corrosive sulphur	IEC 62535	Non-corrosive
Corrosive sulphur	ASTM D1275 (Method B)	Non-corrosive
DBDS (mg kg ⁻¹)	IEC 62697-1	Non-detectable
Antioxidants (wt %)	IEC 60666	0.38
Metal passivator additives (mg kg ⁻¹)	IEC 60666	Non-detectable
Acidity (mg KOH/g)	IEC 62021	<0.01

All solutions were prepared based on dilution by weight and the quantity of addition was dependent on DBDS/elemental sulphur concentration in parts per million (ppm). The parts per million is given by the following equation:

$$\text{parts per million} = \frac{\text{grams of solute}}{\text{grams of solution}} \times 1000000 \quad 3.1$$

In order to simulate a corrosive environment, DBDS (purity: 98 %, Sigma Aldrich) and elemental sulphur (purity: 99.99 %, Sigma Aldrich) were added as solids into the non-corrosive oil to attain the concentration needed. The corrosive oil was prepared in bulk just before the experiment was carried out. The glass bottles were initially cleaned with acetone three times, followed by deionised water and then dried for 2 h at 105 °C in order to eliminate any traces of moisture.

The oil samples with DBDS were prepared according to the following procedure:

- 1) DBDS (solids) was added into clean glass bottles containing the non-corrosive oil samples. It shall be noted that each bottle contained DBDS with a different concentration.
- 2) The solutions were stirred for ~1 h using a hot plate magnetic stirrer in order to attain homogeneous mixtures. The temperature of the hot plate was set within a range of 69–72 °C (Figure 3-1 (a)) based on the melting point of the DBDS [84].

The oil samples with elemental sulphur were prepared according to the following procedure:

- 1) Elemental sulphur (purity: 99.998 % Sigma Aldrich (solids)) was added into clean glass bottles containing the non-corrosive oil samples. Likewise, each bottle contained elemental sulphur with a different concentration.
- 2) The solutions were stirred for ~1 h using a hot plate magnetic stirrer until the yellowish elemental sulphur completely dissolved in the insulating oils samples. The temperature of the hot plate was set at 119 ± 2 °C (Figure 3-1 (b)) based on the melting point of elemental sulphur [85].

During the mixing process of oil with either DBDS or elemental sulphur, the glass bottles were covered with aluminium foil. The glass bottles were then secured with their caps after being cooled to room temperature (20 ± 2 °C) for ~20 min.

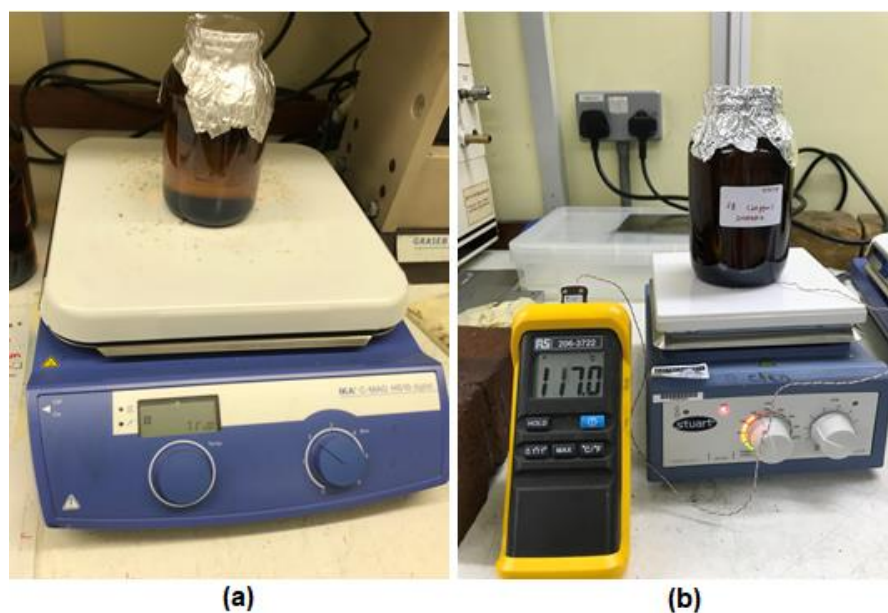


Figure 3-1. Stirring process of the oil via hot plate magnetic stirrer for (a) DBDS and (b) elemental sulphur.

Copper strips (used for the experiments presented in Chapter 3 and 4), each with an area of 200 mm² and thickness of 500 ± 10 µm, were prepared by thoroughly polishing copper sheets with abrasive paper and the sheets were cleaned with cyclohexane (purity: > 99 %, Fisher Scientific UK Ltd., UK) three times. This process is essential in order to remove oxide

layers that may have formed on the surface of the copper sheets. This process was conducted on the same day before the ageing took place to prevent contamination and oxidation of the bare copper sample.

3.3 BS EN 62535 STANDARD TEST METHOD AND SEM–EDX SPECTROSCOPY

Qualitative analysis was conducted on the copper samples according to the BS EN 62535 standard test method. To classify the level of corrosiveness in detail, the ASTM copper strip corrosion standard presented in Figure 2-10 was used. Corrosion occurs if the colour of the copper strip changes into graphite grey, dark brown or black.

3.3.1 FUNDAMENTAL PRINCIPLES OF SEM–EDX SPECTROSCOPY

In principle, the signals originating from SEM (i.e. secondary electrons, backscattered electrons, X-rays) are analysed to obtain information on the behaviour of the sample that is bombarded by the electron beam through interactions between the primary electron beam and sample. In essence, SEM–EDX spectroscopy has the same concept as SEM; however, it also involves X-ray microanalysis, which enables one to determine the elemental composition of a solid sample based on the SEM images. Different detectors are used in SEM–EDX spectroscopy to detect secondary electrons, backscattered electrons, or characteristic X-rays.

Secondary electrons have relatively low energy (<50 eV) compared with backscattered electrons (>50 eV), where the electrons are emitted from within proximity of the sample surface (Figure 3-2). Secondary electrons are produced when the incident electrons from the primary beam excite electrons on the sample surface and lose some of their energy (inelastic) during this process. The advantage of secondary electron images is that one can obtain high-resolution topographic information of the sample. As the name implies, backscattered electrons are produced due to the formation of scattered electrons in elastic form (no energy losses) when the electron beam strikes the sample. Owing to the high energy (>50 eV), backscattered electrons are emitted from the bulk of the sample.

Characteristic X-rays are produced once the EDX fires electrons at a sample through the primary beam. The energies of the X-rays are measured, which are then used to produce spectra of the elements contained in the sample. If the electron beam has an energy greater than the binding energy of the inner shell electron, then the inner shell electron will be knocked out. The outer shell electrons will drop down to the vacant inner shell, emitting an X-ray to balance the energy difference of the two shells. Therefore, the energy of the X-ray is equivalent to the energy difference between the two shells. Each different atomic element emits X-rays at a specific energy due to the interaction between its unique electronic configuration and the beam electrons. The energies of the characteristic X-rays enable one to identify the elements of a sample whereas the intensities of the characteristic X-ray peaks enable quantification of the concentrations of elements [86].

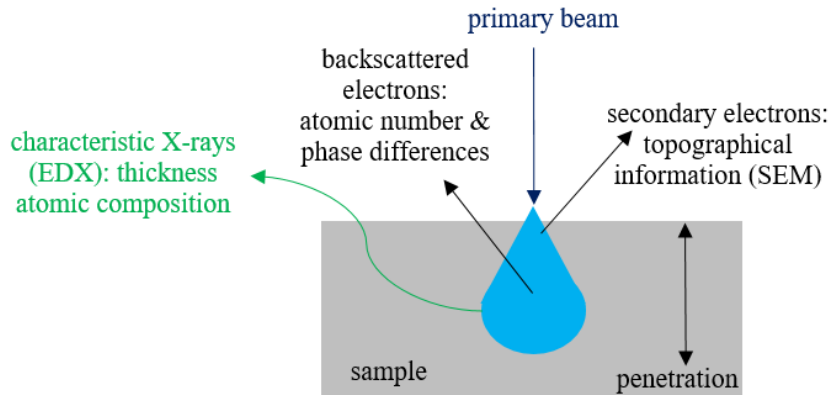


Figure 3-2. Firing of the electron beam on the sample, resulting in the emission of secondary and backscattered electrons as well as X-rays [87].

3.3.2 RESULTS AND DISCUSSION

The qualitative results of the bare copper samples aged in three different DBDS concentrations (100, 200, and 300 ppm) for three days according to the BS EN 62535 standard test method are presented in Figure 3-3–Figure 3-5. It can be seen from Figure 3-3 that the sulphur corrosion process occurs slowly on Day 1 for all of the bare copper samples, as evidenced from the moderate tarnish (Level 2c). In addition, it is difficult to distinguish the three corrosion levels on Day 1.

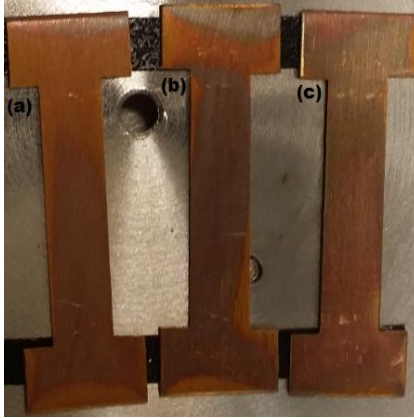


Figure 3-3. Bare copper samples aged in (a) 100 ppm, (b) 200 ppm, and (c) 300 ppm of DBDS on Day 1, according to the BS EN 62535 standard test method.

The corrosion process is accelerated when the ageing time is increased to two days. Based on the appearance of the bare copper samples in Figure 3-4, it is suspected that sulphur corrosion occurs in the insulating oils, based on the specifications given in the ASTM copper strip corrosion standard. It can be observed that there is dark tarnish (Level 3b) on the surface of these bare copper samples. However, it is still quite difficult to distinguish the corrosion level between the three samples on Day 2.

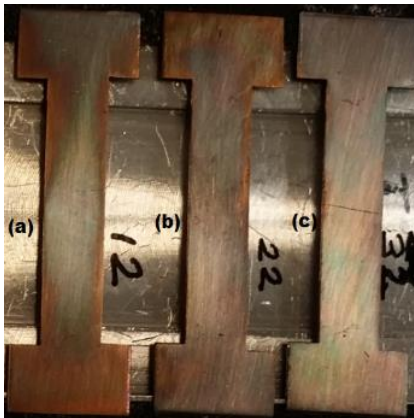


Figure 3-4. Bare copper samples aged in (a) 100 ppm, (b) 200 ppm, and (c) 300 ppm of DBDS on Day 2, according to the BS EN 62535 standard test method.

In contrast, the corrosion levels of the three samples can be clearly distinguished on Day 3, as shown in Figure 3-5. The results are positive since the colours of the bare copper samples are graphite grey, dark brown, and black for the bare copper sample aged in the insulating

oils mixed with 100, 200, and 300 ppm of DBDS, respectively. The results shown in Figure 3-3–Figure 3-5 support the argument that this technique is disadvantageous (as described earlier in Section 2.7), which will lead to misinterpretation of the results. For this reason, it is necessary to analyse the level of sulphur corrosion using a quantitative technique (i.e. SEM–EDX), as recommended in the BS EN 62535 standard test method.

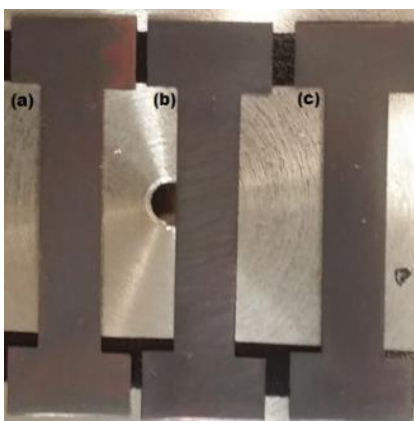


Figure 3-5. Bare copper samples aged in (a) 100 ppm, (b) 200 ppm, and (c) 300 ppm of DBDS on Day 3, according to the BS EN 62535 standard test method.

For the quantitative analysis, SEM–EDX spectroscopy was carried out to analyse the elements present on the surface of the bare copper samples resulting from sulphur corrosion due to the breakdown of DBDS. Carl Zeiss Leo 1450VP SEM with Oxford Instruments EDX spectrometer and AZtecEnergy software system were used for this purpose. The aged copper samples were analysed separately using a multiple pin sample holder. The following settings were used for the quantitative analysis: (1) working distance: 19 mm, (2) accelerated voltage: 20 kV, and (3) current probe: 750 pA. The magnification view was set at 44 \times and the total number of X-ray counts in the EDX spectrum was set at 300000. No sample coating was required to analyse the bare copper samples.

Only sulphur and copper were quantified even though there were other elements identified from the analysis. Therefore, the results presented are based on the per cent by weight normalised to the sum of copper and sulphur. Three different areas on the same surface were chosen for quantitative analysis of the aged copper samples, as shown in Figure 3-6. The mean and standard deviation were calculated for each sample, as shown in Table 3-2. The

samples were evaluated in this manner and the standard deviations are shown in the SEM–EDX graphs using error bars.

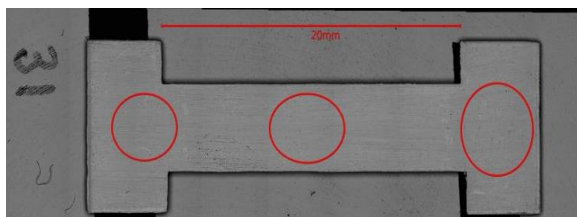


Figure 3-6. SEM image of the bare copper sample aged in 100 ppm of DBDS on Day 1. The circled areas were analysed using SEM–EDX spectroscopy.

Table 3-2. SEM–EDX data of the bare copper sample aged in 100 ppm of DBDS on Day 1.

Site	Sulphur (wt %)	Copper (wt %)
1	2.49	97.51
2	2.41	97.59
3	2.47	97.53
Mean	2.46	97.54
Standard deviation (\pm)	0.03	0.03

The amounts of copper in per cent by weight (wt %) remaining on the bare copper samples after sulphur corrosion were quantified by SEM–EDX spectroscopy and the results are shown in Figure 3-7. It can be observed from Figure 3-7 that on Day 1, the amounts of copper decrease to 98.36, 97.99, and 97.54 wt % for a DBDS concentration of 100, 200, and 300 ppm, respectively. On Day 2, the amounts of copper decrease further to 96.83, 95.04, and 94.36 wt %. In a similar fashion, the amounts of copper decrease gradually to 93.66, 91.29, and 91.17 wt % on Day 3 for a DBDS concentration of 100, 200, and 300 ppm, respectively. In general, increasing the DBDS concentrations from 100 ppm to 200 ppm and 300 ppm decreases the amounts of copper by at least 0.37 % and 0.68 % on Day 1 and Day 2, respectively. This percentage significantly decreases after 3 days of ageing, where there is a minor decrease in the amount of copper present on the surface of the bare copper samples (~ 0.12 %) for a DBDS concentration of 200 and 300 ppm. This suggests that the corrosive by-products resulting from the breakdown of DBDS may not be linear over time. In general, it is evident that the amount of copper on the surface of the bare copper samples decreases with an increase in the DBDS concentration. The results indicate that the possibility that the

DBDS will degrade and form other corrosive sulphur compounds in the mineral oil is extremely high at higher DBDS concentrations. This indicates that the sulphur corrosion process in an actual oil-filled power transformer will accelerate at higher DBDS concentrations, suggesting a higher dissolution of copper in the insulating oil.

As stated in the BS EN 62535 standard test method, SEM–EDX spectroscopy provides a highly reliable elemental analysis. However, this technique is a laboratory-based analysis and it is extremely costly. Thus, researchers are constantly searching for portable, cost-effective, and reliable ways to monitor the progression of sulphur corrosion in transformer insulating oils. An optical approach (UV–vis spectroscopy) was used in this study to monitor the progression of sulphur corrosion. The feasibility of UV–vis spectroscopy in characterising the corrosive oil based on UV–vis spectra is described in detail in Section 3.4.

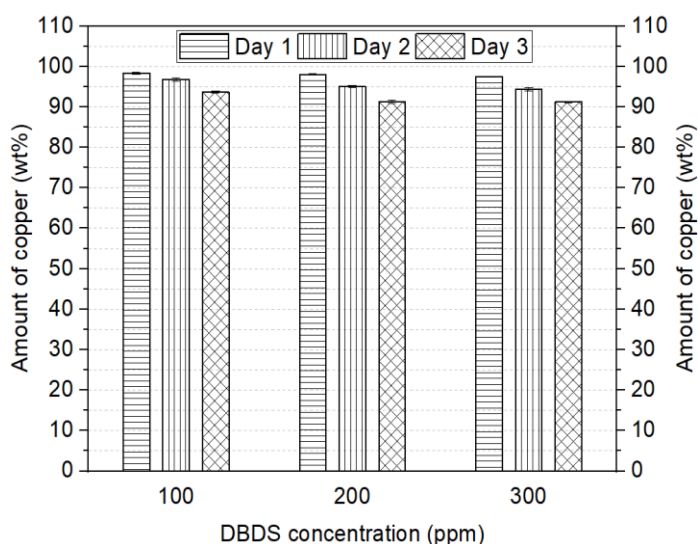


Figure 3-7. Amounts of copper traced on the surface of the bare copper samples using SEM–EDX spectroscopy.

3.4 UV–VIS SPECTROSCOPY

Theoretically, UV–vis spectroscopy is a technique used to quantify the transition of metal ions and highly conjugated electronic compounds. UV–vis spectroscopy allows the operator to determine the concentrations of unknown substances based on the absorption of electromagnetic radiation in the UV and visible range. Any changes in the chemical structure

of molecules leads to the shift in the absorbance of the UV–vis spectrum. The changes in the UV–vis spectrum can be interpreted as follows:

- 1) Hypochromic effect: decrease in molar absorption/decrease in the spectral intensity
- 2) Hyperchromic effect: increase in molar absorption/increase in the spectral intensity
- 3) Hypsochromic effect: shift of bands towards shorter wavelengths/higher energy
- 4) Bathochromic effect: shift of bands towards longer wavelengths/lower energy

The application of UV–vis spectroscopy for condition monitoring of insulating oils has garnered considerable attention from researchers worldwide based on the principle that the light transmitted through the oil sample containing various contaminants is decreased by the fraction of light that is being absorbed. The light transmittance is detected as a function of wavelength. Studies have been carried out from 2008 to 2017 on the application of UV–vis spectroscopy for: (1) measurement of the interfacial tension of transformer oils [88], [89], (2) identification of dissolved decay products in the insulating oil [90], (3) on-site analysis of transformer paper insulation [91], and (4) estimation of furanic compounds in the transformer insulating oil [92]. The same concept was used in these applications, where the light beam (wavelength λ : 200–1100 nm) penetrates through the liquid (i.e. transformer oil) contained within a cuvette. The light penetrates through an input fibre when the sample interacts with the oil and the transmitted light is fired to the spectrophotometer by the output fibre. The spectrophotometer is connected to a computer, which is used to display and analyse the spectral response of the oil sample. The light transmitted through the oil sample containing various contaminants decreases by the fraction of light that is being absorbed. The light transmittance is detected as a function of wavelength in the UV–vis spectrum. According to the Beer Lambert law, the amount of light absorbed or transmitted by a solution can be determined using [93]:

$$A_{\lambda} = -\log_{10} \left(\frac{S_{\lambda} - D_{\lambda}}{R_{\lambda} - D_{\lambda}} \right) = \varepsilon \cdot c \cdot l \quad 3.2$$

where S_{λ} is the intensity of light that penetrates through the sample, R_{λ} is intensity of the light incident on the sample, D_{λ} is the intensity detected by the spectrophotometer without the incident light on the sample, ε is the absorbance coefficient of the absorbing species in the

oil, c is the concentration of the absorbing species in the oil (g/L), and l is the path length of the light through the oil.

In the past five years, UV–vis spectroscopy has been used to investigate the ageing behaviour of dodecylbenzene in the presence of copper and DBDS [94]. The results presented in [94] provide convincing evidence that the absorption edge shifted to longer wavelengths with an increase in ageing time. The same trend could be observed for two different oil samples: (1) without DBDS and (2) with a relatively high DBDS concentrations (2000 ppm). Based on the theory and previous applications presented in this section, it is hypothesised that the amount of copper dissolved in insulating oils may influence the UV–vis spectra.

3.4.1 FUNDAMENTAL PRINCIPLES OF ABSORPTION SPECTROSCOPY

Photons are the source of electromagnetic radiation for absorption spectroscopy. The fundamental principles of absorption spectroscopy are described as follows. A light beam is the source of photons of electromagnetic radiation. The transition of electrons in atoms and molecules from the ground state to the excited state occur when there is an absorption of the photons of electromagnetic radiation such that the energy is equal to the energy difference between the levels. The principle of absorption spectroscopy can be explained based on quantum theory: where once a molecule absorbs radiation, the photon energy growth is proportional to its energy E , which is given by:

$$E = h\nu = \frac{hc}{\lambda} \quad 3.3$$

where h is the Planck's constant (6.626×10^{-34} J s), ν is the frequency, λ is the wavelength (nm), and c is velocity of light (2.998×10^8 m s⁻¹).

The absorption of electromagnetic radiation by molecules depends on the type of transition (electronic, rotational or vibration), resulting in variations of nuclear spins and bond deformations. All of these transitions require an exact amount of energy. The electronic type requires a large energy transition whereas both rotational and vibrational types require small energy transition, resulting in different absorption characteristics in different regions of the

electromagnetic spectrum. Because of the high energy generated by UV–vis radiation, the absorption in UV–vis spectrum is generally associated with molecular electronic transitions.

According to the Beer Lambert law, the fraction of light absorbed by a substance is proportional to the concentration of an absorbing species and it is inversely proportional to the light intensity transmitted through the sample:

$$A_{\lambda} = -\log_{10} \left[\frac{I}{I_o} \right] = \varepsilon \cdot c \cdot l \quad 3.4$$

where, A_{λ} is the light absorbance, I_o is the light intensity transmitted through the reference blank, I is the light intensity transmitted through the sample, T is the light transmittance, ε is the molar absorbance coefficient of the substance at wavelength λ (which is unique for each substance), c is the concentration of the absorbing species (g/L), and l is the path length traversed by the light.

3.4.2 FUNDAMENTAL PRINCIPLES OF UV-VIS SPECTROSCOPY AND PREVIOUS APPLICATIONS

Theoretically, the variations in the absorption and reflectance of UV radiation is due to different types of electronic excitations between different energy levels, namely: (1) bonding (σ , π), (2) non-bonding (n), and (3) anti-bonding (π^* , σ^*), as illustrated in Figure 3-8. The electronic transitions from the bonding (σ) and non-bonding (n) orbitals to the anti-bonding (σ^*) orbital require relatively higher energy and therefore, these electronic transitions are associated with shorter-wavelength radiation in the far UV region. In contrast, the electronic transitions from the non-bonding (n) and bonding (π) orbitals to the anti-bonding (π^*) orbital require relatively lower energy and thus, these electronic transitions are typically associated with longer-wavelength radiation, which is either in the UV or visible region.

The measurement of light absorbance in the UV and visible regions can be performed at a single wavelength or throughout the wavelength range of the spectrum. The light source used in UV–vis spectroscopy is a combination of deuterium (185–390 nm) and tungsten or

halogen (350–800 nm) lamps. The output from the light source is focused onto a diffraction grating, which splits the incoming light into its component colours of different wavelengths.

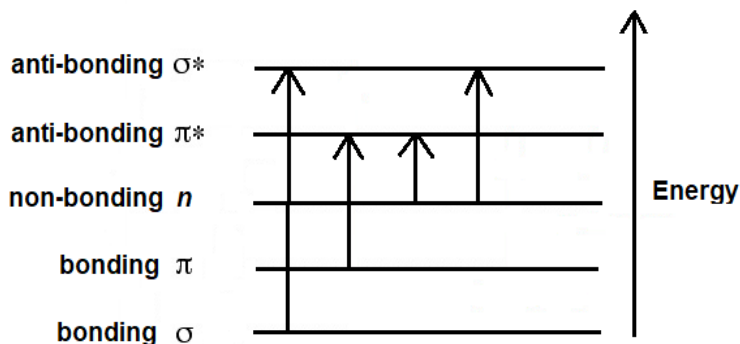


Figure 3-8. Electronic transitions of electrons.

3.5 EXPERIMENTAL SET-UP

The samples were prepared according to the procedure described in Section 3.2. The treated copper samples were placed carefully into headspace glass vials. Each vial contained 15 mL of mineral oil mixed with different concentrations of DBDS: (1) non-corrosive oil (0 ppm), (2) mildly corrosive oil (100 ppm), and (3) highly corrosive oil (1000 ppm). The glass vials were sealed with sulphur-free polytetrafluoroethylene (PTFE)/silicone septum and aluminium caps. The samples were aged in air atmosphere using a fan oven set at 150 ± 1 °C for three days. Once the ageing process was complete, the copper samples were taken out from the vials using a clean pair of tweezers. The copper samples were degreased by rinsing the samples with cyclohexane at least three times until the copper surface was free from oil residues.

Perkin Elmer LambdaTM 35 UV–vis spectrophotometer as shown in Figure 3-9 was used for spectroscopy measurements of the oil samples once the ageing process was completed. This instrument covers a wavelength range of 200–1100 nm and it is equipped with quartz cells with an optical path length of 10 mm. In order to examine the effect of the cuvettes filled with oil samples on the spectroscopy measurements, an empty cuvette was scanned and its spectrum was stored as reference (auto-zero mode). Next, each cuvette was filled

with 3.5 mL of oil sample using Eppendorf Multipette® Stream pipette and the samples were scanned using the spectrophotometer. The spectral absorbance characteristics of the oil samples were determined by identifying the difference between the spectral response of each oil sample and the reference spectral response. The UV–vis spectroscopy measurements were repeated three times for each oil sample using a new cuvette to ensure consistency of the results. It shall be noted that it is crucial to minimise the presence of water bubbles in the insulating oil samples because the bubbles will affect the measurement results. For this reason, the insulating oil samples were left for ~10 min until there were no water bubbles present after each oil sample was poured into a cuvette.



Figure 3-9. Perkin Elmer Lambda™ 35 UV–vis spectrophotometer.

3.6 RESULTS AND DISCUSSION

The UV–vis spectra of the insulating oils with bare copper samples aged in different DBDS concentrations (0, 100, and 1000 ppm) in a fan oven at 150 °C for 72 h are shown in Figure 3-10. It can be observed that the presence of corrosive by-products in the insulating oil resulting from breakdown of DBDS reduces the percentage of light transmission. The results conform with the Beer Lambert law presented in Section 3.4. According to the Beer Lambert law, the light absorbance increases in proportion with the increase in concentration of the absorbance species. Hence, it is expected that the percentage of light transmission decreases with an increase in the DBDS concentration, as evidenced from the results.

Compared with both oil samples (DBDS concentration: 0 and 100 ppm), the oil sample with the highest DBDS concentration (1000 ppm) exhibits hyperchromic effect, as indicated by

the significant increase in the intensity of the spectrum within a wavelength range of 350–700 nm. However, there is no significant difference in the percentage of light transmission between the non-corrosive oil (0 ppm) and mildly corrosive oil (100 ppm) since the UV–vis spectra for both oil samples are almost coincident. In addition, the UV–vis spectra of these oil samples indicate that there are no hypochromic/hyperchromic or hypsochromic/bathochromic effects in these samples. It can be observed that the UV–vis spectra only shift to longer wavelengths (as indicated by the black arrow in Figure 3-10) with an increase in the DBDS concentration. It is evident from Figure 3-10 that it is difficult to distinguish the difference in the UV–vis spectra for low DBDS concentrations within a range of 0–100 ppm.

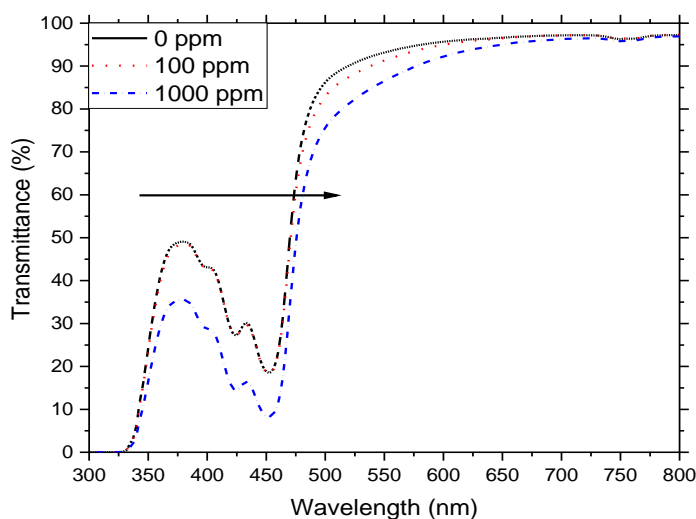


Figure 3-10. UV–vis spectra of the insulating oils aged in (a) 0 ppm, (b) 100 ppm, and (c) 1000 ppm of DBDS.

The UV–vis spectra of the insulating oils are also influenced by the ageing condition (i.e. aged in air or nitrogen) and the ageing time [95]. This is due to the fact that the presence of other compounds resulting from higher oil acidity contributes to changes in the light absorbance characteristics and thus, UV–vis spectra. Hence, it is difficult to differentiate the other compounds present in the insulating oil from the corrosive by-products as a results of the breakdown of DBDS. For this reason, it can be deduced that UV–vis spectroscopy is

impractical for the detection and condition monitoring of corrosive sulphur, particularly at low concentrations of DBDS.

3.7 SUMMARY

The qualitative analysis based on the ASTM copper strip corrosion standard is a visual-based dependent process. This technique may only distinguish either the insulating oil is corrosive or not, however, it is impossible to identify the level of oil corrosiveness. Interestingly, SEM–EDX proved to be a useful lab-based technique to investigate the sulphur corrosion process allowing a clear indication that the amounts of copper in per cent by weight (wt %) remaining on the bare copper samples are reducing with the increasing in DBDS concentrations and ageing time. In contrast, it is far to implement this technique on-site in real-time in order to facilitate timely remedial actions. Besides, the corrosivity level of transformer oil in bulk may not be determined as this tools only required a small sample volume compared to the total oil volume of the transformer.

On the other hand, further investigations to sense the presence of corrosive sulphur in insulating oils was carried out by means of UV–vis spectroscopy, which returned values in contrast with those previously reported in literature. This strong supporting evidence that will be essential for the benefit of other readership in this area, proving that UV–vis spectroscopy is not feasible and reliable to track the progression of sulphur corrosion due to the breakdown of DBDS at low concentration (<100 ppm), although the quantitative results obtained from SEM–EDX analysis presented in Section 3.3.2 showed that the sulphur corrosion phenomenon occurred with the presence of relatively low concentration of DBDS (100 ppm).

To summarise, future experimental work (presented in Chapter 4) concentrates on investigating the characteristics of corrosive oil with regard to variations in capacitance and conductivity, respectively. The most recent developments in the field of IDCs as oil sensors, which allow the study of oil capacitance behaviour, could pave the way to a new way of observing the progression of sulphur corrosion in transformer oils.

4 SULPHUR CORROSION SENSORS UTILISING DC CONDUCTIVITY MEASUREMENTS AND INTERDIGITATED CAPACITIVE SENSORS

4.1 INTRODUCTION

This chapter discusses a series of experiments conducted to identify a feasible method for detecting and monitoring sulphur corrosion in transformer insulating oil. It shall be noted that the results presented in this chapter are based on the characteristics of the oil which contains only the corrosive by-products of DBDS. Section 4.3 and Section 4.4 briefly discuss the fundamental principles, experimental set-up and procedure, as well as the results and discussions on DC conductivity measurements and oil capacitance measurements by means of IDCs. Because the water content in insulating oils contributes to the changes in oil conductivity and capacitance, it was necessary to measure the water content in insulating oils. Therefore, Karl Fischer (KF) Coulometric Titration was used for this purpose and the fundamental procedure, the equipment used and the procedure are explained in Section 4.2.

4.2 KARL FISCHER (KF) COULOMETRIC TITRATION

Variations in water content will lead to significant variations in DC conductivity and oil capacitance measurements. In this study, the water content measurements were conducted by means of KF Coulometric titration on the same day, immediately before the DC conductivity and oil capacitance measurements, respectively. This measure was crucial because the amount of water present in the oil samples has a significant effect on DC conductivity and oil capacitance values.

4.2.1 FUNDAMENTAL PRINCIPLES

The KF Coulometric titration analysis is a reliable moisture detection method that has been documented as an international standard. This method allows users to obtain high accuracy

measurements within a short test period. In addition, the method requires a simple sample preparation and involves the use of an electrolytic reagent that contains iodine, sulphur dioxide, a base, and a solvent. Aquamax KF Plus Coulometric titrator (GR Scientific Ltd.) was used in this research. The Aquamax KF Plus Coulometric titrator is a combination of the Coulometric technique and KF titration and is used to determine the water content of oil samples by measuring the amount of electrolysis current necessary to produce the consumed iodine [96]. As indicated in the stoichiometry of the reaction, 1 mole of iodine will react with 1 mole of water. Therefore, the quantity of water can be determined because it is proportional to the total integrated current [97]. The key feature of this instrument is that it does not require the calibration of the reagent (iodine). The instrument will automatically select the suitable titration speed according to the amount of water contained in the oil samples.

4.2.2 EQUIPMENT USED AND PROCEDURE

A new syringe with needle was used to collect the oil sample for each measurement. The measurement procedure was repeated three times for each oil sample to ensure that the results were consistent. The measurement procedure was initiated by carefully pouring 1 mL of oil sample into a 2-mL syringe. As suggested [96], 1–2 mL of oil sample is required if the expected water content is between 1 ppm and 100 ppm. It is essential to minimise any water bubbles inside the insulating oils since the water bubbles will affect the measurement results. For this reason, the insulating oils were visually inspected to ensure that no water bubbles were present in the oils before the oil samples were placed in the Aquamax KF Plus Coulometric titrator. It shall be noted, however, that the air bubbles could have been ejected through the needle (diameter: 1.10 ± 0.01 mm; length: 50 ± 1 mm) by inverting the syringe. Once the syringe plunger was at 1-mL mark, the excess sample from outside of the needle was wiped using a clean and dry tissue. The needle was then pierced via the injection septa of the titration vessel. The oil sample was then immediately injected into the Aquamax KF Plus Coulometric titrator once the START button was pressed. Finally, the results in ppm on the display were read and recorded.

4.3 DC CONDUCTIVITY MEASUREMENTS

The DC Conductivity measurements of oil samples were conducted in a material room located in The Tony Davies High Voltage Laboratory within University of Southampton. Data collection and analysis were performed entirely by the author.

4.3.1 FUNDAMENTAL PRINCIPLE AND PREVIOUS APPLICATIONS

The DC conductivity measurement is one of the methods used to determine the conduction properties of a test sample. For a power transformer, DC conductivity measurement is one of the common methods used to assess the insulating oils or pressboard deterioration level [98]. According to Ohm's law, conductivity (G) is the inverse of resistance (R) and is determined from the measured voltage and current:

$$G = \frac{1}{R(\Omega)} = \frac{I(A)}{V(V)} \quad 4.1$$

The basic unit of conductivity is Siemens (S) and could be written as Ω^{-1} . The cell geometry effects the oil conductivity, and therefore, to compensate the differences between electrode dimensions, the product of measured DC conductivity measurements is expressed as:

$$\text{Specific conductivity } (C) = \left(G \times \frac{L}{A} \right), Sm^{-1} \quad 4.2$$

where G is the measured conductivity, L is the length between the electrodes, and A is the area of the electrodes. The conduction in liquid comprises a complex physicochemical process involving the dissociation of ionic pairs in the bulk liquids and the charge injection between the electrode and liquid interface [99]. The dissociation mechanism is explained as:



where A^+B^- denotes the density of ionic pairs, A^+ and B^- are the positive and negative ion, k_d and k_r are the dissociation and recombination rate constants.

In liquid (i.e. insulating oil), the dominating electrical conduction is caused by the mobility of charge carriers (the drift process of positive and negative ions). When the DC electric field E is applied, the relationship between electrical conductivity σ and current density J is expressed as:

$$J = \sigma \cdot E \quad 4.4$$

In thermodynamic equilibrium, the ionic conductivity is a function as the sum of the mobility of every type of ion μ_i and the charge density q_i and can be expressed as:

$$\sigma = \sum_i (\mu_i \cdot q_i) \quad 4.5$$

Hence, the charge carrier density is a function of DC electric field strength, temperature, impurities, ageing products, and water content [100], [101].

Oil conductivity is influenced by ageing products such as water, acid, and furan compounds during ageing [102]. As a transformer ages, the ageing products begin to generate. Prolonging the operation time of transformer leads to the growth in thermal, oxidation, and electrical degradation of either oil or paper insulation, which in turn, will increase the ageing products. A pure insulating oil is known to be nonpolar because it comprises saturated hydrocarbons, which are non-ionic or are free of electrons. However, the properties of oil may change from being nonpolar to having polar contaminants, thus enabling the oil to easily conduct the current when ionic dissociation occurs due to the presence of the ageing products, which dominate the charge carriers. Besides the ageing products, other impurities may influence the electrical conductivity of insulating oil. These impurities include conducting particles such as copper, semi-conducting particles like carbon, or electrically insulating particles such as silica and paper [103].

It is accepted that the presence of moisture or water in liquid particularly insulating oils affects its electrical properties by reducing its dielectric strength and increases its electrical conductivity and dissipation factor [104]. The dissociation of moisture or water in insulating oils from H_2O into H^+ and OH^- increases its conductivity value. According to [105], the

conductivity of a fine diluted water in oil is subjected to the concentration of water dissolved in the oil.

To date, various international standards have been proposed to provide guidance for DC conductivity measurements as shown in Table 4-1 [106]–[108]. Considering the availability of the equipment in our laboratory, the DC conductivity measurement was conducted in accordance to the ASTM D 1169 standard test method.

Previous studies have applied PDC measurements in an oil-paper insulation system [109],[110] which showed that the electrical conductivity of mineral oil was associated with the initial value of polarisation current. Another study [37] applied the PDC techniques to monitor oil conductivity and moisture content in mineral oils and found that the polarisation current was divided into polarisation current that occurred at initial time (approximately ≤ 100 s) — due to conductivity of insulating oils, and the polarisation current that occurred at longer period of time ($t \approx 10000$ s) — due to moisture content in insulating oil. As illustrated in Figure 4-1, the initial values of polarisation currents is related to the oil conductivity while the end values is associated with the water content in the oil. The transient values were due to the geometry and oil properties.

Table 4-1. Summary of international standard for DC conductivity measurements of insulating liquids [106]–[108].

Standard	Method	Description	Electrical Stress	Electrification time
IEC 61620	Current measurement, trapezoidal voltage	Conductivity is related to an initial current density	≤ 0.1 kVmm ⁻¹	< 5 s
IEC 60247	Current measurement with DC voltage	Conductivity is read at a steady state current density	0.05–0.25 kVmm ⁻¹	60 s
*ASTM D 1169	Current measurement with DC voltage	Conductivity is read at a given instant of time	0.2–1.2 kVmm ⁻¹	60 s

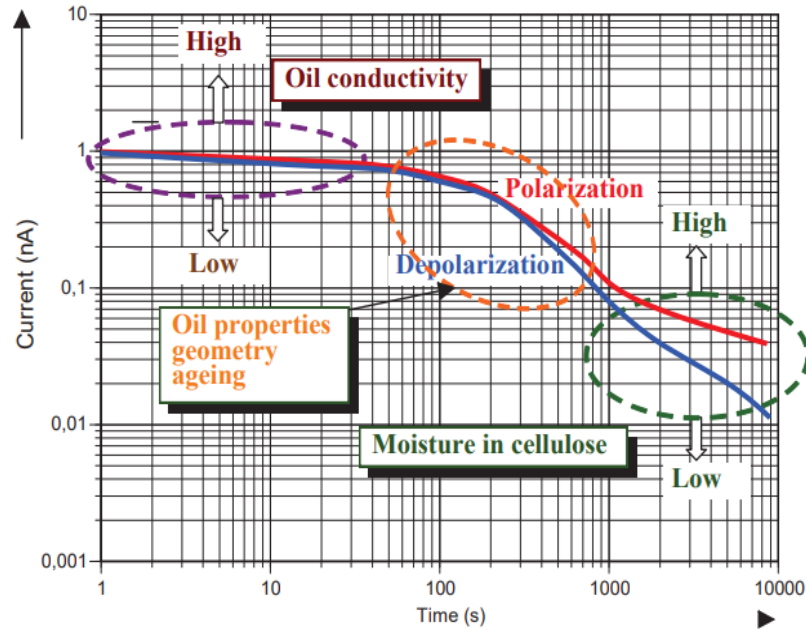


Figure 4-1. Interpretation of PDC measurement for insulating oils [111].

The conductivity of liquid (i.e. insulating oil) is dependent on the temperature, electrical field strength, water content and impurities as a results of ageing. These parameters give an effect on the charge movement in the oil (resistance), resulting in the changes of oil conductivity. It is known that the ageing copper in the oil with DBDS at temperature, range between 80 °C and 150 °C may lead to the breakdown of DBDS into other corrosive by-products such as mercaptans. This process leads to corrosive by-product attack on copper, which in turn, releases the copper ions and form a semi-conductive copper sulphide on the paper insulation. Therefore, it is hypothesised that increments of oil conductivity will occur. Because this form of analysis has not been reported in the literature, the feasibility of DC conductivity measurement in measuring the corrosive sulphur content in insulating oil was further investigated. The mixture of moisture, corrosive by-product compounds and copper ions will complicate the process of oil characterisation because all of these components will increase the DC conductivity value at the same time and therefore, may not be easy to distinguish these effects. Therefore, it is essential to consider using the same ageing conditions (i.e. ageing time, temperature, and base oil) while varying the DBDS concentrations. In addition, it was crucial to obtain constant temperature, electrical field strength, and water content while conducting the DC conductivity measurement to avoid any misinterpretation of the results.

4.3.2 EXPERIMENTAL SET-UP

The oil samples were prepared according to the procedure described in Section 3.2. The DBDS concentrations used were 0, 100, and 200 ppm. However, modifications on the following aspects were made to the experimental set-up due to the limitations of the experiment: (1) the effect of polarisation on the oil samples and (2) the capacity of the test cell (5 mL of oil was needed for each measurement). Therefore, three oil samples (each with the same DBDS concentration) were required to make sure that the oil sample was fully discharged before the following DC conductivity measurement was initiated. In other words, if the oil is not fully discharged after the experiment, the conductivity of the following measurement will be increased. Hence, each sample consists of 40 mL of oil along with a copper strip were added into a 50-mL headspace vial. The dimensions of the copper strip are described in Section 3.2. The samples were aged in air atmosphere using a fan oven set at 130 ± 1 °C for 10 days. It was crucial to cover all the headspace vials with a glass Petri dish to prevent excessive evaporation during the ageing process.

The experimental set-up used for DC conductivity measurements of the oil samples is illustrated in Figure 4-2. The DC power supply was connected in series with a 5-mL cylindrical test cell and picoammeter. A 10-M Ω protection resistor was connected in series in between the DC power supply and 5-mL cylindrical test cell to prevent damage to the picoammeter. Table 4-2 shows the measured test cell geometry used in this experiment. These parameters are used to calculate k , which is a constant based on the test cell geometry.

Table 4-2. Measured test cell geometry

Parameters	Measured values (m)
Outer radius, r_a	0.0120
Inner radius, r_b	0.0100
Height, l_c	0.0364

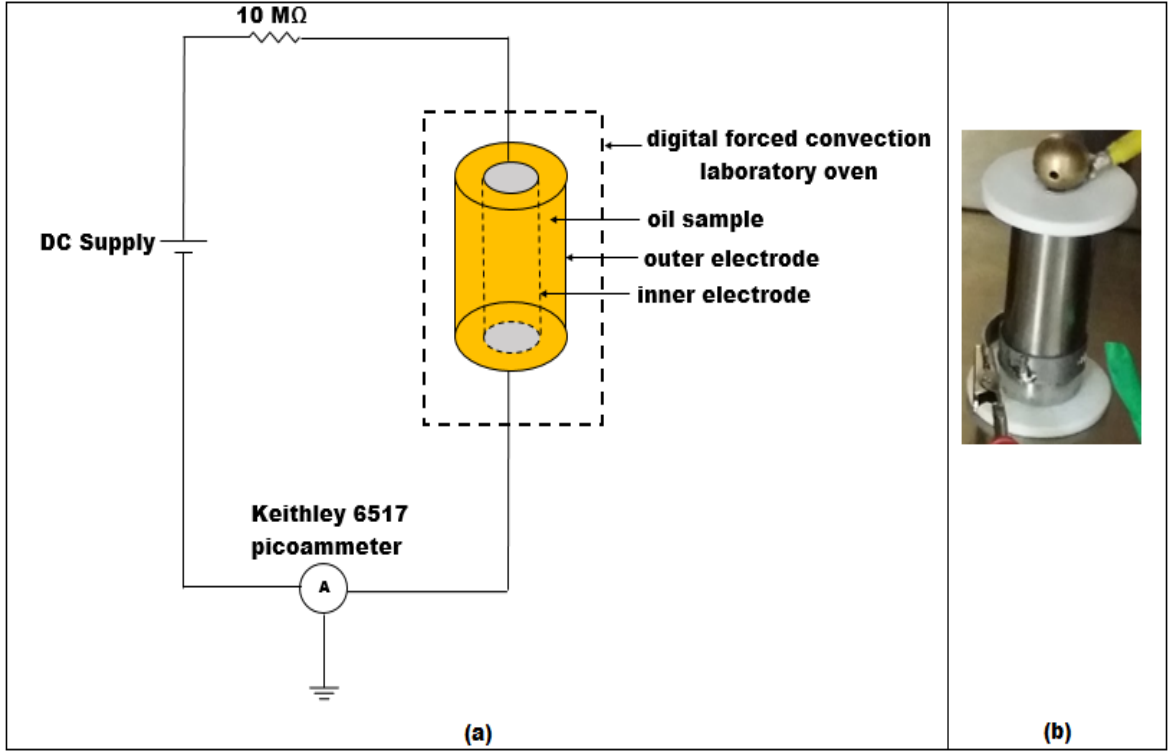


Figure 4-2. DC conductivity measurements: (a) Experimental set-up and (b) Image of the test cell.

Since the test cell is cylindrical, k can be written as [107]:

$$k = \frac{1}{\epsilon_o} \frac{2\pi\epsilon_{air}\epsilon_o l_c}{\ln \frac{r_a}{r_b}} \quad 4.6$$

where r_a and r_b represent the outer and inner radius of the test cell, respectively, l_c is the height of the test cell, ϵ_o is the vacuum permittivity, and ϵ_{air} is the air relative permittivity (≈ 1).

In this experiment, the current flowing through the oil samples was measured and the DC conductivity of the oil samples was determined from the following equation [107]:

$$\sigma = \frac{I}{kV} \quad 4.7$$

Here, σ is the DC conductivity of the oil sample, I is the measured current, and V is the electric potential across the sample.

The DC conductivity measurements were carried out according to the following procedure:

- 1) Gently, 5 mL of non-corrosive insulating oil (0 ppm (Sample 1)) was pipetted into a clean cylindrical test cell using Eppendorf Multipette® Stream pipette equipped with 25 mL Combi-tips® Plus with adapter.
- 2) The lid of the cylindrical test cell was closed and the sample was left for ~10 min. It shall be noted that the time taken varied depending on the presence of bubbles. It was important to ensure that the sample is completely free of bubbles.
- 3) The cylindrical test cell was placed in a fan oven.
- 4) The connection between the cylindrical test cell, power source, and measuring devices was established, as shown in Figure 4-2.
- 5) Because the gap between the inner and outer electrode is 2 mm, the applied voltage was set at 2 kV to achieve 1 kV/mm.
- 6) Because temperature has a significant effect on the results obtained using this technique, the fan oven was set at 25 ± 1 °C. K-type thermocouple connected to a temperature meter was used to monitor the temperature changes in the oven.
- 7) The current for non-corrosive insulating oil (0 ppm (Sample 1)) was measured over a period of 996 s with 12-s intervals using Keithley 6517 picoammeter.
- 8) The conductivity of the non-corrosive insulating oil (0 ppm (Sample 1)) was calculated using Equation 4.6 and 4.7.
- 9) The cylindrical test cell was cleaned gently using acetone and then dried at 105 °C for 1 h to eliminate moisture.
- 10) The cylindrical test cell was then cooled to room temperature for ~10 min.
- 11) Steps 1–10 were repeated for other samples, as presented in Table 4-3.

Table 4-3. The details of oil samples used for DC conductivity measurements.

DBDS concentration (ppm)	Sample no.
0 (non-corrosive)	2 and 3
100 (corrosive)	1, 2, and 3
200 (corrosive)	1, 2, and 3

To analyse the pattern of initial oil conductivity due to corrosive sulphur, the initial current at 60 s was taken into account as suggested by ASTM D 1169 and [37].

4.3.3 RESULTS AND DISCUSSIONS

Because the presence of water in the insulating oils will significantly affect DC conductivity measurements, several tests were conducted to ensure that the water content is approximately the same for all the oil samples used in this study. Through experimentation, the optimum time taken to degas and dry the oil samples in the vacuum oven without any heating process was found to be four days. It was found that the water content of the insulating oils was 15 ± 1 ppm.

The DC conductivity measurement results (for a DBDS concentration of 0 ppm, measured at three different times) are presented in Figure 4-3. The temperature and water variations were measured at 25 ± 1 °C and 15 ± 1 ppm, respectively. The repeatability of this test is acceptable because the relative difference between each curve is no more than 27 % based on the average conductivity values determined every 12 s.

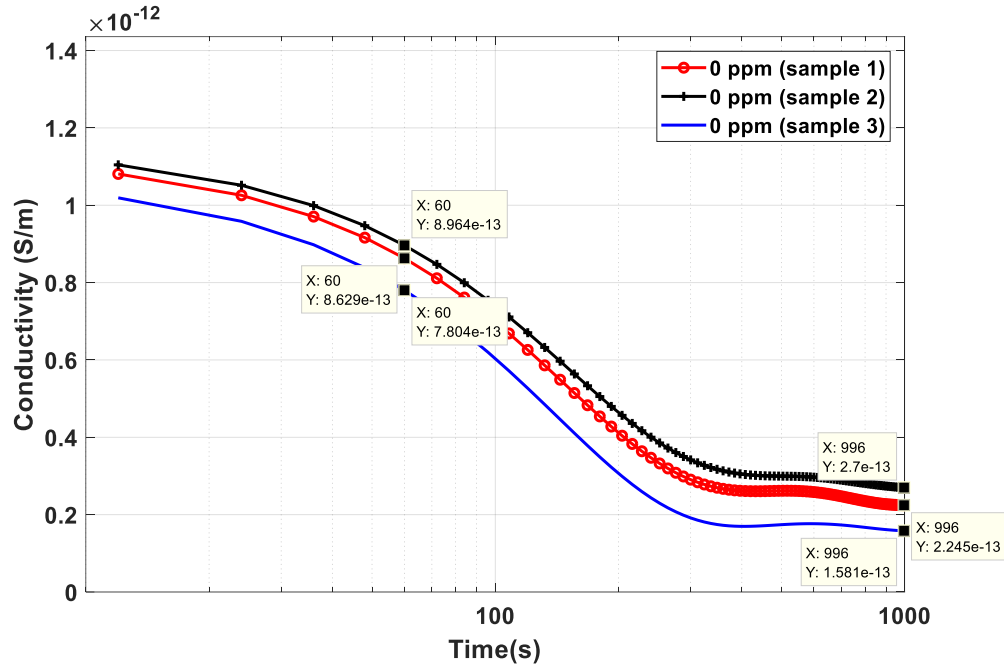


Figure 4-3. DC conductivity results of non-corrosive (0 ppm) oil samples under 1 kV/mm at 25 °C measured at three different times.

Figure 4-4 shows the DC conductivity results of non-corrosive (0 ppm) and corrosive (100 ppm, and 200 ppm) oil samples under 1 kV/mm at 25 °C measured at three different times. The result presented in Figure 4-4 is based on the corrosive and non-corrosive oil that consist of other non-impurities, such as furans, as a result of the degradation of the paper insulation in insulating oil. It is evident from the results that the DC conductivity graphs overlap each other — a result that contradicts the hypothesis mentioned in Section 4.3.1. It was difficult to characterise the oils even though the initial conductivity result revealed the possibility to distinguish between non-corrosive oil (0 ppm) and corrosive oil (200 ppm). This finding is attributed to the fact the same pattern was not observed for the corrosive oil with 100 ppm of DBDS.

The uncertainties in this DC conductivity measurement of corrosive by-product of DBDS, which was due to the breakdown of DBDS in the insulating oil, caused the results to become too complex to be interpreted, and any attempt of doing so might lead to misinterpretation. The difficulty in characterising the oil based on its corrosivity level is due to either uncertainty with respect to the amount of copper ions dissolved in the insulating oil (due to its low solubility) [52], which could not be differentiated by the DC conductivity

measurement or the influence of a very low concentrations of water content (~1 ppm). For this reason, measurement of conductivity was not pursued, instead a method using IDCs to detect changes in electrical capacitance due to the progression of sulphur corrosion in insulating oils was investigated. The variations of electrical capacitance were measured using IDCs fabricated onto a printed circuit board (PCB), which is described further in Section 4.4.

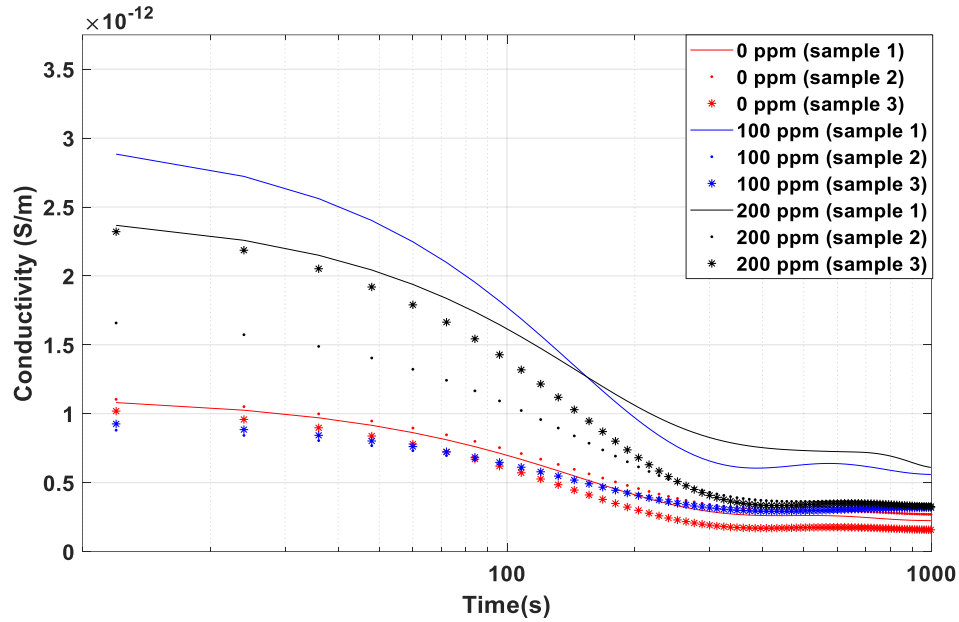


Figure 4-4. DC conductivity results of non-corrosive (0 ppm) and corrosive (100 ppm and 200 ppm) oil samples under 1 kV/mm at 25 °C measured at three different times.

4.4 INTERDIGITATED SENSORS (IDCs)

The IDCs were designed using EAGLE PCB design and schematic software. The IDCs were fabricated by Mr Richard Howell (Senior Engineer), and the calibration of IDCs and oil capacitance measurements were carried out by the author within the Undergraduate Teaching Laboratory, School of Electronics and Computer Science, Faculty of Physical Science and Engineering, University of Southampton.

4.4.1 FUNDAMENTAL PRINCIPLES AND PREVIOUS APPLICATIONS

Parallel plate capacitors (Figure 4-5) consist of two conducting plates with area A placed parallel to each other. The conducting plates are separated by a dielectric at a distance d .

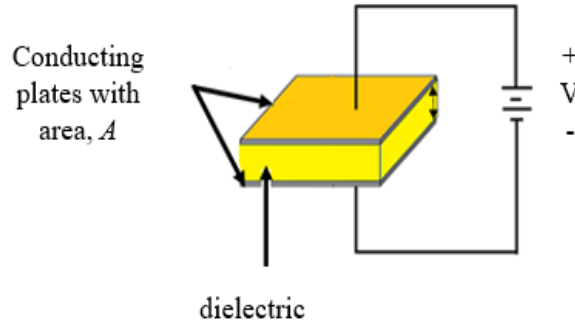


Figure 4-5. Schematic diagram of a parallel plate capacitor.

The main function of a capacitor filled with a medium is to store charge Q as soon as a potential difference ΔV is applied. The charge will remain stored even though the potential is disconnected. As indicated in Equation 4.8, the quantity of the charges being stored is dependent on the magnitude of the applied potential across the capacitor. In other words, capacitance is the ratio between the charges on the capacitor and the magnitude of the potential difference across the two parallel plates. The unit of capacitance is either Coulombs per Volt or Farad (F).

$$C = (Q/\Delta V) \quad 4.8$$

The capacitance of a parallel plate capacitor is determined from Equation 4.9:

$$C = \epsilon_0 \epsilon_r (A/d) \quad 4.9$$

where C is the capacitance, ϵ_0 is the permittivity of the free space (8.854 pF/m), ϵ_r is the dielectric permittivity of the material, A is the plate area, and d is the gap between the two parallel plates.

The electrical properties of insulating oils can be measured using this method by filling the region in between the two parallel plates with the insulating oil. The dielectric constant of the insulating oil can be determined in this manner. Compared to the conventional parallel plate capacitor, IDCs consist of a pair of coplanar interdigitated electrodes (fingers), as

shown in Figure 4-6. Figure 4-6(a) shows the top view of an IDC and Figure 4-6(b) shows the cross-sectional view of an IDC. The operating principle of IDCs is identical to that of a conventional parallel plate capacitor. The electric field between the fingers is generated by applying an AC voltage source between the positive and negative terminals. The capacitance of IDCs changed as the electric field generated penetrates the material under test. Therefore, the sensing behaviour of insulating oils can be observed by measuring the change in the capacitance of the IDCs.

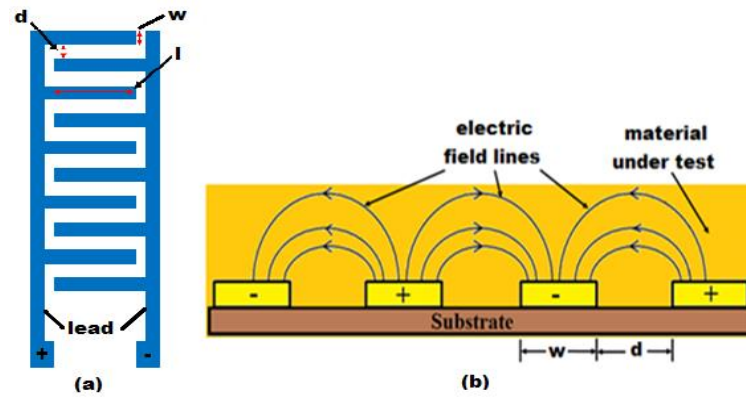


Figure 4-6. Schematic diagram of an IDC: (a) top view and (b) cross-sectional view.

The theoretical calculation of IDCs is inherently complex because it involves complex mathematical calculations such as conformal mappings [112],[113]. However, according to Bilican et al. [114] and Mamishev et al. [115], another easy approximation that can be used to determine the capacitance of IDCs is by applying the concept of a conventional parallel plate capacitor. Therefore, Equation 4.9 can be written as:

$$C = \epsilon_0 \epsilon_r (lwn/d) \quad 4.10$$

where l is the finger length, w is the finger width, n is the number of fingers, and d is the gap between two parallel fingers. However, the limitation of this approximation since the IDCs will not function well if the finger width and finger gap are not identical, which will affect the electric field distribution.

Two types of dielectric media are used in IDCs: solution (material under test) and substrate, as shown in Figure 4-7. Consequently, applying AC voltage creates electric field lines that

penetrate through these dielectric media, creating two parallel plate capacitors. Therefore, the total capacitance is given by [114]:

$$C_{total} = C_{sub} + C_{up} \quad 4.11$$

where C_{sub} is the total capacitance of the substrate and C_{up} is the change in capacitance resulting from exposure of the sensor to air or liquid having a different dielectric constant.

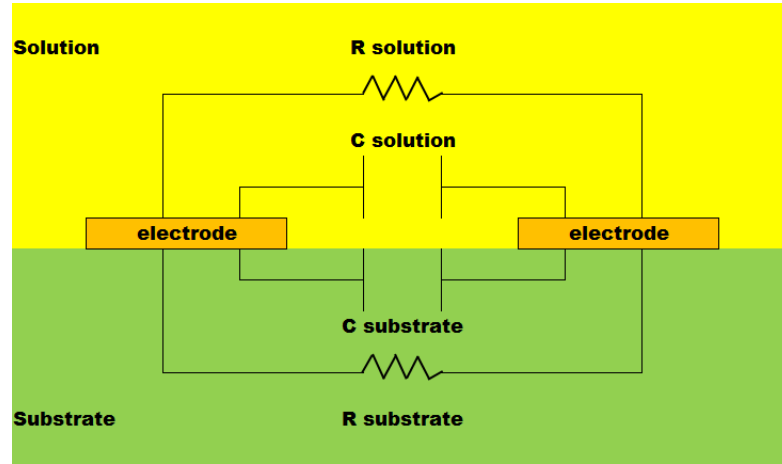


Figure 4-7. Equivalent circuits of interdigitated electrodes [114].

The earliest interdigital electrode design was created by Nikola Tesla in 1891 [115]. According to Tesla, the total capacitance of the “electrical condenser” increases in proportion with the number of fingers when the finger electrode is immersed in an insulating liquid. His idea has inspired many researchers to apply this concept in their own field, particularly in sensing and detection systems.

The use of IDCs is not new — in fact, these sensors have been exploited for a wide range of applications including temperature sensors [116], moisture sensors [117], and biosensors [118]. A number of studies have also been carried out on complex mathematical calculations and simulations of IDCs as well as complex chemical surface treatment of IDCs [114]. Furthermore, Khan et al. [119]–[121] developed IDCs to detect the variation of different taste substances such as sourness, saltiness, sweetness, and bitterness. Interestingly, IDCs have also been applied for real-time analysis of water contaminants [121] and as biosensors [118].

One of the advantages of IDCs is that these sensors use relatively small and simple metal interdigitated electrodes. Thus, the fabrication cost of IDCs is relatively inexpensive compared to the cost of fabricating optical and chemical sensing systems. The interdigital geometry improves the sensitivity of IDCs while reducing the surface area. Hence, IDCs can be fabricated in bulk quantities on simple substrates such as FR-4 PCB or glass by implementing a simple evaporation process. For capacitance measurements, IDCs can be used without the need for complex calibration procedures. Unlike conventional parallel plate capacitors, IDC fingers completely adhere onto the substrate and thus the gap distance is kept at a constant value. Therefore, IDCs improve the accuracy of capacitance measurements.

4.4.2 DESIGN, CONSTRUCTION AND FABRICATION

The main aim of Section 4.4 is to investigate the feasibility of IDCs in sensing the presence of sulphur corrosion in transformer oils by measuring the changes in the capacitance values of the corrosive insulating oil compared to the new insulating oil. In this research, only one IDCs configuration has been tested because the results presented in Section 4.4.4 revealed that this technique is highly affected by the presence of water content in the insulating oils which leads to the misinterpretation of the results.

The variables of the IDCs design are finger length l , finger width w , finger gap d , and number of fingers n . The values of these variables are 8, 0.5, 0.5 mm, and 16 respectively. Ideally, the gap between the fingers should be minimised because this variable will increase the sensitivity of the sensor. However, in this study, a gap of 0.5 mm was chosen because of the limitations of the PCB fabrication set-up in the laboratory. According to Bilican et al. [114], Equation 4.10 is suitable only if the finger gap and finger width are the same. For this reason, the sensor was designed with the finger gap and finger width being equal to 0.5 mm. The capacitance of IDCs is commonly affected by the stray capacitance of the leads (Figure 4-6(a)) and therefore, it is essential to minimise the effect of stray capacitance by having a large number of fingers [115]. A schematic diagram of the proposed IDCs is shown in Figure 4-8.

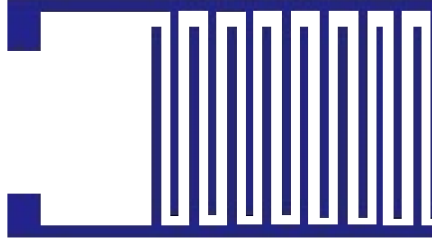


Figure 4-8. Schematic diagram of the proposed IDCs designed using EAGLE PCB design and schematic software.

The IDCs were fabricated using a photolithographic process on a copper clad FR-4 PCB laminate. The IDCs were fabricated on the PCB using the following procedure:

- 1) The pattern was designed using EAGLE PCB design and schematic software.
- 2) The mask for the sensor pattern was prepared by transferring the EAGLE drawing onto a polyester drafting film using a high-resolution laser printer.
- 3) The sensor pattern was transferred onto a photoresist-coated copper clad PCB by ultraviolet (UV) photolithography.
- 4) The sensor pattern was inspected to ensure that there were no defects.
- 5) The sensor pattern was dried.
- 6) The sensor pattern was formed by exposing the copper clad FR-4 PCB to ferric chloride solution, followed by agitation. The PCB was then turned over for ~20 min to remove unwanted copper. The process time generally depends on the amount of copper to be removed. It shall be noted that this process needs to be carried out with painstaking detail since there is a high possibility for the tracks to be over-etched.
- 7) The PCB was washed with water followed by an acetone to clear the photo resist.

The degradation of insulating oils caused by sulphur corrosion was analysed based on the electrical capacitance of the oil samples measured using the IDCs.

4.4.3 EXPERIMENTAL SET-UP AND PROCEDURE

The sample preparation (i.e. corrosive oil samples and bare copper samples) and thermal ageing of the samples in air atmosphere using a fan oven were carried out at the chemical

preparation room in the Tony Davies High Voltage Laboratory, University of Southampton, following the procedure described in Section 3.2. According to Scatiggio et al. [18], the maximum DBDS concentration in an actual oil-filled power transformer is 350 ppm. Therefore, the DBDS concentrations used in this study were below 350 ppm. In total, 9 samples were prepared because the analysis was based on DBDS concentrations (100, 200, and 300 ppm) and ageing time (i.e. Day 1, Day 2, and Day 3). Figure 4-9 shows the schematic diagram of the experimental set-up of the proposed IDC sulphur corrosion sensing system. The list of equipment used for the oil capacitance measurements is provided in Table 4-4.

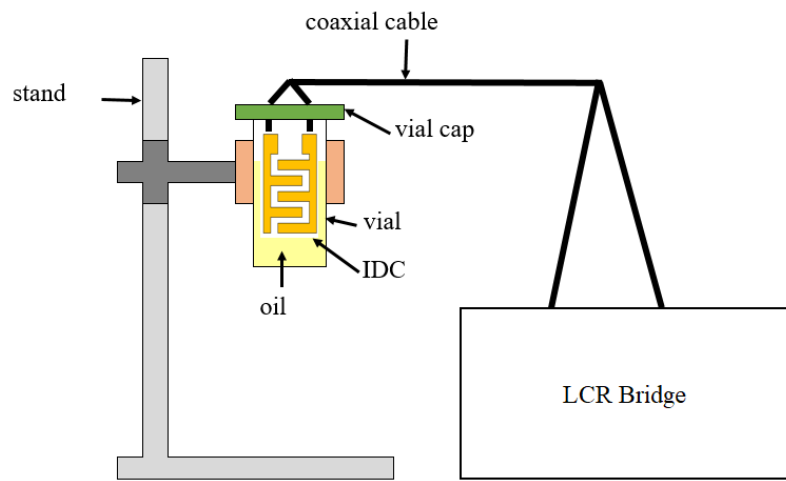


Figure 4-9. Schematic diagram of the experimental set-up of the proposed IDC sulphur corrosion sensing system.

Table 4-4. List of equipment for oil capacitance measurements

1	Clamp stand
2	Eppendorf Multipette® Stream pipette and 25 mL Combi-tips® Plus with adapter
3	15 mL headspace vials with plastic caps
4	IDCs connected via a coaxial cable
5	Fluke 971 temperature humidity meter
6	LCR400 precision LCR bridge
7	Corrosive insulating oil samples

The procedure used for the oil capacitance measurements is presented below:

- 1) The IDCs were placed into an empty 15 mL clean headspace vial and the vial was sealed tightly with the plastic cap.

- 2) The vial was held in place using the clamp stand, as shown in Figure 4-9.
- 3) The IDCs were connected to the LCR400 precision LCR bridge (Aim and Thurlby-Thandar Instruments, UK). The use of a coaxial cable is extremely important since this will improve accuracy of the measurements by minimising the effect of stray capacitance.
- 4) The LCR400 precision LCR bridge was switched on.
- 5) A Fluke 971 temperature humidity meter was used to monitor the ambient temperature. The ambient temperature was within a range of 21 ± 1 °C. This step is vital because variations in temperature will affect the oil capacitance measurements. In addition, the optimum operating temperature range for the Eppendorf Multipette® Stream pipette is 5–40 °C [122].
- 6) Gently, 10 mL of new oil was pipetted into a clean headspace vial (15 mL) using Eppendorf Multipette® Stream pipette equipped with 25 mL Combi-tips® Plus with adapter.
- 7) The sample was left for ~10 min. It shall be noted that the time taken varied depending on the presence of bubbles. It was important to ensure that the sample is completely free of bubbles.
- 8) The IDCs were placed into the vial containing the insulating oil as indicated in Step 7 and the vial was sealed tightly with the plastic cap.
- 9) The capacitance of the new insulating oil C_1 was measured.
- 10) The IDCs were cleaned gently using soft tissues saturated with acetone. The IDCs were left to dry at room temperature for ~10 min.
- 11) Steps 1–8 were repeated by replacing the new insulating oil in Step 6 with the corrosive insulating oil as presented in Table 4-5.
- 12) The capacitance of each corrosive insulating oil C_2 was measured.
- 13) The changes in the capacitance values of the corrosive insulating oil compared to the new insulating oil was calculated using the following formula: $\Delta C = C_2 - C_1$.
- 14) The IDCs were cleaned gently using soft tissues saturated with acetone. The IDCs were left to dry at room temperature for ~10 min.

The measurement procedure was repeated three times for each sample to determine the repeatability of the results.

Table 4-5. The details of oil samples used for capacitance measurements.

Ageing time	DBDS concentration (ppm)
Day 1	100, 200, and 300
Day 2	100, 200, and 300
Day 3	100, 200, and 300

4.4.4 RESULTS AND DISCUSSION

As the presence of water in the insulating oil will significantly affect the oil capacitance measurements, several tests were conducted to ensure that the water content was the same for all the insulating oil samples in this study. It was found that the water content of the insulating oils was 13 ± 1 ppm. Through several experimental works, the optimum time taken to degas and dry the oil samples in the vacuum oven without any heating process was six days.

In general, the presence of contaminants such as cellulose fibres or metallic particles (due to sulphur corrosion) in the insulating oils can lead to oil and paper degradation, as well as internal discharge which results in catastrophic power transformer failures. For this reason, it is essential to monitor the health index of insulating oils to implement countermeasures. One of the possible monitoring tools that can be used to monitor the progression of sulphur corrosion in insulating oils is by measuring the oil capacitance values using IDCs. It is hypothesised that either copper ions or corrosive by-products due to the breakdown of DBDS in the insulating oil (as a result of sulphur corrosion) will increase the oil capacitance values. This hypothesis is validated by the results shown in Table 4-6 and Table 4-7, respectively. The results presented in this section suggest a potential relationship between corrosive by-products due to the breakdown of DBDS and changes in oil capacitance values. It can be seen that the increase in oil capacitance values, ΔC (pF) measured using the IDCs, is proportional to the increase in the amount of copper in per cent by weight, ΔCW (%), which was obtained from the SEM–EDX analysis. The increase in weight percent of the bare copper samples suggests that a dissolution of copper ion occurred due to sulphur corrosion in the insulating oils. These results are comparable with one of the empirical theories proposed by CIGRE through their Working Group A2.40 [9], which suggests that the formation of copper sulphide begins with dissolution of copper in an insulating oil.

On Day 1, there was an increase in ΔC with the range of 0.02–0.03 pF as the DBDS concentrations were increased from 100 ppm to 200 ppm, and from 200 ppm to 300 ppm. The same pattern could be observed in Table 4-7, whereby the ΔCW increased by approximately 0.40 % for both cases. However, it could be observed that the increment of ΔC for Day 2 and 3, was not linear compared with the ΔCW shown in Table 4-7. Interestingly, an increase in ΔC was still noted when the DBDS concentration was increased from 200 ppm to 300 ppm on Day 3 although the amount of copper on the surface of copper sample increased by only 0.12 %. It is believed that the moisture present in the oil can be a contributing factor for the observed increase in the ΔC . As the variations in ΔC were extremely low (0.01–0.13 pF), there is a great possibility that the results obtained via this method can be misinterpreted because some external effects (i.e. temperature and water content) might vary during the measurements.

Table 4-6. Variation in ΔC of insulating oil with respect to the ageing time for three DBDS concentrations.

DBDS concentration (ppm)	Day 1		Day 2		Day 3	
	ΔC (pF)	Standard deviation (pF)	ΔC (pF)	Standard deviation (pF)	ΔC (pF)	Standard deviation (pF)
100	0.01	0.0058	0.05	0.0058	0.06	0.0100
200	0.04	0.0058	0.06	0.0115	0.08	0.0100
300	0.06	0.0173	0.08	0.0100	0.11	0.0100

Table 4-7. Changes in copper weight (%) of the copper strips with respect to the ageing time for three DBDS concentrations.

DBDS concentration (ppm)	Day 1		Day 2		Day 3	
	ΔCW (%)	Standard deviation (%)	ΔCW (%)	Standard deviation (%)	ΔCW (%)	Standard deviation (%)
100	1.64	0.23	3.17	0.41	6.34	0.24
200	2.01	0.15	4.96	0.27	8.71	0.42
300	2.46	0.04	5.64	0.48	8.83	0.23

The increase in ΔC was exceptionally small as the samples were aged under accelerated ageing conditions within a very short period of time. Besides the DBDS concentrations used in this research were very low which contributes to the slow sulphur corrosion process. Therefore, the feasibility of this method in detecting the presence of corrosive sulphur in insulating oils could be enhanced by increasing the ageing time and DBDS concentrations, respectively.

Practically, it is expected that the changes in ΔC of the corrosive oils could be due to three reasons: (1) the presence of copper ions as a result of sulphur corrosion, (2) the effect of water content in the insulating oils, and (3) the presence of other compounds resulting from higher oil acidity. The difficulty in distinguishing between these effects leads to the conclusion that IDCs is not a practical to be implemented as sulphur corrosion sensors.

4.5 SUMMARY

This chapter presents the effect of corrosive oil that contains the corrosive by-products due to the breakdown of DBDS on both DC conductivity measurements and capacitance measurements (via IDCs). The results of DC conductivity measurements show that the graph overlaps each other and therefore it was not feasible to characterise the corrosivity level of oil by means of this method. On the other hand, the changes in the oil capacitance values due to the presence of different corrosive by-product of DBDS were remarkably small which leads to a high possibility of misinterpretation of the results. As a consequence from both studies, a better indication of non-practicality of both methods was obtained. Because these techniques are greatly influenced by moisture and water, it is evident that this technique is unfeasible to be implemented either on-site or in real-time. To summarise, in future experimental work, it would be essential to find a feasible and reliable technique that could monitor the progression of sulphur corrosion in insulating oil without the influence of other external disturbances such as the variations in water and temperature during the measurement activity. It is noteworthy to look into the effect of sulphur corrosion by investigating the changes in the solid (copper) rather than liquid (insulating oil) via electrical techniques.

5 THIN FILM SACRIFICIAL COPPER STRIPS FOR SULPHUR CORROSION SENSING

5.1 INTRODUCTION

The findings presented in this chapter are of significance for online condition monitoring of sulphur corrosion because the developed approach allows quantitative measurement using a thin film sacrificial copper strip to detect the progression of sulphur corrosion in transformer insulating oils. The fabrication of the thin film sacrificial copper strips is first described (Section 5.2), followed by the principle of low-resistance measurements (Section 5.3). The fabrication process, experimental set-up, data collection, and data analysis of these sensors were conducted entirely by the author using the facilities available in the Integrated Photonics Cleanroom, Optoelectronics Research Centre, University of Southampton, and The Tony Davies High Voltage Laboratory, University of Southampton. With access to the Nanofabrication Centre, University of Southampton, the pre-cleaning and cutting processes of *Sensors Type C* were carried out by Dr Kian Kiang from the Optoelectronics Research Centre, University of Southampton. The development of the thin film sacrificial copper strips based on the 2^2 factorial design is described in this Chapter, along with the development of a regression model used to predict the transformed resistance of the sensors as a function of their area and thickness. The feasibility of these sensors in tracking the progression of sulphur corrosion due to the presence of corrosive by-products of DBDS and elemental sulphur is presented in Section 5.5 and Section 5.6. A novel online method was proposed for quantification of elemental sulphur in transformer insulating oils using the thin film sacrificial copper strip sensors, which is elaborated in Section 5.7. A journal paper summarising the findings of this work has been accepted for publication in Measurement [123].

5.2 FABRICATION OF SENSORS

The sensors (thickness: 50–200 nm) were fabricated by evaporating pure copper (purity: 99.99 %) onto a glass substrate/wafer, depending on the application. Solely evaporating a layer of copper onto the glass substrate/wafer leads to the “easily peeling off” issue. To improve the thin film copper adhesion, a titanium layer (thickness: 5 nm) was evaporated prior to copper evaporation. The evaporation of copper and titanium were conducted by using BOC Edwards E500a e-beam evaporator with a vacuum pressure of 10^{-6} mbar in nitrogen atmosphere.

It is essential to clean the surface of the glass substrate/wafer to obtain consistent resistance values for each sensor. Hence, the glass substrates/wafers was pre-cleaned using an ultrasonic bath with acetone (~10 min) and isopropanol (~10 min). After ultrasonic cleaning, the glass substrates/wafers were rinsed with deionised water, blow-dried with nitrogen, and lastly, heated using a hot plate (~5 min). The evaporation process was conducted immediately after the pre-cleaning process to reduce surface contamination of the glass substrates/wafers. The fabricated sensors were stored in a desiccator (whose lower compartment was filled with silica gel) to prevent surface oxidation of the sensors.

Table 5-1 shows the details of the thin film sacrificial copper strips fabricated in this research, namely, the sensor type, substrate type, fabrication type, the method used to obtain the desired area, and the copper and titanium area. Unlike *Sensors Type A* and *Type B* (where each sensor was fabricated individually), *Sensors Type C* could be fabricated simultaneously in bulk (34 sensors at a time), which would significantly reduce fabrication time and cost. Nevertheless, the surfaces of *Sensors Type C* required special coating to protect them from any scratches resulting from the debris produced by the glass wafer during the cutting process. Hence, *Sensors Type C* were coated with ~1.3 μm MICROPOSITTMS1813TM G2 photoresist before they were cut into individual units, as shown in Figure 5-1(b). For the coating process, the photoresist was poured onto the glass wafer, which was placed inside the sample holder of a spin coater (SCS G3P-8, Specialty Coating Systems, Inc., USA). The sensors were spun at a rotation speed of 4500 rpm for ~3 min. Finally, the sensors were soft-baked at 115 °C for ~1 min using a precision hot plate (Model: 1000-1, Electronic Micro Systems Ltd., UK).

As presented in Table 5-1, three type of sensors were used for this research, namely *Sensor Type A*, *Type B*, and *Type C*. *Sensor Type A* was firstly used in this research mainly for proof of concept. *Sensor Type B* was then used to improve the sensitivity of measurement and the quality of the sensors. *Sensor Type C* was the final sensor employed to establish the principle of using a shadow mask approach to allow simultaneous fabrication of single sensors in bulk.

Table 5-1. Details of the thin film sacrificial copper strips fabricated in this research.

Sensor type	Method used to obtain the desired area	Copper and titanium area (mm ²)	Substrate type	Fabrication type
<i>A</i>	Kapton tape (both edges)	1375	Rectangular glass substrate (area: 1875 mm ² , thickness: 0.8–1.0 mm)	Individual fabrication (one sensor on each glass substrate)
<i>B</i>	Shadow mask	100–800	Rectangular glass substrate (area: 1875 mm ² , thickness: 0.8–1.0 mm)	Individual fabrication (one sensor on each glass substrate)
<i>C</i>	Shadow mask (Figures 5-1 and 5-2)	100	6-in glass wafer (thickness: 0.7 mm) * Each sensor has an area of 350 mm ²	Bulk fabrication (34 sensors on a 6-in glass wafer)

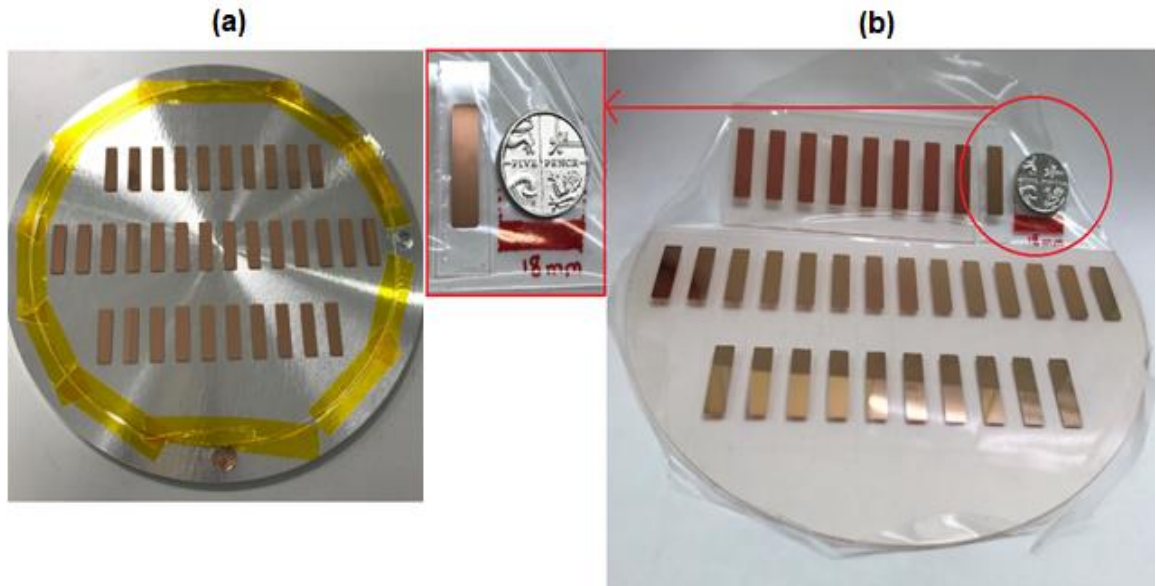


Figure 5-1. Bulk fabrication of *Sensors Type C*. In (a), 34 sensors were fabricated on a 6-in glass wafer. In (b), the sensors were adhered onto a tape before they were cut into individual units. The actual size of the sensors was compared to the size of a five pence (5p) coin (inset).

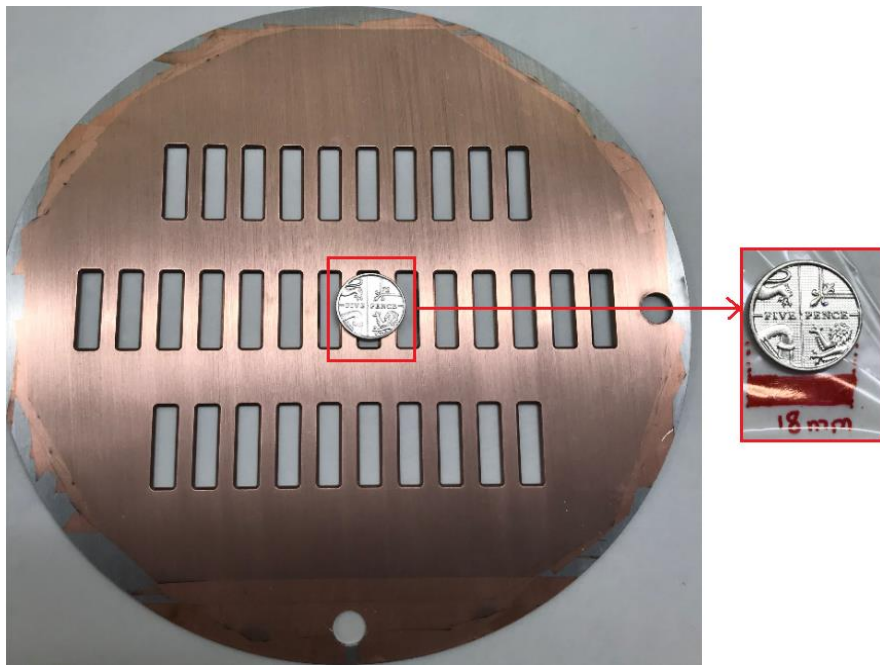


Figure 5-2. Shadow mask used for bulk fabrication of *Sensors Type C*. The size of a cut-out in the shadow mask was compared to the size of a five pence (5p) coin (inset).

5.3 PRINCIPLE OF THE LOW-RESISTANCE MEASUREMENTS

Several experiments have been carried out to investigate the effect of ambient temperature (20 ± 1 °C) towards the resistance measurements of copper samples. As compared to a long and thin copper wire, the resistance of a short and thick copper wire was greatly affected by the variation of ambient temperature (20 ± 1 °C). To overcome this issue, the thin film sacrificial copper strips sensors have been proposed.

The resistance of the thin film sacrificial copper strips was measured based on low-resistance measurements using the four-wire measurement method. Figure 5-3 shows the schematic of the experimental set-up used for the low-resistance measurement. The test cell presented in Figure 5-3 is designed to ensure that all of the probes are at the same position while the resistance measurements are carried out.

The details of each component in the experimental set-up are presented in Table 5-2. The low-resistance measurements were performed in a temperature and humidity-controlled environmental room, where the temperature and relative humidity were set at 20 ± 1 °C and 20 ± 10 %. A digital micro-ohmmeter (Megger DucterTM DLRO-10X, Megger Ltd., UK) was used to measure the resistance of the sensors.

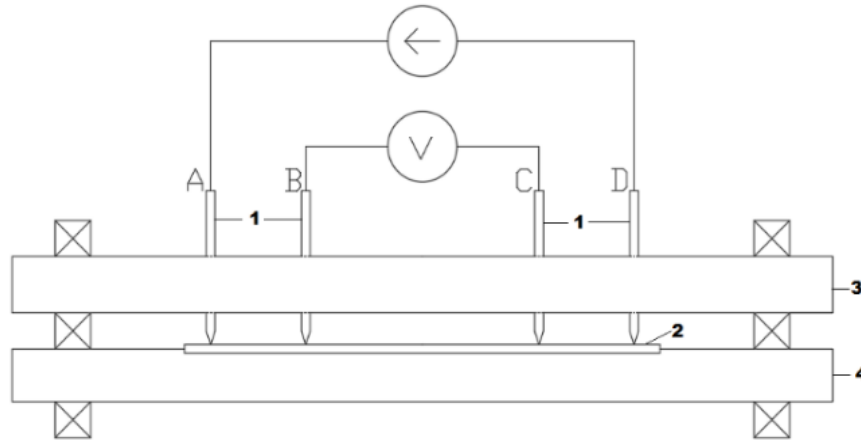


Figure 5-3. Schematic of the experimental set-up used to measure the resistance of the thin film sacrificial copper strips using the four-wire measurement method.

Table 5-2. Structural details of the test cell.

Label	Description
1	Measurement copper needles
2	Thin film sacrificial copper strip sensor
3	Electrode holder made from polyethylene terephthalate (thickness: 6.4 mm)
4	Sensor holder made from aluminium (thickness: 6 mm)

In the four-wire measurement method, the resistance values of the sensors were obtained by measuring the voltage when four collinear probes came into contact with the sensor surface. Because the measured resistance is relatively low, this method eliminates cable and contact resistance. Forward current and reverse current were applied to eliminate thermo-electromotive forces, which would manifest as offset voltage (parasitic voltage). The resistance measurement was repeated at least five times for each experimental condition to ensure that the results were consistent. As shown in Figure 5-3, the potential difference between Probes B and C (V_{BC}) was measured when there was a current of I_{AD} between Probes A and D. The resistance of each thin film sacrificial copper strip was calculated using the following equation:

$$R = V_{BC}/I_{AD} \quad 5.1$$

Table 5-3 shows the separation distance between the probes (i.e. Probes A–B, B–C, and C–D) and the applied current used in this research. The separation distances for *Sensors Type A* were larger compared with those *Sensors Type B and Type C* because these sensors had the largest copper area (Table 5-1). For *Sensors Type B and Type C*, 100 μ A of current was applied to obtain the change in resistance (ΔR) in ohms Ω . Theoretically, the reaction between the corrosive by-products due to the breakdown of DBDS and copper is relatively slow compared with the reaction between elemental sulphur and copper. For this reason, the applied current for the low-resistance measurements was increased to 100 mA so that ΔR can be measured in milliohms ($m\Omega$).

The change in resistance (ΔR) of the thin film sacrificial copper strips as a result of sulphur corrosion caused by the corrosive by-products of DBDS or elemental sulphur was calculated using the following equation:

$$\Delta R = R_i - R_n \quad 5.2$$

where R_n is the measured resistance after a certain ageing period and R_i is the measured initial resistance prior to ageing. It shall be noted that the variations in the initial resistance of the sensors will not have a significant influence on the low-resistance measurements, considering that the effect of sulphur corrosion on the sensors is represented by ΔR .

Table 5-3. Details of the probe separation distances and applied current used in this research.

Sensor type	Separation distance of the probes (mm)	Applied current (A)
<i>A</i>	A–B: 6, B–C: 18, C–D: 6	100×10^{-3}
<i>B</i>	A–B: 5, B–C: 5, C–D: 5	100×10^{-6}
<i>C</i>	A–B: 5, B–C: 5, C–D: 5	100×10^{-6}

5.4 DEVELOPMENT OF THE SENSORS BASED ON THE 2^2 FACTORIAL DESIGN

The OFAT method is a conventional method to design experiments, which involves determining the response variable by varying one input variable while the other input variables are fixed. Despite its ease of implementation [124], the OFAT method is not suitable to determine the effects of multiple input variables simultaneously because it is difficult to define the interactions between the input variables. In this regard, design of experiments (DoE) is suitable to determine the effects of multiple input variables on the response variable. This method significantly reduces the number of test runs, which in turn, reduces production time and cost. For these reasons, the DoE method has been used extensively in the manufacturing industry. Figure 5-4 shows the advantage of using the DoE method compared with the OFAT method for a three-factor experimental design. It can be seen that the DoE method only requires eight test runs whereas OFAT method requires 16 test runs, which is twice the number of runs for the DoE method [125].

In general, there are various DoE methods that can be used to examine the relationship between the main factors and interaction factors in multi-factor experiments such as the 2^k factorial design, Box-Behnken design [124], Taguchi method [126], and response surface methodology [127]. In this research, the 2^2 factorial design was selected to develop a

regression model that is capable in predicting the transformed resistance of the thin film sacrificial copper strips as a function of their area and thickness. Analysis of variance (ANOVA) was performed to access the adequacy of the regression model. For this analysis, *Sensors Type B* were fabricated according to the procedure described in Section 5.2.

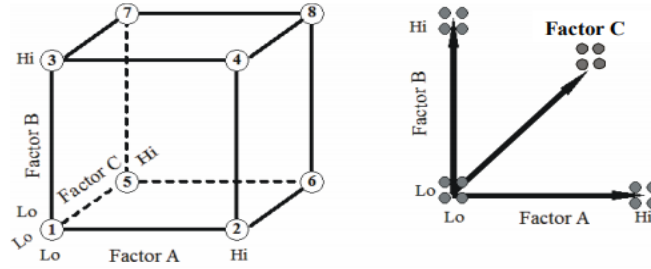


Figure 5-4. Advantage of using the DoE method (left) compared with the OFAT method (right) for a three-factor experimental design [125].

5.4.1 SCREENING EXPERIMENT

The 2^2 factorial design was performed using Design-Expert® software version 10.0 (Stat-Ease, Inc., USA). A screening experiment was carried out to analyse the effects of two independent variables (area and thickness) on the resistance of the sensors, with three repetitions for each test run. The 2^2 factorial design matrix (consisting of 12 test runs) was used to screen the variables, as shown in Table 5-4. Table 5-5 presents the coded levels of each factor, where the minimum and maximum levels were coded as -1 and $+1$, respectively. The resistance measurements of the sensors were conducted based on the 2^2 factorial design matrix. The effects of area and thickness on the transformed resistance of the thin film sacrificial copper strips were examined based on the half-normal and effect list. Next, a regression model was developed to predict the transformed resistance of the thin film sacrificial copper strips as a function of their area and thickness. The statistical significance and adequacy of the regression model were assessed using ANOVA. The outcomes retrieved from 2^2 factorial design will determine the fit of the regression model, which consists of coefficients multiplied by their respective factor levels. The regression equation is given by:

$$Y = \beta_0 + \beta_1 x_1 + \beta_2 x_2 + \beta_{12} x_1 x_2 \quad 5.3$$

Here, Y is the response variable, β_n represents the coefficient associated with Factor n , whereas x_1 and x_2 are the variables that represent Factors A and B , respectively. The product x_1x_2 denotes the interaction between Factors A and B , β_1x_1 and β_2x_2 denote the individual effects of x_1 and x_2 , respectively. $\beta_{12}x_1x_2$ denotes the two-factor interaction between x_1 and x_2 , and β_0 is the model intercept. Next, regression analysis was performed in units that were coded, while coefficients had been based on the coded units. Following this, ANOVA was carried out to obtain the means squares (MS), coefficient of determination (R^2), sum of squares (SS), as well as p -values, and F -values. The response surface plot was employed to visually identify the interaction between the factors that affected the transformed resistance the thin film sacrificial copper strips. Experiments were then carried out to validate the linear regression model that describes the effects of the independent variables (area and thickness) on the dependent variable.

Table 5-4. 2^2 factorial design matrix used to screen the factors.

Test run		1	2	3	4	5	6	7	8	9	10	11	12
Coded level	A: Area (mm ²)	+1	+1	+1	-1	+1	-1	-1	-1	+1	-1	+1	-1
	B: Thickness (nm)	-1	-1	-1	+1	+1	+1	-1	-1	+1	+1	+1	-1

Table 5-5. Uncoded and coded levels of the factors.

Factor 1 (A: Area (mm²)) Type: Numeric	Factor 2 (B: Thickness (nm)) Type: Numeric
100 (-1)	50 (-1)
800 (+1)	70 (+1)

5.4.2 RESULTS OF THE SCREENING EXPERIMENT

Figure 5-5 and Table 5-6 illustrate the half-normal plot and effect list, respectively, obtained from the screening experiment. It can be seen from Figure 5-5 that Factor A (area), Factor B (thickness), and Interaction AB (interaction between area and thickness) are located away from the straight line. In other words, none of these variables are coincident with the straight

line. Factor *A*, Factor *B*, and Interaction *AB* were found to be significant model terms. These outputs were supported by the effect list Table 5-6, where it is evident that Factor *A* was the most significant factor with a percentage contribution and sum of squares of 90.19 % and 2.78, respectively. This was followed by Factor *B* with a percentage contribution and sum of squares of 7.98 % and 0.25, respectively. On the contrary, the Interaction *AB* displayed a contribution of 0.14 %, which signified the least contribution of this particular factor amongst the rest. The sum of squares for Interaction *AB* was 0.004. From the outcomes, Factor *A* significantly contributes higher to the transformed resistance of the sensors, when compared to Factor *B* and Interaction *AB*. It shall be noted that 1.69 % of the percentage contribution was due to error.

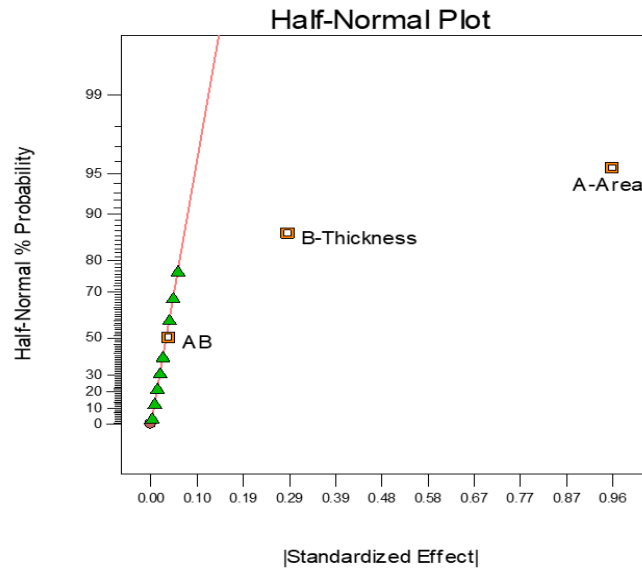


Figure 5-5. Half-normal plot for the screening factors.

Table 5-6. Effect list of all model terms obtained from for the screening experiment.

Model term	Standardised effects	Sum of squares, <i>SS</i>	Percentage contribution (%)
<i>A</i>	0.96	2.78	90.19
<i>B</i>	0.29	0.25	7.98
<i>AB</i>	0.038	0.004	0.14
Error		0.052	1.69

5.4.3 REGRESSION MODEL

The regression model developed based on the 2^2 factorial design, which describes the transformed resistance the thin film sacrificial copper strips as a function of their area and thickness, is expressed as:

$$\frac{1}{\sqrt{R}} = 1.38 + 0.48x_1 + 0.14x_2 + 0.019x_1x_2 \quad 5.4$$

The response plot was plotted to visualise how the factors influence the transformed resistance of the sensors, as shown in Figure 5-6. It can be observed that the transformed resistance increased gradually when the area decreased from 800 mm² to 100 mm² and when the thickness decreased from 70 nm to 50 nm. The predicted transformed resistance values (Y') presented in Table 5-7 were obtained from the regression model (Equation 5.4). The residuals appeared to be reasonably small (below 0.10 Ω), although two of them were found to be slightly higher (0.16 Ω and 0.13 Ω , respectively). These values suggest that while fabricating the thin film sacrificial copper strips, it is necessary to avoid having a large area and higher thickness of copper at the same time. Increasing these two parameters at the same time results in a higher chances of either surface contamination or non-uniform deposition to be occurred.

The ANOVA results for 2^2 factorial design are summarised in Table 5-8. It can be seen that the overall regression model was statistically significant because the p -value was less than 0.0001, which was below the significance level of 0.05. In addition, the p -values of the individual factors were less than 0.05 (<0.0001, 0.0003, and 0.4341 for Factor A, Factor B, and Interaction AB, respectively). The R^2 value was determined to be 0.9831, indicating that the model can describe 98.31 % of the total variation of the transformed resistance of the thin film sacrificial copper strips due to variations in their area and thickness. Based on the results, it can be deduced that the regression model developed in this research was reasonable.

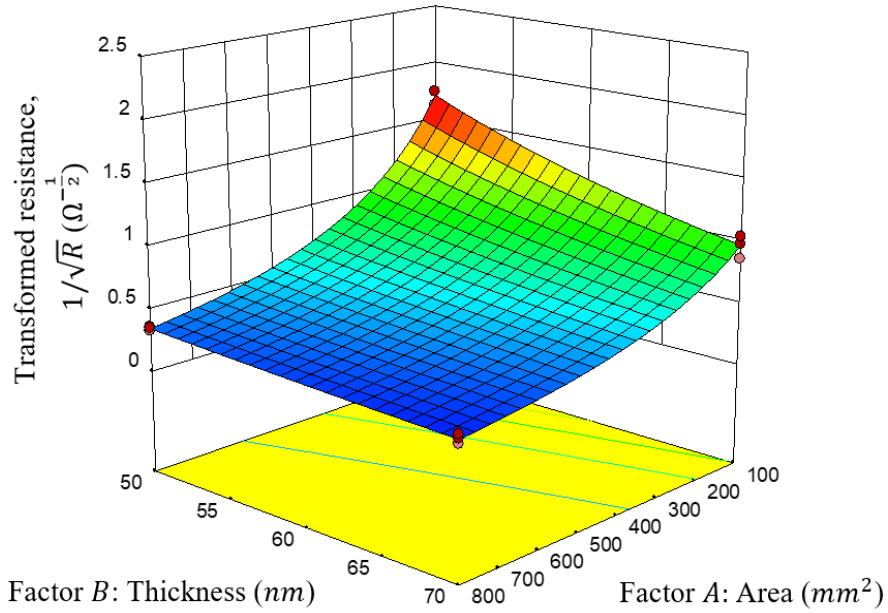


Figure 5-6. Response surface plot of the transformed resistance as a function of the area and thickness of the thin film sacrificial copper strip sensor.

Table 5-7. Measured and predicted transformed resistance values of the thin film sacrificial copper strip sensor obtained from the regression analysis.

Test run	Measured transformed resistance value, Y ($\Omega^{-1/2}$)	Predicted transformed resistance value, Y' ($\Omega^{-1/2}$)	Residual, $Y - Y'$ ($\Omega^{-1/2}$)
1	1.69	1.70	-0.01
2	1.74	1.70	0.04
3	1.67	1.70	-0.03
4	1.01	1.02	-0.01
5	2.18	2.02	0.16
6	0.98	1.02	-0.04
7	0.76	0.77	-0.02
8	0.79	0.77	0.01
9	2.00	2.02	-0.02
10	1.08	1.02	0.06
11	1.89	2.02	-0.13
12	0.78	0.77	0.01

Table 5-8. ANOVA results obtained from the 2² factorial design.

Source	Sum of squares, <i>SS</i>	Degrees of freedom, <i>Df</i>	Mean square, <i>MS</i>	<i>F</i> -value	<i>p</i> -value	Coefficient of determination, <i>R</i> ²
Model	3.030	3	1.010	155.30	< 0.0001	0.9831
Factor <i>A</i> : Area	2.780	1	2.780	427.38	< 0.0001	
Factor <i>B</i> : Thickness	0.250	1	0.250	37.83	0.0003	
Interaction <i>AB</i>	0.004	1	0.004	0.68	0.4341	
Pure error	0.052	8	0.007			
Corrected total sum of squares	3.080	11				

5.4.4 VALIDATION OF THE REGRESSION MODEL

Three additional thin film sacrificial copper strips (area: 300–800 mm², thickness: 60–70 nm) were fabricated in order to validate the regression model (Equation 5.4) developed in this research. The measured transformed resistance values were obtained by measuring the resistance values of the sensors while the predicted transformed resistance values of the sensors were determined using Equation 5.4. The predicted values were compared with the measured values, as shown in Table 5-9. The mean percentage difference between the measured and predicted values was determined to be 5.80 %. The root mean square error (*RMSE*) between the measured values (\hat{y}) and the predicted values (y) was calculated using the following equation:

$$RMSE = \sqrt{\frac{1}{n} \sum_{i=1}^n (\hat{y}_i - y_i)^2} \quad 5.5$$

The *RMSE* was found to be 0.1079 for the three sensors, which was higher than the regression model because the values was determined based on three samples. The *RMSE* can be further decreased by increasing the number of samples in the validation experiment.

Table 5-9. Comparison between the measured and predicted $1/\sqrt{R}$ values of the three new sensors used to validate the regression model.

Sensor	Area (mm ²)	Thickness (nm)	Measured transformed resistance value ($\Omega^{-\frac{1}{2}}$)	Predicted transformed resistance value ($\Omega^{-\frac{1}{2}}$)	Percentage difference (%)
1	300	70	1.43	1.31	8.39
2	450	70	1.49	1.52	2.01
3	800	60	2.00	1.86	7.00

5.5 CHARACTERISTICS OF THE SENSORS IN THE PRESENCE OF CORROSIVE BY-PRODUCTS DUE TO THE BREAKDOWN OF DBDS

Theoretically, an increase in material loss from a metal leads to an increase in electrical resistance [128]. To understand this relationship, the calculated resistance of the thin film sacrificial copper strip was plotted against its thickness, as shown in Figure 5-7. It can be observed that the resistance of the sensor increased by more than one order of magnitude when the thickness of the sensor was decreased from 200 nm to 20 nm for uniform corrosion at a constant rate. Therefore, ΔR is inversely proportional to the thickness of the sensor.

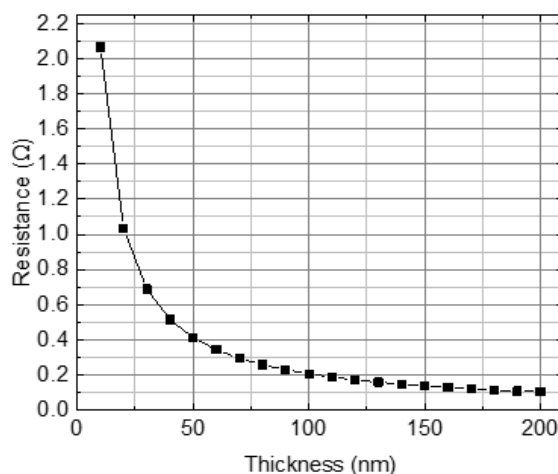


Figure 5-7. Variation of the calculated resistance with respect to the thickness of the thin film sacrificial copper strip sensor.

5.5.1 EXPERIMENTAL SET-UP

Sensors Type A (area: 1375 mm², thickness: 200 nm) were fabricated to examine their characteristics in the presence of corrosive by-products due to the breakdown of DBDS. The sensors were immersed in glass Petri dishes containing 40 mL of insulating oil with different DBDS concentrations: (1) 100 ppm, (2) 250 ppm, and (3) 1000 ppm. Each Petri dish was covered with another Petri dish to prevent oil evaporation during the thermal ageing process. According to Facciotti et al. [43], the ageing time and ageing temperature are the parameters that can significantly influence the chemical reactions between the corrosive by-products and copper immersed in the mineral insulating oil. It is crucial to select the appropriate ageing temperature for the experiments owing to the flash point of the insulating oil. The BS EN 62535 standard is the standard test method typically used to detect potentially corrosive sulphur in insulating oils. According to this standard, a high temperature of 150 °C should be used for the accelerated thermal ageing tests. However, it shall be noted that sulphur corrosion may occur at a temperature of 80 °C and reducing the ageing temperature to 80 °C may prolong the occurrence of sulphur corrosion. Hence, in this research, the thermal ageing experiments were conducted at 120 and 130 °C because these temperatures were found to be a good compromise between the above criteria. The sensors were aged in a fan oven for 25 h, where the sensors were taken out from the oven every 5 h to measure their resistance. The sensors were cleaned by soaking them in a beaker filled with acetone, followed by gentle shaking. This step was performed at least three times, where fresh acetone was used each time to remove oil residue from the surface of each sensor. The sensors were handled using a clean pair of tweezers and a clean pair of nitrile gloves was worn at all times to prevent unnecessary contact, which could cause contamination to the sensor surface.

5.5.2 SURFACE MORPHOLOGIES OF THE SENSORS

Before accessing the feasibility of thin film sacrificial copper strips as sulphur corrosion sensors, it is first necessary to provide evidence on the importance of the low-resistance measurements. Table 5-10 shows the optical photographs of 200-nm thin film copper strips aged in insulating oils with different DBDS concentrations (0, 100, 250, and 1000 ppm) at 130 °C. The colour changes of the sensors were due to the presence of corrosive by-products

in the insulating oil samples resulting from the breakdown of DBDS. The breakdown of DBDS resulted in a loss of copper from the surfaces of the glass substrate. After 5 h of ageing, the colour of the sensors changed in proportion to the DBDS concentration. It can be clearly observed that the colour of the sensor aged in the non-corrosive oil (DBDS concentration: 0 ppm) was orange and the colour changed into gold with a slight tinge of orange for higher DBDS concentrations (100 and 250 ppm). The colour of the sensor changed completely into gold for the highest DBDS concentration (1000 ppm). The same trend was observed for longer ageing periods. After 10 h of ageing, the colour of the sensor changed from partially gold (DBDS concentrations: 100 and 250 ppm) to entirely purple (DBDS concentration: 1000 ppm). There were no significant changes in the colour of the sensors aged in the insulating oils with a DBDS concentration of 100 and 250 ppm for 15 and 20 h. However, the colour of the sensor aged in the insulating oil with a DBDS concentration of 1000 ppm changed from purple to light green after 15 h of ageing. For the longest ageing time (20 h), the sensors changed colour from green to a mix of green, gold, and red. Interestingly, the colour of the sensor aged in the non-corrosive oil changed from orange to darker orange with some tarnish. This suggests that thermal ageing can affect the surface morphology of the thin film sacrificial copper strips. Hence, it is difficult to distinguish between the effects of thermal ageing and sulphur corrosion by merely observing the surface morphological changes of the sensors. Blotch-type corrosion can also occur (Figure 5-8) and thus, it was not possible to assess the feasibility of the sensors based on their thickness. For this reason, low-resistance measurements should be used to assess the feasibility of the sensors in tracking the progression of sulphur corrosion in transformer insulating oils.

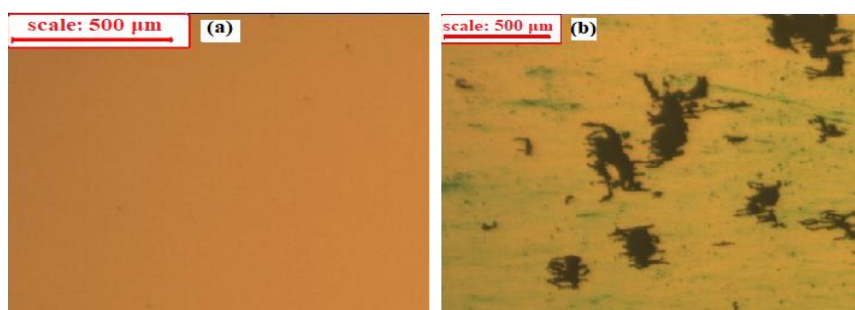

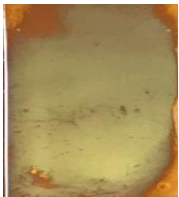
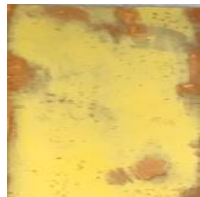



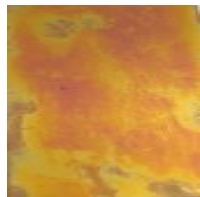



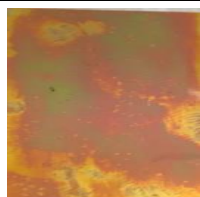
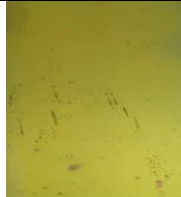

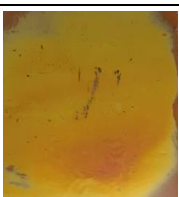
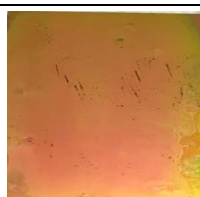
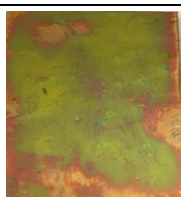


Figure 5-8. Changes in the surface morphology of the sensor surface due to the corrosive by-products of DBDS: (a) new sensor and (b) sensor aged in corrosive oil.

Table 5-10. Optical photographs of 200-nm thin film copper strips aged in insulating oils with different DBDS concentrations at 130 °C as compared to ASTM D130-12.

Ageing period (h)	DBDS concentration (0 ppm)	ASTM D 130-12	DBDS concentration (100 ppm)	ASTM D 130-12	DBDS concentration (250 ppm)	ASTM D 130-12	DBDS concentration (1000 ppm)	ASTM D 130-12
5 h		Freshly polished		Moderate tarnish (Level 2e)		Moderate Tarnish (Level 2e)		Moderate tarnish (Level 2e)
10 h		Slight tarnish (Level 1a)		Moderate tarnish (Level 2e)		Dark tarnish (Level 3a)		Moderate tarnish (Level 2b)
15 h		Slight tarnish (Level 1a)		Moderate tarnish (Level 2e)		Dark tarnish (Level 3a)		Moderate Tarnish (Level 2e)
20 h		Slight tarnish (Level 1b)		Dark tarnish (Level 3a)		Dark tarnish (Level 3a)		Dark tarnish (Level 3a)

5.5.3 CHANGES IN THE RESISTANCE OF THE SENSORS FOR INSULATING OILS WITH DIFFERENT DBDS CONCENTRATIONS

Dissolution of copper occurs at 135 °C and it has been reported that the weight of the copper strip is inversely proportional to the heating time [52]. Hence, the weight of the copper strip decreases because the dissolution of DBDS-Cu complex is more pronounced than the formation of copper sulphide on the copper strip. Experiments were carried out to test this hypothesis and the results showed that at 130 °C, the ΔR of the thin film sacrificial copper strip increased linearly with an increase in the DBDS concentration and ageing time, as shown in Figure 5-9. These results are in good agreement with those of [52], where the degradation of DBDS resulted in corrosion of the sensors at 130 °C. In addition, the increase in ΔR is likely because of the dissolution of DBDS-Cu complex in the insulating oils after the DBDS-Cu complex forms on the sensor surface owing to the reaction between the copper and corrosive by-products of DBDS.

It can be observed from Figure 5-9 that there was a steady increase in ΔR as the DBDS concentration increased. The increase in ΔR was most pronounced at the highest DBDS concentration (1000 ppm), as indicated by the steepness of the red line. The ΔR increased at a relatively slow rate for the lowest DBDS concentration (100 ppm) compared with those for higher DBDS concentrations (250 and 1000 ppm). Based on the results, it is believed that the corrosive by-products of DBDS chemically interact with the copper surface, even for the lowest DBDS concentration (100 ppm). It can be deduced from Figure 5-9 that the corrosive by-products of DBDS begin to attack the copper surface after 5 h of ageing. This process occurs only for the sensor aged in the insulating oils with a DBDS concentration of 250 and 1000 ppm. However, the sensor aged in the insulating oil with a DBDS concentration of 100 ppm showed a slightly different characteristic. It can be deduced that the sulphur corrosion process begins after 5 h of ageing because there are no significant changes in ΔR within the first 5 h of the thermal ageing experiment.

In general, ΔR of the thin film sacrificial copper strip increased with an increase in the DBDS concentration and ageing period. Increasing the DBDS concentration and ageing time will increase the sulphur corrosion rate, as indicated by the higher ΔR , which implies that there is a significant amount of copper loss from the glass substrate.

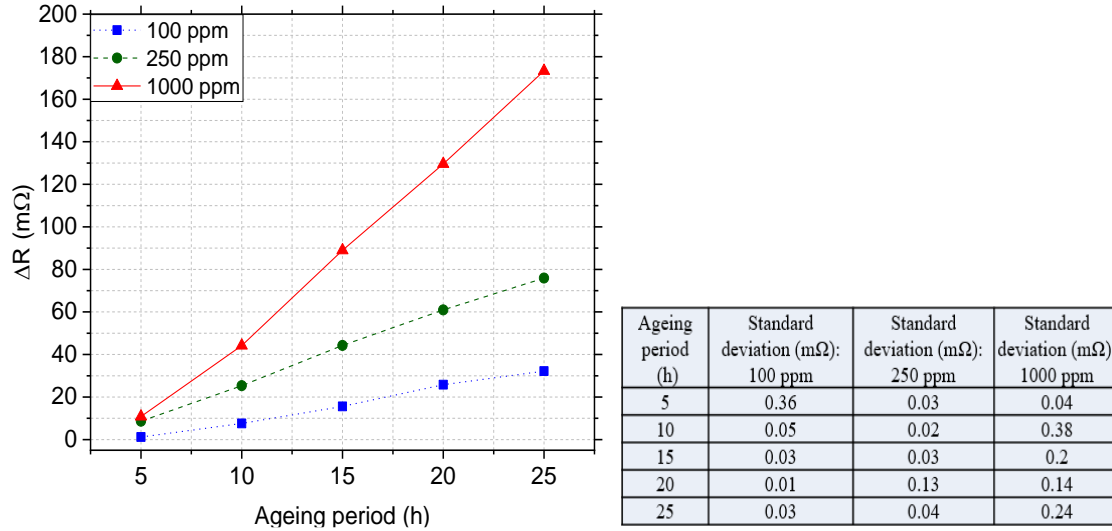


Figure 5-9. Variation of the ΔR of the thin film sacrificial copper strips with respect to the ageing period. The sensors were aged in the insulating oils with different DBDS concentrations at 130 °C.

5.5.4 EFFECT OF AGEING TEMPERATURE ON THE CHARACTERISTICS OF THE SENSORS

Interestingly, there were differences in the ΔR of the thin film sacrificial copper strips when the sensors were aged at different temperatures, shown in Figure 5-10–Figure 5-12. It can be deduced that there is a non-linear relationship between ΔR of the sensors and thermal stresses in the presence of oxygen. The results indicate that temperature plays a vital role in increasing the corrosiveness of the insulating oils, regardless of the DBDS concentration. This suggests that the degradation of insulating oils containing DBDS due to the thermal ageing will accelerate the progression of sulphur corrosion in oil-filled power transformers.

It can be seen from Figure 5-10 that the effect of thermal stresses was only apparent after 10 h of ageing for the sensor aged in the insulating oil with a DBDS concentration of 100 ppm. However, the time taken for the corrosive by-products of DBDS to thermally react with the sensor surface was faster for the sensors aged in the insulating oils with a DBDS concentration of 250 and 1000 ppm (Figure 5-11 and Figure 5-12, respectively), where there were significant changes in the ΔR after only 5 h of ageing. It can be seen from Figure 5-10 and Figure 5-12 that the effects of thermal stresses on the ΔR of the thin film sacrificial copper strips were more pronounced at higher ageing periods even though the DBDS

concentration was the same. However, it can be observed from Figure 5-11 that there were no significant differences between the ΔR of the sensors aged at 120 and 130 °C, where the data markers were almost coincident, which was unexpected. The reason for this is not clear but it may be associated with the variation in the oxygen level of the oils during the thermal ageing process. It has been reported in [40] that the sulphur corrosion can be significantly affected by the oxygen level of the insulating oils. The reaction between an unstable sulphur compound such as DBDS and the copper strip tends to decrease with an increase in the oxygen level. Therefore, the unexpected trend observed in Figure 5-11 may be attributed to the improperly covered Petri dishes used during the thermal ageing experiment, which can affect the oxygen level of the insulating oils.

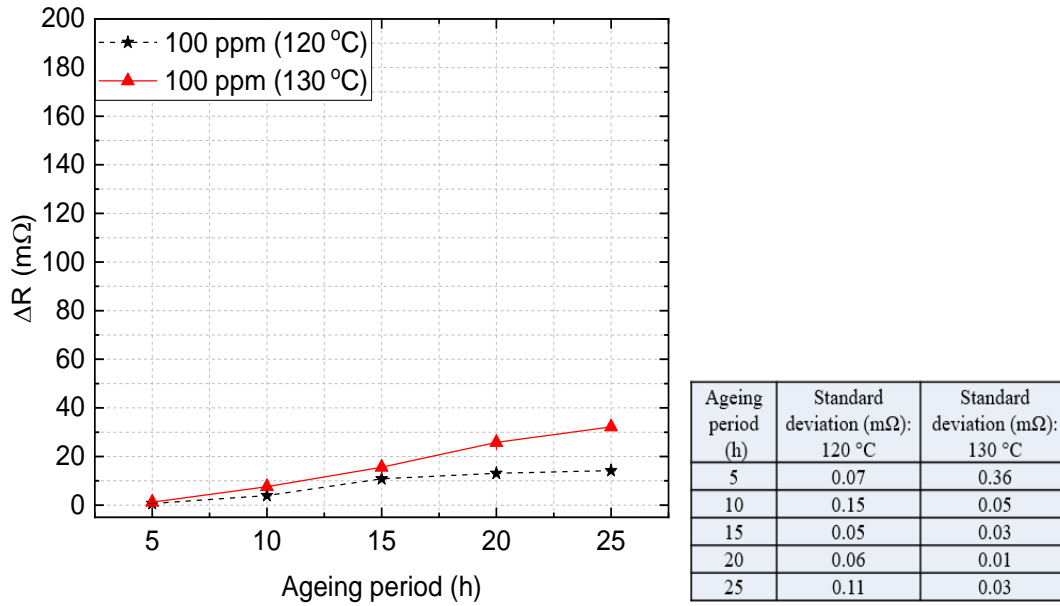


Figure 5-10. Effects of ageing temperature (120 and 130 °C) on the ΔR of the thin film sacrificial copper strips aged in the insulating oils with a DBDS concentration of 100 ppm.

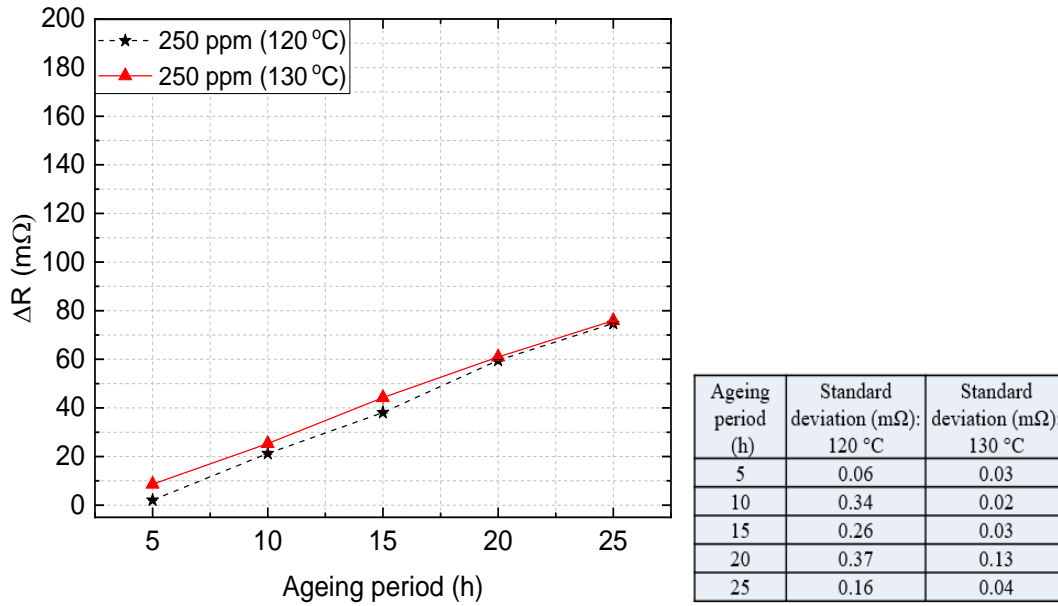


Figure 5-11. Effects of ageing temperature (120 and 130 °C) on the ΔR of the thin film sacrificial copper strips aged in the insulating oils with a DBDS concentration of 250 ppm.

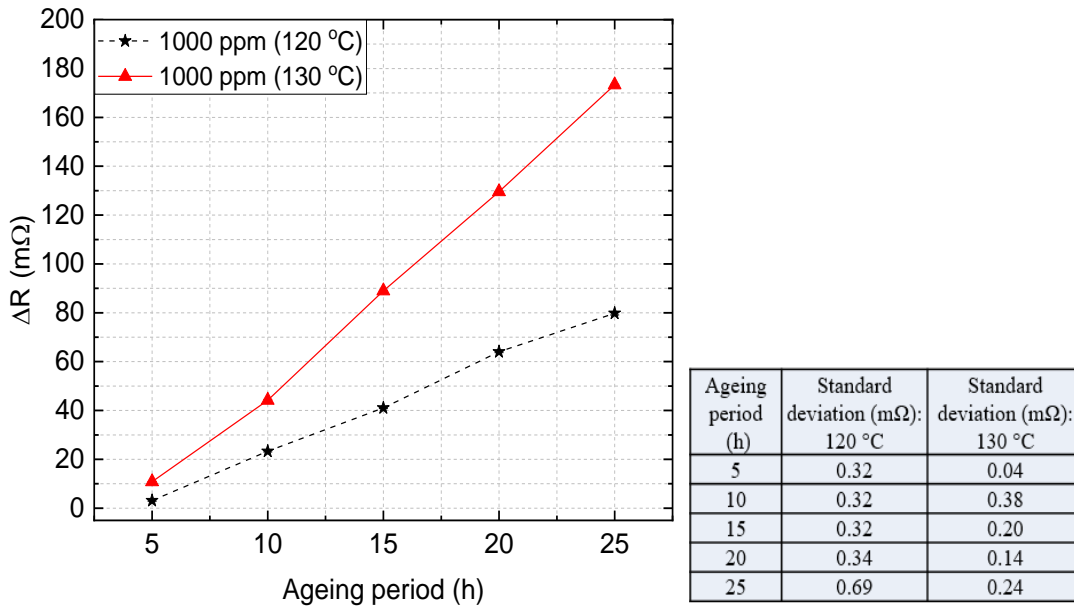


Figure 5-12. Effects of ageing temperature (120 and 130 °C) on the ΔR of the thin film sacrificial copper strips aged in the insulating oils with a DBDS concentration of 1000 ppm.

5.6 CHARACTERISTICS OF THE SENSORS IN THE PRESENCE OF ELEMENTAL SULPHUR

The feasibility of the thin film sacrificial copper strips in sensing and monitoring the progression of sulphur corrosion was further accessed by investigating their characteristics in the presence of elemental sulphur, which is the most corrosive sulphur compound. Chemical analysis based on UHPSFC–MS was carried out to examine the relationship between ΔR of the sensors and the change in elemental sulphur concentration (ΔS_8).

5.6.1 EXPERIMENTAL SET-UP

Sensors Type B (area: 800 mm², thickness: 50 nm) were fabricated to evaluate the feasibility of the sensors in monitoring the progression of sulphur corrosion in the insulating oils due to the presence of elemental sulphur. The sensors were immersed in glass Petri dishes containing 30 mL of insulating oil with different elemental sulphur concentrations (0, 15, 20, and 25 ppm). Each Petri dish was covered with another Petri dish to prevent oil evaporation during the thermal ageing experiment. The sensors were aged in a fan oven at 90 °C for 1 h. Prior to the resistance measurements, a clean pair of tweezers was used to remove the sensors from the glass Petri dishes. The sensors were cleaned by soaking them in a beaker filled with acetone, followed by gentle shaking. This step was performed at least three times, where fresh acetone was used each time to remove oil residue from the surface of each sensor.

5.6.2 SURFACE MORPHOLOGIES OF THE SENSORS

The addition of elemental sulphur into the insulating oils at different concentrations resulted in different sulphur corrosion levels, as indicated by the surface morphologies of the 50-nm thin film sacrificial copper strips shown in Figure 5-13. It is evident that increasing the elemental sulphur concentration increases the amount of copper loss from the glass substrate, which modifies the surface morphology of the sensors. After 1 h of ageing at 90 °C, the surface of the sensor aged in the non-corrosive oil (elemental sulphur concentration: 0 ppm)

remained relatively invariant as that before the ageing process. This indicates that sulphur corrosion did not occur owing to the absence of elemental sulphur in the insulating oil. The amount of copper loss was most pronounced for the highest elemental sulphur concentration (25 ppm), as indicated by the severely corroded copper surface in Figure 5-13(d). However, it was not possible to distinguish between the sulphur corrosion levels for the sensors aged in insulating oils with an elemental sulphur concentration of 15 and 20 ppm. Therefore, low-resistance measurements were carried out to determine the characteristics of the sensors for different elemental sulphur concentrations, which will be described in Section 5.6.3.

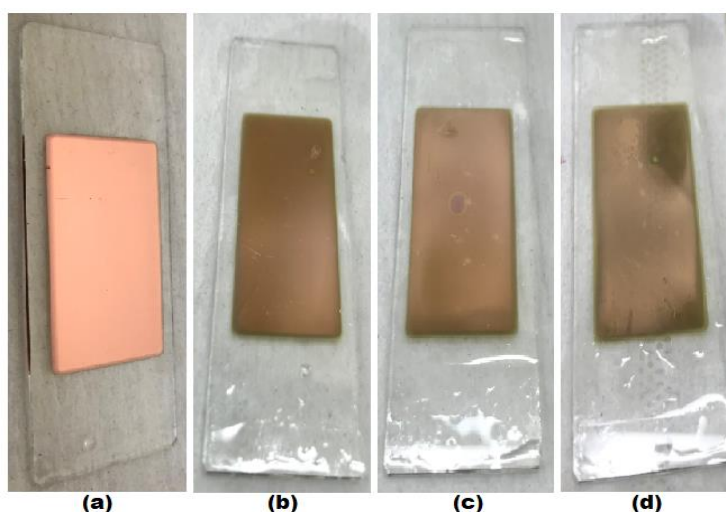


Figure 5-13. Surface morphologies of 50-nm thin film sacrificial copper strips aged in insulating oils with different elemental sulphur concentrations: (a) 0 ppm, (b) 15 ppm, (c) 20 ppm, and (d) 25 ppm. The sensors were aged at 90 °C for 1 h.

5.6.3 CHANGES IN THE RESISTANCE OF THE SENSORS FOR INSULATING OILS WITH DIFFERENT ELEMENTAL SULPHUR CONCENTRATIONS

Figure 5-14 displays the ΔR of the thin film sacrificial copper strips aged in insulating oils with different elemental sulphur concentrations (0, 15, 20, and 25 ppm). The ΔR was found to increase from 0.00 Ω to 8.08 Ω when the elemental sulphur concentration was increased from 0 ppm to 25 ppm, which suggests that there was an increase in the amount of copper loss from the glass substrate (Figure 5-13). The results indicate that increasing the elemental sulphur concentration promotes sulphur corrosion in the insulating oil. In general, the ΔR of the sensor aged in the non-corrosive oil (elemental sulphur concentration: 0 ppm) remained

constant at 0 Ω after the thermal ageing experiment. It can be deduced that the elemental sulphur begins attacking the copper surface at a low concentration (15 ppm), as indicated by the increase in ΔR from 0.00 Ω to 0.48 Ω (Figure 5-14). In addition, the amount of copper loss from the glass substrate increased when the elemental sulphur concentration increased to 20 ppm, as indicated by the slight increase in ΔR . However, it is apparent that the ΔR increased drastically to 8.08 Ω when the sensor was aged in the insulating oil with the highest elemental sulphur concentration (25 ppm), which conforms well with the severely corroded copper surface observed in Figure 5-13(d). Based on the results, it can be inferred that elemental sulphur plays a vital role in creating a corrosive environment, which can cause detriment to copper components in oil-filled power transformers.

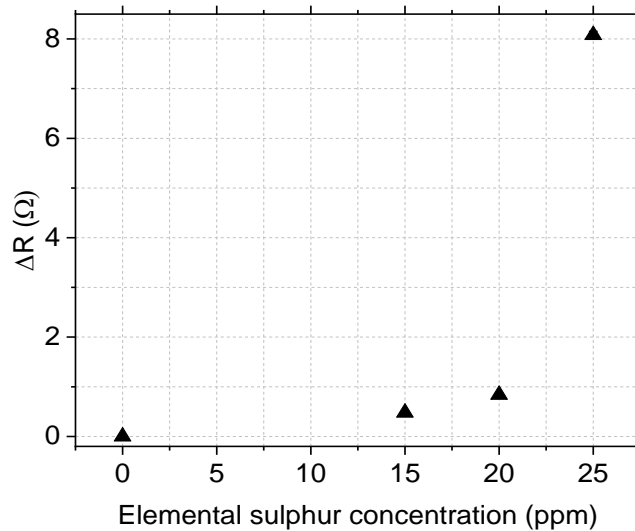


Figure 5-14. The ΔR of the thin film sacrificial copper strips aged in the insulating oils with different elemental sulphur concentrations: (a) 0 ppm, (b) 15 ppm, (c) 20 ppm, and (d) 25 ppm.

5.6.4 VALIDATION OF THE SENSORS BY ULTRA HIGH PERFORMANCE SUPERCRITICAL FLUID CHROMATOGRAPHY–MASS SPECTROMETRY

Chemical analysis based on UHPSFC–MS was performed to validate the feasibility of the thin film sacrificial copper strips in sensing the presence of elemental sulphur in transformer insulating oils. This chemical analysis was carried out in collaboration with Sergio Garcia,

a doctoral student from the School of Chemistry, University of Southampton. The experimental procedures of this novel elemental sulphur detection method is described in [129].

Chromatographic separation was carried out using a convergence chromatography system (Acquity UPC² system, Waters Corporation, USA). This system was fitted with a binary solvent manager, a heated column manager, and an internal autosampler with a cooled sample tray. Acquity HSS C18 SB column (Waters Corporation, USA, particle size: 1.8 μm , inner diameter: 3.0 mm, length: 100 mm) was chosen as the column for chromatographic separation. The abbreviations HSS and SB indicate ‘high-strength silica’ and ‘electivity for bases’, respectively. The column was pre-heated in a column oven at 40 °C before 2.0 μL of an insulating oil sample was introduced into the column. The chromatographic separation process was performed for 3 min. Mass spectrometry was performed using a triple quadrupole mass spectrometer (TQ Detector 2, Waters Corporation, USA).

Elemental sulphur is usually present as S_8 ring structures at room temperature. The novelty of the elemental sulphur detection method in this research is based on the principle that different sulphur allotropes will react with triphenylphosphine (TPP) to form a single compound known as triphenylphosphine sulphide (TPPS), as shown in Figure 5-15.

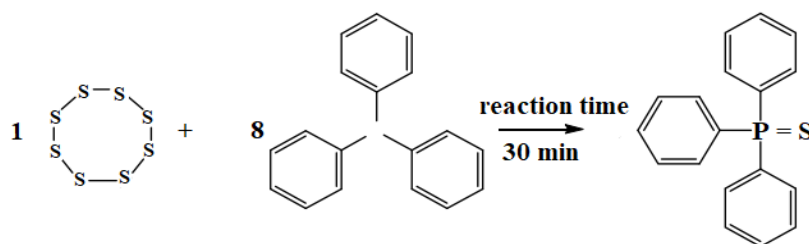


Figure 5-15. Derivatisation between elemental sulphur and TTP.

The resultant TPPS has a higher boiling point and retention time, which makes it easier to distinguish elemental sulphur from other components in the aged insulating oil based on the peaks in the chromatogram. TTP was chosen because further investigation revealed that TPP did not react with other organosulphur compounds such as disulphide, thiophene and dithiophene. This makes it possible to quantify the amount of elemental sulphur in aged insulating oils. The main advantage of this method is that the limit of detection (i.e. the

smallest concentration of elemental sulphur in the insulating oil sample that can be distinguished with confidence) is less than 20 parts per billion (ppb) of TPPS, which corresponds to less than 2.18 ppb of elemental sulphur. It shall be noted that 1 ppm of elemental sulphur contains 9.18 ppm of derivative TPPS.

It is crucial to determine the TPPS concentration calibration curve before quantifying the amount of elemental sulphur in the aged transformer insulating oils using this method. Hence, experiments were performed for this purpose, where three insulating oil samples with the same elemental sulphur concentration were prepared for each calibration point. The mean concentrations range for TPPS were from 0 ppb to 15000 ppb, as shown in Table 5-11. The details of the sample preparation procedure are provided in [129]. Origin software package (OriginLab Corporation, USA) was used to plot the TPPS concentration calibration curve, as shown in Figure 5-16. The data points were fitted using the least squares method.

Table 5-11. Mean TPPS concentrations.

Compound	Mean concentration (ppb)
TPPS	0, 50, 100, 250, 500, 1000, 2500, 5000, 10000, 15000

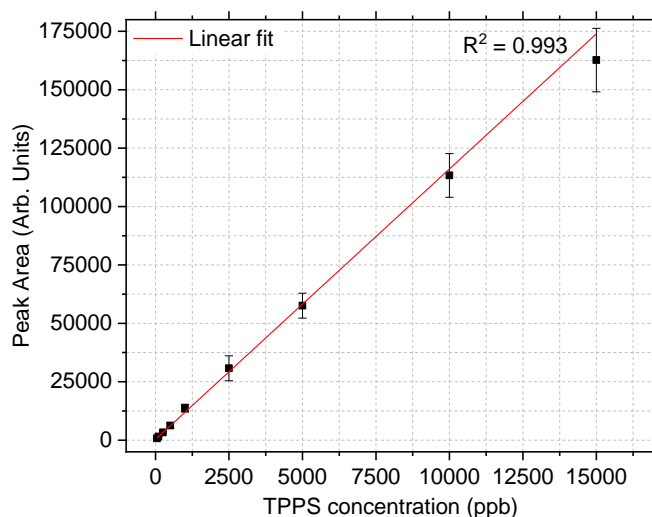


Figure 5-16. Calibration curve for the TPPS concentration. For each calibration point, the mean TPPS concentration was determined from three insulating oil samples with the same elemental sulphur concentration. The error bars indicate the standard deviations of the measured values.

A regression model was developed based on the least squares method, which describes the TPPS concentration in ppb (y) as a function of the area (x), as follows:

$$y = 11.57x + 349.44 \quad 5.6$$

The molecular weights of elemental sulphur and TPP are 32.07 and 262.29 g/mol, respectively which gives 294.36 g/mol of TPPS. Therefore, an insulating oil sample containing 1 ppm of elemental sulphur will contain 9.18 ppm of TPPS. Based on this information, the unknown elemental sulphur concentration can be estimated using Equation 5.6.

Following this, the presence of elemental sulphur in the insulating oils was detected using the thin film sacrificial copper strips developed in this research. Four sensors (each with the same characteristics described in Section 5.6.1) were aged in insulating oils with different elemental sulphur concentrations (0, 10, 20, and 40 ppm) at 100 °C. After 1 h of ageing, 5 mL of each insulating oil sample was collected to measure its final elemental sulphur concentration using UHPSFC–MS. The thermal ageing experiment was conducted in triplicate for each elemental sulphur concentration. The mean and standard deviation of the final elemental sulphur concentration for all insulating oil samples are summarised in Table 5-12.

The results proved that the thin film sacrificial copper strips can be implemented as sulphur corrosion sensors because these sensors are highly sensitive in detecting the corrosivity of insulating oils in the presence of various corrosive sulphur compounds (i.e. corrosive by-product of DBDS and elemental sulphur). The results shown in Figure 5-9 and Table 5-12 were comparable with the theory presented in Section 2.5. Unlike DBDS, elemental sulphur begins to attack the sensor at a very low concentration of 10 ppm, which is 10 times lower than the DBDS concentration (100 ppm). Even at a very low elemental sulphur concentration of 10 ppm, the ΔR of the sensor increased by a factor of 6 from 0.03 Ω despite the fact that the experimental conditions were lower (ageing temperature: 100 °C, ageing period: 1 h) compared with those for the insulating oil with a DBDS concentration of 100 ppm (ageing temperature: 130 °C, ageing period: 25 h).

It can be seen from Table 5-12 that the ΔR of the thin film sacrificial copper strip increased as the concentration of ΔS_8 increased, indicating an increase in the oil corrosivity level. The ΔR of the sensor aged in the non-corrosive oil (elemental sulphur concentration: 0 ppm) was 0 Ω , as expected. Interestingly, the UHPSFC–MS detected 0.22 ppm of elemental sulphur in this oil sample even though elemental sulphur was not added, indicating the high sensitivity of the UHPSFC–MS. This indicates that the mineral insulating oil used in this research contains a trace amount of elemental sulphur, which is not sufficient to cause detectable sulphur corrosion.

Table 5-12. Relationship between the ΔR of the thin film sacrificial copper strips and the ΔS_8 of the insulating oils after 1 h of ageing at 100 °C.

Initial elemental sulphur concentration before ageing (ppm) *	Final elemental sulphur concentration after ageing (ppm)**	Standard deviation (ppm)	Change in elemental sulphur concentration, ΔS_8 (ppm)	Change in resistance, ΔR (Ω)
New oil without any addition of elemental sulphur	0.22	0.07	-	0
10	0.44	0.01	9.56	0.18
20	1.62	0.40	18.38	3.30
40	2.05	0.13	37.95	Not measureable

* Prepared according to the procedure described in Section 3.2

** Measured using UHPSFC–MS

Based on the results in Table 5-12, the rate of sulphur corrosion was highest for the insulating oil with an elemental sulphur concentration of 40 ppm. The results showed that 37.95 ppm of elemental sulphur was sufficient to remove off almost all of the copper from the glass substrate and therefore, the ΔR was infinite for the sensor aged in this insulating oil. In contrast, a small ΔR (0.18 Ω) was obtained for the insulating oil with an elemental sulphur concentration of 10 ppm, indicating that 9.56 ppm of elemental sulphur was not sufficient to

create a highly corrosive environment, resulting in a slow progression of sulphur corrosion. However, the ΔR significantly increased to $3.30\ \Omega$ for the sensor aged in the insulating oil with an elemental sulphur concentration of 20 ppm, indicating that 18.38 ppm of elemental sulphur could create a corrosive environment, resulting in a higher rate of sulphur corrosion.

5.7 A NOVEL ONLINE METHOD FOR QUANTIFICATION OF CORROSIVE SULPHUR IN INSULATING OILS

There is a critical need to develop a method that is capable of quantifying the amount of elemental sulphur in transformer because elemental sulphur results in the fastest progression of sulphur corrosion in oil-filled power transformers compared with other corrosive sulphur species. According to Lewand et al. [40], elemental sulphur can react with copper in the absence of heat unlike DBDS, which reacts only at temperatures above 80 °C. In addition, a trace amount of elemental sulphur (1 ppm) in the transformer insulating oil can corrode the silver material of tap changers [129].

In general, a new condition monitoring tool for sulphur corrosion should fulfil the following criteria: (1) robust, (2) low cost, (3) non-destructive, (4) capable of detecting and quantifying various corrosive sulphur compounds, and (5) the tool is simple such that it can be used as an online assessment tool without the need for expert personnel. At present, there are a few common standard corrosion tests (Table 2-3) and other laboratory-based methods (Section 2.7) available to detect and monitor corrosive sulphur compounds in transformer insulating oils. The thin film sacrificial copper strips developed in this research offer the following advantages over existing methods: (1) the oil corrosivity levels can be monitored quantitatively unlike common standard corrosion tests, which are based on visual observations and (2) the corrosive sulphur species present in the transformer insulating oils can be quantified on-site in real-time. From a financial perspective, the cost to fabricate the thin film sacrificial copper strips and the corrosive sulphur detection system is estimated to be less than GBP 1000, which is at least 10 times cheaper compared with existing equipment (i.e. XRF and UHPSFC–MS).

In order to implement the new thin film sacrificial copper strips as sulphur corrosion sensors, it is first necessary to establish a procedure that will yield accurate, repeatable, and reproducible results. Hence, a non-standard procedure is established to ensure that the sensors are reliable for online condition monitoring of sulphur corrosion. The results presented in Section 5.6 indicate that the thin film sacrificial copper strips are feasible to detect and monitor the progression of elemental sulphur in transformer insulating oils. In this section, a novel online method for quantification of elemental sulphur in transformer insulating oils using the thin film sacrificial copper strips (which is the main aim of this research) is presented.

5.7.1 EXPERIMENTAL SET-UP

To use the thin film sacrificial copper strips for quantification of elemental sulphur in transformer insulating oils, the sensors must have a criteria of having a good repeatability with an accurate results. In addition, the sensors must be highly sensitive to detect the presence of elemental sulphur in ppm. Hence, five sensors were aged in the same ageing conditions (ageing temperature and elemental sulphur concentration) and the standard deviation of ΔR between these sensors was kept within $\sim \pm 1$ standard deviation.

Sensors Type C (thickness: 200 nm) were chosen for this experiment. The sensors were fabricated in bulk according to the procedure described in Section 5.2. The sensors were first cleaned by soaking them in 8-mL vials containing 7 mL of acetone until the purple photoresist layer was removed from the surface of each sensor. This step was performed at least three times, where fresh acetone was used each time to minimise contamination of the sensor surface. The sensors were placed in a fume cupboard at room temperature (20 ± 5 °C) for ~ 15 min to ensure that the acetone residue had completely evaporated from the sensors prior to the initial resistance measurements.

A set of sensors was placed in five 25-mL vials, where each vial contained 20 mL of insulating oil with a different elemental sulphur concentration. Each vial was covered with two layers of aluminium foil to prevent oil evaporation during the thermal ageing process. The samples were aged in air atmosphere using a fan oven set at different ageing

temperatures (80–110 °C) for a maximum period of 16 h. During the course of the thermal ageing experiment, the resistance of the sensors was frequently measured and the ΔR values were recorded because the reaction between the sensors and elemental sulphur would vary during the thermal ageing process. A clean pair of tweezers was used to remove the sensors from the vials. For each resistance measurement, the sensors were cleaned by soaking them in 8-mL vials filled with 7 mL of acetone, followed by gentle shaking. This step was performed at least three times, where fresh acetone was used each time to remove oil residue from the surface of each sensor.

In this research, the effects of two variables (ageing temperature and elemental sulphur concentration) on the ΔR of the thin film sacrificial copper strips were investigated and the experimental conditions are presented in Table 5-13 and Table 5-14, respectively.

Table 5-13. Experimental conditions used to investigate the effect of elemental sulphur concentration on the ΔR of the thin film sacrificial copper strips.

Experiment	1	2	3	4	5	6	7	8	9
Ageing temperature (°C)	80		90				110		
Elemental sulphur concentration (ppm)	20	30	5	10	20	30	3	5	10

Table 5-14. Experimental conditions used to investigate the effect of ageing temperature on the ΔR of the thin film sacrificial copper strips.

Experiment	1	2	3	4	5	6	7	8
Elemental sulphur concentration (ppm)	10				20		30	
Ageing temperature (°C)	90	100	105	110	80	90	80	90

5.7.2 RESULTS AND DISCUSSION

In general, there was a positive relationship between the elemental sulphur concentration and ΔR , which confirmed the feasibility of this detection approach. For all the cases investigated in this research, the ΔR showed significant variations with respect to the ageing temperature and elemental sulphur concentration, indicating the feasibility of these sensors

in investigating the effects of these parameters on the progression of sulphur corrosion in power transformers. To analyse the repeatability of the sensors in tracking the progression of elemental sulphur aged under the same experimental conditions (elemental sulphur concentration, ageing temperature, and ageing period), the ΔR values were measured independently for a set of sensors and the mean ΔR was determined. For each set of sensors, the ΔR values were analysed in this manner and the variability in the measured values (standard deviation) in the plots was indicated using error bars.

Table 5-15 shows the ΔR values measured for five sets of thin film sacrificial copper strips. The differences in the ΔR value between the sensors appeared to be reasonably small. However, there was a slight increase in the standard deviation of ΔR with an increase in the ageing period, which is likely because of the non-linearity of the sulphur corrosion rate during the course of the thermal ageing experiment. In the first hour of ageing, the reaction between elemental sulphur and copper surface was relatively uniform. Based on the initial colour of the sensor prior to ageing (orange), it can be deduced from Figure 5-17(a) that the amount of copper remaining on each sensor was approximately the same. It shall be noted that the slight red tinge on the surface of the sensors (especially sensor 4) is due to thermal ageing at high temperature of 110 °C. However, the presence of this red tinge does not reflect the differences in the ΔR values between the sensors.

In contrast, the increase in the standard deviation of ΔR suggests that the sulphur corrosion process is non-uniform during the course of the thermal ageing experiment. It can be seen from Figure 5-17(b) that the presence of copper was only evident on the surface of Sensors 3 and 5, whereas small amounts of copper were observed for the other sensors which are reminiscent of non-uniform sulphur corrosion. Taking the non-uniformity of the sulphur corrosion process into consideration, the maximum ΔR (i.e. the break-through condition of the sensor) was set as less than 0.35 Ω in order to minimise the differences in the ΔR values between the sensors.

Table 5-15. The ΔR for five sets of thin film sacrificial copper strips aged in insulating oils with an elemental sulphur concentration of 10 ppm at 110 °C.

Ageing period (h)	Change in resistance, ΔR (Ω)						Standard deviation (Ω)
	Sensor 1	Sensor 2	Sensor 3	Sensor 4	Sensor 5	Mean	
0.17	0.00	0.00	0.00	0.00	0.00	0.00	0.00
1.00	0.02	0.02	0.01	0.01	0.03	0.02	0.01
1.50	0.09	0.08	0.09	0.07	0.08	0.08	0.01
2.00	0.20	0.18	0.21	0.16	0.21	0.19	0.02
2.25	0.34	0.29	0.31	0.25	0.34	0.31	0.04

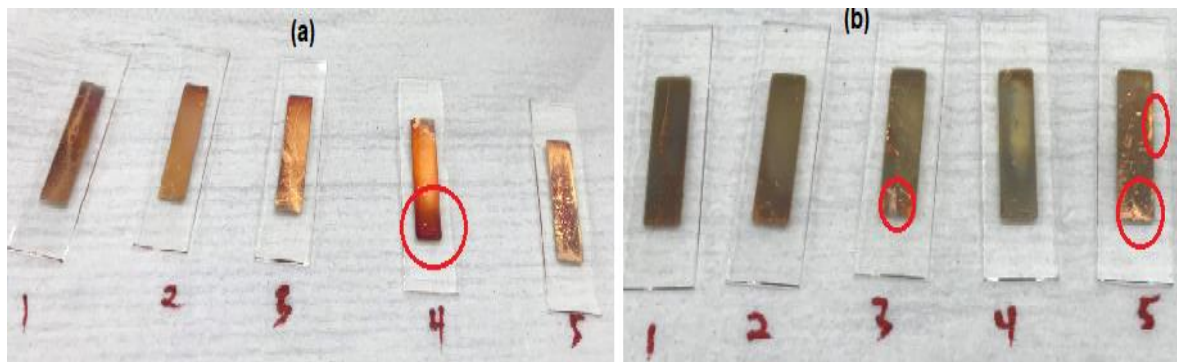


Figure 5-17. Surface morphologies of five thin film sacrificial copper strips aged in insulating oils with an elemental sulphur concentration of 10 ppm at 110 °C after (a) 1 h and (b) 2.25 h of ageing. The high-definition quality images of these sensors are presented in Appendixes D1 and D2.

Figure 5-18–Figure 5-20 illustrate the characteristics of the thin film sacrificial copper strips (i.e. ΔR as a function of the ageing period) when the sensors were aged in insulating oils with different elemental sulphur concentrations and ageing temperature. These results illustrate how copper corrosion is influenced by the presence of elemental sulphur in the insulating oil at different concentrations. It can be observed from Figure 5-19 that at an ageing temperature of 90 °C, increasing the elemental sulphur concentration did not result in severe corrosion of the sensors. It is apparent that a very low elemental sulphur concentration of 5 ppm was indeed insufficient to create a corrosion environment, where the ΔR values were relatively constant at 0 Ω throughout the thermal ageing experiment. In this case, it is expected that sulphur corrosion will occur after 16 h of ageing. In addition, it can be observed that the variation of ΔR changed from an exponential curve to a rather steep

almost linear curve when the oil corrosivity level increased from mildly corrosive (elemental sulphur concentration: 10 ppm) to highly corrosive (elemental sulphur concentration: 30 ppm). It is apparent from Figure 5-18–Figure 5-20 that sulphur corrosion is a time-dependent process. The trends observed for all cases indicate that the break-through condition occurs rapidly for the highly corrosive insulating oil samples, which is indicated by the steepness of the ΔR - ageing period curves. Interestingly, the ΔR remained constant at $0\ \Omega$ in the first hour of ageing, which indicates that this is the minimum time for the elemental sulphur to react with copper.

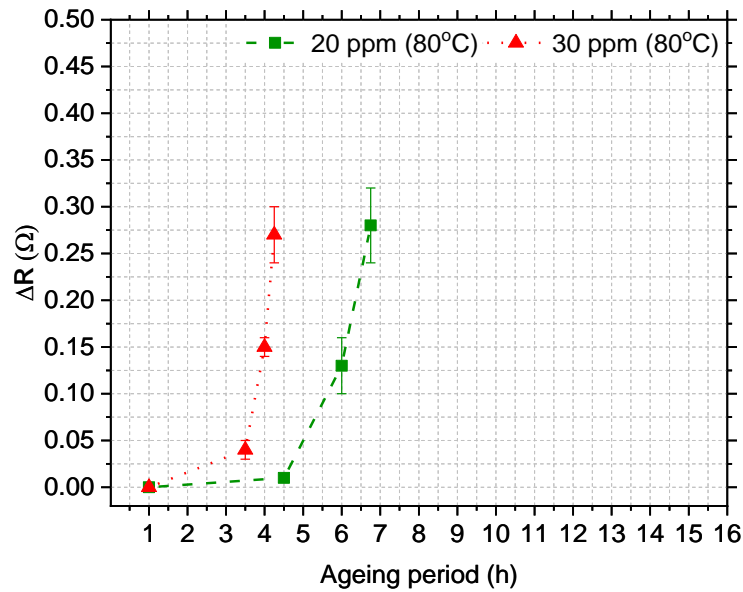


Figure 5-18. Effect of elemental sulphur concentration (20 and 30 ppm) on the ΔR of the thin film sacrificial copper strips aged in the insulating oils at temperature of 80 °C.

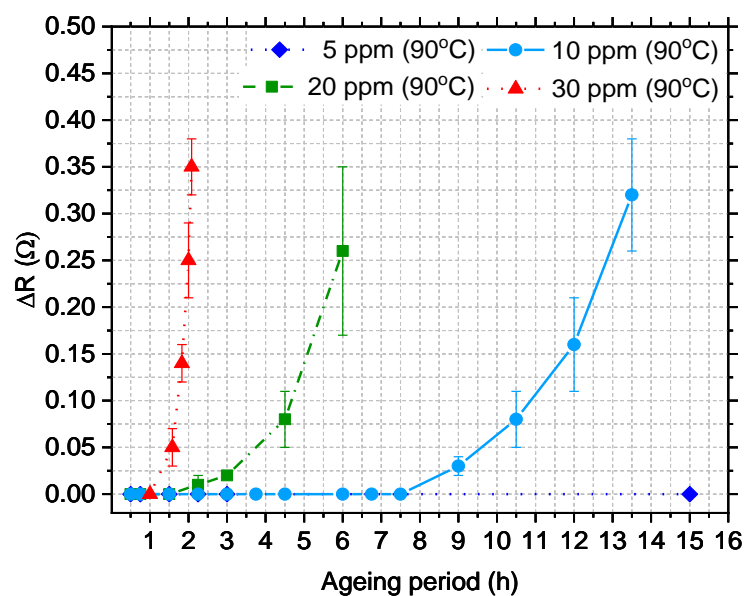


Figure 5-19. Effect of elemental sulphur concentration (5, 10, 20 and 30 ppm) on the ΔR of the thin film sacrificial copper strips aged in the insulating oils at temperature of 90 °C.

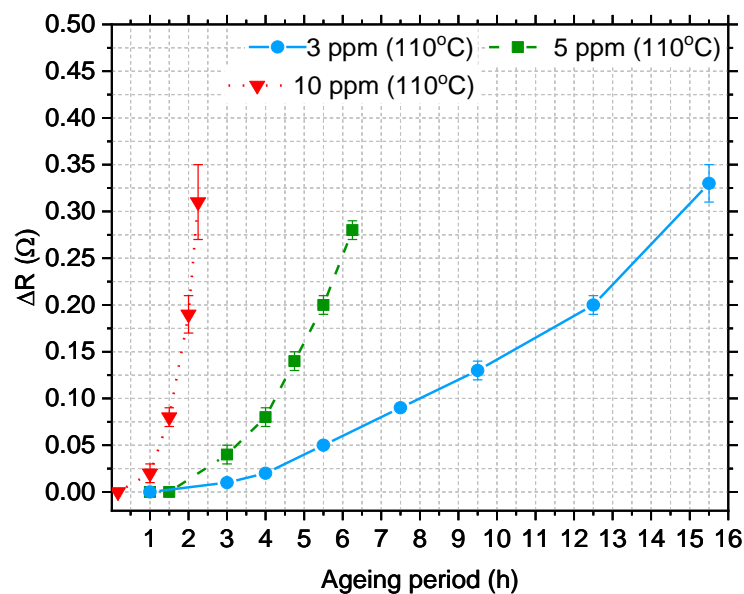


Figure 5-20. Effect of elemental sulphur concentration (3, 5, and 10 ppm) on the ΔR of the thin film sacrificial copper strips aged in the insulating oils at temperature of 110 °C.

Temperature has the most significant effect on sulphur corrosion in transformer insulating oils. This is evident from Figure 5-21, where the ΔR -ageing period curve shifted towards shorter ageing periods as the ageing temperature increased, which indicates that the onset of sulphur corrosion occurs earlier at higher temperature. It can also be observed from Figure 5-22 and Figure 5-23 that the ageing temperature (80 and 90 °C) had a significant effect on the characteristics of the thin film sacrificial copper strips even though the elemental sulphur concentration of the insulating oil samples was the same (20 and 30 ppm, respectively). It is apparent from the results that increasing the ageing temperature promotes the rate of sulphur corrosion, particularly at higher elemental sulphur concentrations. This indicates the feasibility of the thin film sacrificial copper strips in investigating the effect of thermal ageing on the progression of elemental sulphur in the insulating oil. It can be observed from Figure 5-21 that the ΔR was 0.05 Ω after 2.75 h of ageing at 100 °C. At the same ΔR value, increasing the ageing temperature to 110 °C shortened the ageing period by a factor of ~ 2.2 . Conversely, decreasing the ageing temperature from 100 °C to 90 °C prolonged the ageing period by a factor of ~ 3.45 . This highlights the detrimental effects of the formation of hotspots in power transformers (which can occur at temperatures above 100 °C), which can promote the rate of sulphur corrosion. It shall be noted that in normal operating conditions, the operating temperature of the power transformer is ~ 60 °C, which is 30 °C lower compared with the lowest ageing temperature investigated in this research. Owing to the capability of the thin film sacrificial copper strips in detecting corrosive sulphur compounds, it is possible to describe why sulphur corrosion requires a long period to occur.

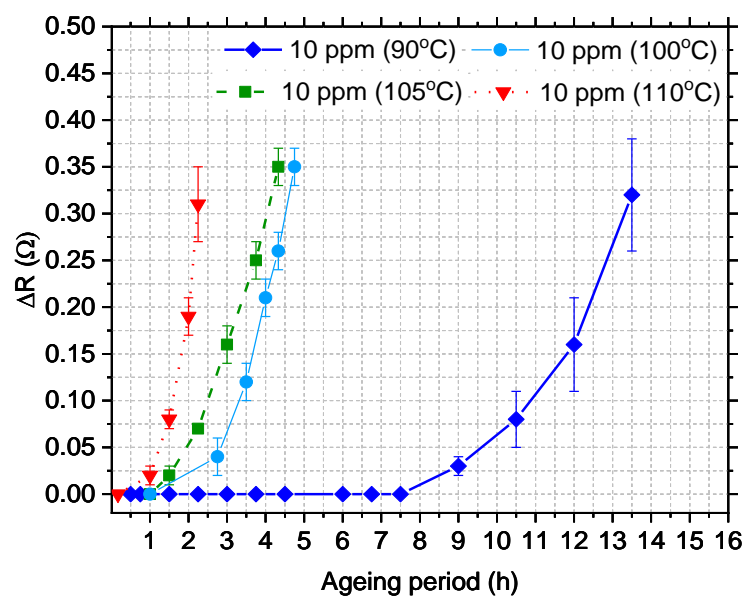


Figure 5-21. Effect of ageing temperature on the ΔR of the sensors aged in the insulating oils with an elemental sulphur concentration of 10 ppm.

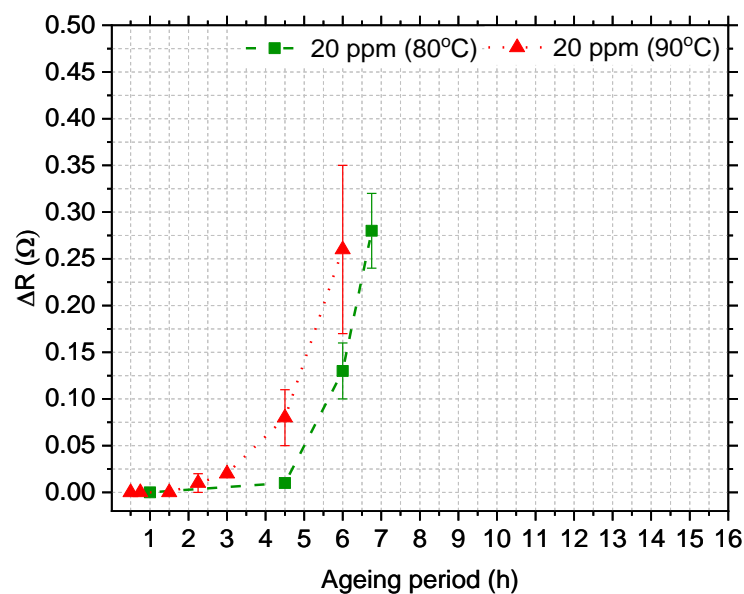


Figure 5-22. Effect of ageing temperature on the ΔR of the sensors aged in the insulating oils with an elemental sulphur concentration of 20 ppm.

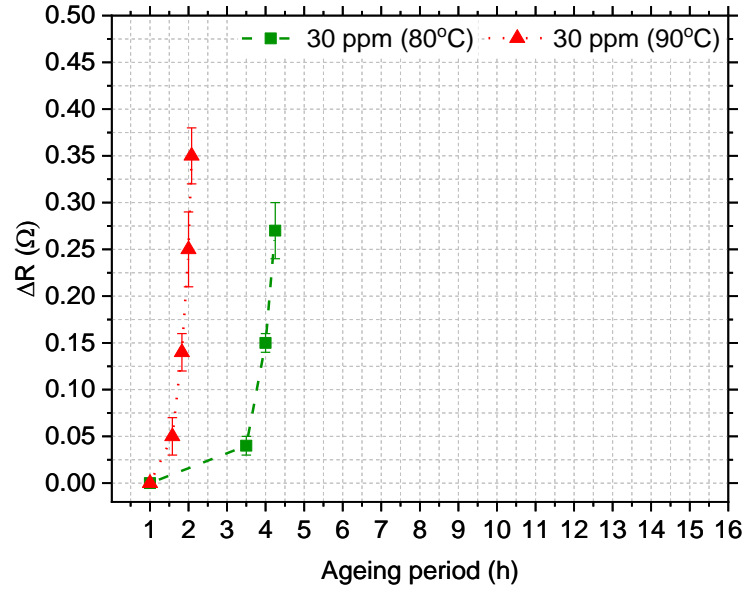


Figure 5-23. Effect of ageing temperature on the ΔR of the sensors aged in the insulating oils with an elemental sulphur concentration of 30 ppm.

Based on the results, each of the thin film sacrificial copper strips exhibited unique characteristics (variations of ΔR with respect to the ageing time, ageing temperature, and elemental sulphur concentration). However, care should be taken when using these sensors for online condition monitoring of sulphur corrosion because of their relatively thin thickness, particularly when ΔR is more than 0.35 Ω , because there will be large differences in the resistance characteristics from one sensor to another (for the same set of sensors). Therefore, the ΔR was set within a range of 0.05–0.25 Ω with an interval of 0.05 Ω in order to ensure the reliability of the sensors. The lookup table block available in MATLAB software (The MathWorks, Inc., USA) was used for this purpose because there are no analytical expressions available for these sensors and the relationships between the ΔR , ageing temperature, ageing period, and elemental sulphur concentration were determined empirically. The lookup table block involves using a data array to map the input values to the output values in order to approximate a mathematical function. The lookup table block can linearly interpolate or extrapolate the nearest adjacent data points (i.e. (x_i, y_i) and (x_{i+1}, y_{i+1})) to obtain the value of y if it comes across an input that does not match any

α -values in the lookup table. The data sets obtained empirically were processed using the lookup table block and the results are presented in Section 5.7.3.

5.7.3 LIMITATIONS OF THE SENSORS

Application-wise, it is also important to highlight the limitations of the thin film sacrificial copper strips before these sensors are used as online condition monitoring tools for sulphur corrosion. First, the quantification of corrosive sulphur is limited only to the quantification of elemental sulphur in transformer insulating oils and therefore, other corrosive sulphur compounds were not considered in the sensor development. Second, the maximum limit of detection of the sensors is 30 ppm for a temperature range of 80–90 °C while the maximum detection is up to 10 ppm for a temperature of 110 °C. Beyond the limits of detection, the response time of the thin film sacrificial copper strips is extremely fast, which makes it difficult to determine the elemental sulphur concentration in the insulating oils, as shown in Figure 5-24–Figure 5-26. Conversely, if the limit of detection is further reduced, it is possible to quantify the amount of elemental sulphur concentration in the insulating oils; however, the process will be time-consuming.

The sensitivity of the thin film sacrificial copper strips appeared to be reasonably good, where the difference in sensitivity was 10 ppm when the sensors were used at a temperature of 80 and 90 °C. However, when the sensors were used at temperature of 110 °C, the difference in sensitivity was reduced to 2 ppm. It may be possible to predict the ΔR with respect to time at the same temperature by interpolating the ΔR values between two elemental sulphur concentrations, which is reserved for future work. This is because the standard deviations of the ΔR between two elemental concentrations appeared to be acceptable, as indicated by the error bars in Figure 5-24–Figure 5-26.

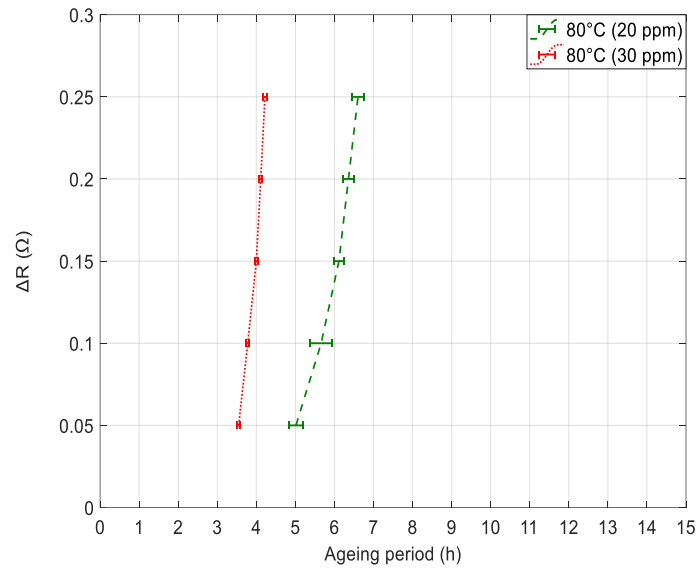


Figure 5-24. The ΔR of the sensors as a function of the ageing period obtained from the lookup table block. The ageing temperature was 80 °C and the elemental sulphur concentrations were 20 and 30 ppm.

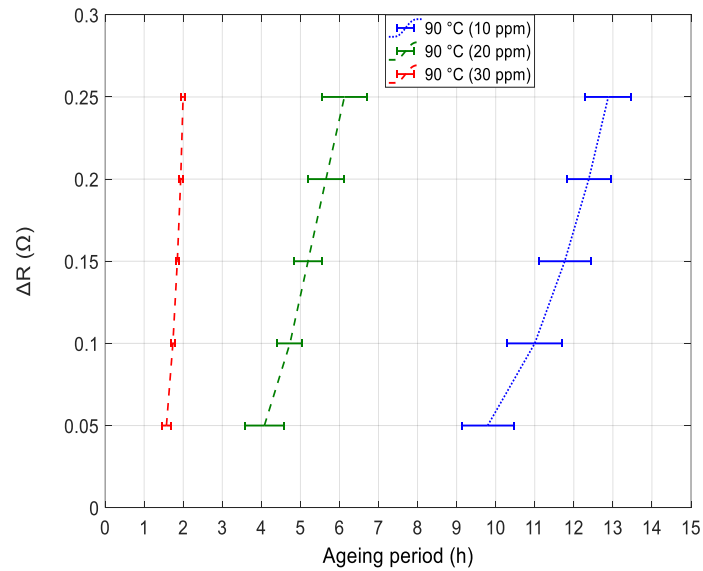


Figure 5-25. The ΔR of the sensors as a function of the ageing period obtained from the lookup table block. The ageing temperature was 90 °C and the elemental sulphur concentrations were 10, 20 and 30 ppm.

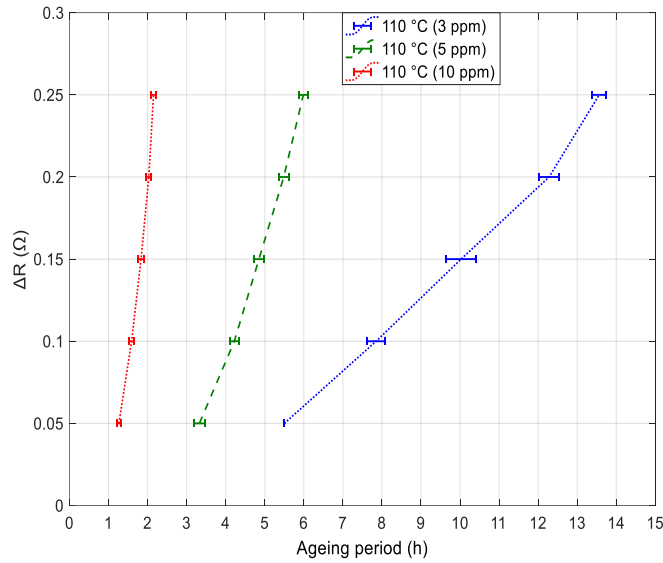


Figure 5-26. The ΔR of the sensors as a function of the ageing period obtained from the lookup table block. The ageing temperature was 110 °C and the elemental sulphur concentrations were 3, 5, and 10 ppm.

5.7.4 PROPOSED ONLINE METHOD FOR QUANTIFICATION OF ELEMENTAL SULPHUR IN INSULATING OILS

An online sulphur corrosion sensors should be low-cost, portable, fool proof, reliable, and provide instantaneously response in detecting the corrosive sulphur compounds present in transformer insulating oils. Based on the results presented in this chapter, thin film sacrificial copper strips are capable of quantifying the amount of elemental sulphur in transformer insulating oils and therefore, they can be used as online sulphur corrosion sensors.

For practical applications, the complete elemental sulphur detection system will comprise a set of thin film sacrificial copper strips, a timer, temperature sensor, and a data logger (to record, display, and store the mean temperature values over time). The data logger and timer will be connected in parallel and both of these devices will be connected in series with a built-in comparator circuit (to determine the ΔR of the sensors by comparing the initial and final resistance values of the sensors based on Equation 5.2). Figure 5-27 highlights the steps involved to implement the thin film sacrificial copper strips as an online tool for quantification of elemental sulphur in the transformer insulating oil.

The first step involves setting the initial value of ΔR within a range of 0.05–0.25 Ω with an interval of 0.05 Ω . As soon as the sensors are inserted into the oil-filled power transformer, the START buttons of the timer and data logger are pressed immediately to count up the time and record the temperature of the power transformer, respectively. The comparator circuit continuously measures the ΔR of the sensors with respect to time. The STOP buttons of the timer and data logger are pressed once ΔR reaches the set value. Following this, the parameters (ΔR , mean temperature of the power transformer, and time) are compared with the master data (Table 5-16) to determine the elemental sulphur concentration of the insulating oil in ppm.

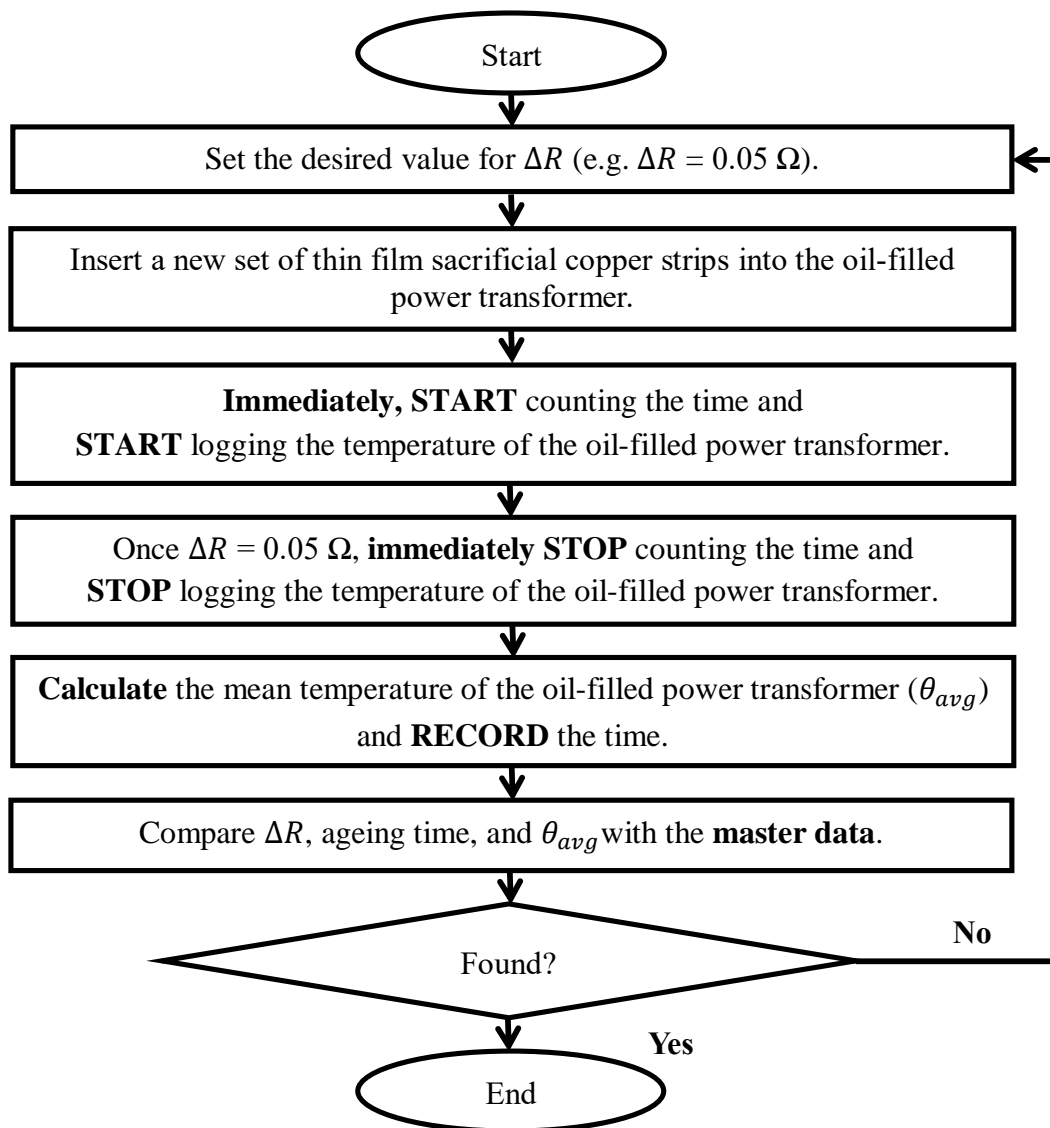


Figure 5-27. Steps involved in implementing the thin film sacrificial copper strips as online sulphur corrosion sensors for quantification of elemental sulphur in transformer insulating oils.

Table 5-16. Master data: The ΔR of the thin film sacrificial copper strips for different elemental sulphur concentrations, ageing period, and ageing temperature.

	Elemental sulphur concentration (ppm)	Ageing period (h)	Ageing temperature (°C)		Elemental sulphur concentration (ppm)	Ageing period (h)	Ageing temperature (°C)
$\Delta R = 0.05 \Omega$	20	5.01	80	$\Delta R = 0.10 \Omega$	20	5.66	80
	30	3.55	80		30	3.78	80
	10	9.80	90		10	11.00	90
	20	4.08	90		20	4.73	90
	30	1.57	90		30	1.74	90
	3	5.50	110		3	7.85	110
	5	3.33	110		5	4.22	110
	10	1.26	110		10	1.59	110
$\Delta R = 0.15 \Omega$	20	6.11	80	$\Delta R = 0.20 \Omega$	20	6.36	80
	30	4.00	80		30	4.11	80
	10	11.77	90		10	12.38	90
	20	5.20	90		20	5.66	90
	30	1.85	90		30	1.94	90
	3	10.03	110		3	12.28	110
	5	4.85	110		5	5.49	110
	10	1.83	110		10	2.03	110
$\Delta R = 0.25 \Omega$		Elemental sulphur concentration (ppm)		Ageing period (h)		Ageing temperature (°C)	
		20		6.60		80	
		30		4.22		80	
		10		12.88		90	
		20		6.13		90	
		30		2.00		90	
		3		13.56		110	
		5		5.99		110	
		10		2.15		110	

5.8 SUMMARY

This chapter presents three significant contributions of this research: (1) the development of a regression model based on the 2^2 factorial design to predict the transformed resistance of the thin film sacrificial copper strips as a function of their area and thickness, (2) the assessment of the feasibility of the thin film sacrificial copper strips in tracking the progression of sulphur corrosion in insulating oils due to the breakdown of DBDS as well as elemental sulphur, and (3) the proposal of an online method for quantification of elemental sulphur in transformer insulating oils using the thin film sacrificial copper strips. Based on the outcomes of the 2^2 factorial design, the sensor area had the most significant effect on the

transformed resistance, with a percentage contribution of 90.19 %. The regression model developed in this research describes the relationship between the transformed resistance (response variable) and area and thickness (independent variables) of the thin film sacrificial copper strips. The regression model was verified using ANOVA and the results showed that the regression model was adequate to predict the transformed resistance of the sensors as a function of their area and thickness, where the R^2 value and p -value of the model were 0.9831 and <0.0001 , respectively. The $RMSE$ was determined to be 0.1079, indicating the reliability of the regression model.

The resistance characteristics of thin film sacrificial copper strips varied in response to the oil corrosivity levels, and the results showed that these sensors were feasible to track the progression of sulphur corrosion in transformer insulating oils due to the breakdown of DBDS as well as elemental sulphur. The effects of DBDS/elemental sulphur concentration and ageing temperature on the characteristics of the sensors were also investigated and the results showed that the increase in the corrosive sulphur compounds (corrosive by-products of DBDS and elemental sulphur) or ageing temperature had a pronounced effect on the rate of sulphur corrosion in the insulating oil. It is evident from the results that the presence of elemental sulphur was more detrimental to oil-filled power transformers compared with the presence of corrosive by-products due to the breakdown of DBDS. Lastly, a novel online method was proposed to quantify the amount of elemental sulphur in transformer insulating oils, which is summarised in the form of a flow chart, as shown in Figure 5-27.

6 CONCLUSIONS

6.1 CONCLUSIONS

It has been proven that insulation failures due to sulphur corrosion are one of the factors that lead to transformer breakdowns. Following this, the main aim of this thesis was to develop a feasible method that can identify if the transformer is at risk of catastrophic failure due to the presence of corrosive compounds in the insulating oils.

In terms of tracking the progression of sulphur corrosion in oil-filled power transformer, the existing standard test methods are very limited. The oil's characterisation based on the BS EN 62535 and ASTM copper strip corrosion standard are imprecise due to visual-based observations as people see colour in their way and therefore different operators might give diverse ratings of the same strip. Interestingly, SEM–EDX proved to be a useful lab-based method to distinguish the oil corrosivity level by detecting a reducing amount of copper in per cent by weight (wt %) of bare copper samples, which indicates the occurrence of sulphur corrosion. However, this technique is costly, requires skilled operators to perform the tests, and could not be performed instantly either online or on-site. Moreover, the corrosivity level of transformer insulating oils in bulk may not be determined as these tools only require a small sample volume compared to the total oil volume of the transformer.

It was found that UV–vis spectroscopy is not a suitable tool to track the progression of sulphur corrosion in insulating oils because it was difficult to distinguish the UV–vis spectra of the aged oil samples, particularly at low DBDS concentrations. In addition, obtained UV–vis spectra indicated that there was no significant shift of bands for the insulating oils aged in 100 ppm of DBDS compared to non-corrosive insulating oils — a result that contradicts the outcomes of SEM–EDX analysis.

It was difficult to characterise the insulating oils based on its corrosivity level through DC conductivity measurements owing to either the uncertainties around the amount of copper ions dissolved in the insulating oil due to its low solubility or the influence of a very low concentration of water content. Meanwhile, remarkably small changes in oil capacitance values were obtained by implementing IDCs as sulphur corrosion sensors. It was assumed

that the changes were due to the presence of corrosive by-products due to the breakdown of DBDS. However, the presence of water and moisture also contributes to changes in oil capacitance values, which complicates the interpretation of results.

Replacement of the existing method (i.e. ASTM D 1275A, ASTM D 1275B, BS EN 62535, ASTM copper strip corrosion standard, and SEM–EDX analysis) with the thin film sacrificial copper strip sensors has the benefit of minimising the possibility of misinterpretation of results because this sensor allows quantitative analysis. This technique is economical and does not require skilled personnel to conduct the tests. In addition, the results provided in Section 5.7 indicate that this technique may be useful in continuously quantifying the elemental sulphur concentrations in transformer insulating oils instantly on-site and has great potential to be implemented online. As a consequence of the use of thin film sacrificial copper strips sensors, it was possible to deduce that: (1) sulphur corrosion is a time-dependent process, (2) the sulphur corrosion rate is accelerated by an increase in either corrosive sulphur compounds (elemental sulphur or corrosive by-products of DBDS) or ageing temperature, (3) elemental sulphur is exceptionally corrosive compared to the corrosive by-products due to the breakdown of DBDS, (4) sulphur corrosion requires a long period to occur in detectable amounts.

6.2 FUTURE WORK

In this research, the quantification of elemental sulphur was based on the ΔR values of the thin film sacrificial copper strips sensors which were obtained randomly without depending on a specific time manner. In addition, the ΔR values were measured at a specific temperature and relative humidity after the thin film sacrificial copper strips sensors were cleaned with acetone. By following this process, the quantification of elemental sulphur concentrations was feasible and could be implemented instantly on-site and has great potential to be implemented online. Therefore, future work could possibly focus on designing a better experimental set-up which allows the quantification of elemental sulphur concentrations based on a continuous measurement of ΔR aged within the range of operating

temperature of power transformers that can ultimately improve the feasibility of the thin film sacrificial copper strips to be applied as an online sulphur corrosion sensor.

From completed work to date, the quantification of elemental sulphur via thin film sacrificial copper strips sensors has been proven (Chapter 5). To completely cover the sulphur corrosion paradigm, further experiments are necessary associated with the quantification of the other corrosive sulphur compounds (i.e. mercaptans and corrosive by-products of DBDS).

In this research, the sulphur corrosion monitoring process was carried out without the influence of metal passivators. However, in a typical field environment, numerous transformer units have been passivated to eliminate the corrosive sulphur-related faults. For further investigation, the technique that have been proposed in this thesis may be tested under the influence of metal passivator because the presence of passivators prevents sulphur attacks on the copper surfaces (explained in Section 2.8), which may influence the quantification of elemental sulphur in the transformer insulating oils.

The other degradation by-products presence in the transformer insulating oils may affect the characteristics of the thin film sacrificial copper strips sensors. In the context of investigating the practicality of this sensor as an online tool for quantification of elemental sulphur concentrations in transformer insulating oils, it is recommended in the future that the technique that has been proposed in this thesis may be further investigated using insulating oil samples obtained from various in-service power transformers.

APPENDIX A: PUBLISHED PAPERS

A.1 CONFERENCE I: M.S.A. KHIAR, R.C.D. BROWN AND P.L. LEWIN, "DETECTION OF SULFUR CORROSION IN TRANSFORMER INSULATION OILS USING AN INTERDIGITATED CAPACITIVE SENSOR BASED ON PRINTED CIRCUIT BOARD TECHNOLOGY," *IN IEEE CONFERENCE ON ELECTRICAL INSULATION AND DIELECTRIC PHENOMENA (CEIDP)*, 2017, PP. 278-281.

Author's Personal Copy

Detection of Sulfur Corrosion in Transformer Insulation Oils Using an Interdigitated Capacitive Sensor Based on Printed Circuit Board Technology

M.S. Ahmad Khiair^{1,2}, R.C.D. Brown³, P.L. Lewin¹

¹ The Tony Davies High Voltage Laboratory, University of Southampton, Southampton SO17 1BJ, United Kingdom

² Universiti Teknikal Malaysia Melaka, Hang Tuah Jaya, 76100 Durian Tunggal, Melaka, Malaysia

³ Department of Chemistry, University of Southampton, Southampton SO17 1BJ, United Kingdom

Abstract- Monitoring sulfur corrosion in insulation oils is essential since sulfur corrosion can result in catastrophic transformer failure when left unchecked. The objective of this study is to analyze the performance of an interdigitated capacitive sensor (IDC) utilizing printed circuit board technology as a potential tool to detect and monitor the progression of sulfur corrosion in mineral insulation oils. The sulfur corrosion is simulated by adding dibenzyl disulfide into 20 ml vials containing 15 ml of vacuum dried and degassed insulation oils at three concentrations: (1) 100, (2) 200, and (3) 300 ppm. Bare copper samples are then added into the oil samples and aged in a forced convection laboratory oven at 150°C for three days. The IDC sensor developed in this study is used to determine the variation in the oil capacitance due to the presence of dibenzyl disulfide. The surface of the bare copper samples is analyzed using scanning electron microscopy-energy dispersive spectroscopy equipped with AZtecEnergy software in order to quantify the variations of the copper and sulfur content. Based on the results, there is a strong positive correlation between the electrical capacitance of the insulation oil and DBDS concentration, whereby the coefficient of determination is within a range of 0.9643-0.9868. In conclusion, the IDC sensor is a simple and inexpensive way of characterizing the quality of insulation oils due to sulfur corrosion and therefore, it has great potential for industrial applications.

I. INTRODUCTION

Degradation in the quality of insulation oils due to sulfur corrosion is one of the main problems of oil-immersed power transformers since the beginning of the 21st century [1] and the problem underlying sulfur corrosion remains unclear to this day. Dibenzyl disulfide (DBDS) is one of the sulfur compounds that play a major role in the sulfur corrosion process, depending on the oil temperature. DBDS is an active sulfur species present in the insulation oil which will react with copper, resulting in the formation of copper sulfide [2]. For this reason, many scientists and researchers use DBDS as the sulfur compound of choice in order to simulate a corrosive environment for non-corrosive oil matrices.

The formation of conductive copper sulfide in transformer insulation oils is a critical issue since the quality of the insulation oil or paper will deteriorate significantly if the amount of copper sulfide reaches the critical value, culminating in catastrophic transformer failure.

At present, there are three measures that can be implemented to mitigate this issue: (1) replacing the insulation oil, (2) treating the insulation oil using an oil passivator, and (3) adding metal passivators into the insulation oil. Replacing insulation oils during periodic maintenance is not a feasible solution since disposing the aged oils into the landfill is detrimental to the environment and moreover, it is costly to replace aged oils with new ones. For these reasons, oil passivation (which is a preventive measure) was introduced in 2005 by oil refiners, and this technique was adopted by transformer manufacturers [3] due to its economic value. Much effort has also been made to mitigate sulfur corrosion using triazole-based passivator [4], Irgamet® 39 passivator [5], as well as blending the insulation oil with turmerone extract, which is a sulfur corrosion retardant [6]. Nevertheless, there is still a lack of understanding on the effects of sulfur corrosion on the quality of insulation oils and the duration of these effects. In general, it is crucial to monitor the progression of sulfur corrosion in insulation oils before implementing any preventive measures.

To date, various techniques have been developed to detect the presence of DBDS in insulation oils. One of these techniques involve using a gas chromatograph interfaced to suitable detectors such as atomic emission detector (AED) or mass spectrometer (MS), which is capable of quantifying the amount of DBDS for concentrations up to 5 mgkg⁻¹ [7]. According to Toyama et al. [7], the presence of DBDS in insulation oils can be detected using alumina-based solid phase extraction (SPE), followed by gas chromatography-mass spectrometry (GC-MS), for concentrations up to 0.1 ppm. More recently, a reliable test procedure using X-ray fluorescence (XRF) spectrometry was developed to determine the corrosion levels of insulation oils [1]. This technique permits quantitative analysis of sulfur and copper in insulation oils up to 4.05 and 1.95 ppm, respectively. In general, all of the aforementioned techniques involve relatively expensive piece of equipment and these techniques require skilled personnel to conduct the tests. In addition, the techniques are time-consuming since the oil samples need to be sent to an external laboratory. On the other hand, common condition monitoring tools such as sweep frequency response analysis (SFRA), return voltage measurement (RVM), partial discharge (PD), turns-ratio, and dissolved gas analysis (DGA) are proven to be inappropriate to monitor the presence and

progression of sulfur corrosion in insulation oils [1]. Thus, there is a critical need to develop a simple, reliable, and inexpensive detection system which will greatly facilitate operators in evaluating the quality of insulation oils due to sulfur corrosion.

For years, interdigitated capacitive sensors (IDCs) have been exploited for a wide range of applications including capacitive pressure sensors, capacitive fingerprint sensors, humidity sensors, and biosensors. A number of studies have been carried out on complex mathematical calculations and simulations of IDCs as well as complex chemical surface treatment of IDCs. However, there are no studies concerning the application of IDCs in detecting the changes in electrical capacitance due to the progression of sulfur corrosion in insulation oils, which forms the motivation of this study. Hence, in this study, the progression of sulfur corrosion is monitored based on the variations of electrical capacitance of the insulation oils. The variations in electrical capacitance are detected using an IDC fabricated onto a printed circuit board (PCB).

II. SAMPLE PREPARATION AND EXPERIMENTAL SETUP

Nyro Gemini X mineral oil (courtesy of Nynas AB, Sweden) was chosen for the insulation oil. Based on the specifications of insulation oils given in the BS EN 62535 standard test method [8], this mineral oil is classified as an inhibited oil since it is free from both DBDS (maximum total sulfur content: 0.05%) and metal passivators.

The oil samples were first treated by vacuum drying and degassing at 85°C in a vacuum oven for 48 h. Next, DBDS (purity: $\geq 98\%$, Sigma-Aldrich, USA) was added into glass bottles containing the treated oil samples at different concentrations: (1) 100, (2) 200, and (3) 300 ppm in order to simulate different corrosion levels. The solutions were prepared based on dilution by weight. Each of the glass bottle was cleaned with acetone and then dried at 105°C for 2 h in order to eliminate moisture. The glass bottles were then cooled to room temperature for 20 min. A hot plate magnetic stirrer was used to thoroughly mix the oil with DBDS (for ~ 1 h) in order to attain a homogeneous mixture. The temperature of the hot plate was set between 71 and 72°C based on the melting point of the DBDS [9]. The oil samples were stirred in tightly sealed glass bottles in order to prevent the samples from moisture ingress.

The copper samples were prepared by polishing copper sheets (area: 200 mm², thickness: 0.5 mm) with abrasive paper. The copper sheets were cleaned three times with cyclohexane (purity: $> 99\%$, Fisher Scientific UK Ltd, UK). This process is essential to remove oxide layers that formed on the surface of the copper sheets.

The treated copper samples were placed carefully into headspace glass vials, whereby each vial contains 15 ml of oil sample mixed with DBDS at a different concentration. The glass vials were sealed with sulfur-free polytetrafluoroethylene (PTFE)-faced silicone septum and aluminum caps, and the vials were placed in a digital forced convection laboratory oven with air atmosphere at $150 \pm 1^\circ\text{C}$

for three days. Once the aging process was complete, the copper samples were taken out from the vials using a clean pair of tweezers. The copper samples were degassed by rinsing the samples with cyclohexane three times. The copper samples were analyzed using scanning electron microscopy-energy dispersive spectroscopy (SEM-EDX) in accordance with the BS EN 62535 standard test method [8]. This quantitative analysis is essential to determine the elemental chemical deposition (particularly, copper sulfide) on the surface of the bare copper samples. Three different areas on the same surface were chosen for analysis for the aged copper samples in order to determine the repeatability and reproducibility of the results.

In addition, the oil samples were degassed in the vacuum oven without heating for six days in order to reduce the moisture content of the oil samples. Since the variations in the moisture content results in significant variations in the oil capacitance measurements, the moisture content of the oil samples was kept within 13 ± 1 ppm. The IDC sensor was then used to characterize the corrosion level of the insulation oils.

The IDC sensor was connected to the LCR400 precision LCR bridge (Aim and Thurlby-Thandar Instruments, UK) with a frequency: 10 kHz via a co-axial cable. The co-axial cable was used to minimize the effect of stray capacitance, which will influence the accuracy of the measured values. The oil capacitance measurements were performed at ambient temperature. The measurement procedure was repeated three times for each sample to ensure that the results were consistent.

III. DESIGN AND FABRICATION OF THE INTERDIGITATED CAPACITIVE SENSOR

The IDC used in this study consists of a pair of coplanar interdigitated electrodes, as shown in Fig. 1. The sensors were fabricated using a photolithographic process on a copper clad flame retardant FR-4 PCB laminate. First, the pattern was designed using EAGLE PCB design and schematic software. Next, the mask for the sensor pattern was prepared by transferring the EAGLE drawing onto a polyester drafting film using a high-resolution laser printer. The sensor pattern was transferred onto a photoresist-coated copper clad PCB by ultraviolet (UV) photolithography. The sensor pattern was inspected for any defects and then dried. The sensor pattern was formed by exposing the FR-4 PCB to ferric chloride solution, agitated, and then turned for ~ 20 min to remove unwanted copper. The process time depends on the amount of copper to be removed. It shall be noted that this process needs to be carried out with painstaking detail since there is a high possibility for the tracks to be over-etched.

The operating principle of the IDC sensor is identical to that for a conventional parallel plate capacitor. As shown in Fig. 2, the electric field lines of the coplanar capacitor are initiated by the parallel plate capacitor. The capacitance of a conventional parallel plate capacitor is determined from the following equation:

$$C = \epsilon_0 \epsilon_r (A/d) \quad (1)$$

where ϵ_0 is the permittivity of the free space, which is equal to 8.854 pF/m, ϵ_r is the dielectric permittivity of material, A is the area of the sensor, and d is the gap between two parallel electrodes. For an IDC, (1) can be written as:

$$C = \epsilon_0 \epsilon_r (lwn/d) \quad (2)$$

where l is the finger length, w is the finger width, n is the number of fingers, and d is the gap between two parallel fingers, having a value of 8, 0.5, 16, and 0.5 mm, respectively. According to [10], (2) is suitable only if the finger gap and finger width values are the same. For this reason, the sensor was designed with the finger gap and finger width equal to 0.5 mm.

The total capacitance is given by [10]:

$$C_{total} = C_{sub} + C_{up} \quad (3)$$

where C_{sub} is the total capacitance of the substrate and C_{up} is the change in capacitance resulting from the exposure of the sensor to air or liquid having a different dielectric constant. In this study, FR-4 PCB ($\epsilon_r = 4.9$) was used as the substrate. For calibration purposes, acetone ($\epsilon_r = 21.01$) was used whereby the measured capacitance values were compared with the theoretical values determined using (3).



Fig. 1. Schematic diagram of the IDC



Fig. 2. Electric field lines of the IDC evaluated from the (a) parallel plate electrode to the (b) intermediate shape, resulting in (c) coplanar interdigitated electrode [10]

IV. RESULTS AND DISCUSSION

A. SEM-EDX Spectroscopy

The quantified sulfur and copper deposits on the bare copper samples obtained using SEM-EDX are shown in Fig. 3 and Fig. 4, respectively. It is evident from Fig. 3 that the amount of sulfur on the bare copper surface increases with an increase in DBDS concentration in the insulation oil. On Day 1, the amount of sulfur on the bare copper samples increases to 1.64, 2.01, and 2.46 wt.% for a DBDS concentration of 100, 200, and 300 ppm, respectively. On Day 2, the amount of sulfur

increases further to 3.17, 4.96, and 5.64%. Likewise, the amount of sulfur deposits on the surface of the bare copper samples increases further on Day 3, with a value of 6.34, 8.71, and 8.83% when the DBDS concentration is 100, 200, and 300 ppm, respectively.

However, a different trend is observed for the copper deposits, as shown in Fig. 4. It can be seen that the amount of copper on the surface of the bare copper samples decreases with an increase in the DBDS concentration. This indicates that the sulfur corrosion process in an actual oil-immersed power transformer is accelerated at higher concentrations of DBDS. This leads to higher dissolution of copper in the insulation oil. It can be observed from Fig. 4 that on Day 1, the amount of copper decreases to 98.36, 97.99, and 97.54 wt.% for a DBDS concentration of 100, 200, and 300 ppm, respectively. On Day 2, the amount of copper decreases further to 96.83, 95.04, and 94.36%. Likewise, amount of copper decreases gradually to 93.66, 91.29, and 91.17% on Day 3 when the DBDS concentration is 100, 200, and 300 ppm, respectively. After 3 days of ageing, there is only 0.12% decrease in the amount of copper present on the surface of the bare copper samples when the concentration of DBDS is 200 and 300 ppm. This suggests that the corrosive by-products resulting from the breakdown of DBDS may not be linear over time.

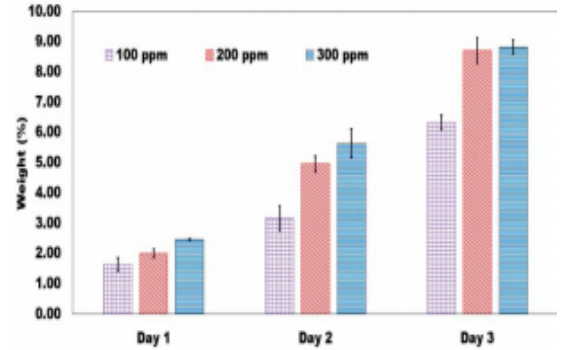


Fig. 3. Amount of sulfur traced on the surface of the bare copper samples using SEM-EDX

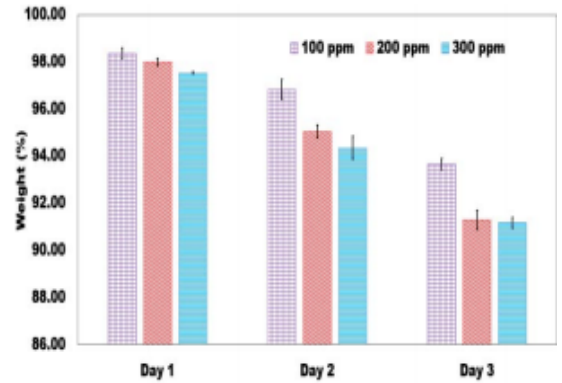


Fig. 4. Amount of copper traced on the surface of the bare copper samples using SEM-EDX

B. Oil Capacitance Measurements Obtained from IDC

The oil capacitance measurements were analyzed to assess the degradation of the insulation oil quality due to the presence of DBDS. Table I shows the relationship between the oil capacitance values measured using IDCs and DBDS concentrations for 3 different days. In general, there is a strong positive correlation between the oil capacitance and DBDS concentration, whereby the coefficient of determination (R^2) value is 0.9643, 0.9643, and 0.9868 for Day 1, 2, and 3, respectively.

TABLE I Relationship between the oil capacitance values measured using IDCs and DBDS concentrations for 3 different days

Time	Fitting Equations	R^2
Day 1	$y = 0.0003x + 6.1133$	0.9643
Day 2	$y = 0.0002x + 6.1733$	0.9643
Day 3	$y = 0.0002x + 6.1733$	0.9868

It can be observed from Fig. 5 that on Day 1, the oil capacitance increases to 6.14, 6.18, and 6.20 pF for a DBDS concentration of 100, 200, and 300 ppm, respectively. On Day 2, the oil capacitance increases further to 6.19, 6.20, and 6.22 pF. Likewise, on Day 3, the oil capacitance increases to 6.20, 6.22, and 6.25 pF. After 3 days of ageing, there is still an increase in oil capacitance when the DBDS concentration is increased from 200 to 300 ppm although there are no significant differences in the amount of copper on the surface of the copper samples. It is believed that the moisture present in the oil can be a contributing factor to the increase in oil capacitance observed in this study. Based on the results, it can be deduced that the DBDS concentration increases the polar materials in the insulation oil. This in turn, increases the dipole density and electric susceptibility of the insulation oil, which is evidenced from the higher oil capacitance values. The increase in oil capacitance values is extremely small because the tests were conducted under accelerated ageing conditions within a very short period. It is anticipated that a significant changes in oil capacitance values could be achieved if the tests are carried out under long-term ageing conditions.

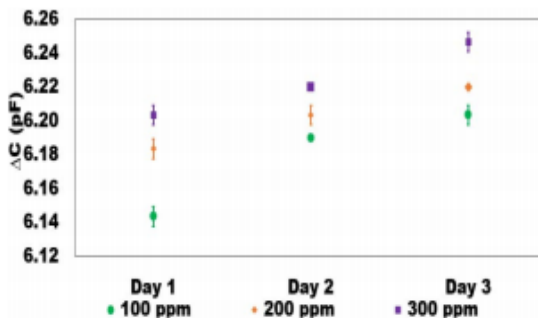


Fig. 5. Variation of oil capacitance with respect to aging time for three DBDS concentrations measured using the IDC sensor

V. CONCLUSION

A low-cost sensor with a highly stable sensing capability for detection and condition monitoring of corrosive sulfur in insulating oils has been developed successfully in this study. The preliminary results presented in this paper indicate that there is a potential relationship between corrosive sulfur and changes in oil capacitance values. In future studies, the sensing capability of the IDC sensor will be further enhanced by considering the use of thin film gold electrode with nano-sized finger gaps.

ACKNOWLEDGMENT

The first author is greatly indebted to the Government of Malaysia and Universiti Teknikal Malaysia Melaka (UTeM) for providing the financial support throughout his PhD study. The authors wish to express their appreciation to Dr. Richard Pearce from Ocean and Earth Science, National Oceanography Centre (NOCS), University of Southampton, for the SEM-EDX analysis. In addition, the authors graciously thank Mr. Richard Howell for manufacturing the PCB.

REFERENCES

- [1] P. S. Amaro, M. Facciotti, A. F. Holt, J. A. Pilgrim, P. L. Lewin, and R. C. D. Brown, "X-Ray Fluorescence as a Condition Monitoring Tool for Copper and Corrosive Sulphur Species in Insulating Oil," *IEEE Trans. Dielectr. Electr. Insul.*, vol. 22, no. 2, pp. 701–708, 2015.
- [2] R. Maina, V. Tumiat, M. Pompili, and R. Bartnikas, "Corrosive Sulfur Effects in Transformer Oils and Remedial Procedures," *IEEE Trans. Dielectr. Electr. Insul.*, vol. 16, no. 6, pp. 1655–1663, 2009.
- [3] F. Scatiggio, M. Pompili, and R. Bartnikas, "Effects of Metal Deactivator Concentration upon the Gassing Characteristics of Transformer Oils," *IEEE Trans. Dielectr. Electr. Insul.*, vol. 18, no. 3, pp. 701–706, 2011.
- [4] T. Amimoto, E. Nagao, J. Tanimura, S. Toyama, and N. Yamada, "Duration and Mechanism for Suppressive Effect of Triazole-based Passivators on Copper-sulfide Deposition on Insulating Paper," *IEEE Trans. Dielectr. Electr. Insul.*, vol. 16, no. 1, pp. 257–264, 2009.
- [5] I. Tronstad, C. M. Roel, W. R. Glomm, and E. A. Blekkan, "Ageing and Corrosion of Paper Insulated Copper Windings: The Effect of Irgamet® 39 in Aged Insulated Oil," *IEEE Trans. Dielectr. Electr. Insul.*, vol. 22, no. 1, pp. 345–358, 2015.
- [6] V. Dukhi, A. Bissessur, and B. S. Martincigh, "Unique Antioxidant and Sulfur Corrosion Retardant Properties of Transformer Oil Blended with Turmerone Extract," *IEEE Trans. Dielectr. Electr. Insul.*, vol. 22, no. 5, pp. 2798–2808, 2015.
- [7] S. Toyama, J. Tanimura, N. Yamada, E. Nagao, and T. Amimoto, "Highly Sensitive Detection Method of Dibenzyl Disulfide and the Elucidation of the Mechanism of Copper Sulfide Generation in Insulating Oil," *IEEE Trans. Dielectr. Electr. Insul.*, vol. 16, no. 2, pp. 509–515, 2009.
- [8] "BS EN 62535:2009: Insulating liquids — Test method for detection of potentially corrosive sulphur in used and unused insulating oil," pp. 1–22, 2011.
- [9] "BS EN 62697-1:2012: Test Methods for Quantitative Determination of Corrosive Sulfur Compounds in Unused and Used Insulating Liquids Part 1: Test Method for Quantitative Determination of Dibenzyl Disulfide (DBDS)," pp. 1–36, 2012.
- [10] I. Bilican, M. T. Guler, N. Gulener, M. Yuksel, and S. Agan, "Capacitive Solvent Sensing with Interdigitated Microelectrodes," *Microsyst. Technol.*, vol. 22, no. 3, pp. 659–668, 2016.

A.2 CONFERENCE II: M.S.A. KHIAR, R.C.D. BROWN AND P.L. LEWIN, “TRACKING THE PROGRESSION OF SULFUR CORROSION IN TRANSFORMER OIL USING THIN FILM SACRIFICIAL COPPER STRIP,” IN *IEEE 2ND INTERNATIONAL CONFERENCE ON DIELECTRICS (ICD)*, 2018, PP. 1-4.

Author's Personal Copy

Tracking the Progression of Sulfur Corrosion in Transformer Oil Using Thin Film Sacrificial Copper Strip

M.S. Ahmad Khiair^{1,2}, R.C.D. Brown³, P.L. Lewin¹

¹The Tony Davies High Voltage Laboratory, University of Southampton, Southampton SO17 1BJ, United Kingdom

²Universiti Teknikal Malaysia Melaka, Hang Tuah Jaya, 76100 Durian Tunggal, Melaka, Malaysia

³Department of Chemistry, University of Southampton, Southampton SO17 1BJ, United Kingdom

Abstract—In this work, thin film sacrificial copper strips are introduced as sensors to provide a direct indication on the corrosiveness of insulating oils. The progression of sulfur corrosion in transformer insulating oils was simulated by adding different concentrations of dibenzyl disulfide into glass Petri dishes, each containing 40 mL of non-corrosive oil. The resistive thin film copper strips were deposited onto a glass substrate using an electron beam evaporator and the strips were then immersed into the corrosive oil samples. The samples were aged in a forced convection laboratory oven at 130 °C for 20 h. The material loss due to the presence of corrosive compounds was monitored by measuring the resistance of the thin film copper strips using four-wire resistance measurements. The preliminary results reveal that the corrosive by-products (due to the breakdown of dibenzyl disulfide) accelerates the corrosion of the thin film copper strips, as evidenced from the amount of copper loss on the surface of the strips. This increases the resistance values of the thin film copper strips. Based on the variations in the resistance of the thin film copper strips, one can infer the level of sulfur corrosion in transformer insulating oils.

Keywords—DBDS; 4-wire resistance measurement; low resistance; sulfur corrosion sensor; thin film copper

I. INTRODUCTION

The deposition of copper sulfide on the cellulose insulation contributes to turn-to-turn breakdowns that lead to transformer catastrophic failure. The presence of copper and corrosive sulfur compounds in insulating oils are identified as the main contributing factor. Hundreds of different sulfur compounds exist in mineral oil [1], nevertheless only a few of them are corrosive.

The most reactive sulfur compounds are elemental sulfur and mercaptans, followed by sulfides [2]. Thiophenes are identified as the most stable sulfur compounds. Disulfide such as dibenzyl disulfide (DBDS) is expected to be stable. DBDS is commonly used as secondary oil antioxidants [3] that provide a protection against the oxygen ingested during transformer operation. However, DBDS could degrade from a stable into a reactive sulfur compound as shown in Fig. 1. Benzyl mercaptan due to the breakdown of DBDS is extremely reactive to copper that will ultimately cause a

copper corrosion.

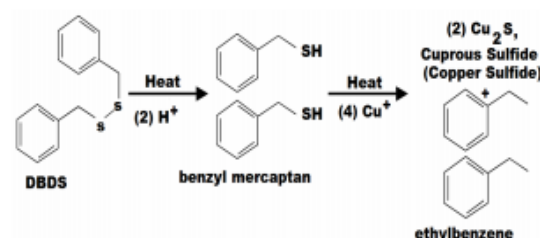


Fig. 1. Degradation of a stable DBDS into a reactive benzyl mercaptan [1]

Consequently, much research has been made on investigating the threshold of DBDS concentration which will result in corrosive oil, and one of them revealed that the minimum concentration of DBDS which will make the oil potentially corrosive according to the BS EN 62535 standard is ~10 mg kg⁻¹ [4].

Various techniques have been developed to detect the presence of DBDS. The most sensitive technique (~0.1 ppm) proposed the use of alumina-based solid phase extraction and gas chromatography-mass spectrometry [5]. Nevertheless, this technique involves relatively expensive equipment and requires skilled personnel to conduct the tests. Besides, there are several standard corrosion tests have been proposed. ASTM D1275B standard test method [6] describes a technique that compares the discoloration of the copper surface with standard reference color scale (ASTM D130-12 standard test method [7]). However, this qualitative test will likely lead to misinterpretation of the results since the analysis of sulfur corrosion depends on visual observations, which may vary from one operator to another.

On the other hand, a preventive measure by means of common oil passivators such as benzotriazole (BTA) and Irgamet®39 are used to protect the copper surface from corrosive sulfur attack [8]. However, the addition of these passivators will not eliminate any corrosive sulfur species and thus, the restoration of insulating oil properties is impossible. Besides, the duration taken for these passivators to be long last is still vague.

To overcome the aforementioned issues, a quantitative method is proposed in this paper whereby we had investigated the practicality of the use of thin film sacrificial copper strip as a direct indicator for monitoring the level of transformer oil corrosiveness. The material loss due to the presence of corrosive compounds was monitored by measuring the resistance of the thin film copper strips using 4-wire resistance measurement.

II. SAMPLE PREPARATION AND EXPERIMENTAL SETUP

A. Sensor Design and Fabrication

The thin film sacrificial copper strips were fabricated on a 25 × 75 mm rectangular Schott® Borofloat glass substrate with a thickness of 1 mm. This type of glass substrate was chosen due to several advantages such as the extremely good scratch resistance with a very good surface homogeneity. This characteristic is essential to ensure a homogenous copper could be evaporated on it.

Besides, the thermal stability of the substrate is crucial to be considered. Borofloat was chosen as a substrate as it could operate at a maximum temperature of 450 °C with a very low thermal expansion effect. Furthermore, Borofloat is resistant to water, alkalis, acids and organic substances and thus, minimizes any effects of acids resulting from the accelerated aging process on the experimental results.

A pure (99.99%) copper wire was used for the evaporation process. The thin copper films with a thickness of 200 nm were deposited using BOC Edwards E500a e-beam evaporator with a base pressure of $\sim 5 \times 10^{-6}$ mBar. To improve the adhesion of the thin film copper layer on the glass substrate, 5 nm titanium layer was firstly deposited. The sensors were then stored in a desiccator equipped with silica-gel under vacuum atmosphere.

B. Oil Samples Preparation

Nytro Gemini X mineral oil (courtesy of Nynas AB, Sweden) was used to prepare the corrosive oil samples. This non-corrosive oil meets the requirement of BS EN 62535 standard test method specifications [6]. The properties (stability) of this non-corrosive oil is presented in Table 1. DBDS normally originates in certain insulating oils between 100 and 1,000 ppm [1]. Due to this reason, DBDS at three concentrations of 100, 250, and 1,000 ppm were chosen to simulate the different corrosion levels.

The solutions were prepared based on dilution by weight. Each glass bottle was cleaned with solvent and then dried for ~ 2 h at 105 °C to eliminate moisture. The glass bottles were then cooled to room temperature for ~ 10 min. Next, the solutions (insulating oils mixed with DBDS) were stirred for ~ 1 h using a hot plate magnetic stirrer to attain homogeneous mixtures. The temperature of the hot plate was set between 71 and 72 °C based on the melting point of DBDS [9]. A sealed tight glass bottles were used during the mixing process to prevent contaminations.

TABLE I. THE PROPERTIES OF MINERAL OIL USED IN THIS EXPERIMENT

Property	Test Method	Typical Data
Total sulfur content (%)	ISO 14596	0.01
Corrosive sulfur	DIN 51353	Non-corrosive
Potentially corrosive sulfur	IEC 62535	Non-corrosive
Corrosive sulfur	ASTM D 1275 B	Non-corrosive
DBDS (mg/kg)	IEC 62697-1	Non-detectable
Antioxidant (wt%)	IEC 60666	0.38
Metal passivator additives (mg/kg)	IEC 60666	Non-detectable
Acidity (mg KOH/g)	IEC 62021	<0.01

C. Experimental Setup

The sensors surfaces were gently cleaned using soft tissue prior the immersing process. The sensors were placed carefully into glass Petri dishes. Each Petri dish contained 40 mL of mineral oil with (100, 250, and 1,000 ppm) and without DBDS (0 ppm). It was crucial to cover all Petri dishes with plate glass to prevent any excessive evaporation during the aging process. The sensors were aged in a fan oven at 130°C for 20 h. During the test period, the samples were taken out every 5 h for measuring their resistance. Prior the resistance measurements, the sensors were taken out from the Petri dishes using a clean tweezer and were gently degreased by rinsing with solvent three times to prevent any scratch on the sensor surface.

D. Low Resistance Measurement

The low resistance measurements were performed at ambient temperature ($21 \pm 1^\circ\text{C}$) using Megger DLRO-10X Ducter digital low resistance ohmmeter. The 4-wire measurement technique determined the resistance of the sensors by measuring the voltage when contacting the four collinear probes on a sensor surface. As the measured resistance is relatively low, this method eliminates the cable and contact resistance. A 100 mA forward and reverse current was applied to eliminate the thermo-EMF and offset voltage. The measurement was repeated seven times for each condition to ensure the consistency of the results. As shown in Fig. 2, 100 mA current I_{AD} flows between probes A and D while measuring the potential different V_{BC} between probes B and C. The resistance of the thin film copper is calculated as:

$$R = V_{BC} / I_{AD} \quad (1)$$

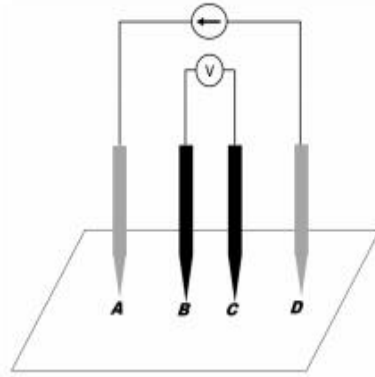


Fig. 2. Measuring resistance of the sensors using 4-wire measurement technique

III. RESULTS AND DISCUSSION

Theoretically, the increasing material loss from metal results in the increase of electrical resistance [10]. To help understand this relationship, the calculated resistance of the proposed sensor versus its thickness is shown in Fig. 3. The resistance of the sensors increases by more than one order of magnitude when the sensors thickness reduces from 200 nm to 20 nm. Due to this reason, the sulfur corrosion phenomenon is possible to be monitored by measuring the resistance of the sensors. However, this method is only applicable for the case of the occurrence of the uniform corrosion at a constant rate.

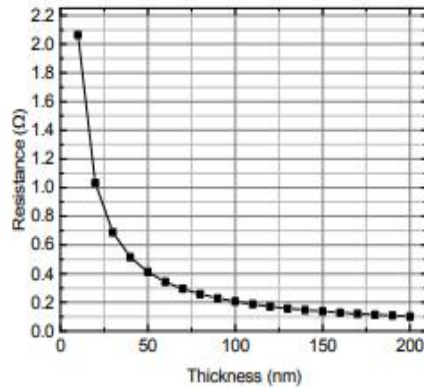


Fig. 3. Calculated thin film copper resistance against thickness

A. Surface Morphology of Sensors

The results presented in Table 2 indicate that the color changes of the sensors were due to the presence of corrosive by-product from the breakdown of DBDS that resulted in copper losses from the surface of the glass substrate. After 5 h of aging, the color of the sensors changed linearly with DBDS concentrations. It can be clearly observed that the sensor without DBDS (0 ppm) was orange and changed to gold with partial orange (100 and 250 ppm) and entirely gold (1,000 ppm). The same pattern could be observed for the longer period of aging. In addition, after 10 h of aging, the

sensors changed its color from partially gold (100 and 250 ppm) to entirely purple (1,000 ppm). There are no significant changes in the color of the sensor aged in 100 and 250 ppm of DBDS, for 15 and 20 h, respectively. However, the color of the sensor that was aged in 1,000 ppm of DBDS changed from entirely purple to entirely light green after 15 h of aging. For the longer aging time (20 h), the sensors changed its color from entirely green to a mix of green, gold, and red. Interestingly, the color of the sensor that was aged without the presence of DBDS changed from orange to tarnished orange. It is assumed that the thermal aging could possibly affect the surface morphology of the sensors. Therefore, it is difficult to distinguish the effect between aging and sulfur corrosion by visual observation on the changes in surface morphology of the sensors. Due to this reason, a low resistance measurement is suggested to further investigate the practicality of this method in tracking the progression of sulfur corrosion in transformer oils.

TABLE II. OPTICAL PHOTOGRAPHS OF 200 NM THIN FILM COPPER STRIPS AGED AT 130 °C IN DIFFERENT DBDS CONCENTRATIONS

Time	DBDS Concentrations			
	0 ppm	100 ppm	250 ppm	1000 ppm
5 h				
10 h				
15 h				
20 h				

B. Resistance Changes of Sensors

Fig. 4 shows the electrical resistance of the sensor as a function of aging time with respect to four different DBDS concentrations. The initial resistance of the sensors were experimentally obtained to be $141 \pm 1 \text{ m}\Omega$. The sulfur corrosion was not occurred in the sensor without DBDS (0 ppm) as evidenced by Fig. 4 where the measured resistances for all interval aging times were slightly less or approximately the same as the initial resistance.

In general, the low resistance measurement data shown in Fig. 4 demonstrate that increasing DBDS concentration accelerated the sulfur corrosion process. It is evidenced by Fig. 4 that the amount of copper losses from the glass substrate was more pronounced at higher DBDS concentration (1,000 ppm) which caused the thin film copper strips to corrode faster. This significantly increased the resistance values of the sensor. This indicates that the presence of DBDS in an actual oil-immersed power transformer plays an important role towards the sulfur corrosion process.

As illustrated in Fig. 4, the sulfur corrosion process started as early as 5 h after the aging took place with the presence of only 100 ppm of DBDS. After 5 h of aging, the resistance of the sensors increased to 143.20, 149.08, and 151.59 $\text{m}\Omega$ for the DBDS concentrations of 100, 250, and 1,000 ppm, respectively. It can be observed from Fig. 4 that aging time is one of the factors that expedited the sulfur corrosion process. After 10 h of aging, the resistance of the sensors increased further to 149.62, 165.73, and 184.91 $\text{m}\Omega$, respectively. The electrical resistance of the sensors increased further after 15 h of aging to 157.59, 184.64, and 229.70 $\text{m}\Omega$ for the DBDS concentrations of 100, 250, and 1,000 ppm, respectively. The corrosive sulfur compounds due to the breakdown of 1,000 ppm of DBDS aged for 20 h increased significantly by 17% compared to 15 h of aging.

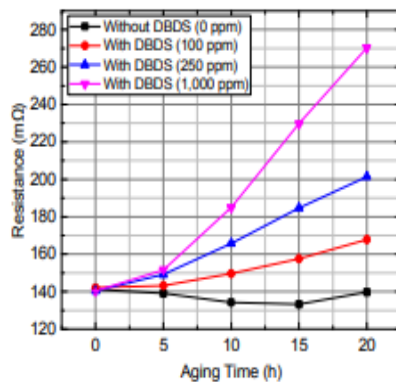


Fig. 4. The electrical resistance of the sensors as a function of aging time for four DBDS concentrations

IV. CONCLUSION

A sensor utilizing the thin film sacrificial copper strip for tracking the progression of sulfur corrosion due to the breakdown of DBDS has been proposed in this research. The results presented in this paper show that there is a potential relationship between the corrosive sulfur and the changes in the thin film resistance values. In future studies, the sensing capability of the thin film sacrificial copper strip as a sensor will be further evaluated under different temperatures as well as the thickness.

ACKNOWLEDGMENT

The first author is greatly thankful to the Government of Malaysia and Universiti Teknikal Malaysia Melaka (UTeM) for the financial support throughout his PhD study. The authors wish to express their appreciation to the Integrated Photonics Cleanroom, Optoelectronics Research Centre, University of Southampton, for the e-beam evaporator.

REFERENCES

- [1] L. R. Lewand and S. Reed, "Destruction of Dibenzyl Disulfide in Transformer Oil," in 75th Annual International Doble Client Conference, 2008, pp. 1–20.
- [2] L. R. Lewand, "The Role of Corrosive Sulfur in Transformers and Transformer Oil," Doble Engineering Company, USA, pp. 1–15, 2002.
- [3] J. M. Lukic, S. B. Milosavljevic, and A. M. Orlovic, "Degradation of the Insulating System of Power Transformers by Copper Sulfide Deposition: Influence of Oil Oxidation and Presence of Metal Passivator," *Ind. Eng. Chem. Res.*, vol. 49, no. 20, pp. 9600–9608, 2010.
- [4] M. A. G. Martins and A. R. Gomes, "Experimental Study of the Role Played by Dibenzyl Disulfide on Insulating Oil Corrosivity—Effect of Passivator Irgamet 39," *IEEE Electrical Insulation Magazine*, vol. 26, no. 4, pp. 27–32, 2010.
- [5] S. Toyama, J. Tanimura, N. Yamada, E. Nagao, and T. Amimoto, "Highly Sensitive Detection Method of Dibenzyl Disulfide and the Elucidation of the Mechanism of Copper Sulfide Generation in Insulating Oil," *IEEE Trans. Dielectr. Electr. Insul.*, vol. 16, no. 2, pp. 509–515, 2009.
- [6] ASTM D1275-15: Standard Test Method for Corrosive Sulfur in Electrical Insulating Oils 1, 2015.
- [7] ASTM D130-12: Standard Test Method for Corrosiveness to Copper from Petroleum Products by Copper Strip Test, 2012.
- [8] M. Facciotti, P. S. Amaro, R. C. D. Brown, P. L. Lewin, J. A. Pilgrim, G. Wilson, P. N. Jarman, and I. W. Fletcher, "Static Secondary Ion Mass Spectrometry Investigation of Corrosion Inhibitor Irgamet 39 on Copper Surfaces Treated in Power Transformer Insulating Oil," *Corros. Sci.*, vol. 98, pp. 450–456, 2015.
- [9] BS EN 62697-1:2012: Test Methods for Quantitative Determination of Corrosive Sulfur Compounds in Unused and Used Insulating Liquids Part 1: Test Method for Quantitative Determination of Dibenzyl Disulfide (DBDS), 2012.
- [10] A. Agoston, E. Svasek, and B. Jakoby, "A Novel Sensor Monitoring Corrosion Effects of Lubrication Oil in an Integrating Manner," in *IEEE Conference on Sensors*, 2005, pp. 1120–1123.

A.3 CONFERENCE III: M.S.A. KHIAR, R.C.D. BROWN AND P.L. LEWIN, “EFFECT OF TEMPERATURE CHANGES ON THIN FILM SACRIFICIAL COPPER STRIPS DUE TO SULFUR CORROSION,” IN *IEEE CONFERENCE ON ELECTRICAL INSULATION AND DIELECTRIC PHENOMENA (CEIDP)*, 2018, pp. 490-493.

Author's Personal Copy

2018 IEEE Conference on Electrical Insulation and Dielectric Phenomena – Cancun – Mexico

Effect of Temperature Changes on Thin Film Sacrificial Copper Strips due to Sulfur Corrosion

M.S. Ahmad Khia^{1,2}, R.C.D. Brown³, P.L. Lewin¹

¹ The Tony Davies High Voltage Laboratory, University of Southampton, Southampton SO17 1BJ, United Kingdom

² Universiti Teknikal Malaysia Melaka, Hang Tuah Jaya, 76100 Durian Tunggal, Melaka, Malaysia

³ Department of Chemistry, University of Southampton, Southampton SO17 1BJ, United Kingdom

Abstract- This paper presents the characteristics of thin film copper strips due to sulfur corrosion at different temperatures. Thin film copper with a layer thickness of 200 nm was deposited onto a glass substrate using an electron beam evaporator. In order to enhance the adhesion of thin film copper on the glass substrate, titanium with a layer thickness of 5 nm was deposited prior to copper evaporation. Three dibenzyl disulfide (DBDS) concentrations were chosen to simulate the different levels of oil corrosiveness: (1) 100, (2) 250, and (3) 1000 ppm. The thin film copper strips were immersed in the corrosive oil samples and then aged in a forced convection laboratory oven at 120 and 130 °C for 25 h. The copper loss due to sulfur corrosion was monitored by measuring the resistance of the thin film copper strips using the 4-wire measurement method. Based on the preliminary results, sulfur corrosion is accelerated by increasing the temperature from 120 to 130 °C. The amount of copper losses from the glass substrate caused by the corrosive by-products due to the breakdown of DBDS is more pronounced at higher temperature, as evidenced from the measured resistance values.

I. INTRODUCTION

Power transformer failures directly or indirectly related to sulfur corrosion are of great interest among researchers for many decades. Sulfur corrosion causes the deposition of copper sulfide onto the insulating paper, resulting in turn-to-turn breakdowns and eventually leads to catastrophic failures of transformers. Periodic replacement of transformer insulating oils such as mineral oils is not a cost-effective solution [1]. In addition, mineral oils are non-biodegradable and toxic, rendering these oils hazardous toward aquatic life in onshore and offshore environments.

A number of mitigation techniques were used to overcome the aforementioned issues. The most common mitigation technique is to use common metal passivators such as benzotriazole (BTA) and Irgamet® 39 because of their cost-effectiveness [2]. However, passivation is not a reliable technique to overcome sulfur corrosion because metal passivators only provide a protective layer on the copper surface and they do not remove any corrosive sulfur species present in the insulating oils [3]. Thus, it is crucial to develop a sulfur corrosion sensing technology that is capable of detecting and tracking the presence of corrosive sulfur compounds in mineral insulating oils.

Many researchers have used dibenzyl disulfide (DBDS) as the main sulfur compound in order to simulate a corrosive environment in a non-corrosive oil matrix. This is due to the fact that at a high temperature (i.e., 120 °C), the stable DBDS

will degrade into an exceptionally reactive sulfur compound, benzyl mercaptan or DBDS-copper complex, which will cause copper corrosion [4].

A number of standard corrosion test methods have been proposed in order to assess the degree of oil corrosiveness, as shown in Table 1. All of these methods involve immersing the copper or silver strip in the insulating oil. It shall be noted that all of the standard corrosion test methods are carried out by visually comparing the discoloration of the copper surface (non-corrosive/suspected corrosive/corrosive surface) with a standard reference color scale (i.e., ASTM D130-12 [5]), as shown in Fig. 1. Since the analysis of sulfur corrosion is subjected to visual observations, it is possible that one will misinterpret the results obtained from these methods.

TABLE I
STANDARD TEST METHODS USED TO DETERMINE CORROSIVITY OF OILS [6]

Method	Description (Oil/Metal/ Paper)	°C	h	O ₂	Remarks
DIN 51353	100ml/1600 mm ² Ag/-	100	18	Absent	Silver plate corrosion
ASTM D1275A	250ml/300 mm ² Cu/-	140	19	Absent	Copper corrosion
ASTM D1275B	220ml/300 mm ² Cu/-	150	48	Absent	Copper corrosion
BS EN 62535	15ml/540 mm ² Cu/ 540 mm ²	150	72	Limited exposure	Corrosion of paper-wrapped conductors

Based on the existing literature, the degree of corrosivity of insulating oils on a copper surface is dependent on the following factors: (1) concentration of the corrosive compounds, particularly DBDS, (2) aging time, and (3) temperature [6]. Our previous work revealed that thin film sacrificial copper strips have great potential as sensors to monitor the progression of sulfur corrosion at different DBDS concentrations as well as aging time [7]. Hence, it is imperative to investigate the characteristics of these sensors due to sulfur corrosion at different temperatures.

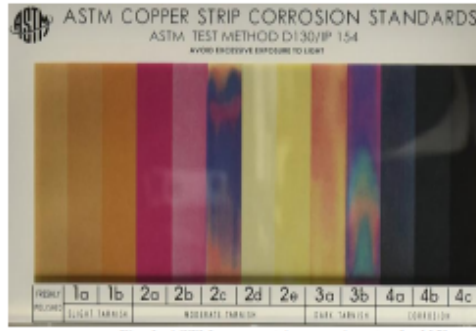


Fig. 1. ASTM copper strip corrosion standard [5]

II. SENSORS: PREPARATION AND TEST PROCEDURE

The thin film sacrificial copper strips (each with an area of 1,375 mm²) were fabricated on a rectangular microscope glass substrate with an area of 1,875 mm². Kapton tape was used to cover both edges of the microscope glass in order to obtain the desired area for copper. Thin film copper with a thickness of 200 nm and purity of 99.99% was evaporated using BOC Edwards E500a e-beam evaporator. In order to enhance the adhesion of thin film copper on the glass substrate, titanium with a layer thickness of 5 nm was deposited prior to copper evaporation. It is essential to keep the sensors in a desiccator with silica-gel in order to reduce surface oxidation of the sensors. We used the same procedure to prepare the corrosive oil samples in order to ensure consistency with our previous work [7].

The tests were conducted in the laboratory, where the sensors were immersed in glass Petri dishes containing 40 mL of corrosive oil with different DBDS concentrations: (1) 100 ppm, (2) 250 ppm, and (3) 1,000 ppm. Each Petri dish was covered with another Petri dish to reduce oil evaporation during the aging process. According to Facciotti et al. [8], the aging time and temperature are the crucial parameters, which will influence the chemical reactions between the corrosive by-products and copper immersed in mineral insulating oils. Selecting the appropriate aging temperature is essential due to the flash point of the insulating oils. The BS EN 62535 standard is the common standard test method used to detect the presence of corrosive sulfur in insulating oils [9]. According to this standard test method, a high temperature (150 °C) should be used to accelerate aging. It is worth noting that sulfur corrosion may occur at an elevated temperature of 80 °C. However, reducing the aging temperature to 80 °C may prolong the occurrence of sulfur corrosion. Hence, in this work, the tests were conducted at 120 and 130 °C because these temperatures have been shown to be a good compromise between the above criteria. The sensors were aged in a forced convection laboratory oven for 25 h. The sensors were taken out from the oven every 5 h in order to measure their resistance. A clean pair of tweezers was used to remove the sensors from the glass Petri dishes. The sensors were cleaned with a solvent and they were gently rubbed with a soft tissue in order to remove oil residue on the sensor surface.

III. LOW RESISTANCE MEASUREMENTS

A sketch of the low resistance measurement equipment is shown in Fig. 2, while the description of each component is given in Table 2. The low resistance measurements were performed in the Temperature and Humidity Controlled Environmental Room where the temperature was set at 20 ± 1 °C. Megger Ducter DLRO-10X digital low resistance ohmmeter was used to measure the resistance of the sensors. The advantages of this technique for low resistance measurements have been described in our previous work [7].

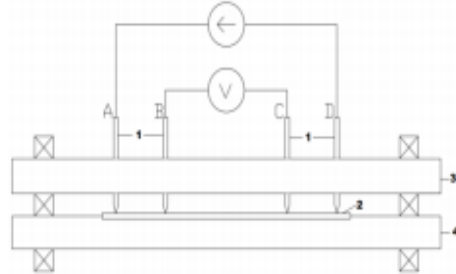


Fig. 2. Sketch of the equipment used to measure the resistance of the sensors using the 4-wire measurement technique

TABLE II
STRUCTURAL DETAILS OF THE TEST CELL

Label	Description
1	Measurement copper needle
2	Sensor
3	Electrode holder made from polyethylene terephthalate with a thickness of 6.4 mm
4	Sensor holder made from aluminum with a thickness of 6 mm

The Megger Ducter DLRO-10X digital low resistance ohmmeter enables current to flow through the outer probe pair (A and D) while the voltage drop is measured across the inner pair probe (B and C). The resistance of the sensor can be determined from the following equation:

$$R = V_{BC} / I_{AD} \quad (1)$$

The change in resistance due to sulfur corrosion is given by:

$$\Delta R = R_t - R_0 \quad (2)$$

where ΔR is the change in the resistance values of the sensors, R_t is the measured resistance value after aging takes place (5-h intervals), and R_0 is the measured initial resistance of the unaged sensors. The measurement procedure was repeated seven times for each sensor to determine the repeatability of the results.

IV. RESULTS AND DISCUSSION

Theoretically, the increase in resistance change of the sensors (ΔR) is due to the copper loss from the glass substrate. For any uniform corrosion at a constant rate, ΔR is inversely proportional to the sensor thickness, as described in our previous work [7]. However, a “blotch” type of corrosion can also occur, as shown in Fig. 3(b).

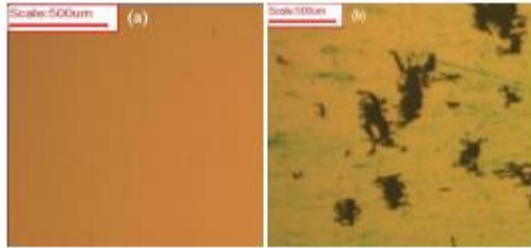


Fig. 3. Morphological changes of the sensor surface due to the presence of corrosive by-products as a consequence of DBDS degradation: (a) new sensor and (b) sensor aged in corrosive mineral oil

A. Changes in Resistance of the Sensors due to Different DBDS Concentrations

Dissolution of copper occurs at 135 °C and it has been reported that the weight of the copper strip is inversely proportional to the heating time [10]. Hence, dissolution of DBDS-Cu complex is more pronounced than the formation of copper sulfide. To test this hypothesis, our experimental results provide evidence that ΔR increases linearly with an increase in the DBDS concentration and aging time, as shown in Fig. 4. These findings are in agreement with the results in [10] where at 130 °C, degradation of DBDS causes the sensors to be corroded. It is believed that this phenomenon promotes the dissolution of the DBDS-Cu complex in the insulating oils.

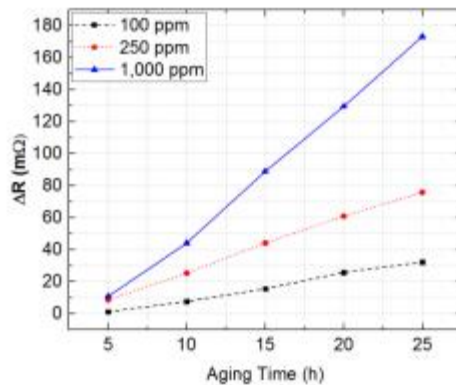


Fig. 4. Variation of ΔR as a function of the aging time when the sensors are aged at 130 °C with three different DBDS concentrations

Fig. 4 shows the low resistance measurement data and it can be observed that there is a steady increase in the ΔR with

respect to the DBDS concentration. The increase in ΔR is most pronounced when the DBDS concentration is 1,000 ppm, judging from the steepness of the line. The ΔR values increase at a relatively slow rate for a DBDS concentration of 100 ppm compared with those for DBDS concentrations of 250 and 1,000 ppm. Therefore, it is assumed that the DBDS chemically interacts with the copper surface even at a small concentration of DBDS (100 ppm).

It can be inferred from Fig. 4 that the corrosive by-products (as a result of the breakdown of DBDS) begin to attack the copper surface after 5 h of aging. This process occurs only for the sensor aged in mineral insulating oils containing 250 and 1,000 ppm of DBDS. However, the sensor aged in mineral insulating oil containing 100 ppm of DBDS shows a slightly different characteristic. It is assumed that the sulfur corrosion process takes place until 10 h of aging because there are no significant changes in the ΔR within the first 5 h of the aging test.

Based on the results presented in Fig. 4, it can be deduced that the ΔR increases with an increase in the DBDS concentration and aging time. Both of these parameters increase the sulfur corrosion rate, which is evidenced from the higher copper losses from the glass substrate.

B. Effect of Temperature Change on the Sensors

Interestingly, the ΔR varies when the sensors are aged at different temperatures. In general, the results presented in Figs. 5–7 show that there is a linear relationship between the ΔR and thermal stresses in the presence of oxygen. It is likely that temperature plays a vital role in increasing the corrosiveness of the mineral insulating oils, as indicated by the measured resistance values in Figs. 5–7. These results indicate that the increase in thermal degradation of the insulating oils containing DBDS in the presence of oxygen will accelerate the progression of sulfur corrosion in oil-immersed power transformers.

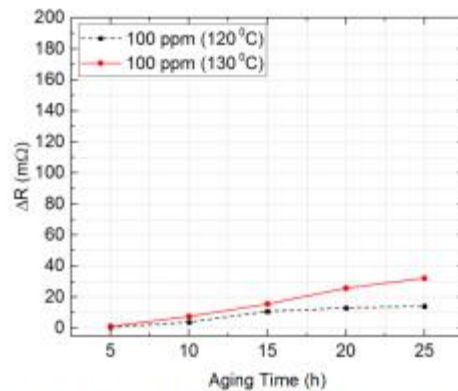


Fig. 5. Variation of ΔR as a function of aging time for the copper surfaces aged in mineral oils containing 100 ppm of DBDS at 120 and 130 °C

As shown in Fig. 5, the effect of thermal stresses on the ΔR aged in 100 ppm of DBDS is only apparent after 10 h of aging. However, the time taken for the corrosive by-products of DBDS to thermally react with the sensor surface is faster for the sensors aged in the mineral oils containing 250 and 1,000 ppm of DBDS (Fig. 6 and Fig. 7), where there are significant changes in the ΔR after only 5 h of aging. The results presented in Fig. 5 and Fig. 7 indicate that, the thermal stresses have a pronounced effect on the ΔR as the aging time is increased at the same DBDS concentration. However, as illustrated in Fig. 6, the sulfur corrosion aging time does not necessarily increase linearly with temperature due to surface effects during the sulfur corrosion process. Therefore, it is imperative that the sensor surface is treated after the resistance measurements because the contaminated surface can be a source of measurement errors.

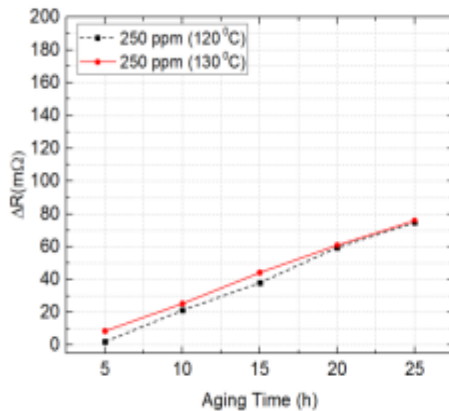


Fig. 6. Variation of ΔR as a function of aging time for the copper surfaces aged in mineral oils containing 250 ppm of DBDS at 120 and 130 °C

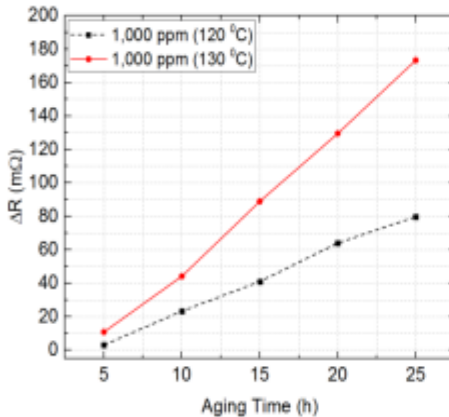


Fig. 7. Variation of ΔR as a function of aging time for the copper surfaces aged in mineral oils containing 1,000 ppm of DBDS at 120 and 130 °C

V. CONCLUSION

The characteristics of thin film sacrificial copper strips in detecting the presence of corrosive by-products resulting from

the breakdown of DBDS at different temperatures have been investigated in this research. The results confirmed that sulfur corrosion is a temperature-dependent process. At the same aging time and DBDS concentration, the amount of copper loss from the glass substrate is more pronounced at higher temperature, based on the measured resistance values. By using the proposed sensors, it is possible to understand how the rate of chemical reaction between corrosive-by products from the degradation of DBDS changes with temperature. Hence, it can be concluded that the proposed thin film sacrificial copper strips can be used as potential sensors to indicate the progression of sulfur corrosion in oil-immersed power transformers.

ACKNOWLEDGMENT

The first author wishes to express his gratitude to the Government of Malaysia and Universiti Teknikal Malaysia Melaka (UTeM) for the financial support during his PhD study. The support of the Integrated Photonics Cleanroom, Optoelectronics Research Centre, University of Southampton, in fabricating the sensors in this study is gratefully acknowledged.

REFERENCES

- [1] M. S. A. Khair, R. C. D. Brown, and P. L. Lewin, "Detection of Sulfur Corrosion in Transformer Insulation Oils Using an Interdigitated Capacitive Sensor Based on Printed Circuit Board Technology," in *IEEE Conference on Electrical Insulation and Dielectric Phenomenon (CEIDP)*, 2017, pp. 278–281.
- [2] T. Wan, B. Feng, Z. Zhou, H. Qian, and S. K. Gong, "Removal of Corrosive Sulfur from Insulating Oil with Adsorption Method," *IEEE Trans. Dielectr. Electr. Insul.*, vol. 22, no. 6, pp. 3321–3326, 2015.
- [3] R. Maina, V. Tumiatti, M. Pompili, and R. Bartnikas, "Corrosive Sulfur Effects in Transformer Oils and Remedial Procedures," *IEEE Trans. Dielectr. Electr. Insul.*, vol. 16, no. 6, pp. 1655–1663, 2009.
- [4] L. R. Lewand and S. Reed, "Destruction of Dibenzyl Disulfide in Transformer Oil," in *75th Annual International Dielectric Conference*, 2008, pp. 1–20.
- [5] "ASTM D130-12: Standard Test Method for Corrosiveness to Copper from Petroleum Products by Copper Strip Test 1," pp. 1–10, 2012.
- [6] F. Scatiggio, V. Tumiatti, R. Maina, M. Tumiatti, M. Pompili, and R. Bartnikas, "Corrosive sulfur induced failures in oil-filled electrical power transformers and shunt reactors," *IEEE Trans. Power Deliv.*, vol. 24, no. 3, pp. 1240–1248, 2009.
- [7] M. S. A. Khair, R. C. D. Brown, and P. L. Lewin, "Tracking the Progression of Sulfur Corrosion in Transformer Oil Using Thin Film Sacrificial Copper Strip," *2nd IEEE International Conference on Dielectrics (ICD)*, in press.
- [8] M. Facciotti, P. S. Amaro, A. F. Holt, R. C. D. Brown, P. L. Lewin, J. A. Pilgrim, G. Wilson, and P. N. Jarman, "Contact-Based Corrosion Mechanism Leading to Copper Sulphide Deposition on Insulating Paper used in Oil-Immersed Electrical Power Equipment," *Corros. Sci.*, vol. 84, pp. 172–179, 2014.
- [9] "BS EN 62535:2009: Insulating liquids — Test method for detection of potentially corrosive sulphur in used and unused insulating oil," pp. 1–22, 2011.
- [10] S. Toyama, J. Tanimura, N. Yamada, E. Nagao, and T. Amimoto, "Highly Sensitive Detection Method of Dibenzyl Disulfide and the Elucidation of the Mechanism of Copper Sulfide Generation in Insulating Oil," *IEEE Trans. Dielectr. Electr. Insul.*, vol. 16, no. 2, pp. 509–515, 2009.

A.4 ACADEMIC JOURNAL: M.S.A. KHIAR, R.C.D. BROWN AND P.L. LEWIN,
“SACRIFICIAL COPPER STRIP SENSORS FOR SULFUR CORROSION DETECTION IN
TRANSFORMER OILS,” MEASUREMENT, VOL. 148, PP. 1–6, 2019.

Author's Personal Copy



Contents lists available at ScienceDirect

Measurement

journal homepage: www.elsevier.com/locate/measurement



Sacrificial copper strip sensors for sulfur corrosion detection in transformer oils



M.S. Ahmad Khia^{a,b,*}, R.C.D. Brown^c, P.L. Lewin^a

^aThe Tony Davies High Voltage Laboratory, University of Southampton, Southampton SO17 1BJ, UK

^bHigh Voltage Engineering Research Laboratory, Centre for Robotics and Industrial Automation, Faculty of Electrical Engineering, Universiti Teknikal Malaysia Melaka (UTeM), Melaka, Malaysia

^cDepartment of Chemistry, University of Southampton, Southampton SO17 1BJ, UK

ARTICLE INFO

Article history:

Received 7 March 2019

Received in revised form 15 July 2019

Accepted 30 July 2019

Available online 2 August 2019

Keywords:

Factorial design

Sulfur

4-Wire measurement

Corrosion sensor

Thin-film copper

ABSTRACT

Existing protocols (e.g., ASTM D 1275-B standard test method) applied to detect and monitor sulfur corrosion in transformer insulating oils are imprecise as it depends on visual observation. As a solution, thin-film sacrificial copper strips are proposed as a corrosive sulfur sensor. A two-level factorial design is utilized to investigate the significant effect of area and thickness upon the sensor's transformation resistance values. Next, a regression model is developed to estimate the sensor's transformation resistance values as functions of area and thickness. The resultant outputs from the two-level factorial design revealed that area, as a variable, exhibited higher significance at 90.19%, compared to either thickness or interaction between area and thickness. The proposed regression model obtained from two-level factorial design is significant in describing the trend displayed by the sensor's transformation resistance values. Finally, this paper details the clear correlation between the sensor's transformation resistance values and elemental sulfur concentration.

© 2019 Elsevier Ltd. All rights reserved.

1. Introduction

Insulating oil serves as a coolant and electrical insulator to ensure reliable operation of high voltage equipment under normal operating conditions. In oil-filled power transformers, mineral oil-based dielectric liquids are used as insulating media and are processed from refined crude petroleum. Petroleum refinement is particularly important because it transforms crude oil into oil-based products with desired physicochemical properties. These oil-based products are carefully refined to fulfil the requirements of specific applications. Although crude oil predominantly comprises of saturated hydrocarbon molecules, it contains a wide range of impurity species; in particular molecules that contain sulfur (hydrogen sulfide, elemental sulfur, mercaptans, alkyl sulfides, thiophenes), oxygen (naphthenic acids), and nitrogen (frequently encountered in asphaltenes), as well as metal species and aromatic compounds. Hence, the oil refinement process should completely remove or minimize these impurities, particularly sulfur, because corrosive elemental sulfur can react with copper and cause a speci-

fic corrosion phenomena that left unchecked will significantly reduce the operational lifetime of the transformer.

Various types of sulfur compounds exist in mineral oil; some originating from virgin oil, while others are unintentionally introduced during the manufacturing process [1]. Sulfur introduced via manufacturing processes is usually due to unsophisticated oil manufacturing technology and refining processes, as well as replenishment of additives, such as antioxidants to prolong the oxidation stability [2] of mineral oils. Sulfur can be found in the mineral oil in elemental form or in organosulfur molecules, namely thiophenes, disulfides, polysulfides, dialkyl sulfides (thioethers), and mercaptans (thiols). Each compound has its own unique reaction rate with copper, which ultimately forms copper sulfide species, as solid corrosion products or complexes, depending upon the concentration of the compounds, copper surface condition, temperature, and aging time [3]. The corrosive levels of sulfur are ranked from elemental sulfur > mercaptans > sulfides > disulfides > thiophenes [3,4]. Hence, elemental sulfur is considered as the most reactive compound with copper, followed by reactive mercaptans. Meanwhile, thiophenes are non-reactive sulfur compounds, whereas disulfides are relatively stable. Nevertheless, disulfides can degrade into benzyl mercaptans, resulting in more corrosive species [5,6].

* Corresponding author.

E-mail addresses: msak15@soton.ac.uk, mohd.shahril@utem.edu.my (M.S. Ahmad Khia), pll@ecs.soton.ac.uk (P.L. Lewin).

<https://doi.org/10.1016/j.measurement.2019.106887>
0263-2241/© 2019 Elsevier Ltd. All rights reserved.

In oil-filled power transformers, sulfur corrosion occurs primarily due to the reaction of existing corrosive sulfur compounds. This particular corrosive sulfur is known as elemental sulfur in insulating oils and copper conductors, which leads to the formation of copper sulfide [4]. For the case of insulating oil, sulfur corrosion is a function of corrosive by-products because of breakdown in stable compounds, namely dibenzyl disulfide (DBDS), which is partly responsible for copper sulfide formation [7–9]. Upon formation, it is likely that copper sulfide will deposit onto the copper surface or insulation paper that is impregnated with insulating oil, thus resulting in turn-to-turn transformer breakdown [2,10].

Although the breakdown of DBDS is believed to be the main cause of copper sulfide formation, insulating oils are still found to be corrosive in the absence of DBDS [9], hence indicating that other sulfur species have the ability to induce a corrosive environment. This phenomenon is reported to be on the increase and worldwide substantial number of transformer units have failed since the beginning of this decade [11]. Passivation techniques and additives have been developed and employed to passivate the corrosive sulfur species in the insulating oils. However, these techniques lead to the generation of passivator-induced stray gas-sing (due to hydrogen, carbon monoxide, and carbon dioxide release) [12]. The released hydrogen in the insulating oils causes difficulties in interpreting the gases results such as dissolved gas analysis because the presence of hydrogen in the insulating oils is not only due to the effect of passivators (i.e. Irgamet®39) but also depends on other mechanisms such as partial discharge. Therefore, reliable condition monitoring tools are absolutely vital to monitor the continuous presence of corrosive sulfur species in transformer oils to avoid catastrophic transformer failure.

Initially, the detection of corrosive sulfur species is carried out by the manufacturers of insulating oils to ensure that the oils comply with the relevant international standards. Thereafter, corrosive sulfur species are detected by transformer system operators, who regularly undertake oil quality monitoring processes. To date, there are four common standard corrosion tests, as presented in Table 1. These tests rely on comparing the color of a silver or copper strip with the ASTM copper strip corrosion standard [13] (see Fig. 1) to deduce the corrosivity levels of the insulating oils under assessment. Unfortunately, this method is imprecise due to visual-based observations and the fact that it is an off-line test dependent on a small sample volume compared with the total oil volume of the transformer.

In order to realize a highly precise corrosion test method, we proposed the use of a quantitative-based thin-film technology [14]. The thin-film copper strips generate resistance values relative to the level of oil corrosiveness. These thin-film technology-based sacrificial copper strips serve as a reliable sensor to track the progression of sulfur corrosion, especially the corrosive by-products that are generated due to degradation in DBDS. The features of the sensors in relation to corrosion of sulfur at varying temperatures were investigated in [15], and further reported that the chemical reaction rate between the corrosive by-products due to degradation of DBDS and thin-film copper was dependent on temperature. However, solely detecting DBDS does not solve issues linked with sulfur corrosion due to presence of other sulfur compounds (i.e., mercaptans, elemental sulfur, and organic sulfides)

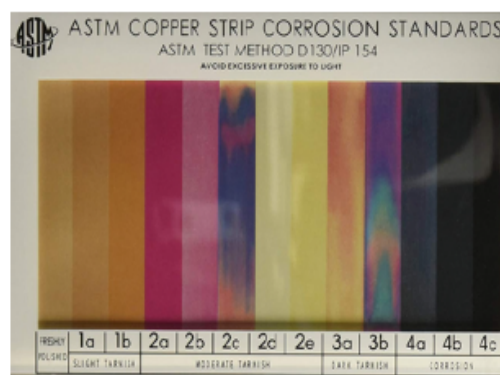


Fig. 1. Copper strip corrosion standard based on ASTM D 130/IP 154.

that induce sulfur corrosion. In order to completely cover the sulfur corrosion paradigm, the proposed method enables two-fold contributions; first, the development of a new test to track one of the corrosive sulfur species, namely elemental sulfur and second, a regression model that estimates the transformation resistance values of the sensors as a function of area and thickness, which has been formulated and verified via two-level (2^2) factorial experimental design.

2. Materials and methods

2.1. Sensors fabrication process

The schematic diagram of the sensors (i.e. area: 800 mm²) is illustrated in Fig. 2. The thin-film copper strip was prepared by evaporating pure copper (purity: 99.99%) onto a rectangular microscope glass substrate with an area of 1875 mm². Pre-cleaning of the glass substrate was first carried out using acetone and isopropyl alcohol, followed by deionized water rinse, and finally, blow-dried with nitrogen. The evaporation was conducted by using a BOC Edwards E500a e-beam evaporator at a vacuum of 10^{-6} mBar in nitrogen condition. In improving thin-film copper adhesion on glass substrate, a 5-nm thick titanium layer was evaporated prior to copper evaporation. Additionally, an aluminum shadow mask was used to obtain a constant desired area of the sensors, as detailed in Tables 2 and 3, respectively.

2.2. Two-level (2^2) factorial design of experiment for screening purpose

One-factor-at-a-time (OFAT) refers to a conventional method for designing experiments that involve testing of variables by changing one variable while retaining the rest at fixed condition. Despite of its ease in implementation, this technique appears to be ineffective in running multiple variables simultaneously. Due to this reason, design of experiments (DoE) has been weighed in as a suitable approach for multi-variable experiments as it significantly eases the number of test runs and ultimately saves manu-

Table 1
Standard test methods to determine corrosivity levels of oils.

Method	Material	Description (Oil/Metal/Paper)	Temperature (°C)	Time (h)
DIN 51353	Ag	100 mL/1600 mm ² /-	100	18
ASTM D1275A	Cu	250 mL/300 mm ² /-	140	19
ASTM D1275B	Cu	250 mL/300 mm ² /-	150	48
BS EN 62535	Cu	15 mL/540 mm ² /540 mm ²	150	72

scale: 20 mm

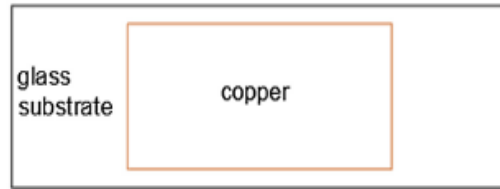


Fig. 2. Schematic diagram of the sensors (top view). The thicknesses of copper are presented in Table 2.

Table 2
Levels of mixing process parameters.

Factor 1 (A: Area (mm ²)) Type: Numeric	Factor 2 (B: Thickness (nm)) Type: Numeric
100 (−1)	50 (−1)
800 (+1)	70 (+1)

Table 3
Factorial design matrix used for factors screening.

Test run	Variable code	
	A: Area (mm ²)	B: Thickness (nm)
1	+1	−1
2	+1	−1
3	+1	−1
4	−1	+1
5	+1	+1
6	−1	+1
7	−1	−1
8	−1	−1
9	+1	+1
10	−1	+1
11	+1	+1
12	−1	−1

facturing time and cost. There are the main reasons for DoE to be applied extensively in the fabricating and manufacturing domains.

A number of techniques are available to assess the correlations between a primary aspect and other interaction factors in experiments that embed multiple factors, for instance, response surface methodology (RSM) [16] and factorial design, as well as Taguchi method [17] and mixture design. In this study, the 2² factorial design of experiment had been selected due to its capability in formulating the regression model that predicts transformation resistance values of the sensors as a function of area and thickness. This regression model can be verified statistically via analysis of variance (ANOVA).

The 2² factorial design of experiment had been performed using Design Expert software version 10.0 (Stat-Ease, Inc., Minneapolis, USA). A screening process was carried out to analyze the significant effect of two independent variables with three repetitions for each test run on the resistance values of the sensors. The 2² factorial design matrix was used to screen the variables that consisted of 12 test runs (see Table 3). Table 2 presents the level of factors, whereby minimum and maximum are designated as −1 and +1, respectively. The measurements of resistance values of the sensors were conducted by adhering to the 2² factorial design matrix. The electrical resistance exhibited by the sensors was measured via 4-wire measurement method in a Temperature and Humidity Controlled Environmental Room with temperature fixed at 20 ± 0.5 °C. The advantages of this method in low resistance measurement have been listed in a prior study [14]. The effects of area

and thickness (variables 1 and 2) on the sensor's transformation resistance values were determined by using a half-normal graph and an effect list, respectively.

Next, a regression model was built to estimate transformation resistance values exerted by sensors as function of thickness and area. Both statistical significance and sufficiency of the regression model were assessed using ANOVA. The outcomes retrieved from 2² factorial design of experiments determined the fit of the regression model, which contained coefficients (multiplied by related factor levels), as follows:

$$Y = \beta_0 + \beta_1 x_1 + \beta_2 x_2 + \beta_{12} x_1 x_2 \quad (1)$$

where Y is response, β_n represents coefficient associated with factor n , whereas x_1 and x_2 are variables that represent factors A and B , respectively. Product $x_1 x_2$ refers to interaction between individual factors. β_0 is model intercept, while $\beta_1 x_1$ and $\beta_2 x_2$ are individual effects of x_1 and x_2 . $\beta_{12} x_1 x_2$ reflects two-factor interaction between x_1 and x_2 . Next, regression analysis had been performed in units that were coded, while coefficients had been based on the coded units. After that, ANOVA was applied to obtain means squares (MS), coefficient of determination (R^2), sum of squares (SS), as well as p -values and F -values. Response surface plot was employed to visually identify the interaction between the factors that affected the sensor's transformation values. The linear regression model that described the correlations between the effect of both variables (area and thickness) and the transformation resistance values of the sensors were verified.

2.3. Preparation of corrosive oil and experimental procedures

The corrosive oil samples were prepared using Nytro Gemini X mineral oil (courtesy of Nynas AB, Sweden). Elemental sulfur (purity: 99.998%, Sigma Aldrich) at three concentrations (15, 20, and 25 ppm) had been selected for simulation of varying levels of corrosion. Oil samples without elemental sulfur were prepared as well to distinguish between corrosive and non-corrosive settings. Dilution based on weight had been used to prepare the solutions. Solvent was used to clean every beaker and later the beakers were dried at 105 °C for about 30 min to ensure that no moisture is retained. Next, the glass bottles were left to cool for about 10 min to room temperature. After that, the solutions (insulating oils mixed with elemental sulfur) had been stirred for ~30 mins until the yellowish elemental sulfur solid homogeneously dissolved in the insulating oils using a hot plate magnetic stirrer. The temperature of the hot plate was fixed to 115 ± 1 °C based on elemental sulfur melting point. The beaker was covered with aluminium foil during the mixing process to avoid excessive evaporation and contamination.

In the attempt of accessing feasibility of sensors in monitoring the progression of corrosive sulfur in insulating oil, a set of sensors with similar area of 800 mm² and thickness of 50 nm was selected. The initial resistance displayed by the sensors had been 0.34 ± 0.01 Ω. The laboratory experimental tests were conducted by immersing the sensors into glass Petri dishes that contained 30 mL of corrosive and non-corrosive oils. The Petri dishes were covered with another Petri dish in order to minimize evaporation of oil over the aging process time. In this study, the samples were aged in a fan-oven for 1 h at 90 °C. Prior to measuring resistance, sensors were removed from the glass Petri dishes with clean pair of tweezers and further cleansing with solvent to discard oil residue on the surface of the sensors. Alteration in resistance because of sulfur corrosion caused by elemental sulfur was calculated as given in the following:

$$\Delta R = R_1 - R_i \quad (2)$$

where ΔR refers to change sensor resistance values, R_i stands for measured resistance values after 1 h of aging, and R_1 is the measured initial resistance prior to aging.

3. Results and discussion

3.1. Screening factor experiment

The 2^2 factorial design, which was applied to screen the factor experiment outcomes in effect list and half-normal plot, is portrayed in Fig. 3 and Table 4, respectively. Fig. 3 illustrates that factors *A* (area), *B* (thickness), and *A-B* interaction (area and thickness) are located away from the straight line. Besides, none of the variables coincide with the straight line. The plot that shows variables *A* and *B*, as well as *A-B* interaction, refers to significant model terms. These outputs are supported by the effect list, which pointed out that variable *A* emerged as the most essential factor with 90.19% of contribution. The *SS* of the variable is 2.78. This is followed by factor *B* with 7.98% contribution and *SS* of 0.25. On the contrary, the *A-B* interaction displayed a contribution of 0.14%, which signified the least contribution of this particular factor amongst the rest. The *SS* for *A-B* interaction is 0.004. From the outcomes, factor *A* significantly contributes higher to transformation resistance values of the sensors, when compared to factor *B* and *A-B* interaction. It shall be noted that 1.69% of the contribution had been due to error.

3.2. Regression model

A regression model based on the 2^2 factorial design, which described the transformation resistance values of the sensors as a function of area and thickness, is presented in Eq. (3).

$$\frac{1}{\sqrt{R}} = 1.38 + 0.48x_1 + 0.14x_2 + 0.019x_1x_2 \quad (3)$$

In order to easily visualize the factors that affected the transformation resistance values of the sensors, the response surface plot was generated (see Fig. 4). As observed from Fig. 4, the transformation resistance values of the sensors increased gradually as the area was decreased from 800 mm² to 100 mm², while the thickness was reduced from 70 nm to 50 nm. The prediction of transformation resistance values of the sensors presented in Table 5 have been based on the regression modeling using the regression equation (see Eq. (3)). Table 5 shows that the highest residual between the measured and predicted value is 0.16 $\Omega^{-\frac{1}{2}}$.

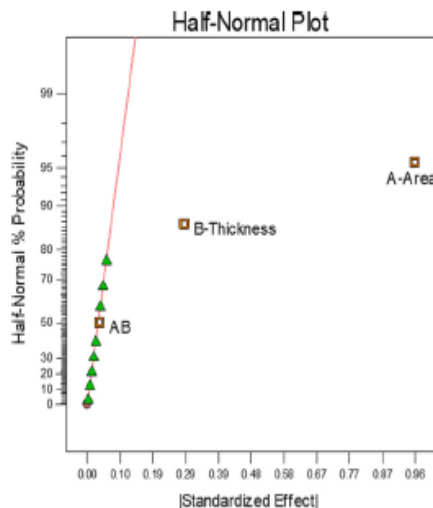


Fig. 3. Half-normal plot for the screening factors.

Table 4

Effect list of all model terms for the screening factor experiment.

Model term	Standardized effects	Sum of squares, <i>SS</i>	Percentage contribution (%)
<i>A</i>	0.96	2.78	90.19
<i>B</i>	0.29	0.25	7.98
<i>A-B</i> interaction	0.038	0.004	0.14
Error		0.052	1.69

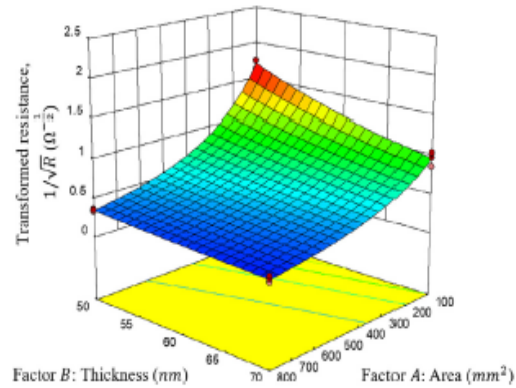


Fig. 4. Response surface plot of transformation resistance values of the sensors vs. area and vs. thickness.

Table 5

Measured and predicted transformation resistance values of the sensors.

Test run	Measured $1/\sqrt{R}$ value, $Y(\Omega^{-\frac{1}{2}})$	Predicted $1/\sqrt{R}$ value, $\hat{Y}(\Omega^{-\frac{1}{2}})$	Residual, $Y-\hat{Y}(\Omega^{-\frac{1}{2}})$
1	1.69	1.70	-0.01
2	1.74	1.70	0.04
3	1.67	1.70	-0.03
4	1.01	1.02	-0.01
5	2.18	2.02	0.16
6	0.98	1.02	-0.04
7	0.76	0.77	-0.02
8	0.79	0.77	0.01
9	2.00	2.02	-0.02
10	1.08	1.02	0.06
11	1.89	2.02	-0.13
12	0.78	0.77	0.01

The details of ANOVA outcomes for the factorial model are summarized in Table 6. The overall regression model seems to be statistically significant since the *p*-value is <0.0001 (below 0.05). In addition, the *p*-values for individual factors are below 0.05 (<0.0001, 0.0003, and 0.4341 for Factors *A* and *B*, as well as *A-B* interaction, respectively). Hence, the regression model built in this research appears adequate as the value of R^2 is 0.9831, signifying that the model can explain 98.31% of the total variation of the sensor's transformation resistance values because of variation in the independent variables (area and thickness).

3.3. Model verification

In order to validate the regression model presented in Eq. (3), three additional sensors (area: 300 mm²–800 mm²; thickness: 60 nm–70 nm) were fabricated. The measured $1/\sqrt{R}$ values of the sensors were obtained by measuring their resistance, while the predicted $1/\sqrt{R}$ values of the sensors were calculated using Eq. (3). The predicted values were compared with the measured val-

Table 6
ANOVA results for the factorial model.

Source	Sum of squares, SS	Degrees of freedom, Df	Mean square, MS	F-value	p-value	Coefficient of determination, R ²
Model	3.030	3	1.010	155.30	< 0.0001	0.9831
A: Area	2.780	1	2.780	427.38	< 0.0001	
B: Thickness	0.250	1	0.250	37.83	0.0003	
A-B Interaction	0.004	1	0.004	0.68	0.4341	
Pure error	0.052	8	0.007			
Corrected total sum of squares	3.080	11				

Table 7
Comparison between the measured and predicted $1/\sqrt{R}$ of 3 new sensors for verification.

Sample	Area (mm ²)	Thickness (nm)	Measured $1/\sqrt{R}$ value ($\Omega^{-1/2}$)	Predicted $1/\sqrt{R}$ value ($\Omega^{-1/2}$)	Percentage difference (%)
1	300	70	1.43	1.31	8.39
2	450	70	1.49	1.52	2.01
3	800	60	2.00	1.86	7.00

ues, as tabulated in Table 7. The average percentage variance between the measured and predicted values is 5.80%. The root mean square error (RMSE) between the actual value, \hat{y} , and the predicted value, y , was obtained using:

$$RMSE = \sqrt{\frac{1}{n} \sum_{i=1}^n (\hat{y}_i - y_i)^2} \quad (4)$$

The RMSE for the three sensor samples is 0.1079. This value is higher than the regression model as it was determined from only three samples. The accuracy of the RMSE can be increased by having larger sample population.

3.4. Thin-film sacrificial copper strips as sulfur corrosion sensors

The addition of elemental sulfur into insulating oils at varied concentrations produced varying corrosion settings. Fig. 5 shows that incremental change in elemental sulfur concentrations leads to increased loss of copper from glass substrate, hence modified the sensor surface morphology. After 1 h of aging at 90 °C in the presence of oxygen, the sensor surface aged in non-corrosive (0 ppm) oil remained unchanged. This indicates that the occurrence of sulfur corrosion is impossible due to absence of elemental sulfur in the insulating oil. Fig. 5 shows that the quantity of copper loss is higher with increased concentration of elemental sulfur

(25 ppm), thus causing corrosion of almost all of the copper. It is relatively challenging to distinguish between the sensors aged in 15 ppm and 20 ppm of elemental sulfur. Therefore, a low resistance measurement method is proposed in this study to assess the feasibility of this method in measuring resistance values of the sensors.

Based on theory, the escalating changes in sensor resistance (ΔR) is linked with the decreasing amount of copper from glass substrate. In order to verify this theory, resistance was measured with a digital micro-ohmmeter (Megger Ducter™ DLRO-10X, Megger Ltd., UK). Fig. 6 displays the variation in ΔR , which serves as a function of elemental sulfur concentrations. The ΔR increases from 0.00 Ω to 8.08 Ω , with increment in elemental sulfur concentrations from 0 ppm to 25 ppm. This increase suggests a decreasing amount of copper from the glass substrate, as observed from Fig. 5. This finding demonstrates that increments in elemental sulfur concentration enhances the process of sulfur corrosion. In general, the value of ΔR aged in non-corrosive oil (0 ppm of elemental sulfur) remained unchanged. The elemental sulfur began attacking the surface of copper at low concentration (15 ppm), whereby ΔR increased from 0.00 Ω to 0.48 Ω . Fig. 6 illustrates that loss of copper from glass substrate had been higher with increased concentration of elemental sulfur (20 ppm), when compared to 15 ppm that led to rapid corrosion of thin-film copper strip and slight increment in the value of ΔR . Meanwhile, the value of ΔR aged in 25 ppm

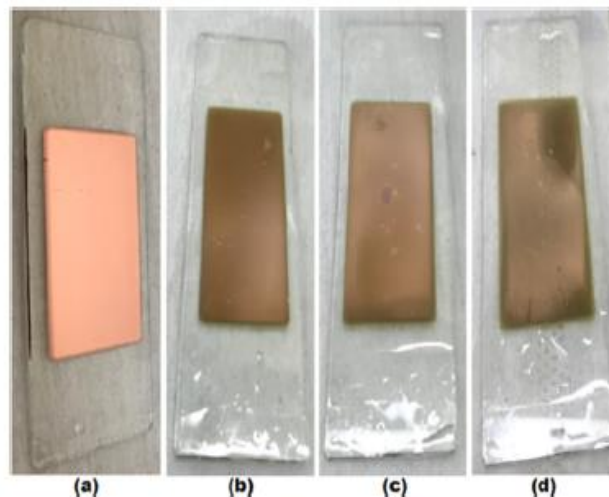


Fig. 5. Surface morphology of 50 nm thin film copper strips aged at 90 °C in different elemental sulfur concentrations: (a) 0 ppm, (b) 15 ppm, (c) 20 ppm, and (d) 25 ppm.

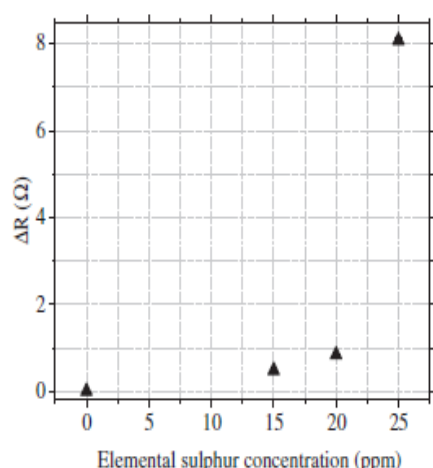


Fig. 6. ΔR of the sensors aged in (a) 0 ppm, (b) 15 ppm, (c) 20 ppm, and (d) 25 ppm of elemental sulfur.

of elemental sulfur increased rapidly to 8.08 Ω as almost all the copper had corroded. Hence, it can be deduced that the experimental results offer evidence that the elemental sulfur plays a vital role in creating a corrosive environment on the copper surface in power transformers.

4. Conclusion

This paper presents evidence that the 2^2 factorial design is indeed a useful method to assess the significant effect of two independent variables on transformation resistance values of sacrificial copper strip sensors. This technique decreases sensor fabricating time and costs as it only requires a small number of test runs, in comparison to those demanded in the OFAT method. Besides, the outputs retrieved from 2^2 factorial design revealed that the sensor area has greatest impact on the sensor's transformation resistance values gave 90.19% contribution. A regression model that describes the correlation between two independent variables (area and thickness) and transformation resistance values of the sensors has been developed. It can be concluded that the model is acceptable in predicting the transformation resistance values of the sensors as a function of area and thickness, whereby R^2 and p -value of the model are 0.9831 and <0.0001, respectively. The regression model generated in this study is remarkably exceptional with an RMSE of 0.1079. The experimental outcomes revealed that the proposed thin-film sacrificial copper strips are indeed feasible in monitoring progress of sulfur corrosion in oil-immersed power transformers via 4-wire measurement technique.

Declaration of Competing Interest

The authors declare that they have no known competing financial interests or personal relationships that could have appeared to influence the work reported in this paper.

Acknowledgments

The first author gratefully acknowledges the financial support extended by Malaysia's Ministry of Education and University Teknikal Malaysia Melaka (UTeM) during his PhD study. The author also would like to express his gratitude to the Integrated Photonics Cleanroom, Optoelectronics Research Centre, University of Southampton, for fabricating the sensors used in this study.

References

- [1] J.M. Lukic, S.B. Milosavljevic, A.M. Orlovic, Degradation of the insulating system of power transformers by copper sulfide deposition: influence of oil oxidation and presence of metal passivator, *Ind. Eng. Chem. Res.* 49 (2010) 9600–9608, <https://doi.org/10.1021/ie1013458>.
- [2] F. Scatiggio, V. Tumiatti, R. Maina, M. Tumiatti, M. Pompili, R. Barnikas, Corrosive sulfur induced failures in oil-filled electrical power transformers and shunt reactors, *IEEE Trans. Power Deliv.* 24 (2009) 1240–1248, <https://doi.org/10.1109/TPWRD.2008.2005369>.
- [3] F. Scatiggio, V. Tumiatti, R. Maina, M. Tumiatti, M. Pompili, R. Barnikas, Corrosive sulfur in insulating oils: its detection and correlated power apparatus failures, *IEEE Trans. Power Deliv.* 23 (2008) 508–509, <https://doi.org/10.1109/TPWRD.2007.911121>.
- [4] L.R. Lewand, The Role of Corrosive Sulfur in Transformers and Transformer Oil, *Doble Eng. Company, USA*, 2002, pp. 1–15, https://www.doble.com/wp-content/uploads/2002_3B.pdf.
- [5] M.A.G. Martins, Experimental study of the thermal stability of Irgamet 39 and dibenzyl disulfide in the laboratory and in transformers in service, *IEEE Electr. Insul. Mag.* (2014) 28–33, <https://doi.org/10.1109/EM.2014.6843765>.
- [6] R. Maina, V. Tumiatti, M. Pompili, R. Barnikas, Corrosive sulfur effects in transformer oils and remedial procedures, *IEEE Trans. Dielectr. Electr. Insul.* 16 (2009) 1655–1663, <https://doi.org/10.1109/TDEI.2009.5361586>.
- [7] M.A.G. Martins, A.R. Gomes, Experimental study of the role played by dibenzyl disulfide on insulating oil corrosivity—effect of passivator Irgamet 39, *IEEE Electr. Insul. Mag.* 26 (2010) 27–32, <https://doi.org/10.1109/EM.2010.5511186>.
- [8] L.R. Lewand, S. Reed, Destruction of dibenzyl disulfide in transformer oil, in: 75th Annu. Int. Doble Client Conf., 2008, pp. 1–20, https://www.doble.com/wp-content/uploads/2008-DBDS_Destruction_Lewand_and_Reed.pdf.
- [9] M. Dahlund, I. Atanasova-Höhlén, R. Maina, N. Dominelli, T. Ohnstad, T. Animoto, C. Claiborne, M.-H. Eise, J. Lukic, V. Mezhyvynskiy, C. Perrier, P. Smith, J. Tanimura, CIGRE WG A2-32 Copper Sulphide in Transformer Insulation, Final Report, 2009.
- [10] C. Bengtsson, M. Dahlund, J. Hajek, L.F. Pettersson, K. Gustafsson, R. Leanderson, A. Hjortsberg, Oil corrosion and conduction Cu₂S deposition in power transformer windings, in: CIGRE, Tech. Rep. A2-111, 2006, pp. 1–10.
- [11] R. Maina, V. Tumiatti, F. Scatiggio, M. Pompili, R. Barnikas, Transformers surveillance following corrosive sulfur remedial procedures, *IEEE Trans. Power Deliv.* 26 (2011) 2391–2397, <https://doi.org/10.1109/TPWRD.2011.2157177>.
- [12] F. Scatiggio, M. Pompili, R. Barnikas, Effects of metal deactivator concentration upon the gassing characteristics of transformer oils, *IEEE Trans. Dielectr. Electr. Insul.* 18 (2011) 701–706, <https://doi.org/10.1109/TDEI.2011.5931055>.
- [13] ASTM D1275-06, Standard Test Method for Corrosive Sulfur in Insulating Oils, 1998.
- [14] M.S. Ahmad Khair, R.C.D. Brown, P.L. Lewin, Tracking the progression of sulfur corrosion in transformer oil using thin film sacrificial copper strip, in: IEEE 2nd Int. Conf. Dielectr., IEEE, 2018, pp. 8–11, <https://doi.org/10.1109/ICD.2018.8514715>.
- [15] M.S.A. Khair, R.C.D. Brown, P.L. Lewin, Effect of temperature changes on thin film sacrificial copper strips due to sulfur corrosion, in: Annu. Rep. – Conf. Electr. Insul. Dielectr. Phenomena, CEIDP, 2018, pp. 490–493, <https://doi.org/10.1109/CEIDP.2018.8544883>.
- [16] S.A. Ghani, N.A. Muhamad, H. Zainuddin, Z.A. Noorden, N. Mohamad, Application of response surface methodology for optimizing the oxidative stability of natural ester oil using mixed antioxidants, *IEEE Trans. Dielectr. Electr. Insul.* 24 (2017) 974–983, <https://doi.org/10.1109/TDEI.2017.006221>.
- [17] S.A. Ghani, N.A. Muhamad, Z.A. Noorden, H. Zainuddin, A.A. Ahmad, Multi-response optimization of the properties of natural ester oil with mixed antioxidants using taguchi-based methodology, *IEEE Trans. Dielectr. Electr. Insul.* 24 (2017) 1674–1684, <https://doi.org/10.1109/TDEI.2017.006589>.

APPENDIX B: NATIONAL GRID REPORTS

B.1 THE EFFECT OF CORROSIVE OIL ON UV-VIS SPECTROSCOPY

Author's Personal Copy



Report issued to:
National Grid plc
National Grid House
Warwick Technology Park
Gallows Hill, Warwick
CV34 6DA

Project:
Corrosive Sulphur Condition Monitoring of
Oil-Filled Power Transformers

Project Engineer:
Email:
Phone:

Deliverable Number:
WRF Ref.:
Order No.:

This report introduces:
The Effect of Corrosive Oil on UV-Vis Spectroscopy

Document Originator:
The Tony Davies High Voltage
Laboratory
Building 20, University Crescent
Electronics and Electrical Engineering
Faculty of Physical Science &
Engineering
University of Southampton
Southampton, SO17 1BJ
UK

Report prepared by:

A handwritten signature in black ink, appearing to read 'Shahril'.

Mohd Shahril Bin Ahmad Khair

Reviewed by:

Tel: 023 8059 4450
Fax: 023 8059 3709
Email: pll@ecs.soton.ac.uk
Contact: Prof Paul Lewin

Prof Paul Lewin CEng FIET FIEEE

Date: 25/07/2018

Executive Summary

Previous project on the aging behaviour of dodecylbenzene in the presence of copper and dibenzyl disulphide (DBDS) funded by the National Grid plc revealed that the absorption edge of ultraviolet-visible (UV-Vis) spectrum shifted to a longer wavelength for a relatively large concentration of DBDS (2000 ppm). For this reason, the corrosive oils with different DBDS concentrations were monitored using the same method. In addition, UV-Vis spectroscopy was used to characterise the sulphur-corrosive oils based on the spectral response parameters of the oils. Based on the results, it can be deduced that this technique is not feasible for detection and condition monitoring of corrosive sulphur for the following reasons. Firstly, this method is not sufficiently sensitive to detect the presence of DBDS at lower concentrations (<100 ppm). Secondly, there is a possibility that one will misinterpret the results obtained from UV-Vis spectroscopy because this method also detects the presence of other compounds in the insulating oils.

EXECUTIVE SUMMARY	2
LIST OF FIGURES.....	4
1 INTRODUCTION.....	5
2 PREPARATION OF CORROSIVE OIL AND BARE COPPER SAMPLES.....	6
3 EXPERIMENTAL SET-UP OF UV-VIS SPECTROSCOPY.....	6
4 RESULTS.....	7
5 CONCLUSION	8
REFERENCES	9

List of Figures

Figure 1. UV-Vis spectra of insulating oils aged in (a) 0 ppm, (b) 100 ppm, and (c) 1000 ppm of DBDS.....	8
---	---

1 Introduction

Within the last ten years (2008-2017), research has been made on the application of ultraviolet-visible (UV-Vis) spectroscopy for: (1) measuring the transformer oil interfacial tension [1], (2) on-site analysis of transformer paper insulation [2], and (3) Furan estimation in transformer oil insulation [3]. Recently, the use of UV-Vis is further applied to investigating the aging behaviour of dodecylbenzene in the presence of copper and dibenzyl disulphide (DBDS) [4]. The results presented in [4] provide evidence that the absorption edge shifted to a longer wavelength in accordance with the aging time. The same pattern could be observed when comparing two different oil samples: (1) without DBDS, and (2) with the presence of relatively large amount of DBDS (2000 ppm). Due to these reasons, it is hypothesised that the semi-conductive copper sulphide results from sulphur-corrosion (due to the breakdown of DBDS) dissolved in insulating oils may influence the spectroscopic performance.

UV-Vis spectroscopy is a powerful non-destructive test that is based on the absorption or reflectance spectroscopy in the ultraviolet visible spectral region. Theoretically, the variations in UV-Vis spectral response are due to the changes in oil colour [5]. This equipment consists of a light source with a wavelength of 200 nm to 1100 nm. This light source is penetrates through any liquid such as transformer oil which is placed in a cuvette. The light is penetrates via input fiber when the sample interacts with the oil, and the passed light is fired to the spectrophotometer by the output fiber. This spectrophotometer is connected to a computer for displaying and analysing the spectral response of the oil sample.

Light transmitted through the oil sample containing various contaminations is decreased by that fraction being absorbed and is detected as a function of wavelength. According to Beer-Lambert Law, the amount of light absorbed or transmitted by a solution can be calculated as:

$$A_{\lambda} = \log_{10} \left[\frac{I_0}{I} \right] = \log_{10} \left(\frac{1}{T} \right) = \epsilon \cdot c \cdot l \quad (1)$$

Where:

A_{λ} : light absorbance

I_0 : light intensity transmitted through the reference blank

I : light intensity transmitted through the sample

T : light transmittance

ϵ : absorbance coefficient of the substance (unique for each substance)

c : concentration of the absorbing species (gram/litre)

l : path length traversed by the light (sample path length measured in centimetres (width of the cuvette almost always 1cm))

2 Preparation of Corrosive Oil and Bare Copper Samples

Nytro Gemini X mineral oil was used to prepare the oil samples. This type of oil was used as a base because it was claimed by manufacturer that it was free from detectable DBDS (maximum total sulphur content: 0.05%) and metal passivators, respectively. To reduce the effect of water towards the experimental results, the oil samples were degassed at 85 ± 1 °C in a vacuum oven for 48 h. Next, the simulation of different corrosion levels is accomplished by adding DBDS with a purity of $\geq 98\%$ into glass bottles containing the dried oil samples at two different concentrations: (1) 100 ppm, and (2) 1000 ppm. Each glass bottle was cleaned with acetone, followed by distilled water and then dried for ~ 30 min at 105 °C in order to eliminate both moisture and impurities. The glass bottles were then cooled to room temperature for ~ 20 min. Subsequently, the solutions (insulating oils mixed with DBDS) were stirred for ~ 1 h using a hot plate magnetic stirrer until all DBDS crystals have dissolved in order to attain homogeneous mixtures. The temperature of the hot plate was set between 70.5 ± 1.5 °C based on the melting point of the DBDS. The bottles were covered with aluminium foil during the mixing process to prevent moisture and impurity ingress.

In contrast, the copper samples with an area of 200 mm² and thickness of 500 ± 10 µm were prepared by polishing copper sheets with abrasive paper. The copper sheets were cleaned three times with cyclohexane (purity: $> 99\%$, Fisher Scientific UK Ltd, UK). This process is crucial to remove oxide layers that have formed on the surface of the copper sheets. The treated copper samples were placed carefully into headspace glass vials that contained 15 mL of mineral oil (with and without DBDS). The glass vials were sealed with sulphur-free polytetrafluoroethylene (PTFE)-faced silicone septum and aluminium caps. The samples were aged in an air atmosphere using a digital forced convection laboratory oven set at 150 ± 1 °C for 72 h. Once the ageing process was complete, the copper samples were taken out from the vials using a clean pair of tweezers. The copper samples were degreased by rinsing the samples with cyclohexane three times. The oil samples were placed in a sealed glass vials before been stored under vacuum conditions inside a desiccator to prevent the samples from moisture ingress.

3 Experimental Set-Up of UV-Vis Spectroscopy

Three oil samples were characterised as: (1) non-corrosive oil (0 ppm), (2) mildly corrosive oil (100 ppm), and (3) highly corrosive oil (1000 ppm). Perkin Elmer Lambda 35 UV-Vis spectrophotometer were used for spectroscopy measurements of the oil samples once the ageing process was completed. This instrument is equipped with quartz cells, with a path length of 10 mm and a wavelength range of 200 – 1100 nm. In order to examine the effect of the cuvettes filled with oil samples on the spectroscopy measurements, an empty cuvette was scanned and its spectrum was stored as reference (auto-zero mode). Next, each cuvette was filled with 3.5 mL of oil sample using

Eppendorf Multipette® Stream pipette and the samples were scanned using a spectrophotometer. The spectral absorbance characteristics of the oil samples were determined by identifying the difference between the spectral response of each oil sample and the reference spectral response. The UV-Vis spectroscopy measurements were repeated three times for each oil sample using a new cuvette to ensure consistency of the results. It shall be noted that it is crucial to minimise the presence of water bubbles in the insulating oil samples because the bubbles will affect the measurement results. For this reason, the insulating oil samples were left for ~ 10 min until there were no water bubbles present after each oil sample was poured into a cuvette.

4 Results

Figure 1 shows the UV-Vis spectra of the insulating oils aged with the copper samples at 150 ± 1 °C for 72 h. It can be observed that there is no significant difference in the percentage of light transmission between the non-corrosive oil (0 ppm) and mildly corrosive oil (100 ppm), since the UV-Vis spectra for both oil are almost coincidental. However, the percentage of light transmission is lowest for the oil sample with the highest DBDS concentration (1000 ppm). This indicates that the presence of relatively highly corrosive by-products in the insulating oil resulting from breakdown of DBDS reducing the percentage of light transmission. The results conform with the Beer-Lambert Law given in Section 1. According to the Beer-Lambert Law, the light absorbance increases in proportion with the increase in concentration of the absorbance species. Hence, it is expected that the percentage of light transmission decreases with an increase in the DBDS concentration, as evidenced from the results shown in Figure 1. In addition, the UV-Vis spectra of the insulating oils are also influenced by the ageing condition (i.e. aged in air or nitrogen) and the ageing time [6]. This is due to the fact that the presence of other compounds resulting from higher oil acidity contributes to changes in the light absorbance characteristics and thus, UV-Vis spectra. Therefore, it is difficult to distinguish between the effect of corrosive oil and ageing using this method.

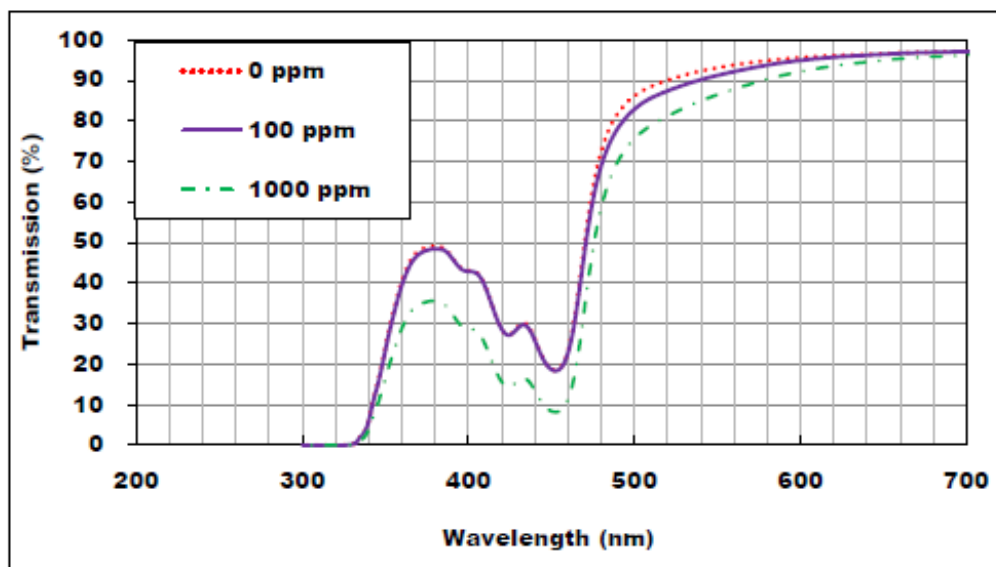


Figure 1. UV-Vis spectra of insulating oils aged in (a) 0 ppm, (b) 100 ppm, and (c) 1000 ppm of DBDS.

5 Conclusion

In conclusion, UV-Vis spectroscopy is impractical for the detection and condition monitoring of corrosive sulphur. The results presented in this report clearly show that the significant changes in UV-Vis spectra only occurred if the DBDS concentration is more than 100 ppm. Besides, it is evident here that the presence of corrosive sulphur species (due to the breakdown of DBDS) in the insulating oil cannot be detected using this method since UV-Vis spectroscopy also detects the presence of other compounds in the oil. Hence, further investigation is essential to analyse the performance of an electrical-based method, in the form of DC conductivity to detect and monitor the progression of sulphur corrosion in insulating oils.

References

- [1] N. Abu Bakar, A. Abu-Siada, S. Islam, and M. F. El-Naggar, "A New Technique to Measure Interfacial Tension of Transformer Oil using UV-Vis Spectroscopy," *IEEE Trans. Dielectr. Electr. Insul.*, vol. 22, no. 2, pp. 1275–1282, 2015.
- [2] P. J. Baird, H. Herman, and G. C. Stevens, "On-Site Analysis of Transformer Paper Insulation Using Portable Spectroscopy for Chemometric Prediction of Aged Condition," *IEEE Trans. Dielectr. Electr. Insul.*, vol. 15, no. 4, pp. 1089–1099, 2008.
- [3] A. Abu-Siada, S. P. Lai, and S. Islam, "A Novel Fuzzy-Logic Approach for Furan Estimation in Transformer Oil," *IEEE Trans. Power Deliv.*, vol. 27, no. 2, pp. 469–474, 2012.
- [4] I. L. Hosier, Linxu Lai and A. S. Vaughan, "Aging Behaviour of Dodecylbenzene in the presence of Copper and Dibenzyl Disulfide (DBDS)," in *IEEE International Conference on Dielectrics (ICD 2016)*, pp. 1032-1035, 2016.
- [5] Y. Zhou, "Electrical Properties of Mineral Oil and Oil/Impregnated Pressboard for HVDC Converter Transformers," PhD Thesis, University of Southampton, 2015.
- [6] I. L. Hosier, A. S. Vaughan, S. J. Sutton, and F. J. Davis, "Chemical, physical and electrical properties of aged dodecylbenzene 2: Thermal ageing of single isomers in air," *IEEE Trans. Dielectr. Electr. Insul.*, vol. 15, no. 5, pp. 1393–1405, 2008.

B.2 THE EFFECT OF CORROSIVE OIL ON DC CONDUCTIVITY MEASUREMENTS

Author's Personal Copy



Report issued to:

National Grid plc
National Grid House
Warwick Technology Park
Gallows Hill, Warwick
CV34 6DA

Project:

Corrosive Sulphur Condition Monitoring of
Oil-Filled Power Transformers

Project Engineer:

Email:
Phone:

Deliverable Number:

WRF Ref.:
Order No.:

This report introduces:
The Effect of Corrosive Oil on DC Conductivity Measurements

Document Originator:

The Tony Davies High Voltage
Laboratory
Building 20, University Crescent
Electronics and Electrical Engineering
Faculty of Physical Science &
Engineering
University of Southampton
Southampton, SO17 1BJ
UK

Report prepared by:

Mohd Shahril Bin Ahmad Khair

A handwritten signature in black ink, appearing to read 'Shahril'.

Mohd Shahril Bin Ahmad Khair

Reviewed by:

Tel: 023 8059 4450
Fax: 023 8059 3709
Email: pll@ecs.soton.ac.uk
Contact: Prof Paul Lewin

Prof Paul Lewin CEng FIET FIEEE

Date: 25/07/2018

Executive Summary

Previous studies have shown that the peak current and saturation current are higher for insulating oils containing dibenzyl disulphide (DBDS) compared with those without DBDS. For this reason, it is hypothesised that the increasing amount of copper in the insulating oils due to sulphur-corrosion (caused by the breakdown of DBDS) affects the charge movement in the oils, resulting in higher oil conductivity. In this research, DC conductivity measurements were carried out using Keithley 6517 picoammeter to monitor the progression of sulphur corrosion in insulating oils. Based on the preliminary results presented in this report, the graphs overlap each other and therefore, it is difficult to distinguish the trends of dissolved copper in the corrosive insulating oils using this method. In addition, the increase in oil conductivity is assumed to be due to the presence of other impurities, particularly moisture. Hence, this method is not suitable to be used as a potential tool for detection and condition monitoring of corrosive sulphur since the small interferences by moisture may lead to misinterpretation of the results.

Table of Contents

EXECUTIVE SUMMARY	2
LIST OF FIGURES.....	4
LIST OF TABLES	5
1 INTRODUCTION.....	6
2 EXPERIMENTAL SET-UP OF DC CONDUCTIVITY MEASUREMENTS.....	6
3 RESULTS.....	8
4 CONCLUSION	10
REFERENCES	11

List of Figures

Figure 1. Experimental set-up for DC conductivity measurements.....	7
Figure 2. DC conductivity results of non-corrosive (0 ppm) oil samples under 1 kV/mm at 25 °C measured at three different times.....	9
Figure 3. DC conductivity results of non-corrosive (0 ppm) and corrosive (100 ppm and 200 ppm) oil samples under 1 kV/mm at 25 °C measured at three different times — steady state conductivity.....	9
Figure 4. DC conductivity results of non-corrosive (0 ppm) and corrosive (100 ppm and 200 ppm) oil samples under 1 kV/mm at 25 °C measured at three different times — initial conductivity.....	10

List of Tables

Table 1. Summary of international standards for DC conductivity measurements of insulating liquids...	6
Table 2. Measured test cell geometry.....	7

1 Introduction

Impurities present in the insulating oils effect the charge movement in the oil (resistance), resulting in changes to the oil conductivity. Due to this, it is hypothesised that DC conductivity measurements are feasible in detecting and monitoring the semi-conductive copper sulphide existing in mineral insulating oils. In addition, higher DBDS concentrations will result in higher DC conductivity values. To date, various international standards have been proposed to provide guidance for DC conductivity measurements as shown in Table 1 [1]–[3].

Table 1. Summary of international standards for DC conductivity measurements of insulating liquids [1]–[3]. (* Used in this research work)

Standard	Method	Description	Electrical Stress	Electrification time
IEC 61620	Current measurement, trapezoidal voltage	Conductivity is related to an initial current density	$\leq 0.1 \text{ kVmm}^{-1}$	$< 5 \text{ s}$
IEC 60247	Current measurement with DC voltage	Conductivity is read at a steady state current density	$0.05 - 0.25 \text{ kVmm}^{-1}$	60 s
*ASTM D 1169	Current measurement with DC voltage	Conductivity is read at a given instant of time	$0.2 - 1.2 \text{ kVmm}^{-1}$	60 s

There is also a research [4] applying Polarisation and Depolarisation Current (PDC) measurements to monitor the conductivity and moisture content in mineral insulating oils. According to the results presented in [4], the polarisation current is divided into two: (1) polarisation current occurred initially (approximately $\leq 100 \text{ s}$) — due to conductivity of insulating oils, and (2) polarisation current occurred after a longer period of time ($t \approx 10\,000 \text{ s}$) — due to moisture content in insulating oil. Considering the suggestions given by ASTM D 1169 and the author in [4], the initial current at 60 s is taken into account in order to analyse the pattern of oil conductivity due to corrosive sulphur.

2 Experimental Set-Up of DC Conductivity Measurements

The DBDS concentrations used in this study were 0, 100, and 200 ppm. Three oil samples (each with the same DBDS concentration) are required to make sure the oil sample was fully discharged before the following DC conductivity measurement was started. Hence, each sample consists of 40 mL of oil along with a copper strip in a 50 mL headspace vial. The dimensions of the copper strip are described in Section 2 (The Effect of Corrosive Oil on UV-Vis Spectroscopy). The samples were aged in an air

atmosphere using a digital forced convection laboratory oven set at 130 ± 1 °C for 10 days. It is crucial to cover all headspace vials with a glass Petri dish to prevent excessive evaporation during the ageing process.

The experimental set-up used for DC conductivity measurements of the oil samples is illustrated in Figure 1. The DC power supply was connected in series with a 5 mL cylindrical test cell and picoammeter. A 10 M Ω protection resistor was connected in series between the DC power supply and 5 mL cylindrical test cell to prevent damage to the picoammeter.

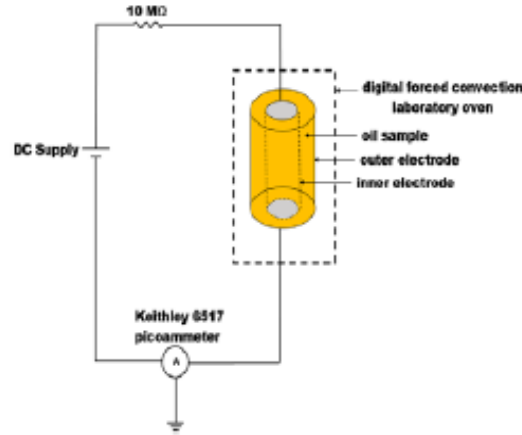


Figure 1. Experimental set-up for DC conductivity measurements.

Table 2 shows the measured test cell geometry used in this experiment. These parameters are used to calculate k , which is a constant based on the test cell geometry.

Table 2. Measured test cell geometry

Parameters	Measured values (m)
Outer radius, r_a	0.0120
Inner radius, r_b	0.0100
Height, l_c	0.0364

Since the test cell is cylindrical, k can be written as [2]:

$$k = \frac{1}{\epsilon_o} \frac{2\pi\epsilon_{air}\epsilon_o l_c}{\ln \frac{r_a}{r_b}} \quad 1$$

where r_a and r_b represent the outer and inner radius of the test cell, respectively, l_c is the height of the test cell, ϵ_o is the vacuum permittivity, and ϵ_{air} is the relative permittivity of air (≈ 1).

In this experiment, the current flowing through the oil samples was measured and the DC conductivity of the oil samples was determined from the following equation [2]:

$$\sigma = \frac{I}{kV} \quad 2$$

Here, σ is the DC conductivity of the oil sample, I is the measured current, and V is the electric potential across the sample.

3 Results

Since the presence of water in the insulating oils will significantly affect the DC conductivity measurements, several tests were conducted to ensure that the water content is approximately the same for all oil samples in this study. Through several experimental works, the optimum time taken to degas and dry the oil samples in the vacuum oven without any heating procedures is four days. It is found that the water content of the insulating oils is 15 ± 1 ppm.

Figure 2 shows the DC oil conductivity values for a DBDS concentration of 0 ppm, measured at three different times. It is found that the relative difference between each curve is less than 32% based on the average conductivity values determined every 12 s. Since the temperature and water measured throughout the experiments are relatively constant, it is considered that the repeatability of this test is acceptable.

Figure 3 and Figure 4 show the DC conductivity results of non-corrosive (0 ppm) and corrosive (100 ppm, and 200 ppm) oil samples under 1 kV/mm at 25 °C measured at three different times for steady-state conductivity and initial conductivity, respectively. It is evident from the results that the graphs overlap each other and therefore, it is difficult to distinguish the trends of dissolved copper and sulphur in the corrosive insulating oils using this method. These findings are contradictory with the results presented in [5] whereby the authors claimed that the insulating oil containing DBDS has a higher peak current and saturation current compared with the oil without DBDS. In addition, the increase in oil conductivity is assumed to be due to the presence of other impurities, particularly moisture.

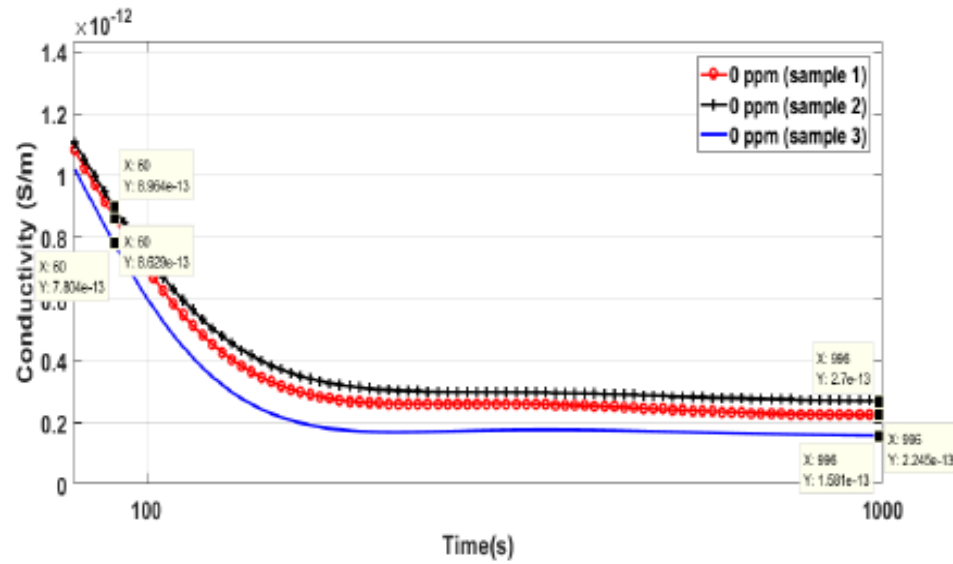


Figure 2. DC conductivity results of non-corrosive (0 ppm) oil samples under 1 kV/mm at 25 °C measured at three different times.

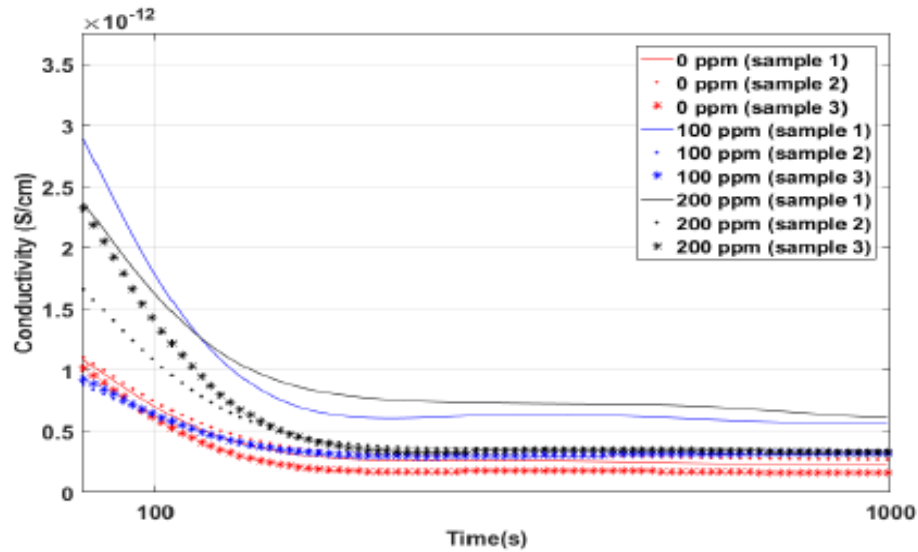


Figure 3. DC conductivity results of non-corrosive (0 ppm) and corrosive (100 ppm and 200 ppm) oil samples under 1 kV/mm at 25 °C measured at three different times — steady state conductivity.

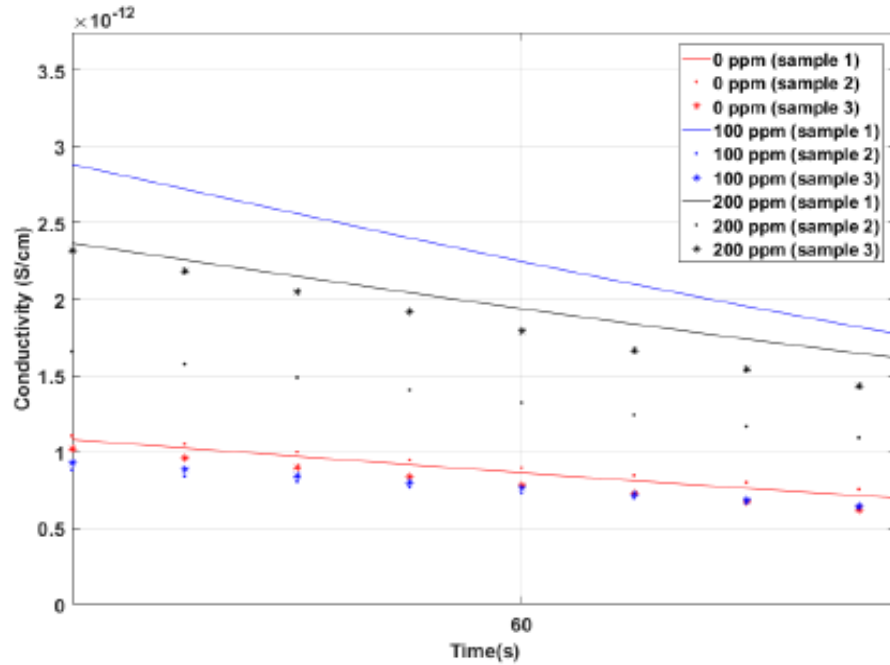


Figure 4. DC conductivity results of non-corrosive (0 ppm) and corrosive (100 ppm and 200 ppm) oil samples under 1 kV/mm at 25 °C measured at three different times — initial conductivity.

4 Conclusion

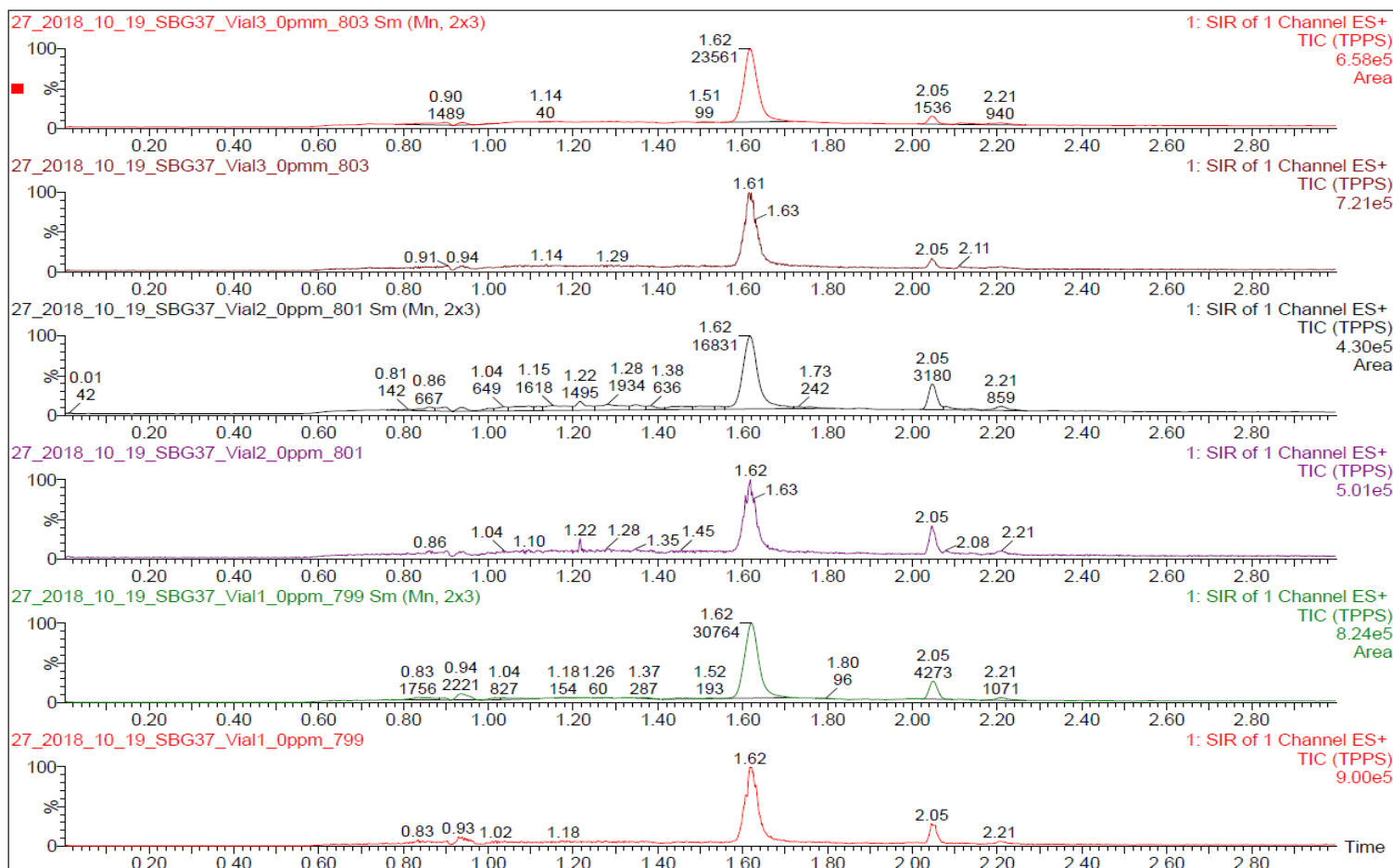
It is proven that this method is not feasible for detection and condition monitoring of corrosive sulphur since the small interferences by moisture could lead to the misinterpretation of the results. For this reason, we are investigating a new method utilising the use of a thin film sacrificial copper strip to detect the changes in electrical resistance due to the progression of sulphur corrosion in insulating oils. The variations of corrosive by-products resulting from the breakdown of DBDS are detected and monitored using thin film copper fabricated onto a glass substrate. The summary of this work has been presented at the 2nd IEEE International Conference on Dielectrics (ICD 2018).

References

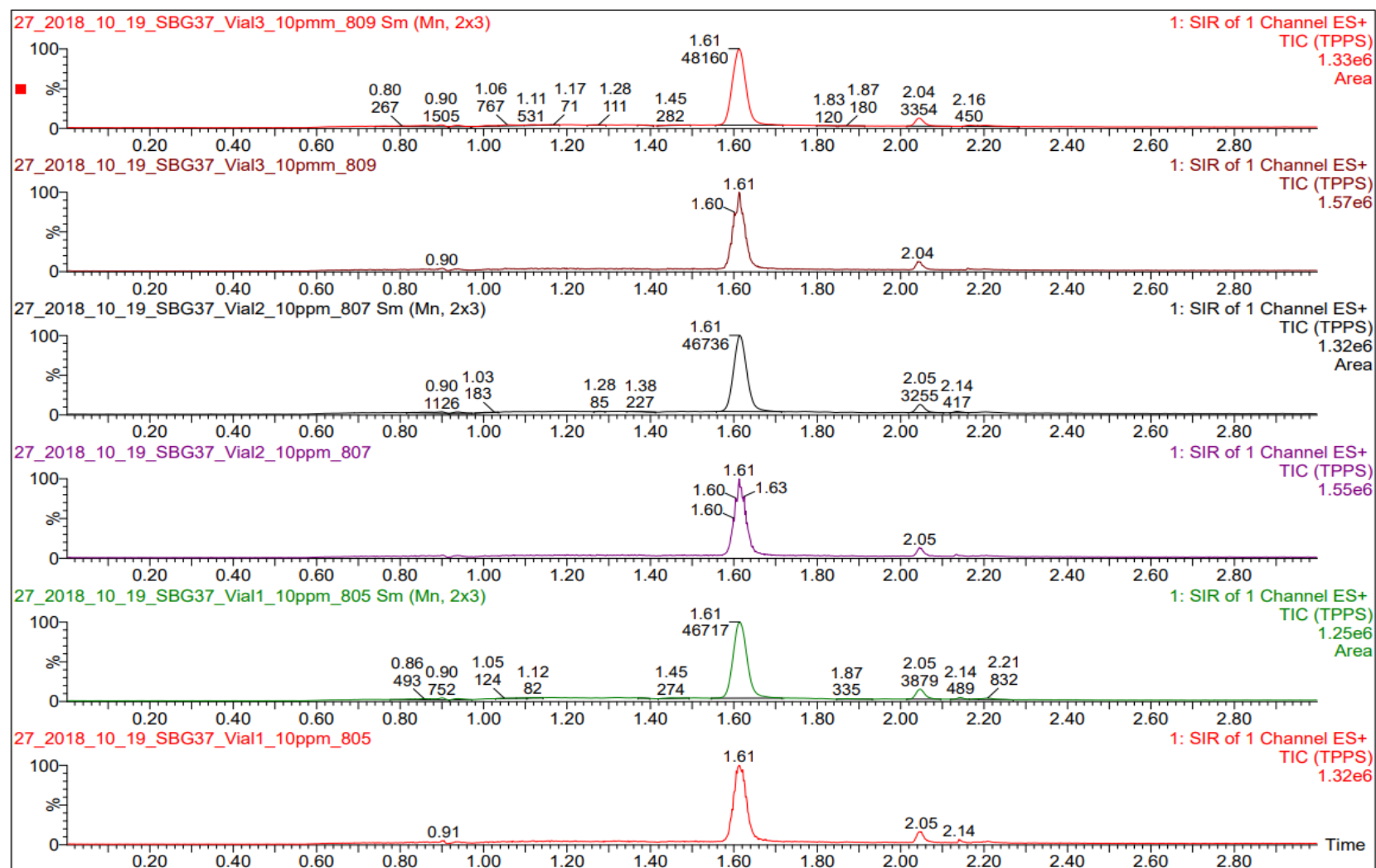
- [1] “BS EN 61620:1999 Insulating liquids— Determination of the dielectric dissipation factor by measurement of the conductance and capacitance – Test method.” pp. 1–20, 1999.
- [2] “BS EN 60247:2004: Insulating liquids—Measurement of relative permittivity, dielectric dissipation factor and d.c. resistivity.” pp. 1–30, 2004.
- [3] “ASTM D1169-11: Standard Test Method for Specific Resistance (Resistivity) of Electrical Insulating Liquids.” pp. 1–7, 2011.
- [4] N. A. Muhamad, “Condition Monitoring of Biodegradable Oil-Filled Transformers using DGA, PD and PDC Measurement Techniques,” PhD Thesis, The University of New South Wales, 2009.
- [5] A. Akshatha, R. Kumar, J. S. Rajan, and H. Ramachandra, “Copper Corrosion Phenomenon in Transformers due to DBDS in Mineral Transformer Oil,” in *IEEE Conference on Electrical Insulation and Dielectric Phenomena (CEIDP 2013)*, 2013, pp. 826–829.

APPENDIX C: UHPSFC-MS DATA SETS

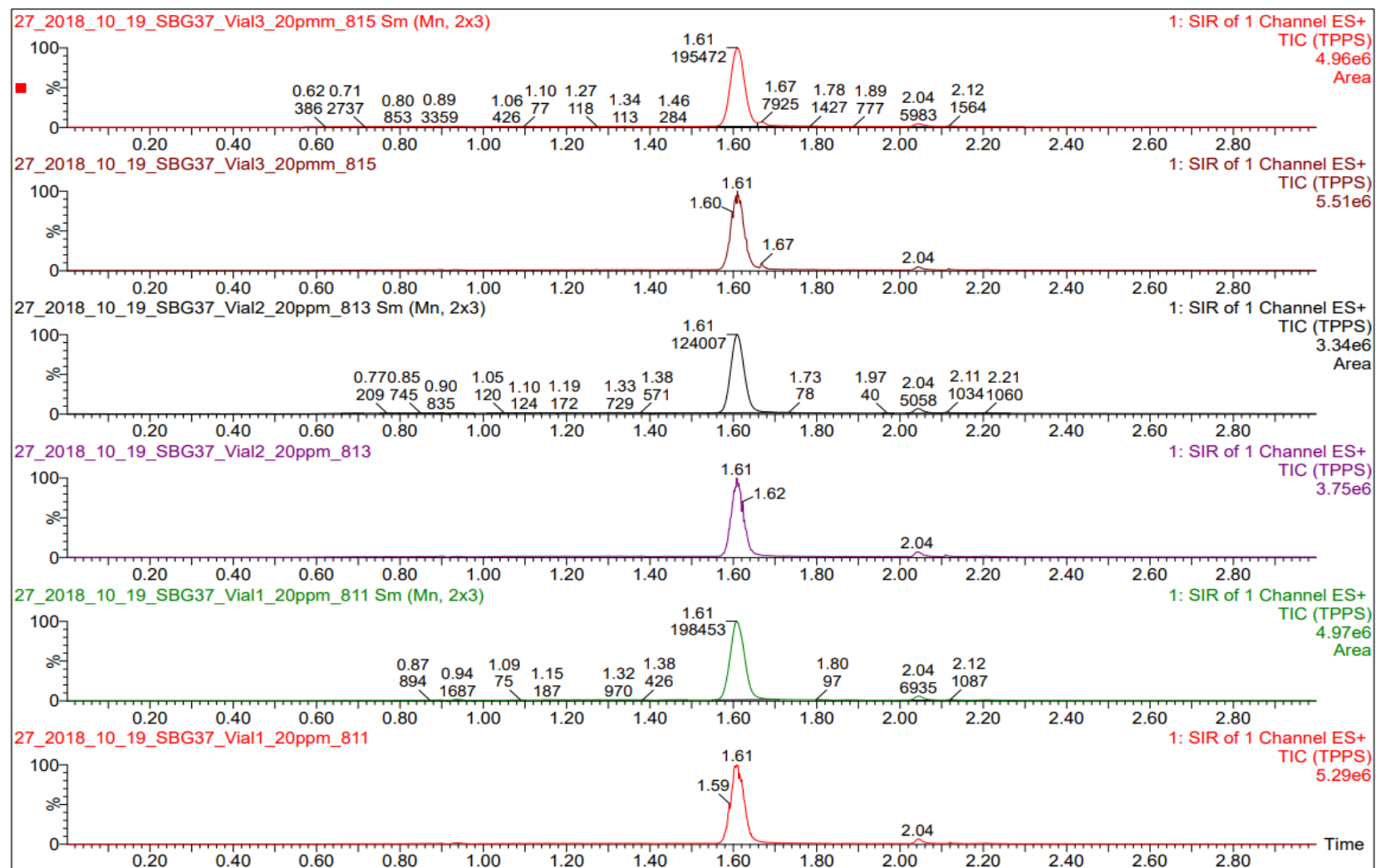
C.1 0 PPM



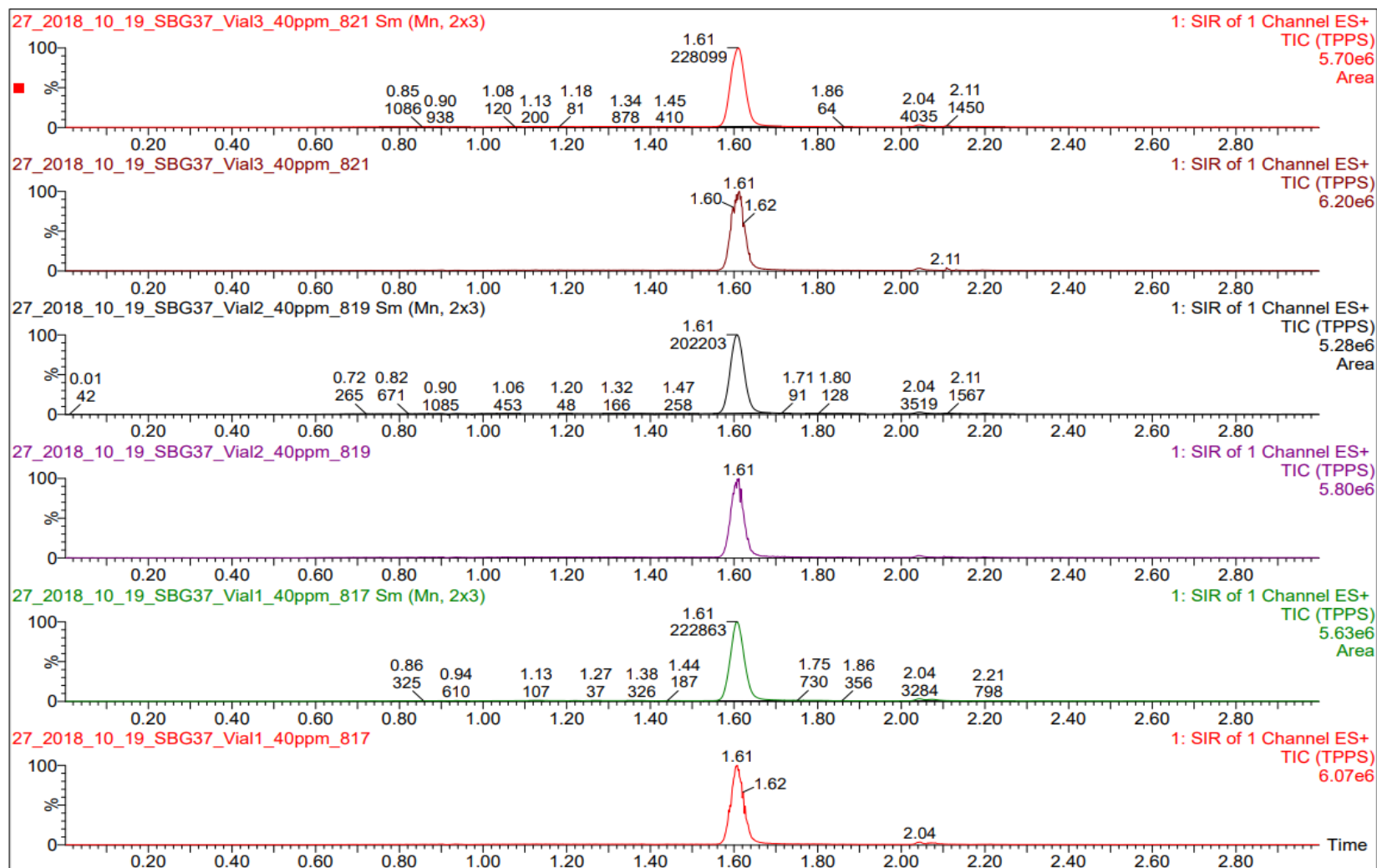
C.2 10 PPM



C.3 20 PPM

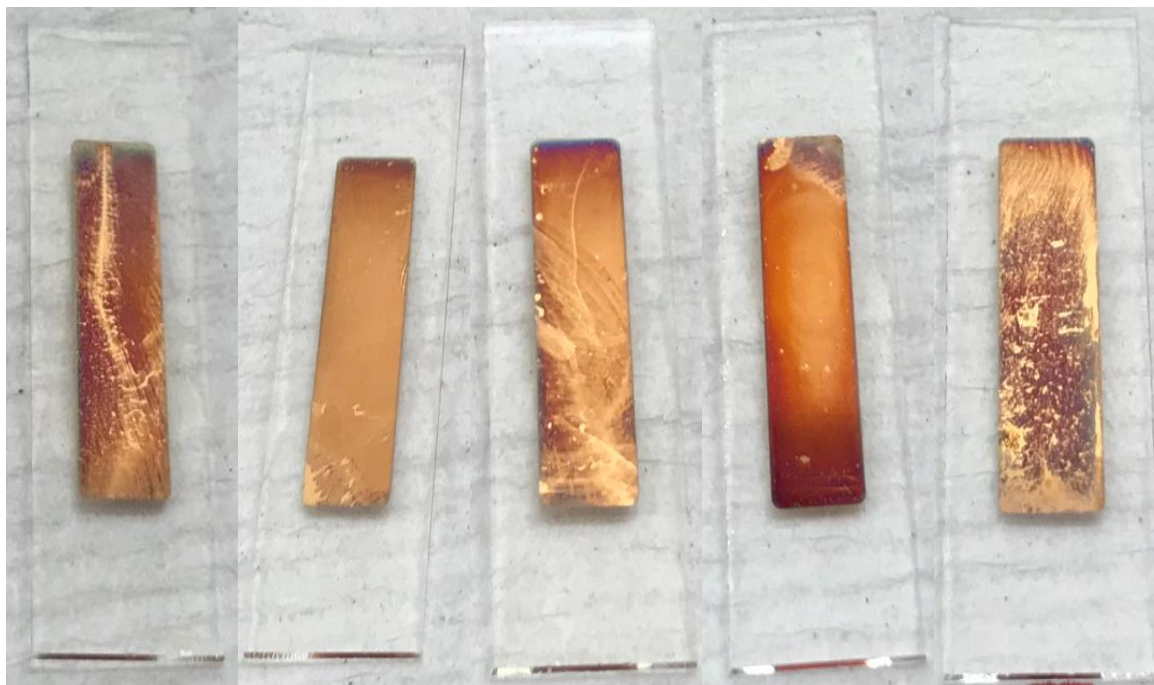


C.4 40 PPM



APPENDIX D: SURFACE MORPHOLOGIES OF THE SENSORS

D.1 HIGH-DEFINITION QUALITY IMAGES OF SENSORS AGED AFTER 1 H
(10 PPM OF S_8 AT 110 °C)



Sensor 1

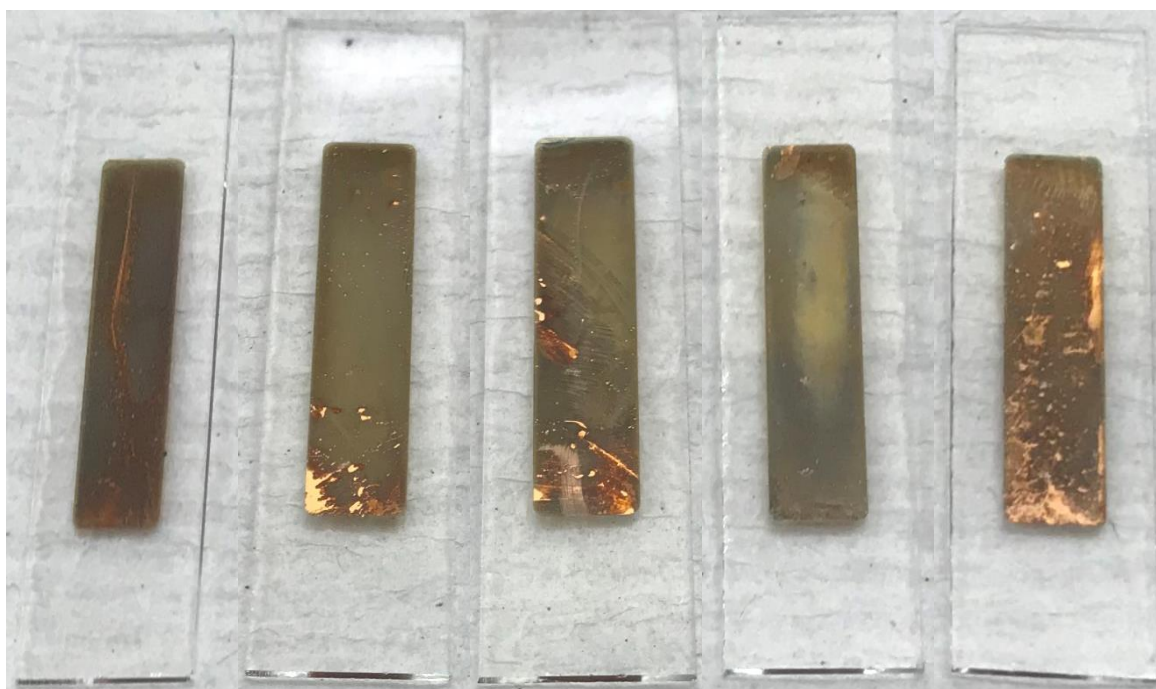
Sensor 2

Sensor 3

Sensor 4

Sensor 5

D.2 HIGH-DEFINITION QUALITY IMAGES OF SENSORS AGED AFTER 2.25 H
(10 PPM OF S_8 AT 110 °C)



Sensor 1

Sensor 2

Sensor 3

Sensor 4

Sensor 5

LIST OF REFERENCES

- [1] M. J. Heathcote, "Operation and maintenance," in *J & P Transformer Book*, Elsevier, 2007, pp. 406–669.
- [2] I. Fofana, "50 Years in the Development of Insulating Liquids," *IEEE Electrical Insulation Magazine*, vol. 29, no. 5, pp. 13–25, 2013.
- [3] P. K. Dooley, "A Comparison of Liquid-Filled and Dry-Type Transformers for Industrial Applications," *IEEE Trans. Ind. Appl.*, vol. 34, no. 1, pp. 222–226, 1998.
- [4] I. A. Metwally, "Failures, Monitoring and New Trends of Power Transformers," *IEEE Potentials*, pp. 36–43, 2011.
- [5] D. J. Allan, "Fires And Explosions in Substations," in *IEEE/PES on Transmission and Distribution Conference and Exhibition*, 2002, pp. 504–507.
- [6] U.S. Department of Energy, "Large Power Transformers and The U.S. Electric Grid." pp. 1–45, 2014.
- [7] O. Seevers, *Power Systems Handbook: Design, Operation and Maintenance*. Prentice Hall, 1991.
- [8] Y. Shirasaka, H. Murase, S. Okabe, and H. Okubo, "Cross-sectional comparison of insulation degradation mechanisms and lifetime evaluation of power transmission equipment," *IEEE Trans. Dielectr. Electr. Insul.*, vol. 16, no. 2, pp. 560–573, 2009.
- [9] J. Lukic *et al.*, "Copper Sulphide Long Term Mitigation and Risk Assessment." CIGRE, Tech. Rep. A2-40, pp. 1–59, 2015.
- [10] C. Bengtsson *et al.*, "Oil Corrosion and Conduction Cu₂S Deposition in Power Transformer Windings." CIGRE, Tech. Rep. A2-111, pp. 1–10, 2006.
- [11] L. Arvidsson, E. Ravnemyhr, J.-P. Haugli, and B. Tandstad, "A Reason for 'Corrosive Sulfur' Failures," in *IEEE International Conference on Dielectric Liquids (ICDL)*, 2014, pp. 1–7.
- [12] T. V. Oommen, "Corrosive and Non-Corrosive Sulfur in Transformer Oils," in *IEEE of Electrical Electronics Insulation Conference (EEIC)*, 1993, pp. 309–311.
- [13] P. J. Griffin and R. Lewand, "Understanding Corrosive Sulfur Problems in Electric Apparatus," in *74th Annual International Doble Client Conference*, 2007, pp. 1–12.
- [14] R. Shuangzan, X. Yang, C. Xiaolong, Z. Lisheng, Y. Qinxue, and J. Robert, "A Research Summary of Corrosive Sulfur in Mineral Oils," in *IEEE International Conference on Properties and Applications of Dielectric Materials (ICPADM)*, 2009, pp. 353–356.
- [15] M. Dahlund, "Failures due to copper sulphide in transformer insulation," *Energize*, pp. 20–23, 2006.

- [16] V. Tumiatti, R. Maina, F. Scatiggio, M. Pompili, and R. Bartnikas, "Corrosive Sulphur in Mineral Oils: Its Detection and Correlated Transformer Failures," in *IEEE International Symposium on Electrical Insulation (ISEI)*, 2006, pp. 400–402.
- [17] F. Scatiggio, V. Tumiatti, R. Maina, M. Tumiatti, M. Pompili, and R. Bartnikas, "Corrosive Sulfur in Insulating Oils: Its Detection and Correlated Power Apparatus Failures," *IEEE Trans. Power Deliv.*, vol. 23, no. 1, pp. 508–509, 2008.
- [18] F. Scatiggio, V. Tumiatti, R. Maina, M. Tumiatti, M. Pompili, and R. Bartnikas, "Corrosive Sulfur Induced Failures in Oil-Filled Electrical Power Transformers and Shunt Reactors," *IEEE Trans. Power Deliv.*, vol. 24, no. 3, pp. 1240–1248, 2009.
- [19] S. Toyama, K. Mizuno, F. Kato, E. Nagao, T. Amimoto, and N. Hosokawa, "Influence of Inhibitor and Oil Components on Copper Sulfide Deposition on Kraft Paper in Oil-immersed Insulation," *IEEE Trans. Dielectr. Electr. Insul.*, vol. 18, no. 6, pp. 1877–1885, 2011.
- [20] F. Kato, T. Amimoto, R. Nishiura, K. Mizuno, and S. Toyama, "Suppressive Effect and its Duration of Triazole-based Passivators on Copper Sulfide Deposition on Kraft Paper in Transformer," *IEEE Trans. Dielectr. Electr. Insul.*, vol. 20, no. 5, pp. 1915–1921, 2013.
- [21] T. Amimoto, E. Nagao, J. Tanimura, S. Toyama, and N. Yamada, "Duration and Mechanism for Suppressive Effect of Triazole-based Passivators on Copper-sulfide Deposition on Insulating Paper," *IEEE Trans. Dielectr. Electr. Insul.*, vol. 16, no. 1, pp. 257–264, 2009.
- [22] F. Kato, T. Amimoto, E. Nagao, N. Hosokawa, S. Toyama, and J. Tanimura, "Effect of DBDS Concentration and Heating Duration on Copper Sulfide Formation in Oil-immersed Transformer Insulation," *IEEE Trans. Dielectr. Electr. Insul.*, vol. 18, no. 6, pp. 1869–1876, 2011.
- [23] R. Maina, V. Tumiatti, F. Scatiggio, M. Pompili, and R. Bartnikas, "Transformers Surveillance Following Corrosive Sulfur Remedial Procedures," *IEEE Trans. Power Deliv.*, vol. 26, no. 4, pp. 2391–2397, 2011.
- [24] "ASTM D130-12: Standard Test Method for Corrosiveness to Copper from Petroleum Products by Copper Strip Test." pp. 1–10, 2012.
- [25] M. Wang and A. J. Vandermaar, "Review of condition assessment of power transformers in service," *IEEE Electr. Insul. Mag.*, vol. 18, no. 6, pp. 12–25, 2002.
- [26] C. Sun, P. R. Ohodnicki, and E. M. Stewart, "Chemical Sensing Strategies for Real-Time Monitoring of Transformer Oil: A Review," *IEEE Sens. J.*, vol. 17, no. 18, pp. 5786–5806, 2017.
- [27] "BS EN 60599:2016: Mineral oil-filled electrical equipment in service — Guidance on the interpretation of dissolved and free gases analysis." pp. 1–44, 2016.
- [28] W. H. Bartley, "Analysis of Transformer Failures," in *International Association of*

Engineering Insurers 36th Annual Conference, 2003, pp. 1–13.

- [29] T. V. Oommen, “Vegetable Oils for Liquid-Filled Transformers,” *IEEE Electr. Insul. Mag.*, vol. 18, no. 1, pp. 6–11, 2002.
- [30] D. Bolliger, G. Pilania, and S. Boggs, “The Effect of Aromatic and Sulfur Compounds on Partial Discharge Characteristics of Hexadecane,” *IEEE Trans. Dielectr. Electr. Insul.*, vol. 20, no. 3, pp. 801–813, 2013.
- [31] “BS EN 60422:2013: Mineral insulating oils in electrical equipment — supervision and maintenance guidance.” pp. 1–50, 2013.
- [32] X. Wang, C. Tang, B. Huang, J. Hao, and G. Chen, “Review of Research Progress on The Electrical Properties and Modification of Mineral Insulating Oils Used in Power Transformers,” *Energies*, vol. 11, no. 3, pp. 1–31, 2018.
- [33] P. S. Amaro, “Corrosive Sulphur in Large Transformers: Impact, Quantification and Detection,” PhD Thesis, University of Southampton, 2015.
- [34] N. Lelekakis, J. Wijaya, D. Martin, and D. Susa, “The Effect of Acid Accumulation in Power-Transformer Oil on the Aging Rate of Paper Snsulation,” in *IEEE Electrical Insulation Magazine*, 2014, vol. 30, no. 3, pp. 19–26.
- [35] R. J. Heywood, “The Degradation Models of Cellulosic Transformer Insulation,” PhD Thesis, University of Surrey, 1997.
- [36] Nynas, “Transformer Oil Handbook.” pp. 1–226, 2004.
- [37] N. A. Muhamad, “Condition Monitoring of Biodegradable Oil-Filled Transformers using DGA, PD and PDC Measurement Techniques,” PhD Thesis, The University of New South Wales, 2009.
- [38] S. D. Cramer and J. Bernard S.Covino, *ASM Handbook Volume 13A Corrosion: Fundamentals, Testing, and Protection*. 2003.
- [39] “ASTM D2864-10: Standard Terminology Relating to Electrical Insulating Liquids and Gases.” pp. 1–7, 2002.
- [40] L. R. Lewand, “The Role of Corrosive Sulfur in Transformers and Transformer Oil,” *Doble Engineering Company, USA*. pp. 1–15, 2002.
- [41] J. R. Smith and P. K. Sen, “Corrosive Sulfur in Transformer Oil,” in *IEEE Industry Applications Society Annual Meeting*, 2010, pp. 1–4.
- [42] “BS EN 62535:2009: Insulating liquids — Test method for detection of potentially corrosive sulphur in used and unused insulating oil.” pp. 1–22, 2011.
- [43] M. Facciotti *et al.*, “Contact-Based Corrosion Mechanism Leading to Copper Sulphide Deposition on Insulating Paper used in Oil-Immersed Electrical Power Equipment,” *Corros. Sci.*, vol. 84, pp. 172–179, 2014.

- [44] L. Arvidsson, "Consequences of State of the Art Transformer Condition Assessment," in *IEEE International Symposium on Electrical Insulation (ISEI)*, 2010, pp. 1–4.
- [45] M. C. Bruzzoniti, R. M. De Carlo, C. Sarzanini, R. Maina, and V. Tumiatti, "Stability and Reactivity of Sulfur Compounds against Copper in Insulating Mineral Oil: Definition of a Corrosiveness Ranking," *Ind. Eng. Chem. Res.*, vol. 53, pp. 8675–8684, 2014.
- [46] L. R. Lewand and S. Reed, "Destruction of Dibenzyl Disulfide in Transformer Oil," in *75th Annual International Doble Client Conference*, 2008, pp. 1–20.
- [47] J. M. Lukić, D. Nikolić, V. Mandić, S. B. Glisić, D. Antonović, and A. M. Orlović, "Removal of Sulfur Compounds from Mineral Insulating Oils by Extractive Refining with N-methyl-2-pyrrolidone," *Ind. Eng. Chem. Res.*, vol. 51, no. 12, pp. 4472–4477, 2012.
- [48] J. M. Lukic, S. B. Milosavljevic, and A. M. Orlovic, "Degradation of the Insulating System of Power Transformers by Copper Sulfide Deposition: Influence of Oil Oxidation and Presence of Metal Passivator," *Ind. Eng. Chem. Res.*, vol. 49, no. 20, pp. 9600–9608, Oct. 2010.
- [49] M. Facciotti, "A Surface Analytical Chemistry Approach to Copper Corrosion and Its Inhibition With Bezotriazole Derivatives in Oil-Filled Power Transformers," PhD Thesis, University of Southampton, 2015.
- [50] S. Annelore and E. Steve, "Effects of Triazole Additives in Transformer Oils." CIGRE, Tech. Rep. D1-102, pp. 1–8, 2012.
- [51] M. Dahlund *et al.*, "CIGRE WG A2-32 Copper Sulphide in Transformer Insulation, Final Report," 2009.
- [52] S. Toyama, J. Tanimura, N. Yamada, E. Nagao, and T. Amimoto, "Highly Sensitive Detection Method of Dibenzyl Disulfide and the Elucidation of the Mechanism of Copper Sulfide Generation in Insulating Oil," *IEEE Trans. Dielectr. Electr. Insul.*, vol. 16, no. 2, pp. 509–515, 2009.
- [53] V. Dukhi, A. Bissessur, and B. S. Martincigh, "Formation of Corrosive Sulfur with Dibenzyl Disulfide in Fluid-Filled Transformers," *Ind. Eng. Chem. Res.*, vol. 55, no. 11, pp. 2911–2920, 2016.
- [54] T. Amimoto, N. Hosokawa, E. Nagao, J. Tanimura, and S. Toyama, "Concentration Dependence of Corrosive Sulfur on Copper-Sulfide Deposition on Insulating Paper Used for Power Transformer Insulation," *IEEE Trans. Dielectr. Electr. Insul.*, vol. 16, no. 5, pp. 1489–1495, 2009.
- [55] T. Amimoto *et al.*, "Identification of Affecting Factors of Copper Sulfide Deposition on Insulating Paper in Oil," *IEEE Trans. Dielectr. Electr. Insul.*, vol. 16, no. 1, pp. 265–272, 2009.
- [56] R. Maina, V. Tumiatti, M. Pompili, and R. Bartnikas, "Dielectric Loss Characteristics

- of Copper-Contaminated Transformer Oils,” *IEEE Trans. Power Deliv.*, vol. 25, no. 3, pp. 1673–1677, 2010.
- [57] R. Maina, V. Tumiatti, M. C. Bruzzoniti, R. M. De Carlo, J. Lukić, and D. Naumović-Vuković, “Copper Dissolution and Deposition Tendency of Insulating Mineral Oils Related to Dielectric Properties of Liquid and Solid Insulation,” in *IEEE International Conference on Dielectric Liquids (ICDL)*, 2011, pp. 1–6.
 - [58] H. Kawarai *et al.*, “Development of Quantitative Evaluation of Copper Sulfide Deposition on Insulating Paper,” in *IEEE Conference on Electrical Insulation and Dielectric Phenomena (CEIDP)*, 2008, pp. 313–316.
 - [59] V. Tumiatti, C. Roggero, M. Tumiatti, S. Di Carlo, R. Maina, and S. Kapila, “IEC 62697-2012: State of the Art Methods for Quantification of DBDS and Other Corrosive Sulfur Compounds in Unused and Used Insulating Liquids,” *IEEE Trans. Dielectr. Electr. Insul.*, vol. 19, no. 5, pp. 1633–1641, 2012.
 - [60] R. Maina, V. Tumiatti, M. Pompili, and R. Bartnikas, “Corrosive Sulfur Effects in Transformer Oils and Remedial Procedures,” *IEEE Trans. Dielectr. Electr. Insul.*, vol. 16, no. 6, pp. 1655–1663, 2009.
 - [61] M. A. G. Martins and A. R. Gomes, “Experimental Study of the Role Played by Dibenzyl Disulfide on Insulating Oil Corrosivity—Effect of Passivator Irgamet 39,” *IEEE Electrical Insulation Magazine*, vol. 26, no. 4, pp. 27–32, 2010.
 - [62] G. A. Oweimreen, A. M. Y. Jaber, A. M. Abulkibash, and N. A. Mehanna, “The Depletion of Dibenzyl Disulfide from a Mineral Transformer Insulating Oil,” *IEEE Trans. Dielectr. Electr. Insul.*, vol. 19, no. 6, pp. 1962–1970, 2012.
 - [63] “BS EN 62697-1:2012: Test Methods for Quantitative Determination of Corrosive Sulfur Compounds in Unused and Used Insulating Liquids Part 1: Test Method for Quantitative Determination of Dibenzyl Disulfide (DBDS).” pp. 1–36, 2012.
 - [64] A. Ravi Kumar, A. Akshatha, and J. S. Rajan, “A New Approach to Monitor Copper Sulphide Migration in Paper Oil Insulation of Transformers,” in *IEEE International Conference on Dielectric Liquids (ICDL)*, 2014, pp. 1–4.
 - [65] S. D. Flora and J. S. Rajan, “Study of Frequency Domain Spectroscopy on Model Transformer Windings at Elevated Temperatures,” in *IEEE International Conference on Properties and Applications of Dielectric Materials (ICPADM)*, 2015, pp. 340–343.
 - [66] P. S. Amaro, A. F. Holt, M. Facciotti, J. A. Pilgrim, G. Wilson, and P. N. Jarman, “Impact of Corrosive Sulfur in Transformer Insulation Paper,” in *IEEE Electrical Insulation Conference (EIC)*, 2013, pp. 459–463.
 - [67] A. Akshatha, R. Kumar, J. S. Rajan, and H. Ramachandra, “Copper Corrosion Phenomenon in Transformers due to DBDS in Mineral Transformer Oil,” in *IEEE Conference on Electrical Insulation and Dielectric Phenomena (CEIDP)*, 2013, pp.

826–829.

- [68] M. Facciotti *et al.*, “XPS Study on Direct Detection of Passivator Irgamet 39TM on Copper Surfaces Aged in Insulating Mineral Oil,” in *IEEE Conference on Electrical Insulation and Dielectric Phenomena (CEIDP)*, 2013, pp. 1097–1100.
- [69] P. S. Amaro *et al.*, “Tracking Copper Sulfide Formation in Corrosive Transformer Oil,” in *IEEE Conference on Electrical Insulation and Dielectric Phenomena (CEIDP)*, 2013, pp. 144–147.
- [70] M. Kai-Bo, L. Yu-Zhen, W. Wei, Z. You, Z. Sheng-Nan, and L. Cheng-Rong, “Influence of Semiconductive Nanoparticle on Sulfur Corrosion Behaviors in Oil-Paper Insulation,” in *IEEE Conference on Electrical Insulation and Dielectric Phenomena (CEIDP)*, 2013, pp. 715–718.
- [71] S. Ren, L. Zhong, Q. Yu, X. Cao, and S. Li, “Influence of the Atmosphere on the Reaction of Dibenzyl Disulfide with Copper in Mineral Insulation Oil,” *IEEE Trans. Dielectr. Electr. Insul.*, vol. 19, no. 3, pp. 849–854, 2012.
- [72] H. Kawarai *et al.*, “Influences of Oxygen and 2,6-di-tert-butyl-p-cresol on Copper Sulfide Deposition on Insulating Paper in Oil-immersed Transformer Insulation,” *IEEE Trans. Dielectr. Electr. Insul.*, vol. 19, no. 6, pp. 1884–1890, 2012.
- [73] Y. Liu, L. Yang, E. Hu, and J. Huang, “Effects of Antioxidants and Acids on Copper Sulfide Generation and Migration Induced by Dibenzyl Disulfide in Oil-Immersed Transformers,” *IEEE Trans. Electr. Electron. Eng.*, vol. 10, pp. 357–363, 2015.
- [74] H. Kawarai *et al.*, “Role of Dissolved Copper and Oxygen on Copper Sulfide Generation in Insulating Oil,” *IEEE Trans. Dielectr. Electr. Insul.*, vol. 16, no. 5, pp. 1430–1435, 2009.
- [75] P. S. Amaro, M. Facciotti, A. F. Holt, J. A. Pilgrim, P. L. Lewin, and R. C. D. Brown, “X-Ray Fluorescence as a Condition Monitoring Tool for Copper and Corrosive Sulphur Species in Insulating Oil,” *IEEE Trans. Dielectr. Electr. Insul.*, vol. 22, no. 2, pp. 701–708, 2015.
- [76] F. Scatiggio, R. Maina, V. Tumiatti, M. Pompili, and R. Bartnikas, “Long Term Stability of Insulating Mineral Oils Following Their Corrosive Sulfur Removal,” in *IEEE International Symposium on Electrical Insulation (ISEI)*, 2010, pp. 1–4.
- [77] K. J. Rapp, A. W. Lemm, L. A. Orozco, and C. P. McShane, “Corrosive Sulfur Phenomena Mitigation by Using Natural Ester Dielectric Fluids - Field Experience in Latin America,” in *IEEE Transmission and Distribution Conference and Exposition (TDCE)*, 2008, pp. 1–6.
- [78] J. S. N’Cho, I. Fofana, A. Beroual, T. Aka-Ngnui, and J. Sabau, “Aged Oils Reclamation: Facts and Arguments Based on Laboratory Studies,” *IEEE Trans. Dielectr. Electr. Insul.*, vol. 19, no. 5, pp. 1583–1592, 2012.
- [79] F. Scatiggio, M. Pompili, and R. Bartnikas, “Oils with Presence of Corrosive Sulfur:

- Mitigation and Collateral Effects,” in *IEEE Electrical Insulation Conference (EIC)*, 2009, pp. 478–481.
- [80] F. Scatiggio, M. Pompili, and R. Bartnikas, “Effects of Metal Deactivator Concentration Upon The Gassing Characteristics of Transformer Oils,” *IEEE Trans. Dielectr. Electr. Insul.*, vol. 18, no. 3, pp. 701–706, 2011.
 - [81] A. F. Holt *et al.*, “An Initial Study into Silver Corrosion in Transformers Following Oil Reclamation,” in *IEEE Electrical Insulation Conference (EIC)*, 2013, pp. 469–472.
 - [82] M. A. Martins, R. M. Martins, and A. Peixoto, “Fuller’s Earth As The Cause of Oil Corrosiveness After The Oil Reclaiming Process,” in *23rd International Conference on Electricity Distribution*, 2015, pp. 1–5.
 - [83] “High Grade Nytro Gemini X High Performance Insulating Oil.” pp. 1–2, 2012.
 - [84] “Dibenzyl Disulphide Data Sheet.” pp. 1–7.
 - [85] “Elemental Sulfur Data Sheet.” pp. 1–7.
 - [86] A. J. Garratt-Reed and D. C. Bell, *Energy-Dispersive X-Ray Analysis in the Electron Microscope*. Taylor & Francis, 2003.
 - [87] T. F. S. P.-W. BV, “Different Types of SEM Imaging – BSE and Secondary Electron Imaging.” pp. 1–7, 2017.
 - [88] N. Abu Bakar and A. Abu-Siada, “A Novel Method of Measuring Transformer Oil Interfacial Tension using UV-Vis Spectroscopy,” *IEEE Electrical Insulation Magazine*, vol. 32, no. 1, pp. 7–13, 2016.
 - [89] N. Abu Bakar, A. Abu-Siada, S. Islam, and M. F. El-Naggar, “A New Technique to Measure Interfacial Tension of Transformer Oil using UV-Vis Spectroscopy,” *IEEE Trans. Dielectr. Electr. Insul.*, vol. 22, no. 2, pp. 1275–1282, 2015.
 - [90] H. Malik, A. K. Yadav, Tarkeshwar, and R. K. Jarial, “Make Use of UV/VIS Spectrophotometer to Determination of Dissolved Decay Products in Mineral Insulating Oils for Transformer Remnant Life Estimation with ANN,” in *Annual IEEE India Conference: Engineering Sustainable Solutions (INDICON)*, 2011, pp. 1–6.
 - [91] P. J. Baird, H. Herman, and G. C. Stevens, “On-Site Analysis of Transformer Paper Insulation Using Portable Spectroscopy for Chemometric Prediction of Aged Condition,” *IEEE Trans. Dielectr. Electr. Insul.*, vol. 15, no. 4, pp. 1089–1099, 2008.
 - [92] A. Abu-Siada, S. P. Lai, and S. Islam, “A Novel Fuzzy-Logic Approach for Furan Estimation in Transformer Oil,” *IEEE Trans. Power Deliv.*, vol. 27, no. 2, pp. 469–474, 2012.
 - [93] S. Ram, A. K. Chandel, G. Singh, and M. Mondal, “UV Spectrophotometer Based AI

- Techniques for Remnant Life Estimation of Power Transformers,” *IOSR J. Electr. Electron. Eng.*, vol. 3, no. 3, pp. 46–55, 2012.
- [94] I. L. Hosier, L. Lai, and A. S. Vaughan, “Aging Behaviour of Dodecylbenzene in the presence of Copper and Dibenzyl Disulfide (DBDS),” in *International Conference on Dielectrics (ICD)*, 2016, pp. 1032–1035.
 - [95] I. L. Hosier, A. S. Vaughan, S. J. Sutton, and F. J. Davis, “Chemical, physical and electrical properties of aged dodecylbenzene 2: Thermal ageing of single isomers in air,” *IEEE Trans. Dielectr. Electr. Insul.*, vol. 15, no. 5, pp. 1393–1405, 2008.
 - [96] “Aquamax KF Coulometric User Manual.” pp. 1–44, 2016.
 - [97] “BS EN ISO 12937:2001: Methods of Test for Petroleum and Its Products- BS 2000:438: Petroleum Products - Determination of Water - Coulometric Karl Fisher Titration Method,” pp. 1–22, 2001.
 - [98] Y. Zhou, “Electrical Properties of Mineral Oil and Oil/Impregnated Pressboard for HVDC Converter Transformers,” PhD Thesis, University of Southampton, 2015.
 - [99] J. K. Park, J. C. Ryu, W. K. Kim, and K. H. Kang, “Effect of Electric Field on Electrical Conductivity of Dielectric Liquids Mixed with Polar Additives: DC Conductivity,” *J. Phys. Chem. B*, vol. 113, pp. 12271–12276, 2009.
 - [100] F. Schober, M. H. Zink, A. Kuchler, M. Liebschner, and C. Krause, “Diagnosis of HVDC insulation systems by use of oil-conductivity measuring methods,” in *IEEE International Conference on Condition Monitoring and Diagnosis (CMD)*, 2012, pp. 250–253.
 - [101] J. C. Scheider *et al.*, “Oil Conductivity – An Important Quantity for the Design and the Condition Assessment of HVDC Insulation Systems,” *Fhws Sci. J.*, vol. 1, no. 2, pp. 59–79, 2013.
 - [102] I. Fofana, V. Wasserberg, H. Borsi, and E. Gockenbach, “Challenge of Mixed Insulating Liquids for Use in High-Voltage Transformers, Part 1: Investigation of Mixed Liquids,” *IEEE Electr. Insul. Mag.*, vol. 18, no. 3, pp. 18–31, 2002.
 - [103] I. L. Hosier and A. S. Vaughan, “Effect of particulates on the dielectric properties and breakdown strength of insulation oil,” in *IEEE Electrical Insulation Conference (EIC)*, 2017, no. June, pp. 376–379.
 - [104] A. Sierota and J. Rungis, “Electrical Insulating Oils-Part I : Characterization and Pre-treatment of New Transformer Oils,” *IEEE Electr. Insul. Mag.*, vol. 11, no. 1, pp. 8–20, 1995.
 - [105] B. Craig, “Predicting the Conductivity of Water-in-Oil Solutions as a Means to Estimate Corrosiveness,” *Corrosion*, vol. 54, no. 8, pp. 657–662, 1998.
 - [106] “BS EN 61620:1999 Insulating liquids— Determination of the dielectric dissipation factor by measurement of the conductance and capacitance – Test method.” pp. 1–20,

1999.

- [107] “BS EN 60247:2004: Insulating liquids—Measurement of relative permittivity, dielectric dissipation factor and d.c. resistivity.” pp. 1–30, 2004.
- [108] “ASTM D1169-11: Standard Test Method for Specific Resistance (Resistivity) of Electrical Insulating Liquids.” pp. 1–7, 2011.
- [109] W. S. Zaengl, “Applications of Dielectric Spectroscopy in Time and Frequency Domain for HV Power Equipment,” *IEEE Electr. Insul. Mag.*, vol. 19, no. 6, pp. 9–22, 2003.
- [110] T. K. Saha and P. Purkait, “Investigations of Temperature Effects on The Dielectric Response Measurements of Transformer Oil-Paper Insulation System,” *IEEE Trans. Power Deliv.*, vol. 23, no. 1, pp. 252–260, 2008.
- [111] J. Sylvestre N’cho, I. Fofana, Y. Hadjadj, and A. Beroual, “Review of Physicochemical-Based Diagnostic Techniques for Assessing Insulation Condition in Aged Transformers,” *Energies*, vol. 9, no. 5, pp. 1–26, 2016.
- [112] S. S. Gevorgian, T. Martinsson, P. L. J. Linner, and E. L. Kollberg, “CAD Models for Multilayered Substrate Interdigital Capacitors,” *IEEE Trans. Microw. Theory Tech.*, vol. 44, no. 6, pp. 896–904, 1996.
- [113] R. Igreja and C. J. Dias, “Analytical Evaluation of the Interdigital Electrodes Capacitance for A Multi-layered Structure,” *Sensors Actuators A*, vol. 112, pp. 291–301, 2004.
- [114] I. Bilican, M. T. Guler, N. Gulener, M. Yuksel, and S. Agan, “Capacitive Solvent Sensing with Interdigitated Microelectrodes,” *Microsyst. Technol.*, vol. 22, no. 3, pp. 659–668, 2016.
- [115] A. V. Mamishev, K. Sundara-Rajan, F. Yang, Y. Du, and M. Zahn, “Interdigital Sensors and Transducers,” in *Proceeding of IEEE*, 2004, vol. 92, no. 5, pp. 808–845.
- [116] M. R. R. Khan and S. W. Kang, “Highly sensitive and wide-dynamic-range multichannel optical-fiber pH sensor based on PWM technique,” *Sensors*, vol. 16, no. 11, pp. 1–37, 2016.
- [117] T. Islam, A. T. Nimal, U. Mittal, and M. U. Sharma, “A Micro Interdigitated Thin Film Metal Oxide Capacitive Sensor for Measuring Moisture in the Range of 175-625 ppm,” *Sensors Actuators, B Chem.*, vol. 221, no. December 2015, pp. 357–364, 2015.
- [118] H. W. Jung, Y. W. Chang, G. yeon Lee, S. Cho, M. J. Kang, and J. C. Pyun, “A Capacitive Biosensor Based on An Interdigitated Electrode with Nanoislands,” *Anal. Chim. Acta*, vol. 844, pp. 27–34, 2014.
- [119] M. R. R. Khan and S.-W. Kang, “Highly Sensitive Multi-Channel IDC Sensor Array for Low Concentration Taste Detection,” *Sensors*, vol. 15, no. 6, pp. 13201–13221, 2015.

- [120] M. R. R. Khan, A. Khalilian, and S. W. Kang, "Fast, Highly-Sensitive, and Wide-Dynamic-Range Interdigitated Capacitor Glucose Biosensor using Solvatochromic Dye-Containing Sensing Membrane," *Sensors*, vol. 16, no. 265, pp. 1–13, 2016.
- [121] M. R. R. Khan, A. Khalilian, and S. W. Kang, "A High Sensitivity IDC-Electronic Tongue using Dielectric/Sensing Membranes with Solvatochromic Dyes," *Sensors*, vol. 16, no. 668, pp. 1–20, 2016.
- [122] Eppendorf, "Multipette® Stream Operating Manual." pp. 1–48.
- [123] M. S. Ahmad Khair, R. C. D. Brown, and P.L. Lewin, "Sacrificial Copper Strip Sensors for Sulfur Corrosion Detection in Transformer Oils," *Measurement*, pp. 1–18, in Press, 2019.
- [124] V. Czitrom, "One-Factor-At-A-Time Versus Designed Experiments," *Am. Stat.*, vol. 53, no. 2, pp. 126–131, 1999.
- [125] M. J. Anderson, "Trimming the FAT out of Experimental Methods," *Optical Engineering*. pp. 1–2, 2005.
- [126] S. A. Ghani, N. A. Muhamad, Z. A. Noorden, H. Zainuddin, and A. A. Ahmad, "Multi-response optimization of the properties of natural ester oil with mixed antioxidants using taguchi-based methodology," *IEEE Trans. Dielectr. Electr. Insul.*, vol. 24, no. 3, pp. 1674–1684, 2017.
- [127] S. A. Ghani, N. A. Muhamad, H. Zainuddin, Z. A. Noorden, and N. Mohamad, "Application of response surface methodology for optimizing the oxidative stability of natural ester oil using mixed antioxidants," *IEEE Trans. Dielectr. Electr. Insul.*, vol. 24, no. 2, pp. 974–983, 2017.
- [128] A. Agoston, E. Svasek, and B. Jakoby, "A Novel Sensor Monitoring Corrosion Effects of Lubrication Oil in an Integrating Manner," in *IEEE Conference on Sensors*, 2005, pp. 1120–1123.
- [129] S. Garcia *et al.*, "Rapid Analytical Method For Elemental Sulphur Detection in Power Transformer Insulation," in *IEEE Electrical Insulation Conference (EIC)*, pp. 1–4, in Press.